Title
Role of cellular microenvironment in non-viral gene transfer

Author
Dhaliwal, Anandika

Publication Date
2012

Peer reviewed|Thesis/dissertation

UNIVERSITY OF CALIFORNIA

Los Angeles

Role of Cellular Microenvironment in Non-Viral Gene Delivery

A dissertation submitted in partial fulfillment of the requirements for the degree Doctor of Philosophy in Biomedical Engineering

by

Anandika Dhaliwal

2012

ABSTRACT OF THE DISSERTATION

Role of Cellular Microenvironment for

Non-Viral Gene Delivery

by

Anandika Dhaliwal

Doctor of Philosophy in Biomedical Engineering

University of California, Los Angeles, 2012

Professor Tatiana Segura, Chair

Gene delivery has widespread application in tissue regeneration and gene therapy. While non-viral gene delivery is less immunogenic as compared to viral gene delivery, it is hindered by its lack of efficiency. Studies aiming to improve the efficiency of non-viral gene delivery have mostly focused on improving the vector system. However, the cellular microenvironment where the cells reside is only beginning to be exploited as a means to enhance gene transfer. In this dissertation, the effect of different densities of extracellular matrix proteins namely collagen I (C I), vitronectin (Vt), laminin (Lm), collagen IV (C IV), fibronectin (Fn) and ECM gel (ECMg), and their combinations on gene transfer to mouse mesenchymal stem cells (mMSCs) were studied. Protein coatings that resulted in well spread cells such as Fn, ECMg and C IV, resulted in 14.6-, 7- and 6.1- fold increase in transgene expression, respectively, when compared to uncoated surfaces. The transgene expression was up to 90% inhibited on C I coated surface,

which led to less spread cells. Interestingly, the same trend was not observed for polyplex internalization, where protein coats that resulted in less spread cells, such as C I and Vt, resulted in higher polyplex internalization. Subsequently, decreased transgene expression corresponded with inhibited trafficking of the internalized complexes to the nucleus. The effect of combining multiple ECM proteins on non-viral gene transfer was also investigated. Surfaces coated with combination including C I resulted in inhibition of transgene expression. In addition, surfaces coated with combination of Vt, C IV and Lm resulted in a statistically similar enhancement in transgene expression as compared to fibronectin. For all ECM combinations analyzed, the extent of cell spreading mediated by the ECM protein had a 70% correlation with the extent of overall gene transfer observed.

The role of different endocytic pathways and cytoskeletal components on gene transfer was later analyzed on collagen I (C I) and fibronectin (Fn), which had opposite influence on gene transfer. The mechanism by which these ECM proteins affect non-viral gene transfer involved the endocytosis pathway used for polyplex uptake and intracellular tension. Fn was found to promote internalization through clathrin-mediated endocytosis and this pathway brought about more efficient transfection than caveolae-mediated endocytosis and macropinocytosis. Likewise, the disruption of actin-myosin interactions resulted in an enhancement of gene transfer for cells plated on Fn coated surfaces, but not for cells plated on C I.

Furthermore, the molecular mechanism by which these ECM molecules affect the process of gene transfer is not completely understood. The Rho subfamily of GTPases regulates a number of cellular processes including cell morphology, cytoskeletal dynamics and uptake pathways and they are activated to different extents by different ECM proteins. The involvement of RhoGTPases in the ECM protein-mediated enhancement of non-viral gene transfer was studied.

Fibronectin was used as the substrate for these studies. The interaction of mouse mesenchymal stem cells (mMSCs) with fibronectin was found to activate RhoGTPases (RhoA, Rac, and Cdc42). Inactivation of RhoGTPases using chemical inhibitor or expression of dominant negative genes resulted in significantly reduced transgene expression. However, the activation of RhoGTPases using chemical activators or expressing constitutively active genes did not further enhance transgene expression for cells plated on fibronectin. But, for cells plated on C I, which did not result in RhoGTPase activation, expression of constitutively active RhoA, Rac, Cdc42 genes resulted in enhanced non-viral gene transfer.

Cells in the body exist in a 3-D microenvironment. Cellular processes like proliferation, differentiation, apoptosis as well as cellular morphology have been shown to be significantly different in 2-D versus 3-D. In part, these differences are due to differential signaling as a consequent of different cytoskeletal assembly and cell-matrix adhesions in 2-D and 3-D. To fully understand the mechanism of gene transfer in cells, L-polyethylenimine (LPEI) mediated non-viral gene transfer mechanism constituting pathways of endocytosis, cytoskeletal dynamics and RhoGTPases, was studied in 3-D using hyaluronic acid hydrogels, in comparison with 2-D using tissue culture plates. Caveolae and clathrin mediated endocytosis were observed to regulate gene transfer in 2-D, while all three pathways of endocytosis namely clathrin and caveolae mediated endocytosis, and macropinocytosis regulated gene transfer in 3-D. Actin polymerization and RhoA mediated contractility highly contributed to efficient transgene expression in 3-D rather than 2-D. Furthermore, Rac and Cdc42 influenced internalization in 2-D but not in 3-D. In conclusion, endocytic pathways, cytoskeletal dynamics and RhoGTPase mediated signaling differentially modulated non-viral gene transfer in cells cultured in 2-D and 3-D. These results

provide an understanding of the dimensionality of cell microenvironment to obtain efficient gene transfer for the purpose of tissue regeneration and gene therapy.

We believe that the cellular microenvironment can be engineered to enhance the ability of cells to become transfected, and through understanding of the mechanisms by which the ECM affects non-viral gene transfer, better materials and transfection protocols can be achieved.

The dissertation of Anandika Dhaliwal is approved.

James Liao

Andrea Kasko

Yi Tang

Lloyd Miller

Tatiana Segura , Committee Chair

University of California, Los Angeles
2012

TABLE OF CONTENTS

LIST OF FIGURES AND TABLES

ACKNOWLEDGEMENTS

First and foremost, I would like to express my heartfelt gratitude and appreciation to my advisor Professor Tatiana Segura, for her insightful comments, critical observations, valuable inputs and sound advice which has led to the successful culmination of my dissertation. Her guidance, encouragement and inspirational interaction helped me to sail through the trying times with ease and perseverance. The opportunities provided by her to present my research at the conferences gave me the necessary exposure, and instilled in me more self-confidence. I also felt challenged to open my mind to new horizons and possibilities. Thanks Professor, for reposing faith in my abilities, and mentoring me with patience and understanding.

I am extremely grateful to my Ph.D committee members, Dr. James Liao, Dr. Lloyd Miller, Dr. Yi Tang and Dr. Andrea Kasko, for their support, useful suggestions, co-operation and encouragement.

I thank all my previous labmates, Lei, Quinn Ng, Sean Anderson and post doc researcher Jianjun Zhang, for their assistance during my initial work.

I also extend my thanks to my fellow lab-mates, Talar Tokatlian, Shiva Gojigni and Jonathan Lam, for their support throughout the period of my research, which I sincerely appreciate. I would also like to render my gratitude to all the other lab-members, Suwei Zhu, Giovanny Acousta, Shouran Li, Jacob Borrajo, Chris Rodman and Shayne Seigman, for making the environment in the lab more intellectually stimulating and friendly.

I also wish to express my sincere thanks to my undergraduate researchers, Maricela Maldonado, Clayton Lin, Zenas Han, Victor Oshita and Fan Wu for trusting me to mentor them. Their

inspiring presence in the lab motivated me to work harder so that I could transfer information and skills to them more effectively.

My gratitude is due to summer undergraduate researchers Yining Zhang, Eleana Manousiouthakis and high school student Caleb Shield.

I am deeply thankful to my loving parents, Jaslene and Rubinder Dhaliwal, for believing in me, and supporting me in all my challenging endeavors. They have always been pillars of strength to me, and have encouraged me to move ahead in life with self-belief and determination. Nurtured by their unconditional love and care, I have always pursued my dreams with confidence. And thanks to my little sister, Divneet Dhaliwal, who has always looked up to me with faith and conviction, and has encouraged me in her own particular way.

A very special thanks to my beloved husband, Kartikeya Bahl, for his selfless, caring and supportive attitude throughout this endeavor. His sense of humor combined with self written poetry lightened many stressful moments, and cheered me during the exhausting times. Thanks so much for providing me the moral and emotional support, and patiently bearing with me through thick and thin.

I thank my mother-in-law and father in-law, Sweety and Shiv Bahl, from the bottom of my heart for bestowing upon me their good wishes, fond affection and warmth, and most importantly for understanding and respecting my work.

Last but not least, I am thankful to my school UCLA for giving me the opportunity to carry out my research in the Segura lab. Surely, I could not have wished for a better supervisor or a lab for my PhD study.

To express my love and gratitude to my deceased grandparents, both maternal and paternal, I dedicate my thesis to them. The relationship and bond I shared with my grandparents holds an enormous meaning for me. May they continue to shower their heavenly blessings on me!

Flowcytometry was performed in the UCLA Jonsson Comprehensive Cancer Center (JCCC) and Center for AIDS Research Flow Cytometry Core Facility that is supported by National Institutes of Health awards CA-16042 and AI-28697, and by the JCCC, the UCLA AIDS institute, and the David Geffen School of Medicine at UCLA.

I would like to acknowledge the NIH grant IR21EB009516.01A1 for funding this research.

Chapters 4 and 5 comprise the content of Dhaliwal A, Lam J, Maldonado M, Lin C and Segura T "Extracellular matrix modulates non-viral gene transfer to mouse mesenchymal stem cells", Soft matter, 2012, 8: 1451-1459.

Chapter 6 comprises the content of Dhaliwal A, Maldonado M and Segura T "Differential uptake of DNA-poly(ethyleneimine) polyplexes in cells cultured on collagen and fibronectin surfaces" Acta Biomater. 2010 Sep;6(9):3436-47

Chapter 7 comprises the content of Dhaliwal A, Maldonado M, Lin C and Segura T "Cellular cytoskeleton dynamics modulates non-viral delivery through RhoGTPases", *PloSOne,* 2012, 7(4):e35046.

Chapter 10 is a version of Dhaliwal A, Oshita V and Segura T " Non-Viral Gene Delivery to Mouse Mesenchymal Stem Cells in 2-D on Tissue Culture Plastic Surface and in 3-D in Hyaluronic Acid Hydrogels", 2012, in preparation.

Dedicated to my family
Grandparents
Mom & Dad
Mummy & Papa
Kartikeya
Divneet
Vinayak

VITA

Education

Ph.D. Biomedical Engineering, University of California Los Angeles, Expected graduation: June 2012

MS Biomedical Engineering, University of California Los Angeles, March 2009. GPA 3.7

B.E. Biotechnology Engineering, Panjab University, Chandigarh, India, May 2007

Diploma Industry Diploma in Biotechnology Intellectual Property Rights Management, Bioinformatics Institute of India, Noida, India, Nov 2005. Grade A+

Professional Activities

2008-2012 Member of American Institute of Chemical Engineers (AIChE)

2011-2012 American Chemical Society (ACS)

2011-2012 Biomedical Engineering Society (BMES)

Research Experience

Jan 2008 - May 2012 Graduate research assistant; Principal Investigator Tatiana Segura
Biomedical Engineering Interdepartmental Program, UCLA
Research area: Non-viral gene delivery, engineering cellular microenvironment
Acquired methods: Tissue culture, gene delivery, fluorescent microscopy, confocal microscopy, flow-cytometry, hydrogels, rheology, molecular biology techniques, basic lab assays

Summer 2006 Research Internship; Principal Investigator Balvinder Singh
Bioinformatics Centre, Institute of Microbial Technology, Chandigarh, India
Research area: Comparative analysis of docking software for protein-protein and protein-DNA docking
Acquired methods: BLAST; RASMOL; docking software like GRAMM, HEX and EscherNG; structure comparison tools like ProFit and LGA server.

Industry Experience

Summer 2005 Industry Internship
R & D Centre, Ranbaxy Laboratories Limited, Gurgaon, Haryana, India
Research area: Gene cloning and expression of cloned gene
Acquired methods: SDS Page, Western Blotting, Molecular Biology techniques

Peer-Reviewed Publications

1. **Dhaliwal, A**, Maldonado, M, Lin, C and Segura, T " Cellular cytoskeleton dynamics modulates Non-Viral Gene Delivery through RhoGTPases , PloSOne, 2012, 7(4):e35046
2. **Dhaliwal, A**, Lam, J, Maldonado, M, Lin, C and Segura, T "Extracellular matrix modulates non-viral gene transfer to mouse mesenchymal stem cells" Soft matter, 2011, 8, 1451.
3. Zhang, J, Du, J, Yan, M, **Dhaliwal, A**, Wen, J, Liu, F, Segura, T and Lu, Y "Synthesis of protein nano-conjugates for cancer therapy" Nano Research, 2011, 4(5): 425–433.
4. Zhang, J, Lei, Y, **Dhaliwal, A**, Ng, Q, Du, J, Yan, M, Lu, Y and Segura, T "Protein-polymer nanoparticles for non-viral gene delivery" Biomacromolecules, 2011 Apr 11;12(4):1006-14.

5. **Dhaliwal, A**, Maldonado, M and Segura, T "Differential uptake of DNA-poly(ethylenimine) polyplexes in cells cultured on collagen and fibronectin surfaces" Acta Biomater. 2010 Sep;6(9):3436-47

Podium Presentations (*represents presenting author)

1. **Dhaliwal, A***, and Segura, T "Role of cellular microenvironment in non-viral gene delivery" BMES annual meeting (Biomedical Engineering Society), Oct **2011**, Connecticut Convention Center, Hartford, Connecticut.
2. **Dhaliwal, A*** and Segura, T "Role of cellular microenvironment and RhoGTPases in non-viral gene delivery" American Institute of Chemical Engineers (AIChE) Nov **2009**, Gaylord Opryland Hotel, **Nashville,** TN
3. **Dhaliwal, A*** and Segura, T "The extracellular matrix modulates non-viral gene transfer to mouse mesenchymal stem cells" American Institute of Chemical Engineers (AIChE) Nov 2008, Downtown Convention Center, Philadelphia PA

Poster Presentations (* represents presenting author)

1. Dhaliwal, A, Maldonado M, Lin, C and **Segura, T*** "RhoGTPases modulate Non-viral gene delivery" American Society of Gene and Cell Therapy, May 2011 Washington State Convention & Trade center, Seattle, WA
2. **Dhaliwal, A***, Maldonado, M, Lin, C and Segura, T "Rho, Rac and Cdc42 RhoGTPases modulate non-viral gene delivery to mouse mesenchymal stem cells" UCLA Engineering Technology Forum March 2011 California Covel Commons, UCLA, Los Angeles CA
3. **Dhaliwal, A*** and Segura, T "The extracellular matrix modulates Non-viral gene transfer to mouse mesenchymal stem cells" UCLA Engineering Technology Forum April 2009 California NanoSystems Institute UCLA, Los Angeles CA

Teaching Assistant Experience (F = fall quarter, W= winter quarter, S= spring quarter)

F 2011, S 2011	Chemical and Biomolecular Engineering 104A " Chemical and Biomolecular Engineering Laboratory I"
W 2009, W 2011	Chemical and Biomolecular Engineering 124/224 "Cell material interactions"
F 2010, W 2010	Chemical and Biomolecular Engineering 104D/L "Molecular Biotechnology Laboratory: From Gene to Product"
S 2008, S 2010	Chemical and Biomolecular Engineering 125/225 "Bioseparations and Bioprocess Engineering"

Mentoring (F = fall quarter, W= winter quarter, S= spring quarter, Su= summer quarter)

W 2012	Fan Wu, Chemical and Biomolecular Engineering, UCLA
Su 2011-W 2012	Victor Oshita, Chemical and Biomolecular Engineering Department, UCLA
Su 2011	Yining Zhang, Chemical and Biomolecular Engineering, MIT, MA
Su 2010-Su 2011	Clayton Lin, Chemical and Biomolecular Engineering Department, UCLA Presently a graduate student in Biomedical Engineering at University of California, San Diego.
Su 2009-F 2011	Maricela Maldonado, Chemical and Biomolecular Engineering Department, UCLA Presently in the PhD program in Bioengineering at University of California, Irvine.
F 2009-S 2010	Zenas Han, Chemical and Biomolecular Engineering Department, UCLA
F 2009-S 2010	Caleb sheilds, Wildflower High School, Los Angeles
Su 2008	Eleana Manousiouthakis, RPI, NY

Honors and awards

- Graduate division fellowship award for 2011-2012
- Graduate division fellowship award for 2008-2009
- **"**Honors**"** in BE Biotechnology which is awarded to select students for achieving excellence (>70%) across all semesters during biotech engineering.
- Awarded a 'Scholar Tie' in class X for being a Distinction holder (>75%) for three consecutive years at The Lawrence School, Sanawar, India

Chapter 1

Overview of Thesis and Objective

1.1 Motivation and objective

Gene therapy is the use of DNA as a pharmaceutical agent to supplement or alter genes within an individual's cells, as a therapy to treat diseases. Gene therapy addresses the various diseases caused by genetic disorders. ADA deficiency, gaucher's disease and lesch-nyhan disease are due to the defect in a single gene. Sickle cell anemia, hemophilia, cystic fibrosis, duchenne's muscular dystrophy and huntington disease are some other diseases which are curable using gene-therapy.

Different cells like nerve cell, muscle cell and bone cell differ in their gene expression. The cell character and function is directed by the expression of a specific set of genes in the cell. When stem cells are employed for tissue engineering, gene delivery to these stem cells can help induce the expression of a particular set of genes that then direct the cell towards differentiating into a specialized cell type, that would constitute a tissue (**Figure 1-1**).

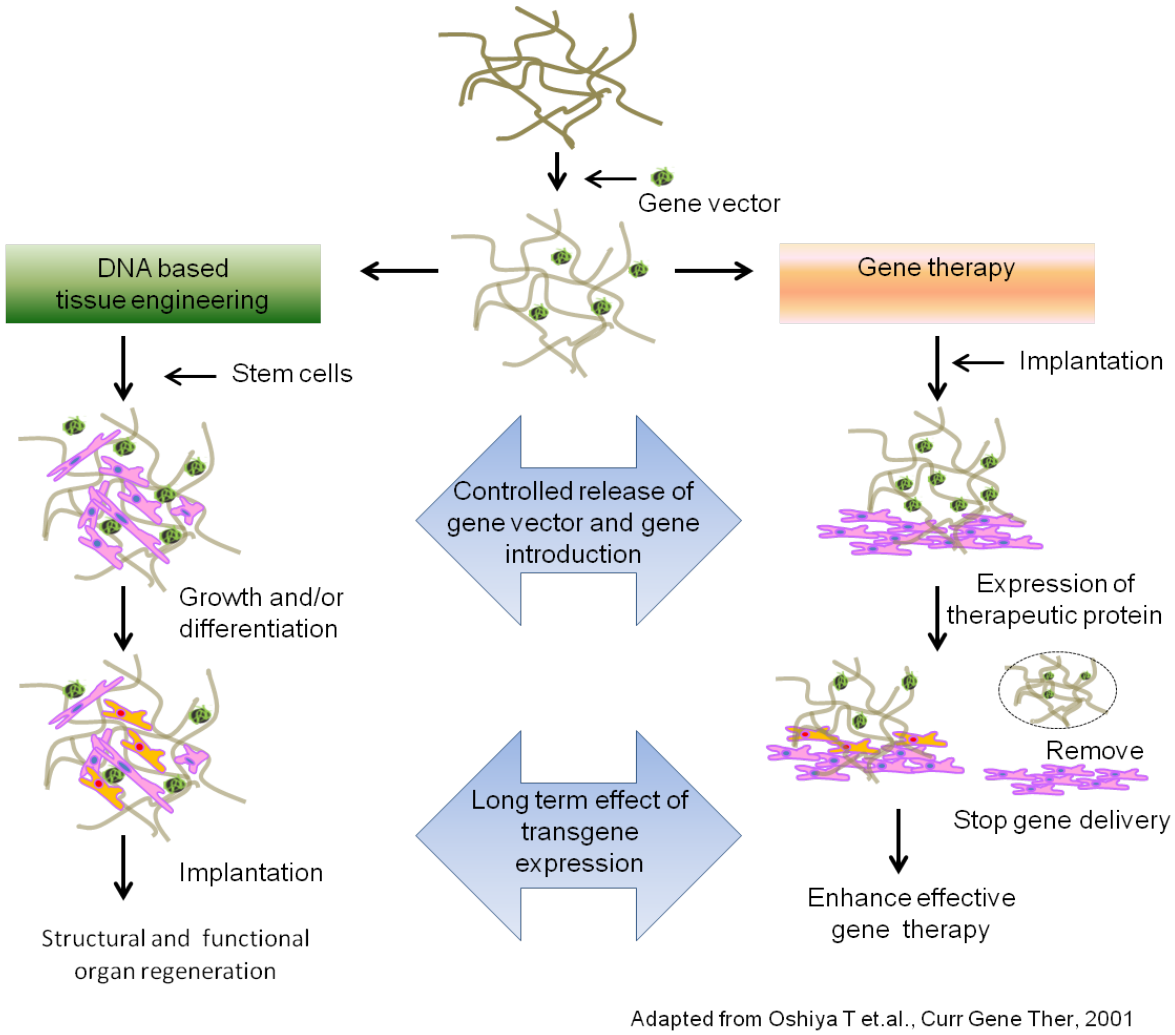

Adapted from Oshiya T et.al., Curr Gene Ther, 2001

Figure 1-1: Biomaterial based gene transfer has immense potential for tissue engineering and gene therapy. Stem cells can be embedded in biomaterial incorporating gene delivery systems in-vitro, or migrate within the implanted material. Controlled release of the gene vector takes place and the gene is introduced in the embedded cells. The transgene expression can promote growth or differentiation of the cells and the construct can then be implanted to restore structure and function of the organ. Furthermore, the transgene expression can also be of a therapeutic protein that can aid in enhancing effective gene therapy

Hence, the application of gene delivery has the potential of meeting the challenge to treat various diseases by gene therapy, and augment tissue regeneration by guiding cell differentiation and proliferation.

Gene delivery is basically of two types: Viral and non- viral gene delivery. Viral gene delivery is widely used and makes use of the natural ability of a virus to transfect mammalian cells.

However, non-viral gene delivery has several advantages over viral gene delivery. It is safer, not immunogenic, simple to use, facilitates large scale production, and can carry larger genetic load. Even so, *the use of non-viral gene delivery is mainly limited by low efficiency and limited targeting.*

The process of introduction or uptake of genetic material into cells, specifically eukaryotic cells, using means other than viral infection is known as transfection. The delivery agent or carrier used to deliver genes to cells is known as a gene delivery vector. Most of the studies that have focused on increasing the efficiency of non-viral gene delivery have aimed at improving the delivery vector systems. However, the role of the cellular microenvironment in which the cell resides has not been studied in detail.

Cells alone do not constitute tissues. A substantial part of the tissue volume is the extracellular space. The extracellular space is largely filled by the extracellular matrix (ECM). In other words, the microenvironment of the cell is known as the extracellular matrix. It consists of physical signals and soluble signals. Physical signals involve various structural proteins like fibronectin, vitronectin, laminin, etc. which form the structure of the matrix. The soluble signals consist of growth factors and other agents that are entrapped or embedded in the matrix. Cells interact with the signals in the ECM via cell surface receptors. This leads to signaling cascades that direct cells towards proliferation (cell growth), migration (cell motility), differentiation (change in type of cell) and apoptosis (cell death).

We hypothesized that the interactions of the cell surface receptors with ECM proteins could affect signaling pathways that direct and influence gene transfer. Recent studies have shown that the cell microenvironment has the ability to influence gene transfer. The stiffness of the matrix [1], macro and nanotopography [2], different densities and nano-scale arrangements of the

integrin binding peptide RGD through which the cells are bound, [3] and ECM proteins constituting the matrix [4-7]. However, the precise role of the ECM in modulating non-viral gene transfer and the intracellular mechanisms by which it does so have not been fully elucidated. The understanding of the influence of the microenvironment in gene transfer to stem cells and the possible mechanisms involved would aid in developing more efficient non-viral gene delivery systems. Therefore, in this study we aimed to identify if changing the type cell-matrix interaction could modulate gene transfer to mMSCs and the mechanisms underlying any such effect.

1.2 Specific aims

The objective of this research was to understand the role of cell microenvironment in modulating non-viral gene transfer. We hypothesized that the composition of the extracellular matrix (ECM) environment modulates non-viral gene transfer to cells seeded in two and three dimensions and that the Rho family of small GTPases plays a role in the mechanism by which ECM modulates gene transfer in two and three dimensions. To test this hypothesis, the *first step* was to identify an optimum microenvironment to achieve efficient gene transfer to mouse mesenchymal stem cells (mMSCs) on 2-D surfaces. The *second step* involved understanding the underlying physical and molecular mechanisms involving internalization, proliferation, cell area and polyplex trafficking, endocytic pathways and cytoskeletal dynamics and RhoGTPases, by which the ECM proteins were likely to modulate gene transfer. The *last step* was to compare the mechanism of non-viral gene transfer to mMSCs plated in 2-D and 3-D in hyaluronic acid hydrogels functionalized with RGD adhesion peptide.

The following section describes the proposed specific aims, which guided the experimental research. Following each aim specific hypothesis will be described.

1.2.1 Specific Aim 1 (Chapter 4 and 5)

This aim screened the effect of different ECM proteins at varied densities and combinations, in non-viral gene transfer to mouse mesenchymal stem cells cultured on a two dimensional surface. This aim also examined the role of polyplex internalization, cell proliferation, integrin expression, cell area and intracellular trafficking in mediating efficient gene transfer, in response to a specific microenvironment.

> *Hypothesis 1:* The composition of the extracellular matrix (ECM) modulates non-viral gene transfer to cells seeded in two dimensions by influencing internalization and cell spreading.

1.2.2 Specific Aim 2 (Chapter 6)

This aim determined the role of different endocytic pathways and cytoskeletal dynamics in mediating non-viral gene transfer to cells cultured in two dimensions, with respect to a specific ECM protein.

> *Hypothesis 2:* The varied ECM proteins influence the efficiency of gene transfer by mediating differential endocytic pathways and cytoskeletal dynamics that subsequently modulate the process of gene transfer.

1.2.3 Specific Aim 3 (Chapter 7 and 8)

This aim investigated the role of the Rho family of small GTPases specifically RhoA, Rac and Cdc42 in modulation of non-viral gene transfer in cells seeded on fibronectin coated surfaces.

Hypothesis 3: the Rho family of small GTPases plays a role in the mechanism by which fibronectin modulates gene transfer in two dimensions

1.2.4 Specific Aim 4 (chapter 9 and 10)

This aim studied and compared the process of non-viral gene transfer in cells plated in two dimensions on tissue culture plastic and cells plated in three dimensions in hyaluronic acid hydrogels functionalized with adhesion peptide.

Hypothesis 4: The gene transfer mechanism is different in cells seeded in two and three dimensions because of different cell-matrix adhesions which result in different intracellular signaling cascades.

The accomplishment of the above mentioned aims provided an understanding of the cellular environment to obtain efficient gene transfer for the purpose of tissue regeneration and gene therapy. This would assist in making artificial extracellular matrix environment (aECM) which is able to incorporate complete biological cues that maintain cellular function while enhancing gene transfer to cells in-vitro and in-vivo.

1.3 Thesis outline

After this introductory chapter, *chapters 2 and 3* provide relevant background to the topic of the thesis. First in *chapter 2*, importance of mesenchymal stem cells (MSCs), gene delivery with an emphasis on linear polyethylenimine (LPEI) mediated non-viral gene delivery and endocytic pathways involved in the process of gene transfer has been reviewed. *Chapter 3* describes the role of the cellular microenvironment on gene transfer. This is followed by a brief overview

about the differences in cell behavior including proliferation, differentiation, gene expression, etc., when cells are cultured in a 2-D and 3-D microenvironment. The cell cytoskeleton and its components have been subsequently reviewed in *chapter 3*, followed by a review of RhoGTPases, which mediate the crosstalk between the cell microenvironment and cell cytoskeleton.

An overview of the experimental work presented in this thesis is illustrated in **Figure 1-2**.

In *chapters 4 and 5*, different ECM proteins at different densities and in different combinations have been screened to assess their effect on gene transfer. C I and Fn maximally inhibited and enhanced transgene expression, respectively. Subsequently, the reasoning behind the influence of ECM proteins on gene transfer was studied by analyzing cell area, polyplex internalization, cell proliferation and intracellular trafficking. After elucidating the role of cell area and intracellular trafficking in ECM modulated non-viral gene transfer, the role of different endocytic pathways and cytoskeletal dynamics on Fn and C I was analyzed in *chapter 6.* To further determine the mechanism related to intracellular signaling molecules that is involved in ECM modulated non-viral gene transfer, the role of RhoGTPases specifically RhoA, Rac and Cdc42 in gene transfer in 2-D was studied in *chapters 7and 8.* Chapter 3 gives the background on RhoGTPases.

After having analyzed and shown the influence of cell microenvironment on non-viral gene transfer in cells cultured on 2-D surfaces, chapter 9 examines the role of fibrin gels for 3-D culture of mMSCs and hMSCs. *Chapter 10* moves on to study the effect of dimensionality on gene transfer. The mechanisms directing gene transfer in 2-D that have been elucidated in chapters 6 and 7, namely endocytic pathways, cytoskeletal dynamics and RhoGTPases, were also studied in cells cultured in 3-D in HA hydrogels in *chapter 10.* The objective was to determine and compare the non-viral gene delivery mechanism employed by MSCs cultured in 2-D on

tissue culture plastic surfaces with MSCs cultured in 3-D in HA gels. Chapter 3 gives the background describing the differences and relevance of cell culture in 2-D and 3-D. Hyaluronic acid hydrogels functionalized with adhesion peptide (RGD) were used for 3-D culture of cells. Chapter 10 contains the conclusions and future directions for the research.

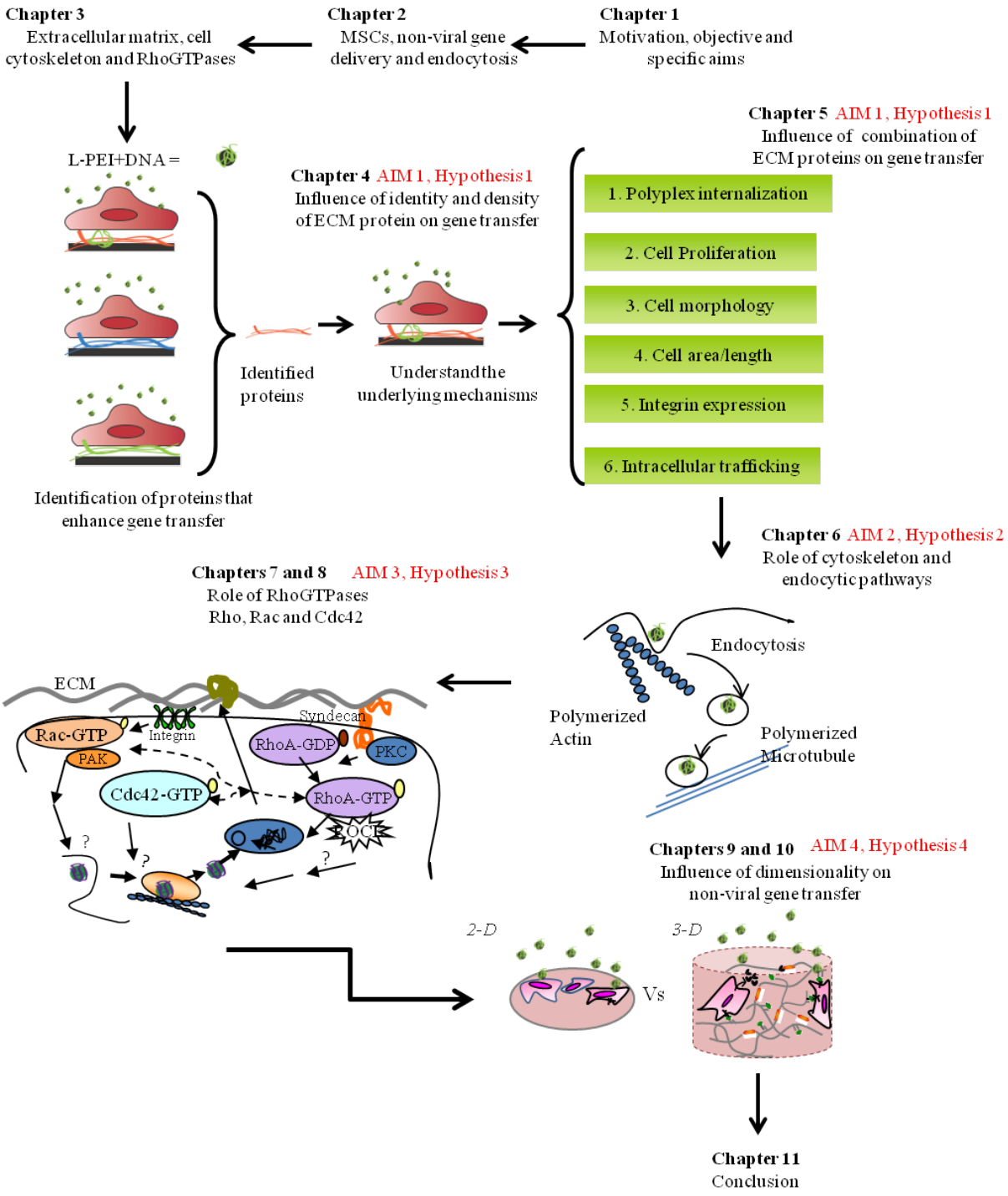

Figure 1-2: Thesis outline with an overview of the AIMs and Hypothesis covered in each chapter .

Chapter 2

Mesenchymal Stem Cells, Non-Viral Gene Delivery, and Endocytosis

2.1 Application of mesenchymal stem cells

MSCs are an attractive tool for cell therapy [8, 9] due to their ease of isolation, ability to expand in culture and the potential to differentiate into osteoblasts [10], chondrocytes [11], myocytes, adipocytes [12], and beta-pancreatic islets cells. They are applicable for autologous transplantation with no associated immunogenicity and possess local immunosuppressive properties [13]. Bone marrow derived mesenchymal stem cells (MSCs) can be genetically modified to serve as cell carriers for local and systemic delivery [14]. MSCs have the potential to migrate to tumor tissues and have therefore received attention for tumor therapy. Recent studies have shown that transduced NK4 in MSCs genetically modified using adenovirus vectors significantly increased the lifespan of mice having colon-26 cell line xenograft in lungs by inhibiting angiogenesis, and inducing apoptosis of tumor cells [15]. MSCs with forced expression of IFN-β using adenovirus have been shown to inhibit the growth of malignant cells in-vivo [16]. Other studies have shown that MSCs modified to transiently express VEGF after transplantation led to improvement of the heart function in myocardial infarction models [17],

whereas MSCs expressing BMPs (using adenoviral gene delivery) enhance bone formation in mice [18, 19]. However, viral gene delivery has limited applicability in clinical studies due to complications related to immunogenicity [13], while non-viral gene delivery is limited by its efficiency [20, 21].

The development of safer vector systems that efficiently transfect MSCs will assist in therapies where gene transfer can be targeted in in-vivo sites and expand the applicability of MSCs in regenerative medicine.

In this research study, we have investigated the influence of ECM proteins on non-viral gene delivery to MSCs, in an effort to enhance transfection to this cell type due to their broad applicability for regenerative studies.

2.2 Gene delivery

Gene delivery has widespread applications in gene therapy and regenerative medicine [22] which have the potential of impacting human life. Gene delivery for tissue regeneration has been applied in studies aiming to promote regeneration of blood vessel [23], bone [19, 24], nervous system [25], soft tissues [26, 27] and cartilage [28-30]. Gene delivery can be achieved with the use of modified viruses (viral delivery) or polymers (non-viral delivery) that encapsulate or condense plasmid DNA into particles which can transport the DNA inside the cell. Viral gene delivery makes use of the

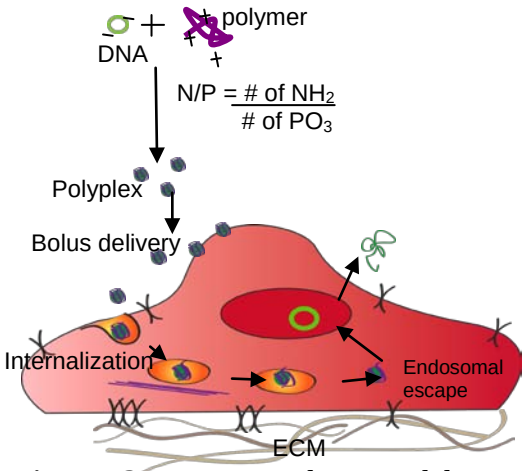

Figure 2-1. Non-viral gene delivery. Polyplexs are formed by complexation of DNA with a polycation, and are delivered as a bolus to cells. Polycation such as PEI shield the negative charge on DNA, thereby enhancing cellular uptake as well as aid in endosomal escape.

natural ability of viruses to efficiently transfect cells.

However, *non-viral gene delivery has the added advantages* of being: 1) safer, 2) non-immunogenic, 3) having the ability to carry larger loads, 4) overcoming the deleterious effects of insertions and mutations posed by viral gene delivery and 5) facilitate large scale production.

Though non-viral gene delivery remains to be a promising technology with wide applications in tissue regeneration and treating disease, it is limited with respect to its efficiency and targeting.

2.3 Non-viral gene delivery

Non-viral gene transfer provides a safe method to transfect cells for the purpose of clinical treatments. The introduction of foreign genetic material into cells using non-viral approaches can be achieved through a variety of methods, including physical and chemical methods such as:

I Physical Methods: 1) Naked DNA delivery by injection, 2) electroporation, 3) microinjection, 4) ultrasonic gene transfer and 5) hydrodynamic gene transfer;

II Chemical Method: 1) Particle mediated gene transfer, 2) calcium phosphate precipitation and 3) DEAE-dextran and polybrene.

Particle mediated gene transfer has been used as the method for non-viral gene delivery in the study reported in the following chapters.

2.3.1 Chemical method (particle mediated gene transfer)

It offers ease of manipulation, targeting and broad applicability [31] while not being as invasive as the physical methods. Further the in-vivo application of electroporation is significantly limited as its effective range to transfect is ~1 cm between the electrodes, it requires a surgical procedure

to place the electrodes deep into the internal organs and the high voltage applied can result in irreversible damage to the tissue [18].

On the other hand, chemical methods including calcium phosphate precipitation, DEAE-dextran and polybrene make use of inexpensive reagents, but require careful preparation of reagents ($CaPO_4$ solutions are pH sensitive), DEAE-dextran is limited to transient transfections, cell toxicity and reproducibility can be problematic.

While electroporation and microinjection can be used to inject the DNA in tissues and cells, gene transfer via other routes of administration, such as intratracheal and intravenous injection require the use of a delivery vector that stabilizes the DNA and protects it from nucleases. Hence, various viral and non-viral vectors have been developed. Cationic lipid and polymer based systems are most widely used among the synthetic vector systems.

2.3.1.a Cationic lipids based gene delivery systems. The use of cationic lipids in gene delivery was first introduced by Felgner et al in 1987 [32]. Cationic polymers were introduced in the same year by Wu and Wu, while Behr and coworkers introduced the second generation PEI in 1995 [33]. Typically DNA is complexed with a lipid or a polycation to form a lipoplex or a polyplex, respectively *(***Figure 2-1***)*, and targeted to the specific cell type. Furthermore, endocytosis has been demonstrated to be the main mechanism for the cellular uptake of non-viral gene delivery systems [34, 35]. Though positively charged lipoplexes enhance gene expression due to ionic interactions with the negative cell membrane and facilitate the endosomal escape, this charge also makes them susceptible to interaction with the negative constituents in the circulation after in-vivo administration, thereby limiting their application via systemic delivery.

2.3.1.b Cationic polymer based gene delivery systems. Cationic polymers condense the DNA more efficiently resulting in smaller DNA condensed particles, as compared to cationic lipids. The size of the particles ranges between a few hundred nanometers to micrometers in the absence and presence of salt, respectively [36]. Previous studies [37] have shown that complexing with a polycation not only protects DNA from degradation by nucleases, but also helps in its uptake.

2.4 Polyethylenimine (PEI) -DNA complexes (polyplexes)

PEI based Polyplexes have been widely used as it has the ability to cause endosomal escape. A 'proton sponge hypothesis' has been proposed to explain this ability [33] and has been confirmed by recent studies [38]. This hypothesis suggests that PEI becomes more protonated at low pH as in endosomes. This protonation triggers an influx of Cl^- ions with protons leading to water influx which causes the swelling and rupturing of the endosomes. In addition, linear PEI-DNA complexes **(Figure 2-2)** have been shown to have improved cell viability, promote nuclear localization, and increase the transfection efficiency as compared to branched PEI-DNA complexes [39, 40].

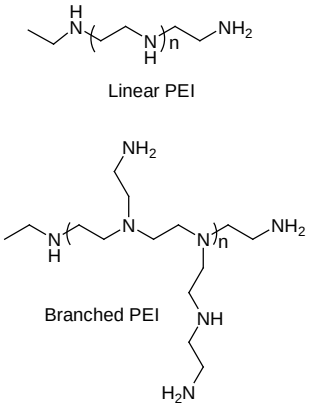

Figure 2-2: Structure of linear and branched PEI

The investigation of effective ways to deliver genes using a non-viral approach has focused on (1) the vector used to condense DNA into a nanoparticle, (2) the sustained release of DNA or DNA nanoparticles from scaffolds [27], (3) the design of the plasmid DNA used [41], and more recently, (4) the engineering of the cell and the cellular microenvironment to enhance the process of gene transfer [6, 42]. Most of the effort has been focused on (1), the design of more

sophisticated condensing agents for DNA that can more efficiently target desired cells and achieve enhanced internalization, intracellular trafficking and nuclear entry [31]. Efficiency of the plasmid expression can be significantly improved by optimizing promoter, enhancer, introns, terminator sequences and codon usage, as well as episomal vectors have been developed to increase the duration of gene expression [20].

Among all the condensing agents, cationic polymers, such as poly(ethylenimine) (PEI), are widely utilized for non-viral gene delivery because they are able to condense DNA through electrostatic interactions between the positively charged amines in the cationic polymer and the negatively charged phosphates on the DNA. The condensation of DNA with PEI forms particles (polyplexes) in the range of 50 to 200 nm in diameter [43]. DNA/PEI polyplexes enter the cell through endocytosis and are believed to be able to escape the endosome through endosomal buffering (the proton sponge effect, [44, 45]). Apart from DNA condensation, the amines in PEI have been heavily modified with ligands, peptides, polymers to enhance targeting [46], endosomal escape [47], nuclear localization [47, 48] and stability [49]. After each iteration a new condensing agent for DNA is realized and the field gets closer to an efficient vector for non-viral gene delivery. However, other aspects of the non-viral gene delivery process such as the role of the cellular microenvironment and the mechanistic pathways involved within the cell should be considered to arrive at an optimal solution for efficient and targeted gene transfer.

The role of the microenvironment surrounding the cell in gene transfer has not been investigated in detail. In this study, it was aimed to understand the role of cellular microenvironment in non-viral gene delivery by employing LPEI-DNA polyplexes as vector systems to deliver genes to mouse bone marrow mesenchymal stem cells (mMSCs).

2.4.1 In-vitro PEI mediated non-viral gene delivery : Pros and cons

One of the drawbacks of non-viral gene delivery vectors is the toxicity associated with large dosage. The increase in cell toxicity with an increase in the N/P ratio (more incorporation of polymer) was seen in the in-vitro studies conducted [50, 51]. Moreover non-viral vectors have a relatively short duration of gene expression and little is understood about the fate of the plasmid DNA after it reaches the cell nucleus. Free PEI is toxic to cells but when bound to DNA, its detrimental effects are significantly reduced. Due to the fusogenic effects of PEI, one possible reason for toxicity that has been proposed is that PEI will permeabilize the cell membrane [52]. However, studies showing the lysosomal disruption by PEI have not been conducted mostly on mammalian cells [53, 54]. Another study showing lysosomal degradation by PEI was conducted at concentration above 0.001 M_{amine} on rat hepatocytes and not on lower concentration of 0.0002 M_{amine}, which is more representative of the concentration used to transfect cells [55]. The data from other similar studies collectively suggests that low concentrations of PEI will not harm plasma membranes [52, 56, 57]. In a study conducted on three murine pulmonary target cell lines, it was observed that low molecular weight PEI resulted in cytotoxicity only at high doses while a cytokine response was observed at low dosage of PEI. Consequently, it was concluded that low molecular weight PEI is powerful tool for respiratory tissue with reduced cytotoxicity and minor proinflammatory potency [46].

2.4.2 In-vivo PEI mediated non-viral gene delivery : Pros and cons

On the other hand, studies have shown that the systemic delivery of DNA or siRNA mediated by LPEI has no associated inflammatory response in-vivo in mice [58]. Furthermore, PEI has been employed as the gene delivery system for many in-vivo and clinical studies. L-PEI has been

used to deliver genes in-vivo into a wide range of organs, such as lung [46, 59], brain [60], pancréas [21], retina [61], as well as tumor [62] in mice and rat models. Clinical trials using linear PEI and a mannosylated derivative as gene delivery systems are underway for bladder cancer [58] and human immunodeficiency virus (HIV) therapy [63] respectively. Though these studies demonstrate the applicability of non-viral gene delivery mediated via PEI for the purpose of gene therapy, no long term studies on the cytotoxicity of PEI and possible side effects has been reported. PEI cannot therefore be considered completely harmless and further in-vivo and long term studies need to be conducted.

2.5 Endocytosis pathways for non-viral gene delivery

The process of uptake of macromolecules and solute by the cell, in vesicles derived by the invagination and pinching off of the membrane is known as 'endocytosis'. Endocytosis can be broadly classified into two types: 1) phagocytosis and 2) pinocytosis.

Phagocytosis is the uptake of large particles by specialized cells. *Pinocytosis* is the uptake of fluid and solutes which occurs in all cells. The terms 'endocytosis' and 'pinocytosis' are mostly used as synonyms, when referring to internalization in cells in general.

Endocytosis is the main mechanism of uptake of non-viral gene delivery systems [34, 35].

There are three main types of endocytic pathways: 1) clathrin mediated endocytosis, 2) caveolae mediated endocytosis and 3) macropinocytosis .

In all three endocytic pathways the internalization step begins with the invagination of plasma membrane and the conversion of this membrane into a closed vesicle called an endosome. Each of the pathways has its own set of molecules that control internalization. These molecules

assemble at the cell surface and physically deform the membrane into the shape of a vesicle. The vesicle, the endosome, then detaches and migrates to other locations within the cell.

In clathrin mediated endocytosis and macropinocytosis, the endosomes often fuse with lysosomes that contain many different hydrolytic enzymes.

Contrarily, in caveolae mediated endocytosis, small particles (50-60 nm) do not require further processing and are delivered directly to the cytoplasm

2.5.1 Clathrin-mediated endocytosis

It is specialized for receptor-mediated endocytosis using clathrin-coated pits (CCPs). This pit is recognized by the particles by the presence of a polygonal lattice on the cytoplasmic surface of the membrane. The CCP then invaginates and is pinched off from the plasma membrane by dynamin to form intracellular clathrin coated vesicles (CCVs). It is an energy-dependent process that involves the assembly of the clathrin lattice underlying the plasma membrane. This is necessary for the detachment of the invaginations as vesicles. The lattice shapes the plasma membrane into a coated vesicle (CCVs) that immediately uncoats and fuses with endosomes. The endosome functions as a switching area, which directs membrane and content particles to specific locations within the cell.

2.5.2 Caveolae-mediated endocytosis

It uses membrane proteins that are anchored by lipid. The lipid anchor causes the attached proteins to migrate in the plane of the membrane and cluster in a membrane specialization called a caveolae. Clustering ensures that any ligand bound to these receptors will be concentrated in this location. When caveolae close, they create a tiny compartment of uniform size that is sealed

off from the extracellular space. When the ligand dissociates from its receptor, it reaches such a high concentration that it naturally flows through water-filled membrane channels into the cell. The closed caveolar compartment appears to be a unique space for the cell. It is transient, does not merge with other organelles, and can selectively concentrate extracellular molecules or ions and deliver them to the cytoplasm.

2.5.3 Macropinocytosis

It refers to the formation of large endocytic vesicles of irregular shape and size, as a consequence of actin-driven invagination of the plasma membrane. It involves the cell membrane ruffling induced by growth factors or other signals. Macropinocytosis is induced by formation of a linear band of outward directed actin polymerization near the plasma membrane which lengthens into a planar extension of the cell surface is known as a 'ruffle' (membrane protrusions). Subsequently these protrusions collapse onto and fuse with the plasma membrane to generate large endocytic vesicles known as 'macropinosomes'. Macropinosomes have no coat, do not concentrate receptors and vary in size up to 5 µm. Macropinosomes are an efficient route for nonselective endocytosis of solute macromolecules, as they are relatively large in size.

An overview of the endocytic pathways with their advantages, disadvantages, and size of internalized molecule, has been represented in ***table 2-1***.

ENDOCYTIC PATHWAYS

Pinocytosis **Phagocytosis**

Various Pinocytotic Pathways

Endocytic pathway	Disadvantages	Advantages	Size of vesicle
Clathrin mediated endocytosis	▪ Leads to lysomal degradation ▪ Poor availability of gene near target site	▪ In all cells ▪ Targeted using ligands like transferrin ▪ Targeting increases internalization	100-150 nm
Caveolae mediated endocytosis	▪ Slowly internalized, small in size ▪ Unlikely to contribute in most cells	▪ Avoids lysomal degradation ▪ Gives significant internalization	50-60 nm
Macropinocytosis	• Increased uptake of macromolecules • Avoidance of lysomal degradation • Ease of escape from macropinosomes because of leaky nature	• Pathway is still under investigation	5 μm
Receptor mediated endocytosis	Promising approach to deliver DNA efficiently in defined populations	Exploring and targeting new receptors internalized by clathrin independent endocytosis	

Table 2-1: Overview of the endocytic pathways with their advantages, disadvantages, and size of internalized molecule.

Chapter 3

Extracellular Matrix, Cell Cytoskeleton, and RhoGTPases

3.1 Cellular Microenvironment

The cellular microenvironment is also known as the extracellular matrix (ECM). It comprises physical and soluble signals. Cells interact with different signals using cell surface receptor leading to signaling cascades within the cell, that guide cell fate and behavior.

3.1.1 ECM and cell fate

The cellular microenvironment plays a pivotal role in deciding the cell fate [64] by interacting with cellular receptors which result in activation of different signal transduction pathways that lead to cell proliferation, migration, differentiation and apoptosis [64, 65]. ECM made by bone marrow cells has been shown to promote replication of mesenchymal progenitors and retention of their multipotentiality as compared to tissue culture plastic [10]. Collagen II ECM significantly influences the chondrogenic differentiation of MSCs [11] while denatured collagen I has been shown to significantly maintain the adipogenic differentiation potential of MSCs [12].

Further studies have shown that the differences in the material properties of extracellular matrix are able to guide cell adhesion, migration [66, 67] and proliferation [68].

3.1.2 ECM and gene transfer

The cellular microenvironment plays a key role in directing cell adhesion, migration, proliferation and differentiation. Recent studies have implicated the role of ECM in gene transfer. The stiffness of the matrix where the cells are bound affects their ability to internalize and process DNA with stiffer substrates achieving higher polyplex internalization and overall gene transfer efficiency [1]. Further, macro and nanotopography affects gene delivery by modulating endocytic pathways. Highest transfection efficiency in hMSCs was observed on micro and nanopillars using FITC-dextran, and on nanopillars using GFP coded plasmid transfection with lipofectamine [2]. The integrins through which the cells are bound and the ligand density have also been found to modulate the process of gene transfer. Cells plated on surfaces with different densities and nano-scale arrangements of the integrin binding peptide RGD, demonstrated that surfaces with the highest density of RGD and shortest distance between RGDs tested enhanced transgene expression [3]. Cationic lipid-mediated gene transfer to rat smooth muscle cells is enhanced when the cells are plated on surfaces that promote $\alpha_v ß_3$ binding, with antibodies against $\alpha_v ß_3$ and $ß_3$ decreasing the amount of gene transfer [69]. Fibronectin (Fn) has been found to enhance non-viral gene transfer to mesenchymal stem cells [4, 5]. The recent studies that compared gene transfer on different structural ECM proteins showed that gene transfer to NIH/3T3 fibroblast was enhanced when the cells were plated on Fn, as compared to cells plated on collagen I (C I), laminin and BSA [6] and that gene transfer to PC12 cells was enhanced on collagen IV (C IV) compared to C I, laminin, Fn, and polylysine [7]. The effect of

ECM on transgene expression in NIH3T3 cells [6] and PC12 [42] was correlated to nuclear area and ability to influence endocytosis pathways, respectively.

Though this indicates that the constituents of the cellular microenvironment as well as their properties may influence gene transfer, the nature of the role of extracellular matrix (ECM) and its implications in guiding gene transfer are not fully understood. *The understanding of the influence of the microenvironment in gene transfer and the possible mechanisms involved would aid in developing more efficient non-viral gene delivery therapies.*

3.1.3 2-D versus 3-D in-vitro microenvironment

The cellular function and behavior on 2-D surfaces does not correlate with cellular responses in 3-D matrices. Cells in tissues are in a three-dimensional environment having characteristic biophysical and biomechanical signals. The biophysical signals embedded in three dimensional matrix influence cell functions like migration, adhesion, proliferation and gene expression [70-73]. The ligands presented by the matrix bring about adhesion clustering, thereby altering cell behavior. The integrin (integrins alpha1, beta1 and beta3) and ECM protein (collagen Type I and III, and tropoelastin) expression in vascular smooth muscle cells has been shown to be upregulated in 3-D matrices of fibrin, collagen as well as in composite matrices having 1:1 ratio of fibrin: collagen; as compared to in 2-D surfaces coated with the respective proteins [74]. The integrin expression guides the cellular response to particular ECM components and directs cell function. Certain cellular processes of differentiation and morphogenesis for tissue engineering [75, 76] have been shown to occur preferentially in 3-D instead of 2-D. MSCs significantly up regulate the expression of smooth muscle specific proteins such as αSMA and myosin when cultured in 3-D PEG hydrogels as compared to on a tissue culture plastic surface [77]. It is likely

that scaffolds mimicking the natural milieu may play a role in modulating gene transfer to cells while having the ability to enhance cell growth and differentiation processes in 3-D. Data from the preliminary studies indicates that the cellular microenvironment is able to modulate gene expression and internalization in 2-D. However, 2-D studies are not indicative of cellular responses in 3-D as 2-D cannot emulate a 3-D environment. The study of the effect of cell response to ECM proteins on gene transfer in 3-D would help decipher the differences in cellular gene transfer in 2-D and 3-D, and to be able to demonstrate our hypothesis in 3-D and in-vivo.

3.2 Hydrogels as scaffolds for 3-Dimensional cell culture

Scaffolds with incorporated biological cues mediate tissue formation by guiding the adhesion, proliferation and differentiation of the transplanted cells or the native infiltrating cells at the site of tissue regeneration. The 3-D scaffold is typically biocompatible, while degrading and resorbing at a rate corresponding to tissue growth, thereby defining the shape and function of the assimilated cell structure [78]. Both, synthetic and natural materials have advantages as 3-D scaffolds over 2-D surfaces. While natural materials provide essential cues that mediate biocompatibility they usually lack the mechanical strength of the synthetic scaffold. There is a lot of interest in tissue like hydrogels as scaffolds since they embody tissue like flexibility while possessing viscoelastic properties, interstitial flow and diffusive transport characteristics similar to tissue.

In chapt ers 9 and 10 of this thesis, hyaluronic hydrogels functionalized with an adhesion peptide were used to culture mouse mesenchymal stem cells (mMSCs) in three dimensions.

3.3 Cell cytoskeleton

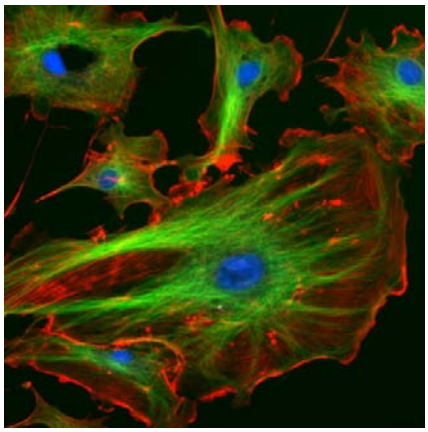

Figure 3-1: The eukaryotic cytoskeleton. Actin filaments are shown in red, microtubules in green, and the nuclei are in blue.
Source:*http://en.wikipedia.org/wiki/Cytoskeleton*

Eukaryotic cells contain three main kinds of cytoskeletal filaments, which are: 1) microfilaments, 2) intermediate filaments and 3) microtubules. The cytoskeleton provides the cell with structure and shape.

Microfilaments (actin filaments): These are the thinnest filaments of the cytoskeleton. They are composed of linear polymers of actin subunits, and generate force by elongation at one end of the filament coupled with shrinkage at the other, causing net movement of the intervening strand.

The average size of these filaments is 10 nanometers in diameter and are more stable (strongly bound) than actin filaments, and heterogeneous constituents of the cytoskeleton. Like actin filaments, they function in the maintenance of cell-shape by bearing tension Intermediate filaments organize the internal tridimensional structure of the cell, organelles and serving as structural components of the nuclear lamina.. They also participate in some cell-cell and cell-matrix junctions.

Microtubules: They are hollow cylinders about 23 nm in diameter, most commonly comprising 13 protofilaments which, in turn, are polymers of alpha and beta tubulin. They have a very dynamic behavior, binding GTP for polymerization. They are commonly organized by the centrosome.

In short, actin filaments are responsible for resisting tension and maintaining cellular shape, forming cytoplasmic protuberances and participating in some cell-to-cell or cell-to-matrix

junctions while the microtubules play a role in intracellular transport and mitotic spindle formation. Recent studies have demonstrated the role of actin and microtubules in endocytosis and gene transfer [79, 80] (**Figure 3-2**).

3.3.1 Role of microtubules in endocytosis and gene transfer.

Nocodazole, a microtubule depolymerizing agent, has been shown to increase the transfection efficiency of the lipid–DNA complexes by enhancing perinuclear accumulation [81] in CV-1 cells as well as increase the transfection efficiency in 293-T7 cells [82]. The transfection efficiency of lipid-bilayer coated gold nanoparticles was also increased prior to nocodazole treatment and this was attributed to interrupted transportation of complexes to lysosomes [83], using TEM in HEK 293T cells. Another study showed that nocodazole treatment inhibited the transgene expression in cystic fibrosis airway epithelial cells [84]. It has been shown that internalization via caveolae requires microtubules in contrast to internalization via clathrin while both pathways converge at the late endosome/lysosome stage in CHO cells [85]. *This indicates that though microtubules are involved in gene transfer, the role played is dependent on the cell type, vector system and route of internalization; since microtubule inhibition resulted in inhibition of DNA transport to nucleus in caveolae mediate internalization in CHO cells as well as can increase the DNA transport by assisting endosomal escape due to interruption of the endosome to lysosome routing in HEK 293T cells.*

3.3.2 Role of actin in endocytosis and gene transfer.

The inhibition of actin polymerization via cytochalasin treatment has also been shown to decrease the transgene expression in 293-T7 cells, in cystic fibrosis airway epithelial cells and

fibroblasts [79, 82, 84]. Actin affects the vector uptake but not the cellular localization, while microtubules affect cellular localization [84]. Another study showed that interruption of actin microfilament polymerization processes led to reduced internalization in 293T cells (60%), but had no significant effect on COS7 (5%) or CHO cells (7%), indicating that the role of actin in uptake is cell dependent [86]. Though the role of the cytoskeleton in gene transfer has been implicated, its correlation with the cellular microenvironment has not been investigated before.

Since the cell cytoskeleton responds to cellular interactions with the ECM, regulating cell morphology, spreading and migration, we hypothesized (AIM2) that it is likely that the influence exerted by the ECM on gene transfer is orchestrated via the cell cytoskeletal dynamics. The role of cytoskeleton in gene transfer has been studied in chapter 6.

3.4 RhoGTPases

3.4.1 RhoGTPases modulate cell behavior, morphology and migration [87].

Rho proteins alternate between an active GTP-bound state and an inactive GDP bound state. In the active conformation, GTPases interact with and stimulate the activity of effectors which participate in signaling cascades that coordinate various cell processes such as migration, proliferation and gene expression. The cell migration is regulated in many ways by the RhoGTPases such as by affecting actin and microtubule dynamics, cell-cell and cell-extracellular matrix adhesion and intracellular trafficking of proteins required for cell motility [88]. Studies have shown that Cdc42 mediates cell polarity and filipodia, Rac mediates protrusion of lamellipodia, and Rho maintains cell adhesion during migration. Furthermore, *there exists a cross talk between the ECM and the RhoGTPases* [89]. The Rho GTPases are localized at

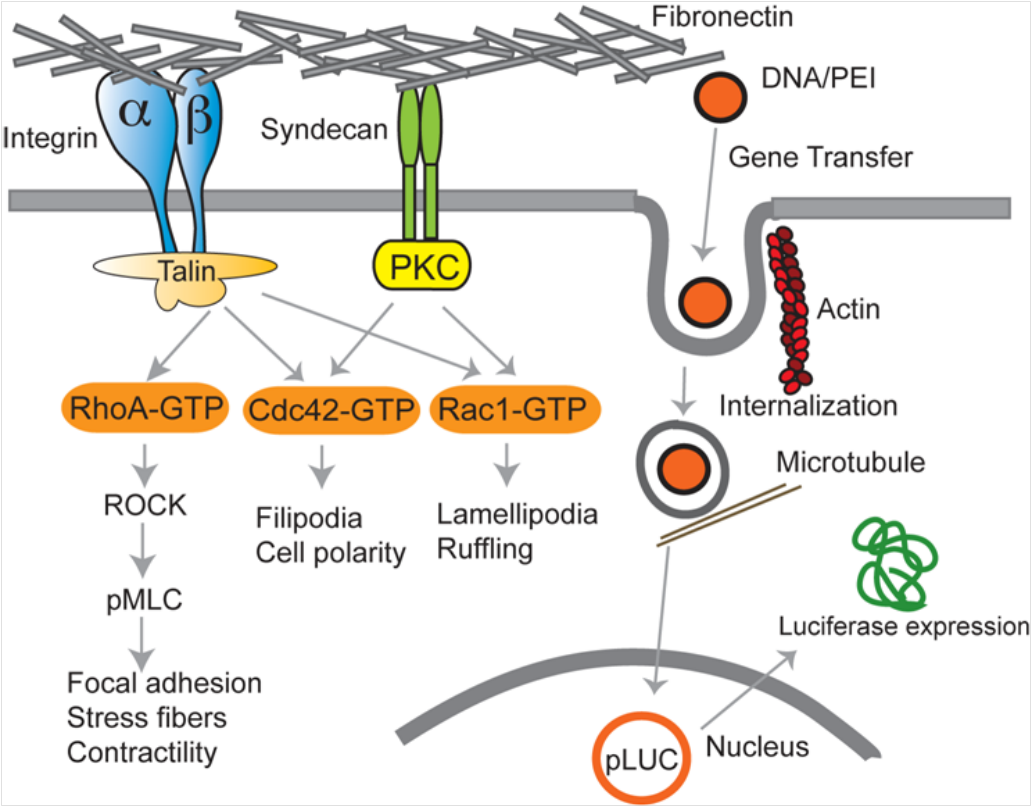

Figure 3-2: Mediation of non-viral gene delivery by the cell and role of RhoGTPases. The interaction of Fn with cell surface receptors namely integrins and syndecans regulates the activity of RhoGTPAases. Active Rho interacts with downstream effector ROCK to phosphorylate MLC mediating contractility by influencing focal adhesion complex and stress fiber formation. On the other hand active Rac and Cdc42 mediate cell motility and endocytosis by influencing ruffling as well as lamellipodia and filipodia extensions.

membranes and become activated upon stimulation of cell surface receptors. Consequently, they act as a focal point for adhesion signaling [89]. It has been shown that large focal adhesion assembly seems to be dependent of RhoA, the adhesion induced membrane ruffling seems to be dependent on Cdc42 and Rac, whereas all three seem to regulate cell spreading [90] (**Figure 3-2**). The assembly of integrin complexes has been shown to require both, the ECM and the intracellular Rac and RhoGTPases for fibroblast cells plated on fibronectin coated surfaces [91].

Besides mediating the focal adhesions, cell motility and cytoskeleton dynamics, RhoGTPases also influence cell proliferation [92] and gene transcription via integrin-dependent intracellular signaling pathway [93]. The various RhoGTPases have further been shown to interact among themselves. It has been shown that in 3T3 fibroblasts, Cdc42 activates Rac, which in turn activates Rho [94]. *It is likely that the interplay between ECM and integrins [95] is communicated via the RhoGTPases and the resultant signaling cascades affecting cytoskeletal dynamics, migration, proliferation and transcription factors are also able to regulate the gene transfer in cells.*

3.4.2 Effectors of RhoGTPases

Many proteins act as the downstream effectors of small RhoGTPases and mediate their effects on cell morphology, focal adhesion and migration. RhoGTPase binds to kinases [96] such as serine/threonine kinases, Rho kinase, ROK and the related p160ROCK; and elevate their activity. Activated Rho-Kinase can phosphorylate myosin light chain (MLC), which enhances the binding to actin filaments and subsequently leads to formation of stress fibers. Phosphatidyl inositol 4-phosphate 5-kinase (PIP5-kinase) and p140mDia also act as downstream Rho effectors that regulate actin polymerization [97, 98]. On the other hand, serine threonine kinase PAK1 is an effector for Cdc42 and Rac that has been shown to play a role in the motility of fibroblasts, while POR1 acts as a target of Rac that plays a role in Rac-mediated membrane ruffling. Furthermore, wiskott-alrich syndrome protein (WASP), related NWASP and Arp2/3 complex play a role in the Rac and Cdc42 mediated signaling involving lamellipodial protrusions and formation of filipodia.

3.4.3 Role of RhoGTPases in gene transfer

RhoGTPases have been primarily implicated as the controlling factors in guiding cell motility, morphology, contractility and proliferation [99]. Bacterial internalization [100, 101], adenovirus internalization [102] and recently receptor mediated internalization of transferrin [103] have been shown to be a resultant of host cell actin cytoskeleton manipulation at level of RhoGTPases. RhoGTPases regulate phagocytosis [104], endocytic trafficking [105] as well as mediate the various steps of vesicular trafficking [106]. However, the role of RhoGTPases in non-viral gene transfer has not been earlier investigated.

Fibronectin has been previously shown to enhance signaling through RhoGTPases [89, 107-109]. Initial activation of Rac and Cdc42 by fibronectin has been shown to mediate cell spreading in NIH/3T3 cells [108, 109]. *The study of the expression of active RhoGTPases particularly RhoA, Rac and Cdc42, and their role in gene transfer in cells plated on Fn (Chapter 7), provided important cues regarding the mechanisms that can modulate gene transfer while mediating the crosstalk between the cell and its microenvironment (Fn).*

Chapter 4

Effect of ECM Identity and Density on Non-Viral Gene Transfer.

4.1 Introduction

Genetically modified MSCs are an attractive tool for cell therapy [14] due to their ease of isolation, ability to expand in culture and the potential to differentiate into osteoblasts [10], chondrocytes [11], myocytes, adipocytes [12], and beta-pancreatic islet cells [110, 111]. They are applicable for autologous transplantation with no associated immunogenicity and possess local immunosuppressive properties [13]. However, efficient and safe delivery remains the major limitations for the use of gene therapy in tissue engineering and to genetically modify MSCs as cell therapeutics. Although viral delivery is generally more efficient than non-viral approaches, it has limitations due to its potential immunogenicity and insertion mutagenesis [112]. Because of the mentioned safety concerns, non-viral approach was investigated. Non-viral gene delivery has been discussed in detail in Chapter 2. In the research project reported in this thesis, linear has been employed as the non-viral gene delivery vector.

Most studies on gene delivery to mammalian cells have focused on improving the vector systems [113] to enhance efficiency and achieve targeting to specific cells types. As a result, many functionalized vector systems have been developed [114]. Although not as widely studied, the cellular microenvironment has been successfully engineered to enhance gene transfer to a variety of cell types [1-7, 69]. In chapter 3, the effect of cell microenvironment on non-viral gene delivery has been described. We hypothesized that the extracellular matrix (ECM) environment modulates non-viral gene transfer. By understanding the role of ECM in gene transfer
better delivery vectors and transfection protocols can be engineered.

Hence, to elucidate the role of the cellular microenvironment in mediating non-viral gene delivery to mMSCs we initiated the study by analyzing the influence of several ECM proteins on transgene expression and polyplex internalization. To understand the underlying mechanisms of the observed changes in transgene expression, cell proliferation, cell morphology, and cell integrin expression was analyzed. *Aims and hypothesis covered in this chapter are: Aim 1 and Hypothesis 1.*

4.2 Material and methods

4.2.1 Materials. pCMV-Gluc plasmid was purchased from New England BioLabs (Ipswich, MA) and expanded using an endotoxin free Giga Prep Kit from Qiagen following the manufacturer's protocol. Linear poly-(ethylenimine) (25 Kg/mol, PEI) was purchased from Polysciences (Warrington, PA). ECM proteins such as vitronectin were purchased from Invitrogen (Carlsbad, CA). Laminin and ECMg were purchased from Sigma Aldrich (St Louis, MO), fibronectin was purchased from Millipore (Billerica, MA), collagen IV was purchased from BD Bioscience (San Jose, CA) and collagen I was purchased from R&D Systems

(Minneapolis, MN). All other reagents were purchased from Fisher Scientific unless otherwise specified.

4.2.2 Cell culture. Mouse bone marrow cloned mesenchymal stem cells (D1, CRL12424) were purchased from ATCC (Manassas, VA, USA). Cells were maintained in Dulbecco's modified eagle's medium (Sigma-Aldrich) containing 10% bovine growth serum (BGS, Hyclone, Logan, Utah) and 1% penicillin/streptomycin antibiotics (Invitrogen, Grand Island, NY) and cultured at 37˚C and 5% CO_2.

4.2.3 Protein coating. Concentrations used for protein coatings were those recommended by manufactures' protocols; collagen I (R&D Biosystems, 5 μg/cm^2 or 50 μg/ml), fibronectin (Sigma Aldrich, 1-5 μg/cm^2 or 0.5-50 μg/ml), laminin (Sigma-Aldrich 1-2 μg/cm$^{2)}$, collagen IV BD biosciences at 1-5 μg/ cm^2, Vitronectin (Invitrogen 3 μg/ml) and ECMg (Sigma-Aldrich, 96-well 50-100 μl/well of stock solution at a concentration of 8-12 mg/ml for a 96 well plate). Two times and half this concentration was tested, leading to 3 conditions. In addition, 20 μg/ml was used as a standard concentration since this concentration overlapped with most of the suggested concentrations. For the experiments with combinations of proteins the concentration suggested by the manufacturer was used.

Stocks of vitronectin (0.5 mg/ml), laminin (0.89 mg/ml), fibronectin (1 mg/ml), collagen I (5 mg/ml), collagen IV (0.694 mg/ml in 0.05M HCl), BSA (1% in PBS) and ECMg (8.54 mg/ml) were made. The stock solutions of various proteins were further diluted in PBS to obtain the final densities and composition used for coating. Protein solution at specific initial densities was added in each well of a tissue culture plate and the plate was incubated over night at 4˚C in a

humid environment, followed by incubation at 37°C for 2 hrs. The solution was removed and wells were washed twice with PBS to remove unbound proteins. Wells were further incubated with BSA (1% in PBS) for at least 30 minutes at 37˚C followed by two washes with PBS.

4.2.4 Imaging of coated proteins. The homogeneity of the immobilized proteins was qualitatively observed using the NanoOrange Protein Quantitation Kit (Invitrogen, Carlsbad, CA) following the manufacturer's instructions with minor modifications. The NanoOrange solution was added to ECM coated plates (96 well or 48 well tissue culture plates) coated prior to BSA blocking. The plate was then incubated at 95°C for 10 minutes and at room temperature for 20 minutes before reading the plate using a typhoon scanner. The scan was visualized for protein homogeneity and was quantified using gray scale intensity readings.

4.2.5 Transfection. mMSCs were seeded on 48 well plates that were previously modified with ECM proteins at cell densities of 20,000 cells/well. The cells were allowed to attach and incubated on the surfaces for 16 hours before DNA/PEI polyplexes were added. DNA/PEI polyplexes were formed by mixing equal volumes of plasmid DNA with 25 kDa-Linear PEI**.** For every 1 µg of DNA, 1.65 µg of PEI was added to the DNA solution to get N/P of 12, vortexed for 15 seconds and incubated at room temperature for 15 minutes. Salt was added directly to the wells post addition of transfection solution to get the final concentration of 150 mM NaCl. Polyplexes were added directly to the medium of the plated cells at a final DNA concentration of 0.5 µg for 48 well plates. Transfection was quantified at 48-hours post transfection using the Gaussia Luciferase Assay System following the manufacturer's instructions. Subsequently, cells were lysed and the total amount of protein in samples was analyzed using Peirce BCA assay kit

as per manufacturer's protocol. Experiments were carried out in triplicates and results were expressed as relative light units (RLU) per mg of cell protein.

4.2.6 Cell proliferation. The Cell Titer 96®Aqueous One Solution Cell Proliferation Assay (Promega) was performed to determine the cytotoxicity and proliferation of the cells in different ECM proteins. The Aqueous One Solution (20 µl) was added in each well to be assayed and incubated for 2 hours. SDS (25 µl of a 10% solution) was added to each well after the incubation. The fluorescence was measured using a plate reader at 490.

4.2.7 Cell morphology. mMSCs cells (20,000 cells/well) were seeded on 8-well coverslip bottom plates pre-coated with ECM proteins. The cells were allowed to incubate for 16 hours before being fixed and stained for actin and nuclear DNA using Alexa488-phalloidin and Hoechst dye following the manufacturer's instructions and standard staining protocols. Briefly, after two PBS washes the cells were fixed with 4% paraformaldehyde (PFA) for 15 minutes at room temperature and the cell membrane was weakened with 0.1% tritonX100 in PBS for 3 minutes. Hoechst dye and Alexa488-phalloidin were then added and left in the dark for 60 minutes at room temperature followed by two washes with 0.05% tween-20. The samples were imaged using a Zeiss Axio Observer inverted fluorescence microscope.

4.2.8 Internalization of polyplexes. Plasmid DNA and the fluorescent DNA-intercalator YOYO-1 were mixed at a ratio of 1 YOYO-1 molecule per 50 base pairs and were allowed to complex for 60 minutes at room temperature. YOYO-1 labeled DNA was then used to prepare PEI/DNA complexes at an N/P of 12 (as mentioned above) and bolus transfection was

performed. Two hours after exposure to the polyplexes, cells were washed with PBS, trypsinized with 50 µl of 0.25% trypsin-EDTA and finally suspended in 350 µl of 0.04% tryphan blue in 1% BGS in PBS. Fluorescent cells were detected by flow cytometry with a FACScan X and data was analyzed with CELLQuest (Beckton Dickinson). Experiments were performed in triplicates analyzing 7000 total events per sample.

4.2.9 Analyzing integrin expression. Cells were cultured in T75 flasks till 80% confluency. Cells were removed via standard trypsin/EDTA incubation. Subsequently, cells were centrifuged and re-suspended in PBS with 1% BSA solution for 10 minutes, to prevent nonspecific binding. For each sample 50,000 cells were incubated in 10 µg/ml PE or FITC conjugated antibody solution for 30 minutes on ice, centrifuged and re-suspended in 1% Paraformaldehyde (PFA). Following which the percent of cells expressing a specific α or β subunit and the level of expression was assessed using flow cytometry with FACScan X and data analysis with Flowjo. Experiments were performed in triplicates analyzing 3000 total events per sample. For all samples, gating was done such that the negative control had 5% positive events (i.e. 5% of the negative control had no antibody stain).

4.2.10 Statistics. All statistical analysis were performed using the computer program Instat (GraphPad, San Diego, CA). Experiments were statistically analyzed using the Tukey test, which compares all pairs of columns, using a 95% confidence interval or using the Dunnett test which compares all columns versus a control column.

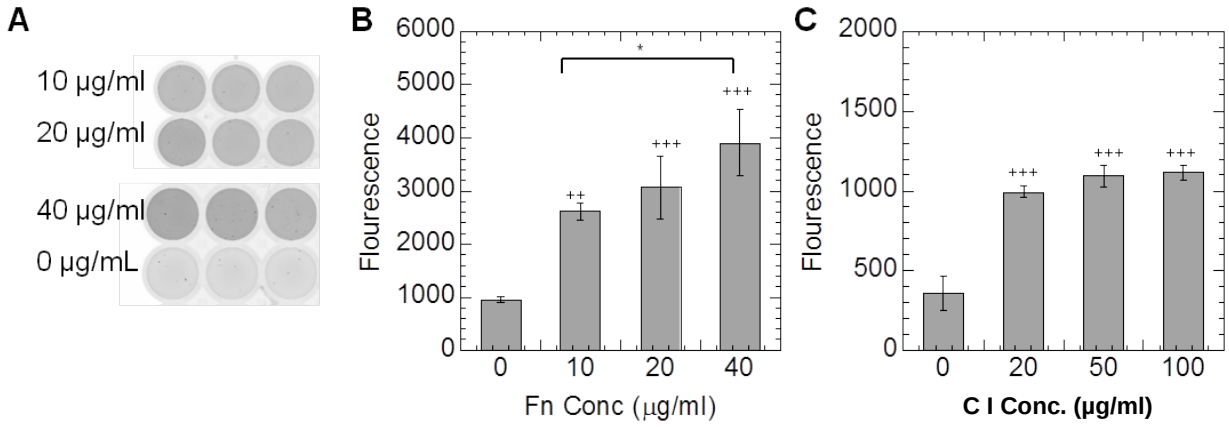

Figure 4-1: NanoOrange staining of immobilized proteins. Picture of wells coated with Fn at an initial density of 0, 10, 20, and 40 µg/ml respectively (**A**). Mean NanoOrange fluorescence of wells coated with Fn (**B**) and C I (**C**) respectively using a typhoon scanner. Statistical analysis was done using the Tukey-Kramer multiple comparison test. The symbol * represents a significant change in fluorescence between the two surfaces at a level of $p < 0.05$, while + and +++ represents a significant change with respect to an uncoated surface at a level of $p<0.05$ and $p < 0.001$, respectively.

4.3 Results and discussion

4.3.1 Imaging of coated proteins

To investigate how extracellular matrix proteins that bind through different integrin receptors affect non-viral gene transfer to MSCs, the role of ECM proteins on efficiency of non-viral gene transfer with DNA/PEI to mMSCs was studied by plating mMSCs on surfaces that had been pre-coated with ECM proteins and then performing a traditional bolus transfection. Protein coatings are reported as the solution concentration used to coat the surface. The solution concentrations used are those suggested by the manufacturer for the protein type. For C I higher coating densities are recommended (50 to 100 µg/ml) than for Fn (10 to 40 µg/ml). Increasing protein coating with increasing protein solution concentration was confirmed through staining the protein with a fluorescence protein quantification assay (**Figure 4-1**). The protein-modified surfaces were imaged through a typhoon scanner. The protein coating was found to be uniform

(**Figure 4-1A**) with the fluorescence intensity increasing with increasing protein solution concentration (**Figure 4-1B, C**).

4.3.2 Effect of ECM protein identity and density on transgene expression and polyplex internalization

ECM proteins namely Vt, C I, C IV, Lm, and Fn were chosen for the study because they simulate various physical signals in the cellular microenvironment by interacting with cells through different integrin receptors including $\alpha_v ß_5$[115, 116], $\alpha_1 ß_1/\alpha_2 ß_1$[117], $\alpha_1 ß_1$[117], $\alpha_3 ß_1/\alpha_6 ß_1$[118], and $\alpha_5 ß_1$[119], respectively. In addition, ECMg (analogous to Matrigel) was reported by Sigma to be mainly composed of Lm, C IV, heparin sulfate proteoglycan and entactin, and it provided a more complex microenvironment to investigate.

Overall transgene expression was enhanced with statistical significance (at least $p < 0.05$) when mMSCs were plated on C IV, Fn and ECMg compared to uncoated surfaces, leading to 6.1-, 14.6-, and 7-fold increase in gene expression respectively (**Figure 4-2A**). On the contrary, overall transgene expression was significantly decreased ($p < 0.05$) when mMSCs were plated on C I coated surfaces, resulting in up to 90-percent decrease in transgene expression. Lm and Vt had no significant effect. However, the trend did not correspond with the levels of polyplex internalization. The level of internalization on ECMg and C IV was statistically the same as that for uncoated surfaces (**Figure 4-2B**). Fn coated surfaces resulted in significantly lower internalization ($p < 0.001$), while higher densities of C I coated surfaces significantly increased internalization (at least $p < 0.05$) as compared to uncoated surface.

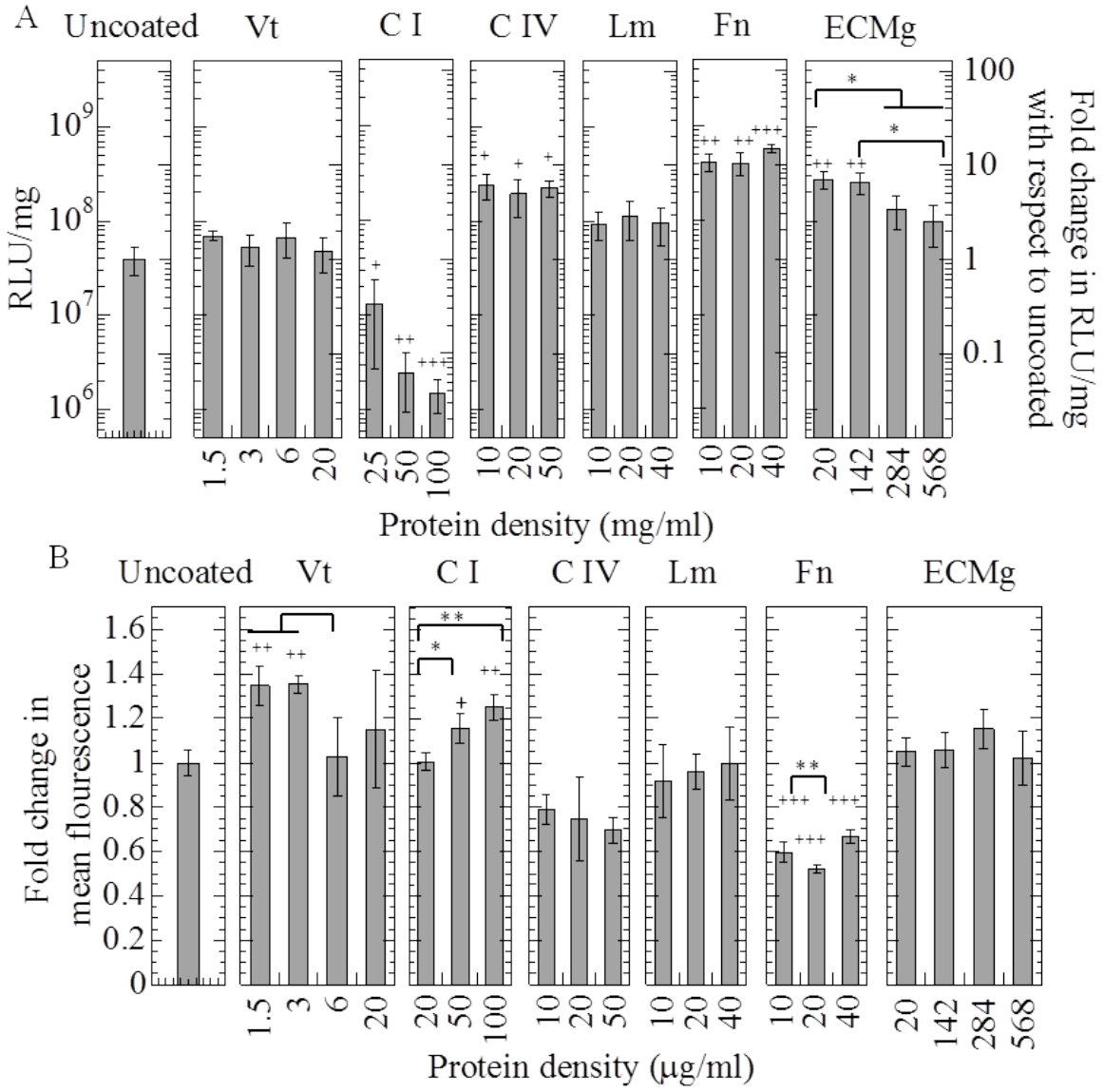

Figure 4-2: Effect of protein identity and density on gene expression and internalization. **(A)** Different proteins were coated at various initial densities and D1 cells were plated. 16 hrs after cell attachment bolus transfection was done with or without YOYO-1 labeled polyplexes. Transgene expression was analyzed 48 hours post transfection using luciferase assay and normalized with total protein quantified using Peirce BCA assay. **(B)** Internalization was assessed 2 hours post transfection using flow cytometry. A total of 7000 events were analyzed per sample. Gating was done such that the negative control had 5% positive events. Fold increase was calculated with respect to uncoated control and statistical analysis was done using the Tukey-Kramer multiple comparison. The symbols +, ++ and +++ represent the significant change in transgene expression or internalization with respect to uncoated to the level of $p < 0.05$, $p < 0.01$ and $p < 0.001$, respectively. The symbols * and ** represent the significant change in gene expression or internalization between two different protein densities to the level of $p < 0.05$ and $p < 0.01$, respectively.

A dose dependent response in gene transfer was seen with respect to ECM protein density for ECMg, Fn and C I. Transgene expression (**Figure 4-2A**) statistically increased from 2.5- to 6.5-fold as the concentration of ECMg decreased from 568 to 142 μg/ml ($p < 0.05$). Although not statistically significant, the expression increased from 10.5- to 14.6- fold for an increase in Fn concentration from 10 to 40 μg/ml and decreased by 67- fold to 90- fold for an increase in C I concentrations from 25 to 100 μg/ml. Internalization (**Figure 4-2B**) significantly increased on higher densities of C I at 50 and 100 μg/ml) and lower densities of Vt (1.5 and 3 μg/ml, at least $p < 0.05$).

Fn coating was shown to enhance gene transfer of lipoplexes to HEK cells from PLG surface relative to collagen I, laminin and uncoated PLG, in-vitro [120]. Fn also enhanced gene transfer, in-vivo at the site of spinal cord injury, from PLG multiple channel bridges [120]. Our results suggested that protein identity as well as density influence gene transfer efficiency. Further, the overall polyplex internalization rate decreased for Fn, demonstrating that polyplexes internalized on Fn are likely to be more efficiently trafficked to the nucleus than the polyplexes internalized on C I, resulting in increased transgene expression. A possible reason for differential gene transfer on Vt, C I, Fn, C IV and ECMg could be that the varied ECM proteins employ different pathways for internalization, which also influence the efficiency of intracellular trafficking and transgene expression. Further, the effect of ECM on non-viral gene transfer is likely to be cell-type specific. PC12, HEK293, NIH/3T3 and mMSCs have all shown enhancement of transfection efficiency with specific ECM coatings [6, 42, 120], but not the same ECM achieved the highest transgene expression.

4.3.3 Effect of protein identity and density on cell proliferation

mMSCs proliferated at similar rates on protein coated surfaces and uncoated surfaces by 24 hours. However, by 48 hours a statistical increase in cell proliferation was observed for cells plated on Fn and Lm ($p < 0.01$, **Figure 4-3**), which is sustained till 72 hours. On the other hand a statistically significant decrease was observed for cells plated on C I ($p < 0.01$) as compared to uncoated. The increase in proliferation observed on Fn and the decrease observed on C I correlate with the level of transgene expression; this finding can be correlated with efficient trafficking to the nucleus when the nuclear membrane is compromised during cell division [121-123].

The proliferation rate of mMSCs on surfaces coated with Lm, C IV, Fn and ECMg was statistically the same (**Figure 4-3**). Cell proliferation was also statistically the same on surfaces with increasing concentration of ECM proteins. Thus, proliferation rate alone cannot explain the observed protein identity and density dependent changes in the efficiency of gene transfer.

4.3.4 Effect of protein identity and density on cell morphology and area

The morphology of mMSCs (**Figure 4-4**) plated on protein-coated surfaces was different for the different protein coats as well as for different protein densities. Cells plated on Lm, C IV, Fn and ECMg resulted in more elongated and widely spread cells compared to cells plated on uncoated, Vt and C I. To quantify the cell morphology images, cell area and length were measured using the Zeiss Axiovision 4.6 software**.** Interestingly, surface coatings that resulted in cells with significantly larger areas (**Figure 4-5**), such as C IV, Fn and ECMg, resulted in significantly enhanced transgene expression ($p < 0.05$) compared to uncoated surfaces (**Figure 4-2A**). On the contrary, surface coatings that resulted in lower cell areas, such as Vt and C I (**Figure 4-5**),

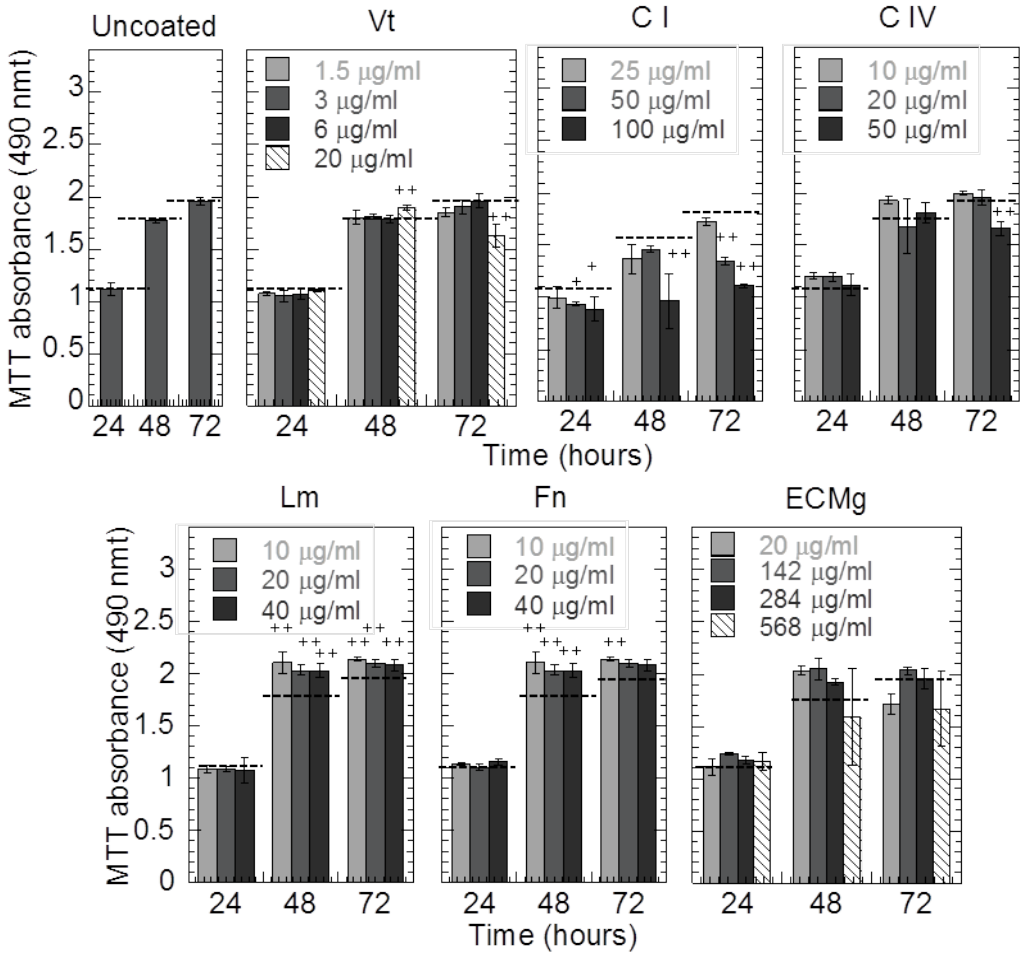

Figure 4-3: Effect of protein identity and density on cell proliferation. Cells were plated on different densities of ECM proteins and MTS assay was done to determine the proliferation rate at 24, 48 and 72 hours after transfection. Cell viability was assessed by measuring and plotting MTS absorbance at 490 nmt. **S**tatistical analysis was done using Dunnett multiple comparison test, which compares all columns with a control column. The symbols + and ++ represent the significant change in MTS absorbance for cells plated on protein coated surface with respect to cells on uncoated surface to the level of $p < 0.05$ and $p < 0.01$, respectively

resulted in higher polyplex internalization rates, but lower or similar transgene expression when compared to cells seeded on uncoated surfaces (**Figure 4-2).** Furthermore, the lower transgene expression observed on higher protein concentration of ECMg and C I correlated with the significantly lower cell area. Our results indicate that the degree of cell spreading mediated by C I, Vt, Lm, Fn and C IV affects the efficiency of gene transfer to mMSCs. The extent of cell spreading is likely to depend on adhesion and cell-ECM interactions via ECM proteins on gene

transfer by affecting cell adhesion and integrin interactions [124].

4.3.5 Integrin expression

The integrin expression of mMSCs was analyzed to determine the correlation of cell-ECM interactions mediated by the integrin expression and the influence of ECM proteins observed on cell spreading and gene transfer. Flowcytometry data was analyzed for the percentage of cells expressing the respective integrin (e.g. % gated cells, **Figure 4-5B**) and the total amount of expression of the respective integrin (e.g. mean fluorescence intensity, **Figure 4-5C**). mMSCs expressed high levels of α_5, α_3, β_1 and β_3, with the percentage of cells expressing α_5 and α_3 being significantly more than the percentage of cells expressing α_2 and α_v (p at least < 0.01). There was no statistical significance for the percentage of cells expressing β_1 and β_3. In terms of the amount of integrin expressed, as determined by the mean fluorescence intensity, α_5 was statistically higher than α_2, α_3 and α_v and β_1 was expressed to a higher level than β_3 (p at least < 0.01). These results correspond with the integrin profile reported for bone marrow derived MSCs [77]. Furthermore the observed morphology and transgene expression agrees with the integrin expression profile for mMSCs; highest expression of Fn receptors α_5 and β_1, moderate expression of collagen and laminin receptors α_2 and α_3,, and negligible expression of vitronectin receptor α_v [125]. Adhesion molecules specifically β_1 integrin have been shown to mediate transfection of lipoplexes in MDCK cells and recruitment of the same in EL4 T lymphocytes by laminin enhanced their transfection [126]. $\alpha_v\beta_3$ integrin has been shown to be involved in the process by which HUVECS internalize microparticles under flow [127]. $\alpha_v\beta_3$ integrin binding is required for adenovirus entry after receptor binding with a deficiency of these integrins limiting transduction [128]. Our results indicate that the ability of the cells to interact with different ECM proteins

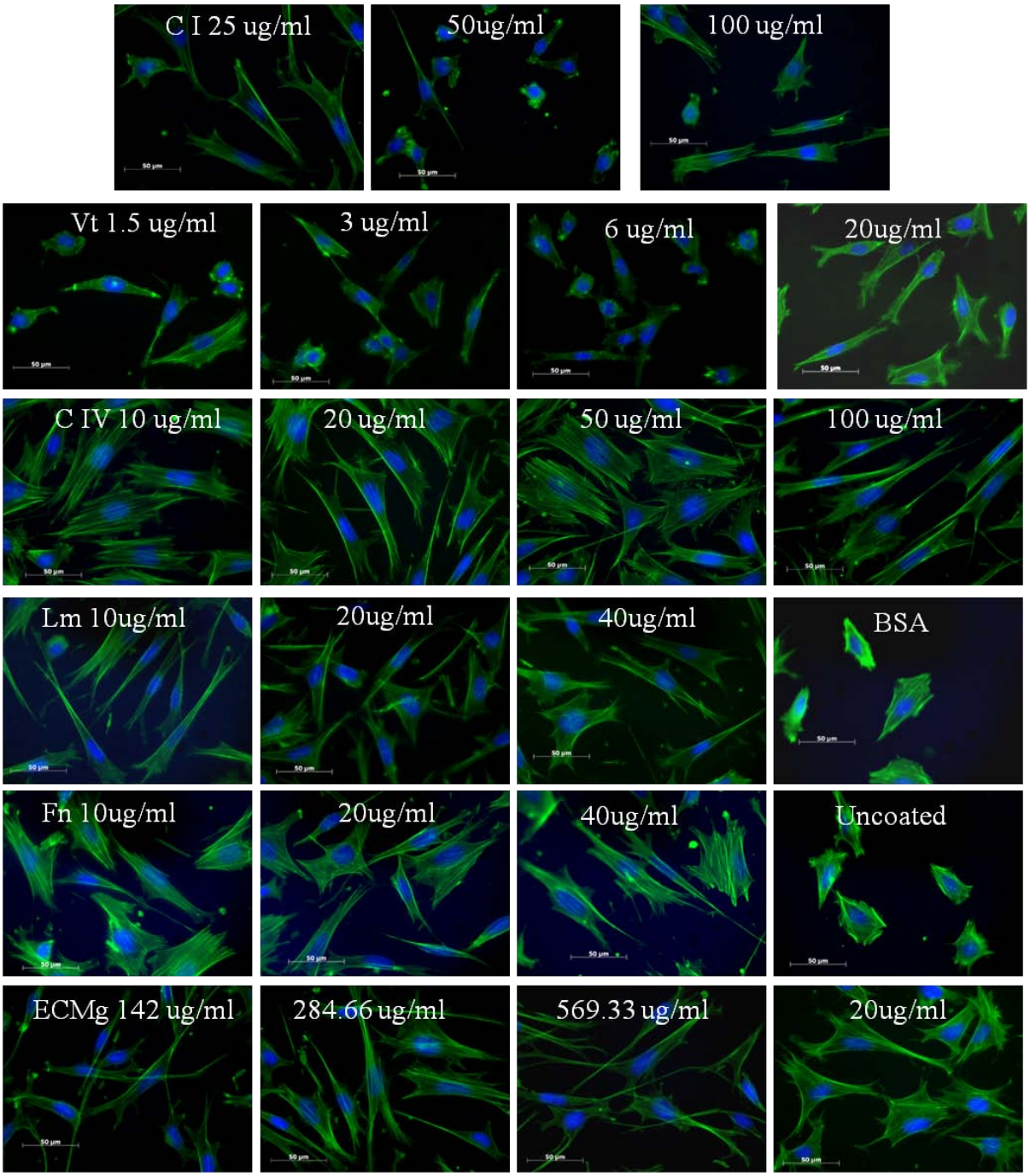

Figure 4-4: Effect of ECM protein identity and density on cell morphology. Extracellular matrix proteins and ECM gel were coated at different densities on plastic slides. 14 hours post cell attachment cells were fixed and stained with Hoechst and phalloidin dyes. Cell pictures were taken using the Zeiss microscope at 40x magnification.

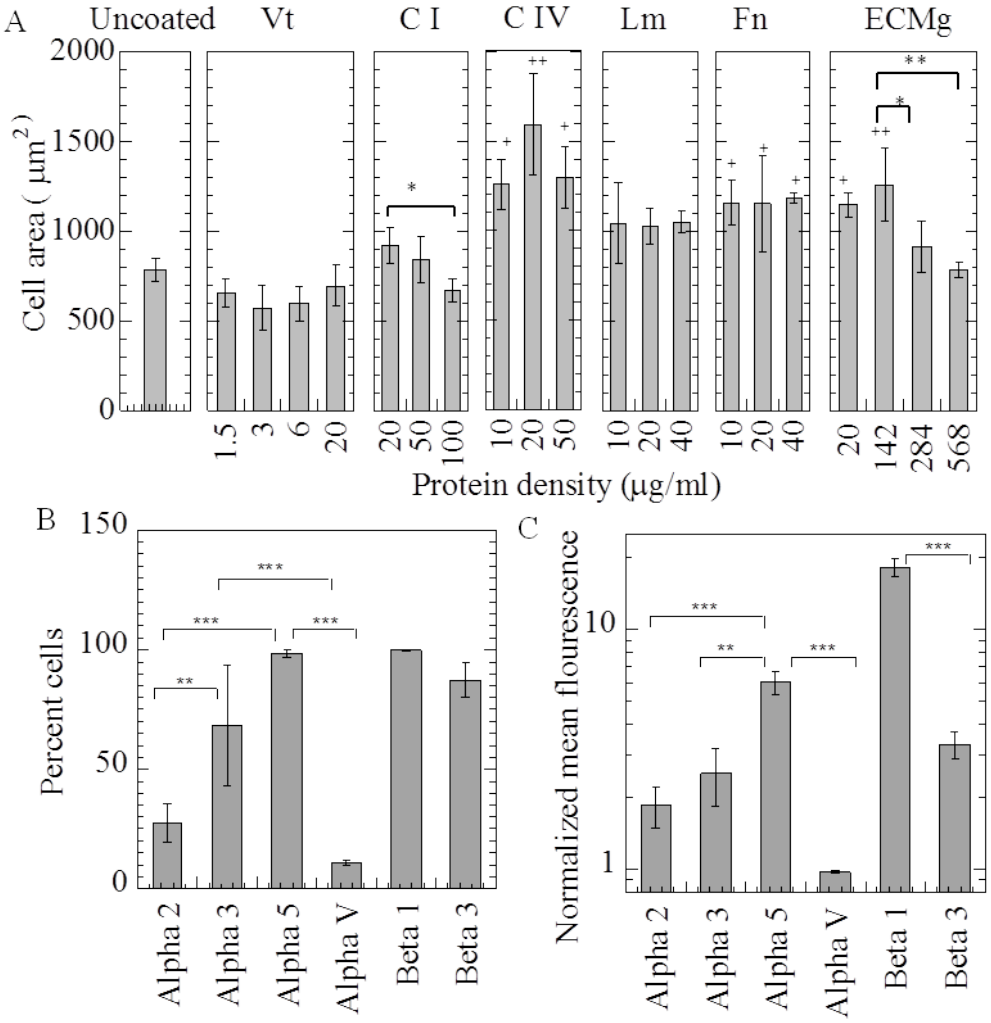

Figure 4-5: Effect of ECM protein identity and density on cell area, and integrin expression of mMSCs. (**A**) Extracellular matrix proteins and ECM gel were coated at different densities on plastic slides. 14 hours post cell attachment; cells were fixed and stained with Hoechst and phalloidin dyes. Cell pictures were taken using the Zeiss microscope. The cell area was quantified using Axiovision4.6 software. Statistical analysis on the quantified data was done using Dunnett multiple comparison test where cell length on each surface was compared with the cell area on uncoated. The symbols + and ++ represent the significant change in cell area on the protein surface with respect to cell area on uncoated surface, to the level of $p < 0.05$ and $p < 0.01$. (**B and C**) Cells cultured in tissue culture flasks were removed with trypsin/EDTA. Subsequently, cells were stained with PE or FITC conjugated antibodies specific for the different integrins The percent of cells expressing a specific α or β subunit and the level of expression was assessed using flow cytometry with FACScan X and data analysis with Flowjo. Experiments were performed in triplicates analyzing 3000 total events per sample. For all samples, gating was done such that the negative control had 5% positive events (i.e. 5% of the negative control had no antibody stain). Statistical analysis was done using the Tukey-Kramer multiple comparison test. The symbols ** and *** represent the significant difference between two integrins to the level of $p < 0.01$ and $p < 0.001$, respectively.

using integrins is an important factor determining the extent of cytoskeletal rearrangement and spreading, which correlated with enhanced transfection.

Also interactions of structural components of the ECM such as Fn with cell surface receptors, specifically integrins [89] and syndecans [129], are able to actively mediate crosstalk between the ECM and RhoGTPases. This effectively engages RhoGTPases leading to adhesion signalling [109, 130]. RhoGTPases have been primarily implicated as the controlling factors in guiding cell motility, morphology, contractility and proliferation [99]. Bacterial internalization [100, 101], adenovirus internalization [102] and recently receptor mediated internalization of transferrin [103] have also been shown to be a resultant of host cell actin cytoskeleton manipulation at level of RhoGTPases. Thus, the cell integrin expression profile as well as the ECM coat used during transfection can influence the level of activation of RhoGTPases and dictate the ability of the cells to become transfected.

4.4 Conclusions

Gene delivery has widespread application in regenerative therapies. The objective of such therapies is to induce tissue regeneration at damaged tissues of organs with either transplanted cells or host cells, by promoting the cell proliferation [131] and differentiation [14] as well as the secretion of biological molecules by gene transfection. While non-viral gene delivery is safe and less immunogenic as compared to viral delivery, it is severely limited in terms of efficiency. In this study, ECM proteins have been identified that significantly enhance transgene expression in mMSCs. It was observed that proteins that significantly enhance cell proliferation and area significantly increase gene expression despite lower polyplex internalization. The observed cell morphology on different ECM proteins corresponded with the integrin expression on mMSCs.

To explain the role of ECM proteins in more detail, the role of combination of ECM proteins on non-viral gene transfer was investigated in the following chapter. Moreover, internalization, proliferation and cell area were analyzed as the factors modulating the influence of combination of ECM proteins on gene transfer.

Chapter 5

Effect of Combination of ECM Proteins on Non-Viral Gene Delivery

5.1 Introduction

In chapter 4, we have shown that the ECM protein identity and density influence transgene expression.

To further evaluate the role of ECM on non-viral gene transfer, the effect of combining multiple ECM proteins on non-viral gene transfer was investigated in this chapter. Chapter 4 revealed that proteins which essentially enhanced cell proliferation and area, significantly increased gene expression while the opposite was observed for internalization. Therefore, to elucidate the underlying mechanisms by which the different combinations of ECM proteins influence transgene expression, cell proliferation, cell morphology, and intracellular trafficking were analyzed. In chapter 4, the transgene expression was maximally enhanced in cells plated on fibronectin (Fn) whereas cells plated on collagen I (C I), a >90% decrease in transgene expression was observed.

In this chapter an attempt was made to determine: 1) if inclusion of Fn could rescue the transgene expression on C I

2) if combinations of different proteins with Fn could further increase the transgene expression as compared to Fn alone.

3) proteins having a dominant influence on gene transfer in the different combinations.

Aims and hypothesis covered in this chapter are: Aim 1 and Hypothesis 1.

5.2 Material and methods

5.2.1 Materials. pCMV-Gluc plasmid was purchased from New England BioLabs (Ipswich, MA) and expanded using an endotoxin free Giga Prep Kit from Qiagen following the manufacturer's protocol. Linear poly-(ethylenimine) (25 Kg/mol, PEI) was purchased from Polysciences (Warrington, PA). ECM proteins such as vitronectin were purchased from Invitrogen (Carlsbad, CA), laminin and ECMg were purchased from Sigma Aldrich (St Louis, MO), fibronectin was purchased from Millipore (Billerica, MA), collagen IV was purchased from BD Bioscience (San Jose, CA) and collagen I was purchased from R&D Systems (Minneapolis, MN). All other reagents were purchased from Fisher Scientific unless otherwise specified.

5.2.2 Cell culture. Mouse bone marrow cloned mesenchymal stem cells (D1, CRL12424) were purchased from ATCC (Manassas, VA, USA). Cells were maintained in Dulbecco's modified eagles medium (Sigma-Aldrich) containing 10% bovine growth serum (BGS, Hyclone, Logan, Utah) and 1% penicillin/streptomycin antibiotics (Invitrogen, Grand Island, NY) and cultured at 37˚C and 5% CO_2.

5.2.3 Protein coating. Concentrations used for protein coatings were those recommended by manufactures' protocols; collagen I (R&D Biosystems, 5 μg/cm^2 or 50 μg/ml), fibronectin (Sigma Aldrich, 1-5 μg/cm^2 or 0.5-50 μg/ml), laminin (Sigma-Aldrich 1-2 μg/cm$^{2)}$, collagen IV BD biosciences at 1-5 μg/ cm^2, Vitronectin (Invitrogen 3 μg/ml) and ECMg (Sigma-Aldrich, 96-well 50-100 μl/well of stock solution at a concentration of 8-12 mg/ml for a 96 well plate). Two times and half this concentration were tested, leading to 3 conditions. In addition, 20 μg/ml was used as a standard concentration since this concentration overlapped with most of the suggested concentrations. For the experiments with combinations of proteins the concentration suggested by the manufacturer was used.

Stocks of vitronectin (0.5 mg/ml), laminin (0.89 mg/ml), fibronectin (1 mg/ml), collagen I (5 mg/ml), collagen IV (0.694 mg/ml in 0.05M HCl), BSA (1% in PBS) and ECMg (8.54 mg/ml) were made. The stock solutions of various proteins were further diluted in PBS to obtain the final densities and composition used for coating. Protein solutions at specific initial densities were added in each well of a tissue culture plate and the plate was incubated over night at 4˚C in a humid environment, followed by incubation at 37˚C for 2 h ours. The solution was removed and wells were washed twice with PBS to remove unbound proteins. Wells were further incubated with BSA (1% in PBS) for at least 30 minutes at 37˚C followed by two washes with PBS.

5.2.4 Transfection. mMSCs were seeded on 48 well plates that were previously modified with ECM proteins at cell densities of 20,000 cells/well. The cells were allowed to attach and incubated on the surfaces for 16 hours before DNA/PEI polyplexes were added. DNA/PEI polyplexes were formed by mixing equal volumes of plasmid DNA with 25 kDa-Linear PEI**.** For

every 1 µg of DNA, 1.65 µg of PEI was added to the DNA solution to get N/P of 12, vortexed for 15 seconds and incubated at room temperature for 15 minutes. Salt was added directly to the wells post addition of transfection solution to get a final concentration of 150 mM NaCl. Polyplexes were added directly to the medium of the plated cells at a final DNA concentration of 0.5 µg for 48 well plates. Transfection was quantified at 48-hours post transfection using the Gaussia Luciferase Assay System following the manufacturer's instructions. Subsequently, cells were lysed and the total amount of protein in samples was analyzed using Peirce BCA assay kit as per manufacturer's protocol. Experiments were carried out in triplicates and the results were expressed as relative light units (RLU) per mg of cell protein.

5.2.5 Cell proliferation. The Cell Titer 96®Aqueous One Solution Cell Proliferation Assay (Promega) was performed to determine the cytotoxicity and proliferation of the cells in different ECM proteins. The Aqueous One Solution (20 µl) was added in each well to be assayed and incubated for 2 hours. SDS (25 µl of a 10% solution) was added to each well after the incubation. The fluorescence was measured using a plate reader at 490 nm.

5.2.6 Cell morphology. mMSCs cells (20,000 cells/well) were seeded on 8-well coverslip bottom plates pre-coated with ECM proteins. The cells were allowed to incubate for 16 hours before being fixed and stained for actin and nuclear DNA using Alexa488-phalloidin and Hoechst dye following the manufacturer's instructions and standard staining protocols. Briefly, after two PBS washes the cells were fixed with 4% paraformaldehyde (PFA) for 15 minutes at room 9temperature and the cell membrane was weakened with 0.1% tritonX100 in PBS for 3 minutes. Hoechst dye and Alexa488-phalloidin were then added and left in the dark for 60

minutes at room temperature followed by two washes with 0.05% tween-20. The samples were imaged using a Zeiss Axio Observer inverted fluorescence microscope.

5.2.7 Internalization of polyplexes. Plasmid DNA and the fluorescent DNA-intercalator YOYO-1 were mixed at a ratio of 1 YOYO-1 molecule per 50 base pairs and were allowed to complex for 60 minutes at room temperature. YOYO-1 labeled DNA was then used to prepare PEI/DNA complexes at an N/P of 12 (as mentioned above) and bolus transfection was performed. Two hours after exposure to the polyplexes, cells were washed with PBS, trysinized with 50 µl of 0.25% trypsin-EDTA and finally suspended in 350 µl of 0.04% tryphan blue in 1% BGS in PBS. Fluorescent cells were detected by flow cytometry with a FACScan X and data was analyzed with CELLQuest (Beckton Dickinson). Experiments were performed in triplicates analyzing 7000 total events per sample.

5.2.8 Intracellular trafficking of polyplexes. mMSCs were seeded on 8-well Lab-Tek chambered coverglass (Thermoscientific) that was previously modified with ECM proteins, at cell densities of 17,000 cells/well. Plasmid DNA was labeled using TM- rhodamine labeling kit from Mirus Bio, as per manufacturer's protocol and PEI/DNA complexes were made at an N/P of 12. The cells were allowed to attach and incubated on the surfaces for 16-hours before DNA/PEI polyplexes were added. Six hours post transfection, cells were washed twice with PBS and two times with cell scrub (Genlantis) solution to remove extracellular complexes. Later the cells were fixed with 4% paraformaldehyde (PFA) for 15 minutes at room temperature and nuclear DNA was stained using Hoechst dye. Intracellular trafficking was analyzed by taking

fluorescent and brightfield images using a Zeiss Axio Observer microscope at 100x magnification.

5.2.9 Statistics. All statistical analysis were performed using the computer program Instat (GraphPad, San Diego, CA). Experiments were statistically analyzed using the Tukey test, which compares all pairs of columns, using a 95% confidence interval or using the Dunnett test which compares all columns versus a control column

5.3 Results

5.3.1 Effect of combination of ECM proteins on transgene expression

Combinations of ECM proteins were studied next to better understand the role of the ECM on non-viral gene transfer. The final concentration of Fn was 20 μg/ml, Lm was 20 μg/ml, C IV was 25 μg/ml, C I was 50 μg/ml and Vt was 3 μg/ml in the combinations. Gene transfer in an uncoated surface was used as the control. Combining Vt and C IV (Vt+C IV) enhanced the transgene expression by 5.4-fold (**Figure 5-1A**), which was statistically significant compared to either C IV or Vt by themselves ($p < 0.001$). The combination of Vt, Lm and C IV (Vt+Lm+C IV) enhanced the transgene expression by 5.6-fold, which is statistically higher ($p < 0.01$) than the transgene expression observed for the same individual proteins, and for Vt and Lm (Vt+Lm) (**Table 5-1**). Further, the transgene expression on Vt+Lm+C IV was statistically the same to C IV+Vt and to Fn, indicating that combining C IV with Vt increases the gene transfer efficiency to mMSCs. A possible explanation for this could be that the extent of adhesion signalling on recruiting multiple integrins including α_2, α_v and β_1 on C IV and Vt, is similar to that achieved by recruiting α_5 and β_1 on Fn.

Protein coatings that contained C I namely Fn+C I, Lm+C I, Fn+C I+Lm, and Fn+C I+Vt, decreased the transgene expression by 70% (**Figure 5-1A**). Moreover, the transgene expression on Fn+C I+Vt and Fn+C I+Lm was statistically lower than the expression on Fn, Fn+Vt and Fn+Lm (**Table 5-1A**). These results indicate that the transgene expression in mMSCs is strongly inhibited by C I even in combination with Fn.

Protein coatings that contained Fn and no C I, namely Fn+C IV, Fn+Vt, and Fn+C IV+Vt, resulted in statistically similar transgene expression as observed on Fn (**Figure 5-1A**).

Moreover, Fn+Lm and Fn+Vt, mediated transgene expression that is statistically higher ($p < 0.05$) than on Vt or Lm. (**Table 5-1A**). These results indicate that even in the presence of Vt, Lm and C IV, Fn strongly enhances transgene expression and this association is likely mediated by the α_5 and β_1 integrins.

It was interesting to note that protein coating with Fn+Vt+Lm improved the transgene expression by 2.7-fold, which is statistically lower than the transgene expression observed on Fn alone (7.2-fold) and Fn+Vt (8.6-fold), and statistically the same to the enhancement observed on Fn+Lm, indicating that Lm reduces the effect of Fn.

5.3.2 Effect of combination of ECM proteins on internalization

As observed for individual proteins, the level of polyplex uptake (**Figure 5-1B**) did not correspond with the level of transgene expression. Combination of Fn+C I significantly increased internalization ($p < 0.001$) as compared to internalization on Fn alone, indicating the dominant influence of C I on cells, as was observed for transgene expression. Interestingly, a

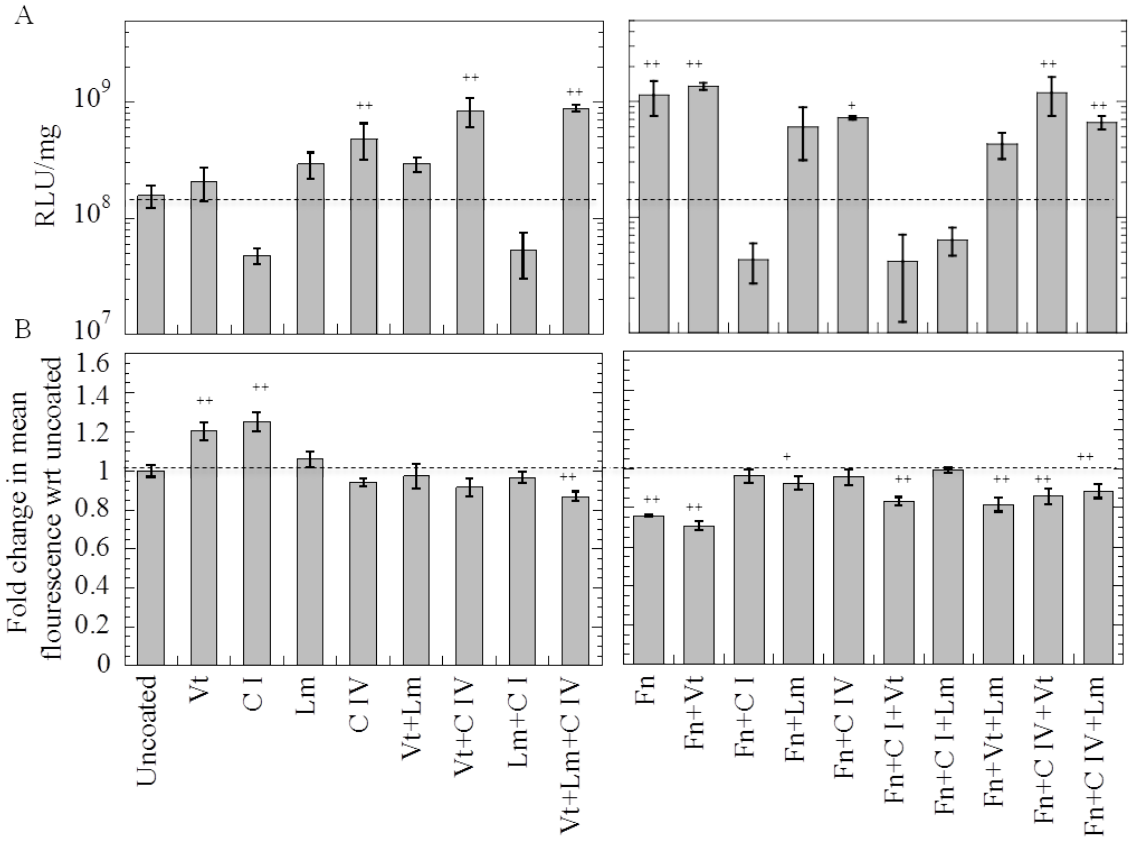

Figure 5-1: Effect of combination of different ECM proteins on gene expression and internalization. Combination of 2 or 3 different proteins comprising C I (50 µg/ml), Vt (3 µg/ml), Lm (20 µg/ml), Fn (20µg/ml) and C IV (25 µg/ml) were coated and D1 cells were plated. 16 hrs after cell attachments bolus transfection was done with or without YOYO-1 labeled polyplexes. (**A**) Transgene expression was analyzed 48 hours post transfection using luciferase assay and normalized with total protein quantified using Peirce BCA assay. (**B**) Internalization was assessed 2 hours post transfection using flow cytometry. A total of 7000 events were analyzed per sample. Gating was done such that the negative control had 5% positive events. Statistical analysis was done using Dunnett multiple comparison test where the transgene expression or internalization on each surface was compared to that on uncoated. The symbols + and ++ represent the significant change in transgene expression or internalization with respect to uncoated to the level of $p < 0.05$ and $p < 0.01$, respectively

significant decrease ($p < 0.01$) in internalization as compared to uncoated surfaces, correlated with a significant increase ($p < 0.05$) in transgene expression for Vt+Lm+Cl IV, Fn+Vt, Fn+C IV+Vt and Fn+C IV+Lm as was seen for Fn.

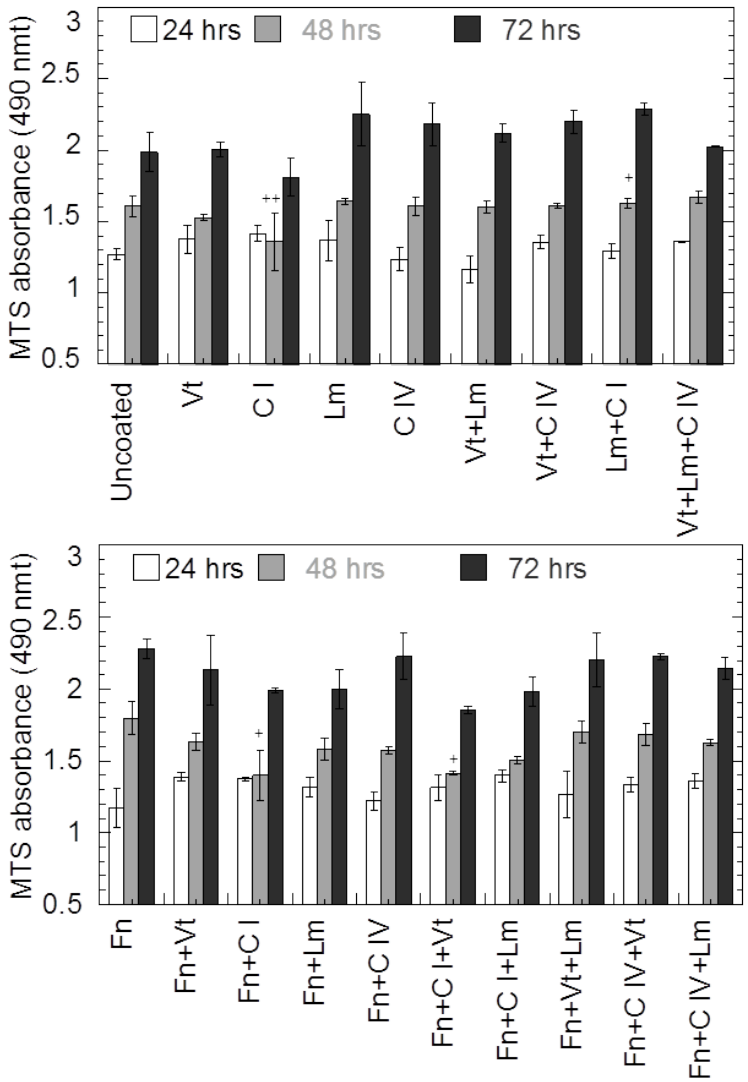

Figure 5-2: Effect of combination of ECM proteins on cell proliferation. Cells were plated on surfaces pre-coated with combination of 2 or 3 different proteins including C I (50 µg/ml), Vt (3 µg/ml), Lm (20 µg/ml), Fn (20 µg/ml) and C IV (25 µg/ml). MTS assay was done to determine the proliferation rate at 24, 48 and 72 hours after transfection. Cell viability was assessed by measuring MTS absorbance at 490 nmt. **S**tatistical analysis was done using Dunnett multiple comparison test, which compares all columns with a control column. The symbols + and ++ represent the significant change in MTS absorbance for cells plated on protein coated surface with respect to cells on uncoated surface to the level of $p < 0.05$ and $p < 0.01$.

5.3.3 Effect of combination of ECM proteins on proliferation

mMSCs proliferated at similar rates on protein coated surfaces and uncoated surface by 24 hours (**Figure 5-2**). By 48 hours, a significant decrease in cell proliferation for cells plated on C I,

Fn+C I, and Fn+C I+Vt corresponded with the low expression on these surfaces. For all other conditions there was no difference in cell proliferation as compared to cells on uncoated surface. This indicates that the transgene expression for all other ECM combinations was independent of proliferation.

5.3.4 Effect of combination of ECM proteins on cell morphology and area

The combination of ECM proteins was found to substantially influence the cell morphology and area as compared to cells plated on uncoated surfaces and single protein coated surfaces. Combination of Fn+C I, Lm+C I and Fn+C I+Vt reduced the extent of cell spreading (**Figure 5-3A**) as compared to spreading on Fn, Lm and Fn+Vt. Increased cell spreading was observed for combination of Fn or C IV with Vt (Fn+Vt, Vt+C IV) as compared to only Vt. A significant increase in cell area (**Figure 5-3B**) corresponded with an increase in transgene expression as was observed for cells plated on C IV, Vt+C IV, Vt+Lm+C IV, compared to uncoated. On the other hand, the cell area (**Figure 5-3B**) on Vt, C I, Lm, Vt+Lm, Lm+C I, Fn+C I, Fn+C I+Vt and Fn+C I+Lm protein coated surfaces was statistically similar to uncoated surface and corresponded with either a significant decrease or no change in transgene expression with respect to uncoated surfaces.

To determine if there was a statistical correlation between transgene expression and cell area statistical analysis was done to compare the different conditions (**Table 5-1A**). Each condition was compared with all combinations inclusive of Fn and exclusive of Fn using the Dunnett multiple comparisons test. Similar analysis was done for cell area on different protein coated surfaces (**Table 5-1B**) as was done for transgene expression (**Table 5-1A**). The 161 conditions were classified as containing one, two or three ECM protein coatings. These coating conditions

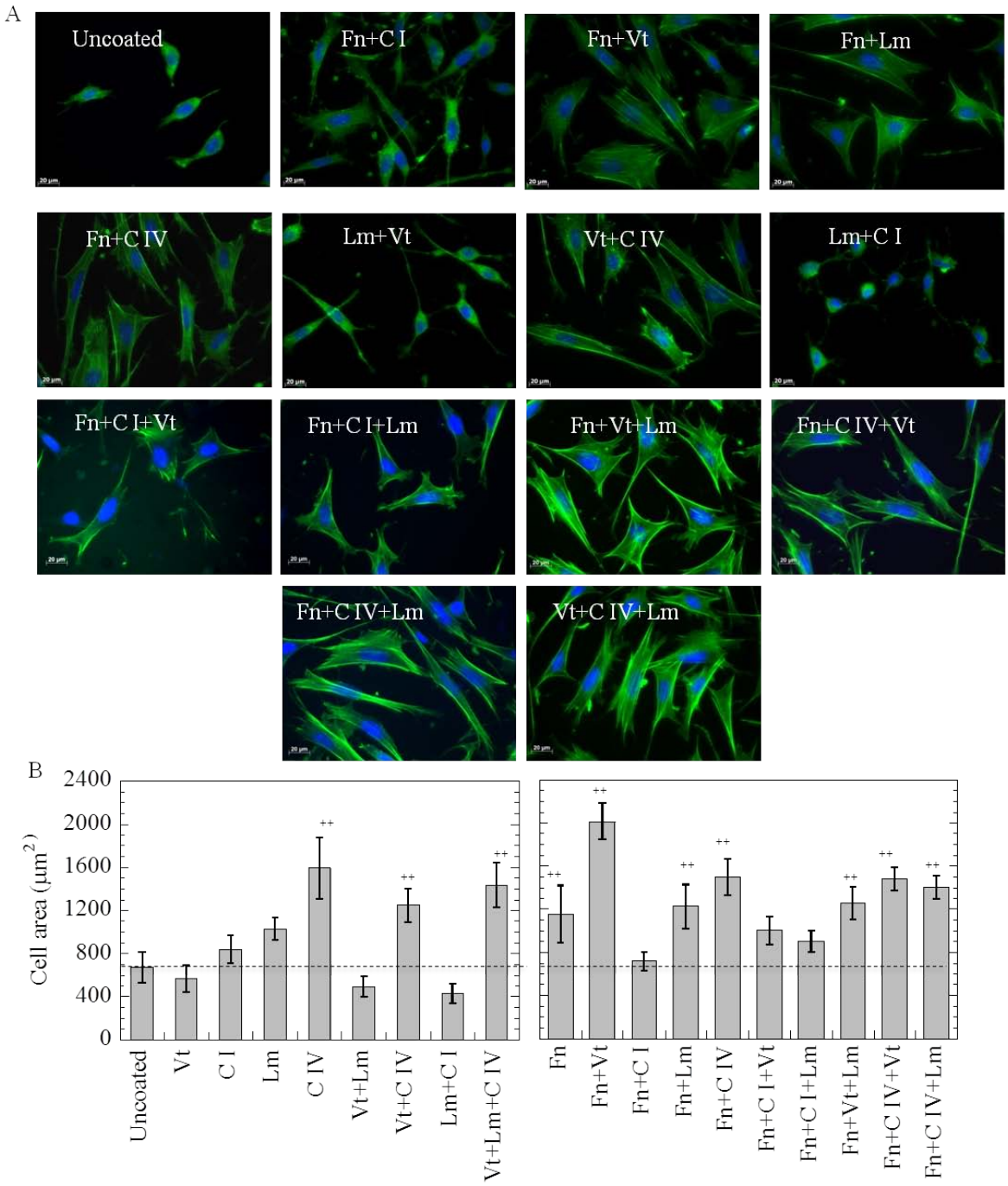

Figure 5-3: Effect of combination of ECM proteins on cell morphology and area. Combination of 2 or 3 different proteins comprising C I (50 µg/ml), Vt (3 µg/ml), Lm (20 µg/ml), Fn (20 µg/ml) and C IV (25 µg/ml) were coated on plastic slides. 14 hours post cell attachment, cells were fixed and stained with Hoechst and phalloidin dyes. (**A**) Cell pictures were taken using the Zeiss microscope at 40x magnification. (**B**) The cell area was quantified using Axiovision4.6 software. Statistical analysis on the quantified data was done using Dunnett multiple comparison test where cell length on each surface was compared with the cell area on uncoated. The symbols + and ++ represent the significant change in cell area on the protein surface with respect to cell area on uncoated surface, to the level of $p < 0.05$ and $p < 0.01$, respectively.

were analyzed to see if there is a correlation between spreading and transgene expression (**Table 5-1C**). For example, there is a 73% statistical correlation between spreading and transfection for single ECM protein coated surfaces. The correlations between all conditions can be found in **Tables 5-1C and 5-1D**. Together this suggests that the interactions of the cell with the ECM that promote adhesion and spreading are highly likely to influence the efficiency of non-viral gene transfer.

ECM adhesion molecules on cells such as integrins and syndecans are also involved in focal adhesion and stress fiber formation [95]. Microfilaments play a role in trafficking and depolymerization of actin has been shown to decrease DNA/PEI polyplex trafficking >60% [84]. Recently, internalization of DNA/polyethylenimine polyplexes associated with cell surface receptor syndecan in Hela cells has been shown to be mediated by actin polymerization and the resultant stress fibers near the cell cortex [132]. Thus, the extent of actin polymerization and stress fiber formation on different ECM coated surfaces is likely to play a role in the efficiency of gene transfer.

5.3.5 ECM proteins modulate intracellular trafficking of polyplexes.

To further investigate the mechanism by which ECM proteins modulate gene transfer, fluorescently labeled polyplexes were tracked after gene transfer to determine their intracellular location. ECM proteins were found to modulate the extent of trafficking to the nucleus. For cells plated on C I and combinations including C I (Lm+ C I, Fn+C I, Fn+C I+Lm and Fn+ C I+Vt) the trafficking of complexes to the nucleus was inhibited, with polyplexes located in the cytoplasm or at the periphery of the nucleus (**Figure 5-4A and B**). The reduced trafficking on

Combination vs constituent single protein Combination of three vs constituent combination of two

A

	Uncoated	Vt	CI	Lm	Fn	CIV	Fn+CI	Fn+Vt	Fn+Lm	Fn+CIV	Vt+Lm	Vt+CIV	Lm+CI	Vt+Lm+CIV
Uncoated		ns	ns	ns	**	**	ns	**	ns	**	ns	**	ns	**
Vt	ns		ns	ns	**	*	ns	**	ns	*	ns	**	ns	**
CI	ns	ns		ns	**	**	ns	**	*	**	ns	**	ns	**
Lm	ns	ns	ns		**	ns	ns	**	ns	ns	ns	**	ns	**
Fn	**	**	**	**		**	**	ns	*	ns	**	ns	**	ns
CIV	**	*	**	ns	**		ns	**	ns	ns	ns	**	**	**
Fn+CI+Vt	ns	ns	ns	ns	**	ns	ns	**	*	**	ns	**	ns	**
Fn+CI+Lm	ns	ns	ns	ns	**	ns	ns	**	*	**	ns	**	ns	**
Fn+Vt+Lm	ns	ns	ns	ns	**	ns	ns	**	ns	ns	ns	ns	ns	ns
Fn+CIV+Vt	**	**	**	**	ns	**	**	ns	*	ns	**	ns	**	ns
Fn+CIV+Lm	*	ns	**	ns	ns	ns	**	**	ns	ns	ns	ns	**	ns
Vt+Lm+CIV	**	**	**	**	ns	**	**	ns	ns	ns	**	ns	**	

B

	Uncoated	Vt	CI	Lm	Fn	CIV	Fn+CI	Fn+Vt	Fn+Lm	Fn+CIV	Vt+Lm	Vt+CIV	Lm+CI	Vt+Lm+CIV
Uncoated		ns	ns	ns	**	**	ns	**	**	**	ns	**	ns	**
Vt	ns		ns	*	**	**	ns	**	**	**	ns	**	ns	**
CI	ns	ns		ns	ns	**	ns	**	*	**	ns	*	*	**
Lm	ns	*	ns		ns	**	ns	**	ns	**	**	ns	**	*
Fn	**	**	ns	ns		*	*	**	ns	ns	**	ns	**	ns
CIV	**	**	**	**	*		**	*	ns	ns	**	ns	**	ns
Fn+CI+Vt	ns	*	ns	ns	ns	**	ns	**	ns	**	**	ns	**	*
Fn+CI+Lm	ns	ns	ns	ns	ns	**	ns	**	ns	**	*	ns	**	**
Fn+Vt+Lm	**	**	*	ns	ns	ns	**	**	ns	ns	**	ns	**	ns
Fn+CIV+Vt	**	**	**	*	ns	ns	**	**	ns	ns	**	ns	**	ns
Fn+CIV+Lm	**	**	**	*	ns	ns	**	**	ns	ns	**	ns	**	ns
Vt+Lm+CIV	**	**	**	*	ns	ns	**	**	ns	ns	**	ns	**	

C

	Uncoated	Vt	CI	Lm	Fn	CIV	Fn+CI	Fn+Vt	Fn+Lm	Fn+CIV	Vt+Lm	Vt+CIV	Lm+CI	Vt+Lm+CIV
Uncoated														
Vt														
CI														
Lm														
Fn														
CIV														
Fn+CI+Vt														
Fn+CI+Lm														
Fn+Vt+Lm														
Fn+CIV+Vt														
Fn+CIV+Lm														
Vt+Lm+CIV														

D

Surfaces compared	% correlation
All ECM protein combinations	69.57
Two different single protein coated surfaces	73.33
A single protein coated surface with a surface coated with two proteins	69.05
A single protein coated surface with a surface coated with three proteins	63.89
A surface coated with three proteins and surface coated with two proteins.	64.29

Table 5-1: To fully analyze the role of individual proteins versus their combinations on transgene expression (**A**) and area (**B**), statistical analysis was done using the Dunnett multiple comparison test. Each condition was compared with all combinations inclusive of Fn and exclusive of Fn. The symbols *, ** and ** represent the significant difference in transgene expression or cell area between two different surfaces to the level of $p < 0.05$, $p < 0.01$ and $p < 0.001$, respectively. The symbols 'ns' represents no significant difference in transgene expression or cell area between two different surfaces. (**C**) The correlation between extent of spreading and transgene expression observed was analyzed. ▭ represents that a significant difference in cell area corresponded with a significant difference in transgene expression, and no significant difference in cell area corresponded with no significant difference in transgene expression between the two surfaces compared. ▭ represents no correlation in statistical difference in cell area with trangene expression on two different protein coated surfaces. (**D**) Correlation between extent of spreading and transgene expression.

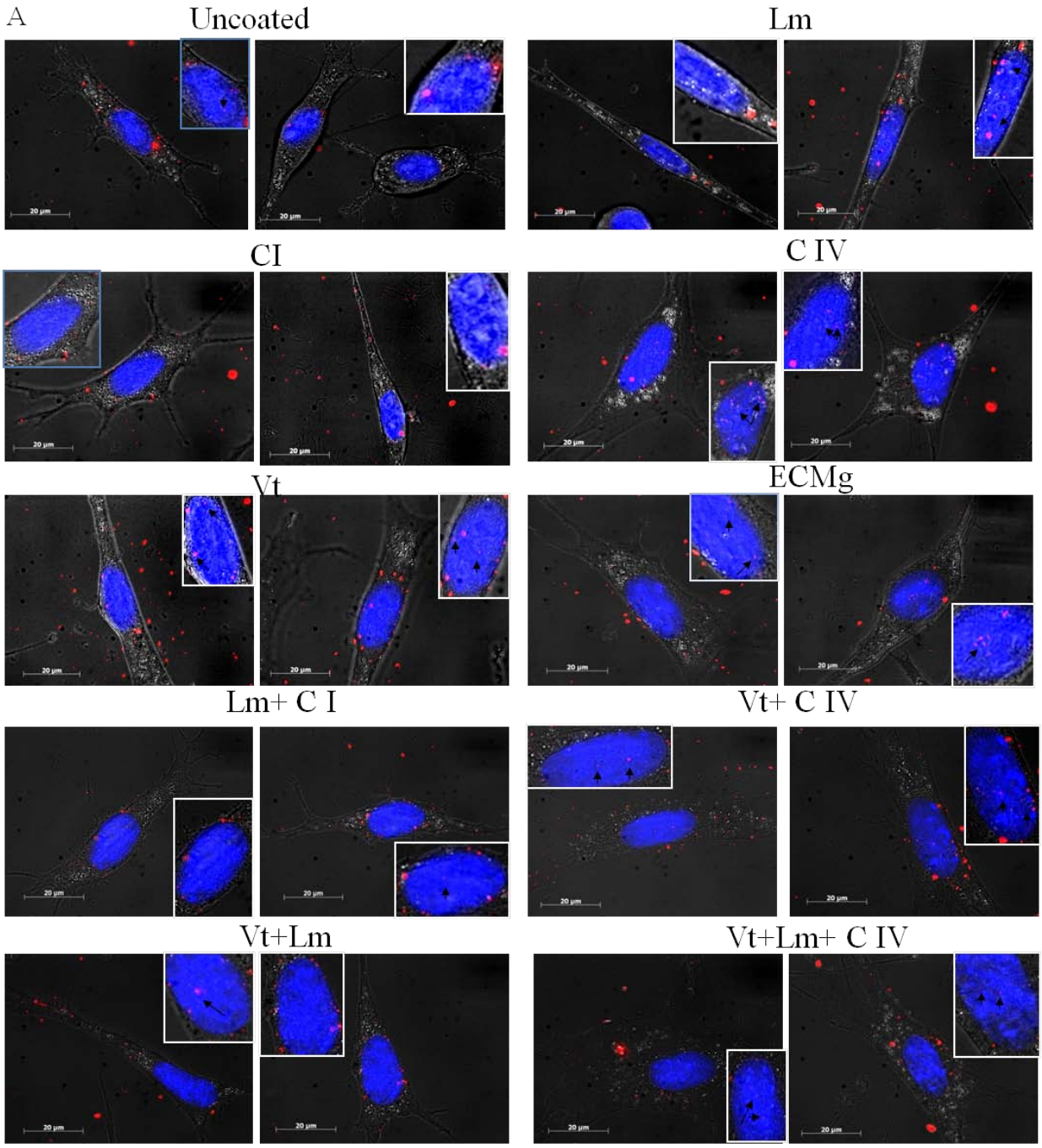

Figure 5-4: Effect of combination of ECM proteins on intracellular trafficking. (**A**) Cells were plated on surfaces pre-coated with single or combination of different proteins including C I (50 µg/ml), Vt (3 µg/ml), Lm (20 µg/ml), and C IV (25 µg/ml). 16 hrs after cell attachment bolus transfection was done with TM-rhodamine labeled polyplexes. 6 hours post transfection cells were washed with PBS and cellscrub solution, fixed and the nucleus was stained using the Hoechst dye. Trafficking of the polyplexes to the nucleus was analyzed by taking combined 100x fluorescent and brightfield pictures using the Zeiss microscope. These images are a maximum intensity projection of three deconvoluted z-stacks, 0.3-0.5 µm apart

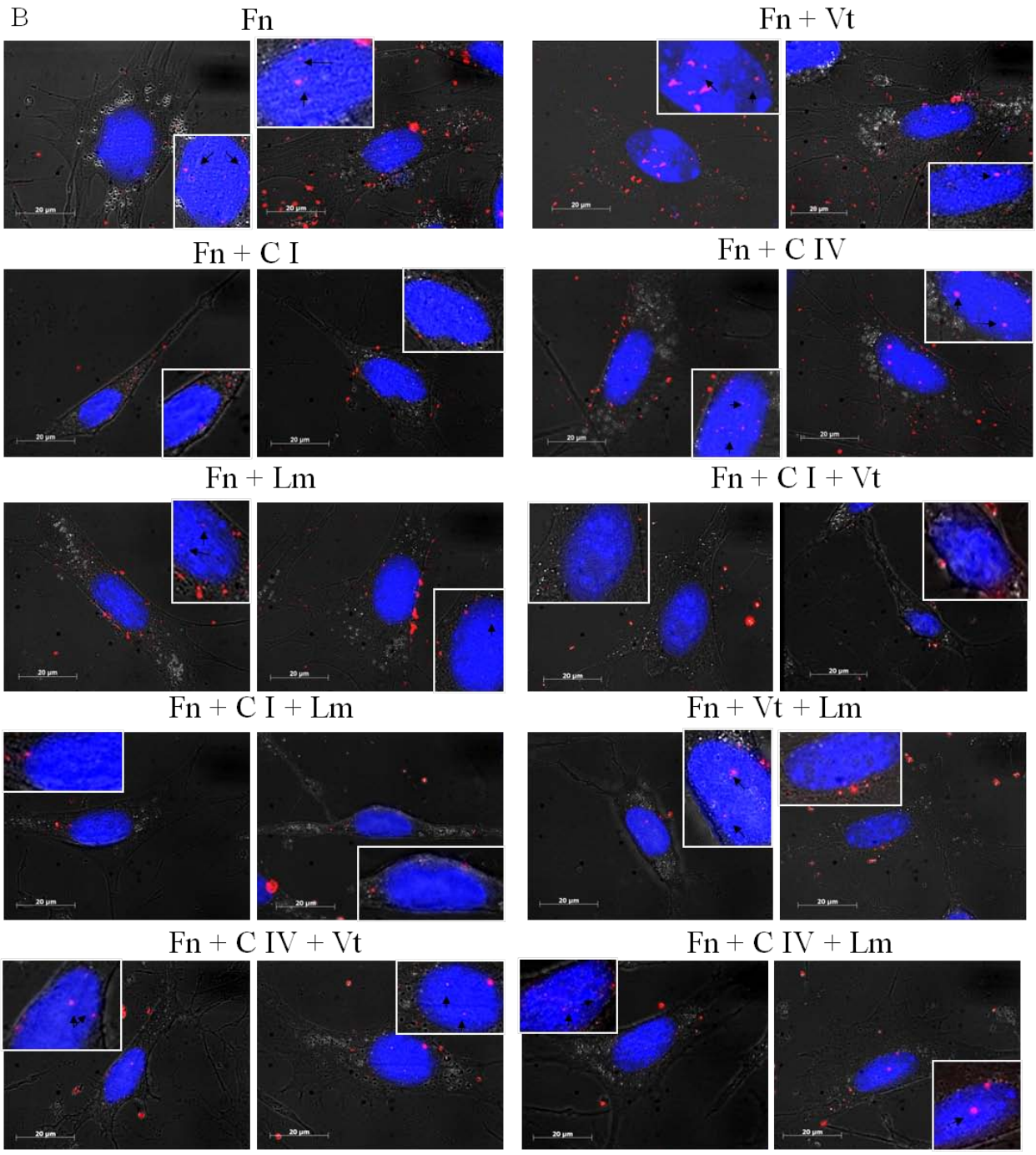

Figure 5-5: Effect of combination of ECM proteins on intracellular trafficking. (**B**) Cells were plated on surfaces pre-coated with Fn (20 µg/ml) alone or a combination of Fn with different proteins including C I (50 µg/ml), Vt (3 µg/ml), Lm (20 µg/ml), and C IV (25 µg/ml). 16 hrs after cell attachment bolus transfection was done with TM-rhodamine labeled polyplexes. 6 hours post transfection cells were washed with PBS and cellscrub solution, fixed and the nucleus was stained using the Hoechst dye. Trafficking of the polyplexes to the nucleus was analyzed by taking combined 100x fluorescent and brightfield pictures using the Zeiss microscope. These images are a maximum intensity projection of three deconvoluted z-stacks, 0.3-0.5 µm apart

surfaces coated with C I and protein combinations constituting C I correlates with considerably decreased transgene expression. On the other hand, Fn and combination of Fn with C IV, Vt and Lm (Fn+C IV, Fn+Vt, Fn+Lm, Fn+Vt+Lm, Fn+C IV+Lm and Fn+C IV+Vt) mediated efficient trafficking of the internalized complexes to the nucleus (**Figure 5-4B**). Trafficking of the polyplexes to the nucleus was also observed on Vt, ECMg and C IV, while uncoated tissue plastic and Lm mediated trafficking of internalized complexes to the nucleus in a few cells (**Figure 5-4A**). A possible reason governing gene transfer is the cell response to ECM as a resultant of affinity for respective integrins. Taken together, these results indicate that gene transfer on different ECM protein microenvironments is modulated by integrin receptor engaged and the resulting cell spreading and trafficking**.**

5.4 Conclusions

In this chapter, combinations of ECM proteins that significantly enhance transgene expression in mMSCs have been identified. As was observed for single ECM proteins in chapter 4, the combinations of ECM proteins that enhanced cell proliferation and area, significantly increased gene expression while the opposite was observed for internalization. C I had a stronger influence and inhibited the transgene expression when combined with Fn or Lm, which also correlated with lower cell area on these surfaces. In contrast, Fn had a dominant influence as compared to Lm and Vt, and enhanced the transgene expression. Interestingly, by combining Vt, Lm, and C IV, similar influence as Fn was observed on the internalization, transgene expression, and cell area. When comparing any two protein coated surfaces a 70% statistical correlation was present between the extent of cell spreading and transgene expression. Moreover, efficient trafficking of

the internalized complexes to the nucleus was observed to be a factor for enhancement of transgene expression correlated on respective ECM coated surfaces.

On the whole, in this chapter the efficiency of gene-transfer was governed by the trafficking of internalized polyplexes and cell area, which pointed towards a role of endocytosis and cell cytoskeleton. To further understand the mechanism by which the ECM regulated gene transfer, the role of endocytic pathways and cytoskeleton in ECM protein mediated non-viral gene transfer was studied in the following chapter.

After determining the affect of ECM proteins in gene transfer, a scaffold or hydrogel can be designed constituting a combination of ECM proteins. ECM proteins that specifically promote proliferation or differentiation or have a dominant influence on gene transfer even in presence of other proteins, can be incorporated.

Chapter 6

Role of Endocytic Pathways and Cell Cytoskeleton in Non-Viral Gene Delivery on Different ECM Coated Surfaces.

6.1 Introduction

Chapter 4 and 5 have evidenced that ECM proteins modulate non-viral gene transfer by influencing cell area, cellular internalization and intracellular trafficking. Fn enhanced transgene expression by increasing cell area and promoting efficient trafficking of the fewer polyplexes internalized. On the other hand C I reduced transgene expression by not increasing area and by not inducing efficient trafficking of the increased polyplexes internalized. Moreover, a 70% correlation was observed between extent of cell spreading and transgene expression. This indicated the possibility of involvement of different internalization pathways and cell cytoskeleton in gene transfer in cells plated on Fn and C I.

Studies investigating the mechanism of PEI/DNA complex internalization and overall gene transfer efficiency into adherent cells concluded that actin polymerization into stress fibers, microtubule motor proteins, as well as protein kinase C (PKC) induced phosphorylation have a

major role in polyplex internalization and trafficking [3, 4, 80, 132]. Chapter 3 had reviewed the role of actin and microtubule in gene transfer.

The Fn induced enhancement of gene transfer to fibroblast was correlated to endocytosis [6], while for PC12 cells the enhancement on collagen IV was correlated to the relative projected nuclear area of the plated cells [42].

We had hypothesised that the varied ECM proteins influence the efficiency of gene transfer by mediating differential endocytic pathways and cytoskeletal dynamics, that subsequently modulate the process of gene transfer (hypothesis 2). To further investigate the mechanism by which C I and Fn mediate either the inhibition or enhancement of non-viral gene transfer to mMSCs, the roles of cell cytoskeleton and internalization pathways were studied in this chapter. mMSCS were seeded on C I or Fn coated dishes and transfected in the presence or absence of pharmacological inhibitors for cytoskeletal components or endocytic pathways. *Aims and hypothesis covered in this chapter are: Aim 2 and Hypothesis 2.*

6.2 Materials and methods

6.2.1 Materials. pEGFP-luc plasmid was purchased from clontech (Palo Alto, CA) and expanded using a Giga Prep Kit from Qiagen following the manufacturer's protocol. Linear poly-(ethylenimine) (25 Kg/mol, PEI) was purchased from Polysciences (Warrington, PA). Various inhibitors namely Amiloride hydrochloride hydrate, Cytochalasin D, Nocodazole, and Butanedione monoxime (BD) were purchased from Sigma Aldrich (St Louis, MO). Endothelin I was purchased from Calbiochem (Gibbstown, NJ). Genistein, Chlorpromazine hydrochloride and chloroquine diphosphate salt were purchased from Fisher scientific. Fn was purchased from

Sigma and C I was purchased from R&D Systems (Minneapolis, MN). All other reagents were purchased from Fisher Scientific unless otherwise specified.

6.2.2 Cell culture. Mouse bone marrow cloned mesenchymal stem (D1, CRL12424) were purchased from ATCC (Manassas, VA, USA). Cells were maintained in Dulbecco's modified eagle's medium (Sigma-Aldrich) containing 10% bovine growth serum (BGS, Hyclone, Logan, Utah) and 1% penicillin/streptomycin antibiotics (Invitrogen, Grand Island, NY) and cultured at 37˚C and 5% CO_2.

6.2.3 Protein coating. Proteins were coated using a method described by Kruger et al. [133] with minor modifications. The stock solutions of various Fn and C I were diluted in PBS to obtain the final densities used for coating. Protein solution at specific initial densities was added in each well of a tissue culture plate and the plate was incubated over night at 4˚C in a humid environment, followed by incubation at 37˚C for 2 hours. The solution was removed and wells were washed twice with phosphate buffer saline (PBS) to remove unbound proteins. Wells were further incubated with BSA (1% in PBS) for 30 minutes at 37˚C followed by two washings with PBS.

6.2.4 Transfection. mMSCs were seeded on 48 well plates that were previously modified with ECM proteins at cell densities of 20,000 cells/well, respectively. The cells were allowed to attach and incubated on the surfaces for 16 hours before DNA/PEI polyplexes were added. DNA/PEI polyplexes were formed by mixing equal volumes of plasmid DNA with 25 kDa-Linear PEI**.** For every 1 μg of DNA, 1.65 μg of PEI was added to the DNA solution to get N/P of 12, vortexed

for 15 seconds and incubated at room temperature for 15 minutes. Polyplexes were added directly to the medium of the plated cells at a final DNA concentration of 0.5 μg for 48 well plates. Salt was added directly to the wells post addition of transfection solution to get a final concentration of 150 mM NaCl. Transfection was quantified at 48 hours post transfection using the Promega Luciferase Assay system using a Luminometer (Turner biosystems, modulus, Sunnyvale, CA) and an integration period of 10 seconds.

6.2.5 Cell proliferation. The Cell Titer 96®Aqueous One Solution Cell Proliferation Assay (Promega) was performed to determine the cytotoxicity and proliferation of the cells exposed to different conditions. The Aqueous One Solution (20 μl) was added in each well to be assayed and incubated for 2 hours. SDS (25 μl of a 10% solution) was added to each well after the incubation. The fluorescence was measured using a plate reader at 490 nm.

6.2.6 Internalization of polyplexes. Plasmid DNA (pGFPluc) and the fluorescent DNA-intercalator YOYO-1 were mixed at a ratio of 1 YOYO-1 molecule per 50 base pairs and were allowed to complex for 60 minutes at room temperature. YOYO-1 labeled DNA was then used to prepare PEI/DNA complexes at a N/P of 12 (as mentioned above) and bolus transfection was performed. Two hours after exposure to the polyplexes, cells were washed with PBS, trysinized with 50 μl of 0.25% trypsin-EDTA and finally suspended in 350 μl of 0.04% tryphan blue in 1% BGS in PBS. Fluorescent cells were detected by flow cytometry with a FACScan X and data was analyzed with CELLQuest (Beckton Dickinson). Experiments were performed in triplicates analyzing 7000 total events per sample. For all samples, gating was done such that the negative control had 5% positive events (i.e. 5% of the negative control had internalized DNA).

6.2.7 Studying the role cytoskeleton in gene transfer. For treatment, the cells were allowed to attach for 14-15 hours before the media in the wells was replaced with media containing the inhibitor for 30 minutes. The media in the wells was changed with fresh complete medium after treatment prior to transfections. 10 μM Nocodazole (Noc) treatment was given to depolymerize microtubules, 10 mM Butanedione monoxime (BD) treatment was given to inhibit myosin ATPase and 20 μM Cytochalasin D (CD) treatment was given to inhibit actin polymerization and the resultant tension. Immediately after treatment, cell morphology was analyzed. Transfections were done to study cell viability, internalization and gene expression after treatment, using previously mentioned methodologies. Cell viability was studied 4 and 48 hour post treatment and transfection.

6.2.8 Cell morphology. Cell morphology was analyzed to assess the effect of cytoskeletal inhibitors. Wells were placed on a plastic coverslip using an 8 well flexiperm and the assembly was placed inside a tissue culture sterile petridish. mMSCs cells (20,000 cells per 250 μl media) were seeded per well on the coverslip pre-coated with Fn or C I and incubated for 16 hours before being treated with cytoskeletal inhibitors. Immediately after treatment, cells were fixed and stained for actin, microtubulin and nuclear DNA using rhodamine-phalloidin, Alexa488-microtubulin stain and Hoechst dye, respectively, following the manufacturer's instructions and standard staining protocols. Briefly, after two PBS washes the cells were fixed with 4% paraformaldehyde (PFA) for 15 minutes at room temperature. Cell membrane was weakened with 0.1% tritonX100 in 1x PBS for 3 minutes. The staining solution consisted phalloidin and Hoechst dyes. The staining solution was added in each well and left in dark for 30-60 minutes at room temperature followed by washings with 0.05% tween-20. The sample was observed with a

fluorescence microscope. The cell nucleus was observed as a blue stain, the actin filaments were observed as a red stain, while the microtubulin was observed as a green stain. Images were taken with a Zeiss AxioObserver Z1 inverted microscope at 40x magnification, keeping the same exposure for all images and analyzed using Image J software to obtain the mean gray-scale values.

6.2.9 Analyzing endocytic pathways. Cells were treated with inhibitors for endocytosis 16 hours post cell attachment prior to transfection to determine the endocytotic pathways active in cells plated on Fn and C I coated surfaces. Clathrin-mediated endocytosis was inhibited by using 10 μg/ml chlorpromazine, caveolae-mediated endocytosis was inhibited using 200 μM genistein and macropinocytosis was inhibited using 100 μM Amiloride hydrochloride. A 30 minutes pretreatment was given followed by incubation with polyplexes for 4 hours in presence of inhibitors. The media was then replaced with fresh media. Gene expression and internalization were analyzed as described above. Cell proliferation after inhibitor treatment was analyzed 4 hours and 48 hours post transfection using above-mentioned method.

6.2.10 Statistics. All statistical analysis were performed using the computer program Instat (GraphPad, San Diego, CA). Experiments were statistically analyzed using the Tukey test, which compares all pairs of columns, Dunnet test which compares all columns versus a control column or the unpaired t-test (two tail p-value) which compares two columns, as mentioned in the figure legend. All test were done using a 95% confidence interval.

6.3 Results and Discussion

6.3.1 Clathrin-mediated endocytosis mediates efficient gene transfer to mMSCs

As shown in chapter 3 the endocytosis rate did not explain why mMSCs plated on Fn coated surfaces had enhanced gene transfer over uncoated and C I coated surfaces. Hence, we turned to determine if the specific endocytosis pathway used for uncoated, C I coated and Fn coated surface was different.

Because the reagents used to block specific endosomal pathways require the use of pharmacological inhibitors, we wanted to ensure that they were not toxic to the cells. We considered 65% percent viability an acceptable viability to conduct our assay. The treatment with all endosomal inhibitors and polyplexes was found to have at least 65% percent viability (**Figure 6-1**) compared to untreated cells. Inhibition of macropinocytosis, caveole-mediated endocytosis and clathrin-mediated endocytosis in mMSCs played a role in the internalization and the overall gene transfer efficiency of PEI/DNA complexes. To be able to compare the effect of the inhibitors directly, the data was normalized to make the no treatment condition (NT) for each surface coating as one. Inhibition of macropinocytosis resulted in a statistical ($p < 0.001$) increase in gene expression on all surfaces, indicating that directing internalization via other pathways results in more efficient intracellular trafficking (**Figure 6-2A**). The increase in transgene expression was highest for cells plated on C I coated surfaces (10-fold increase), indicating that for cells plated on C I more polyplexes are actively internalized and routed using this endosomal pathway. Inhibition of macropinocytosis resulted in a statistical decrease of internalized polyplexes for all the surfaces ($p < 0.001$), confirming that all surfaces promote internalization through this pathway (**Figure 6-2B**).

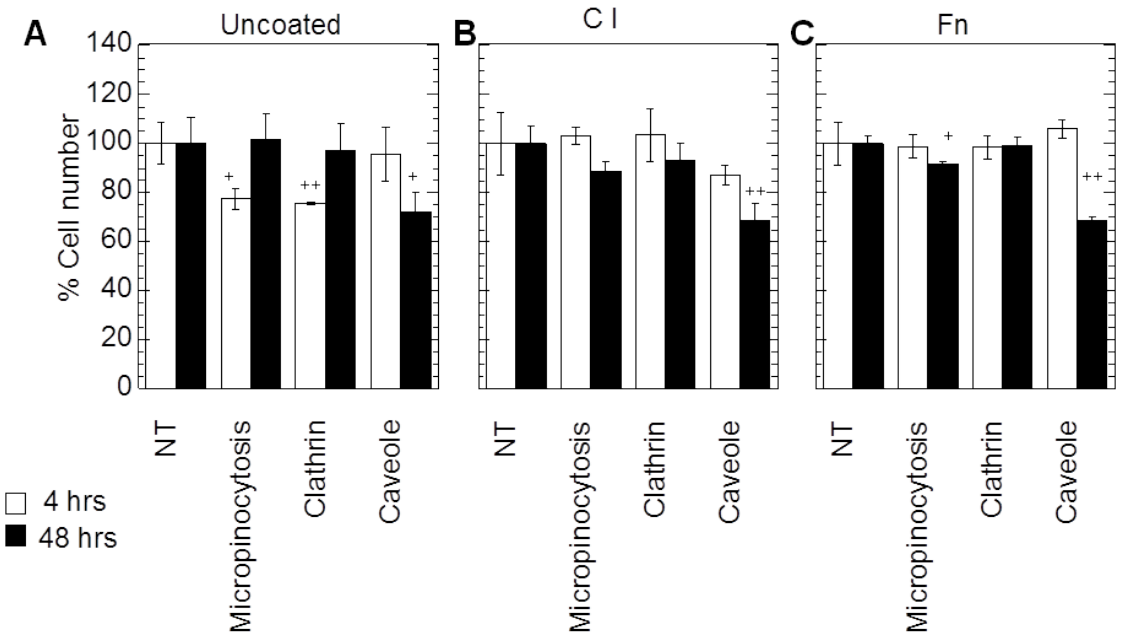

Figure 6-1: Cell viability after endocytosis inhibitor treatment. Cells were plated on uncoated (**A**), or C I coated (**B**) or Fn coated (**C**) surfaces. Cells were pretreated with the inhibitors for 30 minutes followed by incubation with the DNA/PEI polyplexes for 4 hours in presence of the inhibitors. Cell viability was analyzed at 4 and 48 hours post addition of the polyplexes using the MTT assay. Statistical analysis was done using Dunnett multiple comparison test, which compares each treatment condition to the control. The symbols + and ++ represent the significant change to the level of $p < 0.05$ and $p < 0.01$, respectively

Inhibition of clathrin-mediated endocytosis resulted in a statistical decrease in gene expression for cells plated on uncoated and Fn coated surfaces (p at least < 0.01) and no change in gene expression for cells plated on C I coated plates (**Figure 6-2A**). Internalization of polyplexes after clathrin-mediated endocytosis inhibition resulted in a significant decrease in polyplex internalization for all the surfaces tested ($p < 0.001$, **Figure 6-2B**). Since gene transfer was not affected after clathrin inhibition on C I, this indicated that clathrin is not an effective route for gene transfer on C I. On the other hand, the significant decrease in gene transfer after clathrin-

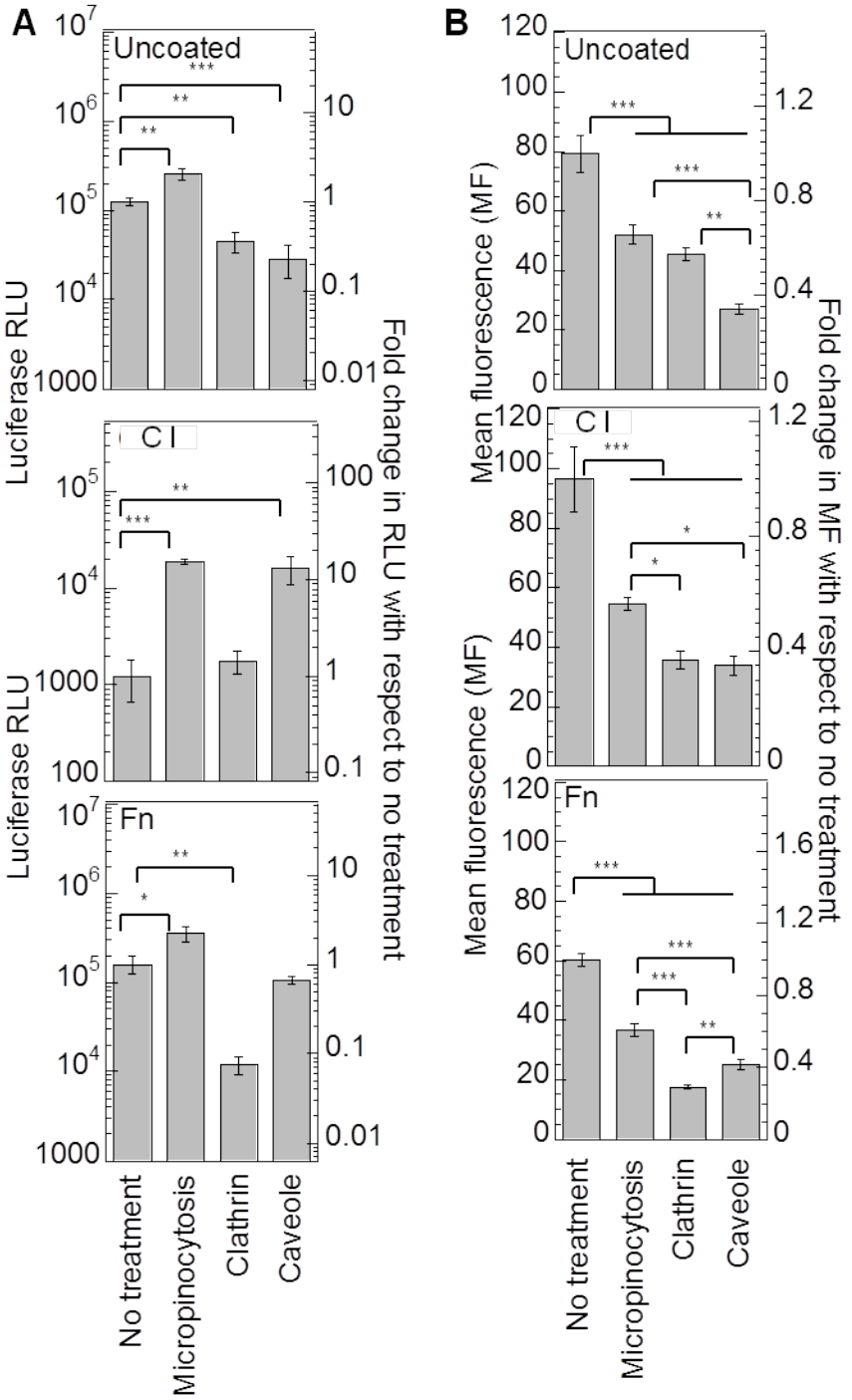

Figure 6-2: Effect of endocytic pathways in transgene expression and polyplex internalization. Cells were plated on uncoated, C I (50 µg/ml) coated or Fn (40 µg/ml) coated surfaces for 14-16 hours prior to treating the cells with amileroide, chlorpromazine and genistein to inhibit macropinocytosis, clathrin and caveolae mediated endocytosis.
Cells were pretreated for 30 minutes following which bolus transfection was done with our without YOYO-1 labeled polyplexes for 2 or 4 hours in presence of inhibitors. Medium was replaced 2 or 4 hours after transfection with treatment. Transgene expression was analyzed 48 hours post transfection using luciferase assay (**A**) and internalization was assessed 2 hours post transfection using flow cytometry (**B**). 7000 total events were analyzed per sample. Gating was done such that the negative control had 5% positive events. The transgene expression obtained after treatment with specific inhibitor was compared to untreated sample using the unpaired t-test (two tail p value). Statistical analysis for internalization was done using Tukey-Kramer multiple comparison test which compares all pairs within the same protein coat. The symbols *, **, *** represents the significant change to the level of $p < 0.05$, $p < 0.01$, and $p < 0.001$, respectively.

mediated endocytosis inhibition (92% decrease) on Fn coated surfaces, suggested that this pathway is critical for efficient gene transfer to cells plated on Fn.

Inhibition of caveolae-mediated endocytosis resulted in a significant decrease in transgene expression for cells plated on uncoated surfaces ($p < 0.001$), a 13.2-fold increase for cells plated on C I coated plates, and no significant change for cells plated on Fn coated plates, indicating that caveolae-mediated endocytosis is activated to different extends for mMSCs seeded on the different surfaces (**Figure 6-2A**). Internalization of polyplexes after caveolae-mediated inhibition resulted in a significant decrease in polyplex internalization for all the surfaces tested ($p < 0.001$, **Figure 6-2B**). Interestingly, although caveolae-mediated endocytosis plays a role in internalization on Fn, it does not affect transgene expression, further suggesting that this internalization pathway is not an effective route for gene transfer to mMSCs plated on Fn. Overall, our results show that for mMSCs plated on protein coated surfaces, polyplexes internalized through caveolae-mediated endocytosis do not lead to efficient gene transfer, while polyplexes internalized through clathrin-mediated endocytosis result in efficient gene transfer.

Although genistein is widely used as a caveolae-mediated endocytosis inhibitor, it is a tyrosine kinase inhibitor that has been reported to affect cell growth and proliferation [134]. Thus the observed changes in internalization and overall gene transfer efficiency could be due to changes in proliferation. Likewise treatment with chlorpromazine does not specifically block clathrin-mediated endocytosis. It is also an antipsychotic and acts as an antagonist (blocking agent) on different postsynaptic receptors [135]. However, since all the different conditions were treated the same, we assumed that differences between protein coatings are beyond changes in proliferation.

Clathrin-mediated endocytosis has been previously reported to result in more efficient transgene expression than macropinocytosis and caveolae-mediated endocytosis for histidylated polylysine/DNA polyplexes [136] and alginate-chitosan particles [86]. The efficacy of the clathrin pathway in transfection has been attributed to complexes being trafficked to the endosome where they are released by the proton-sponge effect, while caveolae mediated endocytosis can lead to vesicle entrapped complexes [86]. In addition, a recent study has shown that the effective mode of endocytosis depends on the cell type along with the type of PEI used [137]. In COS-7 cells, the clathrin dependent pathway was observed as the main contributor to efficient gene transfer [137]. In HUH-7 cells, gene transfer by linear PEI polyplexes occurred mainly via the clathrin dependent route, whereas both pathways mediated transfection by branched PEI polyplexes [137]. In HeLa cells, both pathways were observed to mediate successful transfection with the caveole pathway being more efficient [137]. Our results indicate that the effective route of internalization can be modulated by the cellular microenvironment.

6.3.2 Reduction of cytoskeletal tension and microtubule polymerization enhances gene transfer to mMSCs

To further investigate the mechanism by which the extracellular matrix environment affects non-viral gene transfer to mMSCs, the role of the cellular cytoskeleton in cells plated on Fn coated, C I coated and uncoated surface was investigated. In particular, we investigated the role of actin polymerization, myosin-actin interactions and the microtubular network because they have been previously implicated in the modulation of non-viral gene transfer or endocytosis. To visualize and quantify the changes in the cytoskeleton network of cells after inhibitor treatment, cells were plated on Fn and C I coated surfaces, treated with the inhibitor, fixed and stained for actin,

microtubules and the nucleus. Images were taken at 40x magnification, and analyzed to obtain the grey scale values. After treatment with cytochalasin D (CD), an actin destabilizing agent, the cellular actin network was severely compromised for cells plated on Fn as well as C I (**Figure 6-3B and 6-4B**). However, no change was observed in the actin (**Figure 6-3E and 6-4E**) and microtubulin (**Figure 6-3F and 6-4F**) fluorescence intensity. After treatment with nocodazole (Noc), a microtubule polymerization-destabilizing agent, no significant change was observed for microtubule fluorescence (**Figure 6-3F and 6-4F**). However, the cellular morphology was significantly affected on both C I and Fn coated surfaces with cell becoming rounder and less spread (**Figure 6-3D and 6-4D**). For cells plated on Fn coated surfaces a significant increase in actin stress fibers was observed after Noc treatment (**Figure 6-3D, E,** $p < 0.05$). After treatment with butanedione monoxime (BD), an inhibitor of the actin-myosin interaction, a significant increase in actin stress fibers was observed for cells plated on Fn coated surfaces (**Figure 6-3E**, $p < 0.05$), but not for cells plated on C I coated surfaces (**Figure 6-4E**, $p < 0.05$).

As with the endocytosis inhibitors, we wanted to ensure that the cells plated on C I coated, Fn coated and uncoated surfaces and treated with cytoskeleton inhibitors were viable before conducting our transfection studies. We considered 65% viability an acceptable viability to conduct our assay using cytoskeletal inhibitors. We found that the treatment with CD and BD inhibitors had at least 65% percent viability (**Figure 6-5**) compared to untreated cells. However, treatment with Noc had 50% viability at 48 hours. This is likely due to the prevention of cell division since the microtubules are key contributors of mitosis. Nevertheless, Noc has been previously used in gene transfer studies [80-82, 84] and was used here to test the role of the microtubular network.

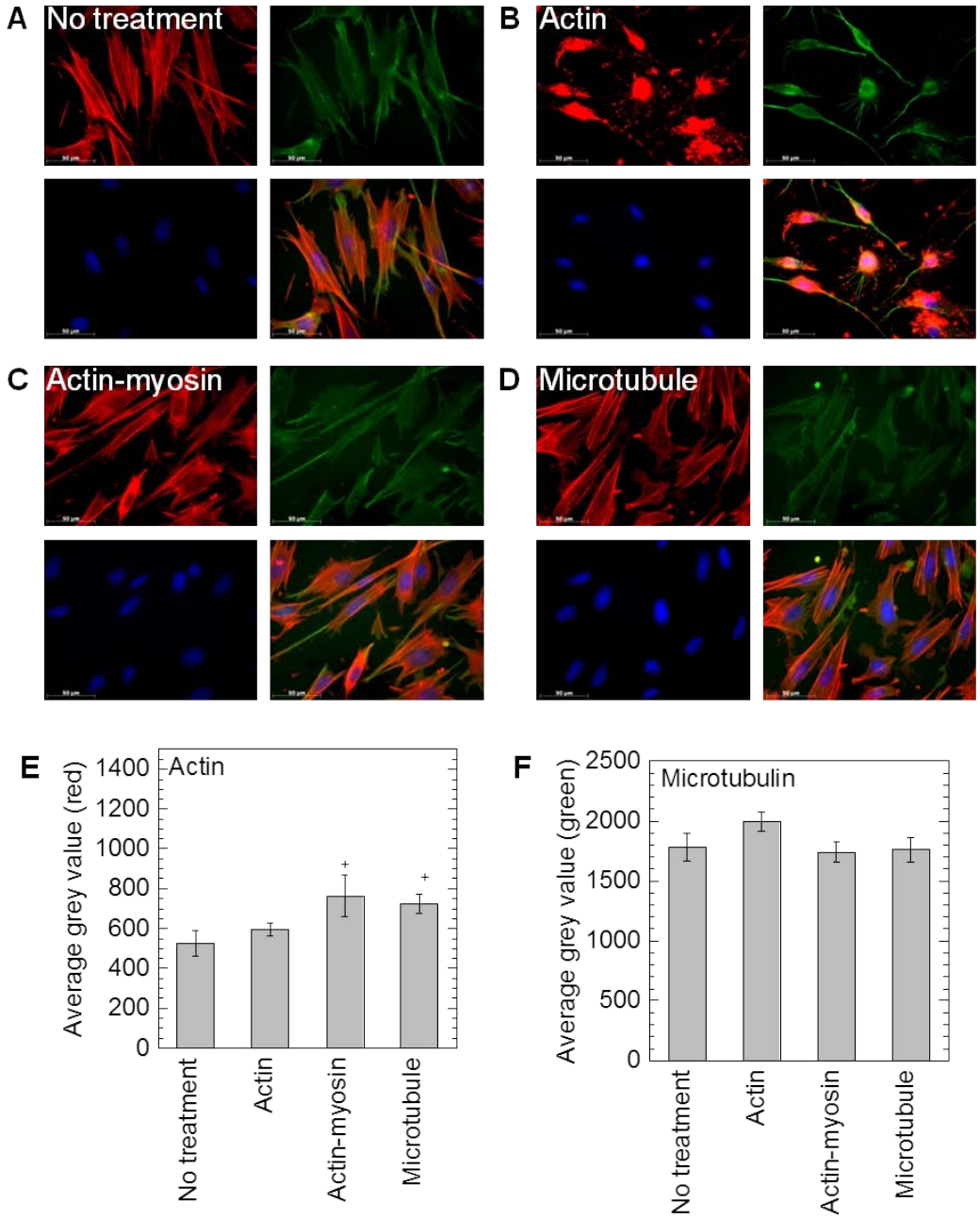

Figure 6-3: Effect of treatment with cytoskeletal inhibitors on actin and microtubular networks on Fn. Cells were seeded on Fn coated surfaces and 14 hours post cell seeding treatment with no inhibitor (**A**) or inhibitors against the actin network (**B**), actin-myosin interactions (**C**) and the microtubular network (**D**) were given. Immediately post inhibitor treatment, changes in cell morphology were visualized through staining for actin using rhodamine-phalloidin, microtubulin using Alexa488 conjugated anti α-tubulin stain and for DNA using Hoechst dye. Images were taken with a Zeiss AxioObserver Z1 inverted microscope at 40 x magnification, and analyzed with Image J to obtain mean gray scale value for the actin (red), tubulin (green) and DNA (blue). The mean gray scale values for actin and tubulin were normalized with mean gray values for DNA and plotted (**E and F,** respectively). Statistical analysis was done using Tukey-Kramer multiple comparisons, which compares all pairs within the same protein coat. The symbols * represents the significant change to the level of $p < 0.05$.

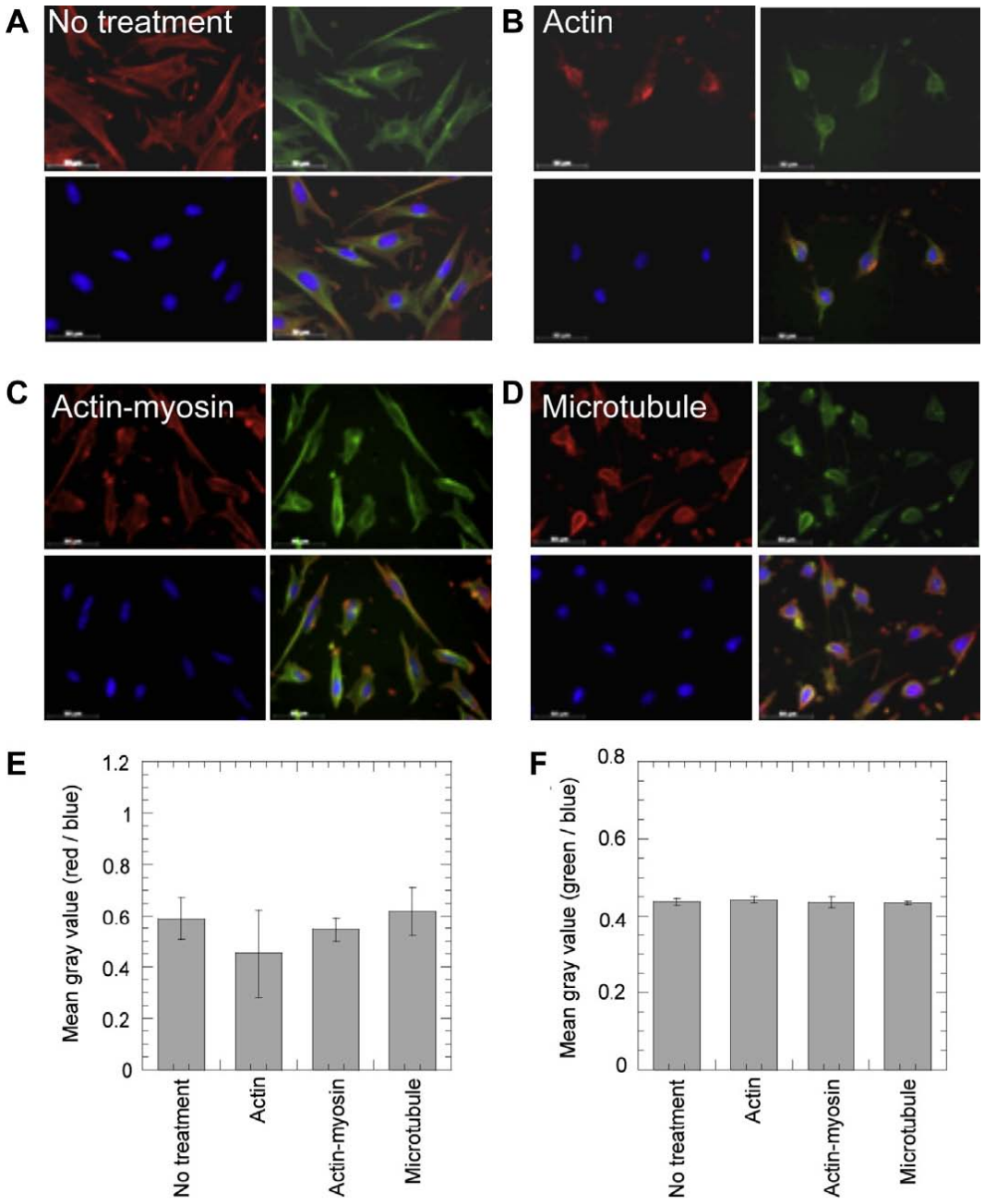

Figure 6-4: Effect of treatment with cytoskeletal inhibitors on actin and microtubular networks on C I. Cells were seeded surfaces precoated with C I and 14 hours post cell seeding no treatment (**A**) or treatment with inhibitors against the actin network (**B**), actin-myosin interactions (**C**) and the microtubular network (**D**) were given. Immediately post inhibitor treatment, changes in cell morphology were visualized through staining for actin using rhodamine-phalloidin, microtubulin using Alexa488 conjugated anti α-tubulin stain and for DNA using Hoechst dye. Images were taken with a Zeiss AxioObserver Z1 inverted microscope at 40 x magnification, and analyzed with Image J to obtain mean gray scale value for the actin (red), tubulin (green) and DNA (blue). The mean gray scale values for actin and tubulin were normalized with mean gray values for DNA and plotted (**E and F**, respectively)

Disruption of actin stress fibers statistically increased the transgene expression for cells plated on uncoated and Fn coated surfaces ($p < 0.05$), while the expression on C I was severely inhibited ($p < 0.01$, **Figure 6-6A**). Internalization of polyplexes after actin stress fiber disruption was enhanced for cells plated on Fn ($p < 0.01$), but no significant difference was observed for cells plated on uncoated or C I coated surfaces ($p < 0.05$, **Figure 6-6B**). This indicates that for cells seeded on Fn coated surfaces, which had poor internalization (**Figure 4-2B**), the disruption of the actin network enhanced endocytosis. Since the enhancement in endocytosis resulted in enhanced gene transfer, it is likely that this internalization was through the clathrin pathway, since this pathway showed efficient gene transfer for cells seeded on Fn coated surfaces. Further, for cells seeded on C I, the actin network appeared critical for gene transfer. The already inhibited gene transfer to mMSCs seeded on C I coated surfaces was further inhibited when the actin stress fibers were disrupted. Together, these results suggest that cells seeded on Fn have a more significant actin network than cells seeded on C I, and that the amount of actin stress fibers to achieve efficient gene transfer goes through a maximum where too much actin reduces gene uptake (Fn case) and too little actin reduces effective intracellular transfer (C I case). Therefore, the disruption of actin network on Fn reduces stress fibers and cellular tension, and our results indicate that this promoted gene transfer.

Disruption of actin-myosin interactions statistically increased transgene expression for cells seeded on uncoated and Fn coated surfaces, while the expression on C I was unchanged (**Figure 6-6A)**. However, the internalization of polyplexes was significantly decreased after disruption of the actin-myosin interactions on all surfaces (**Figure 6-6B**). These results suggest that for cells plated on Fn coated surfaces decreasing the contractility of the cell increases intracellular

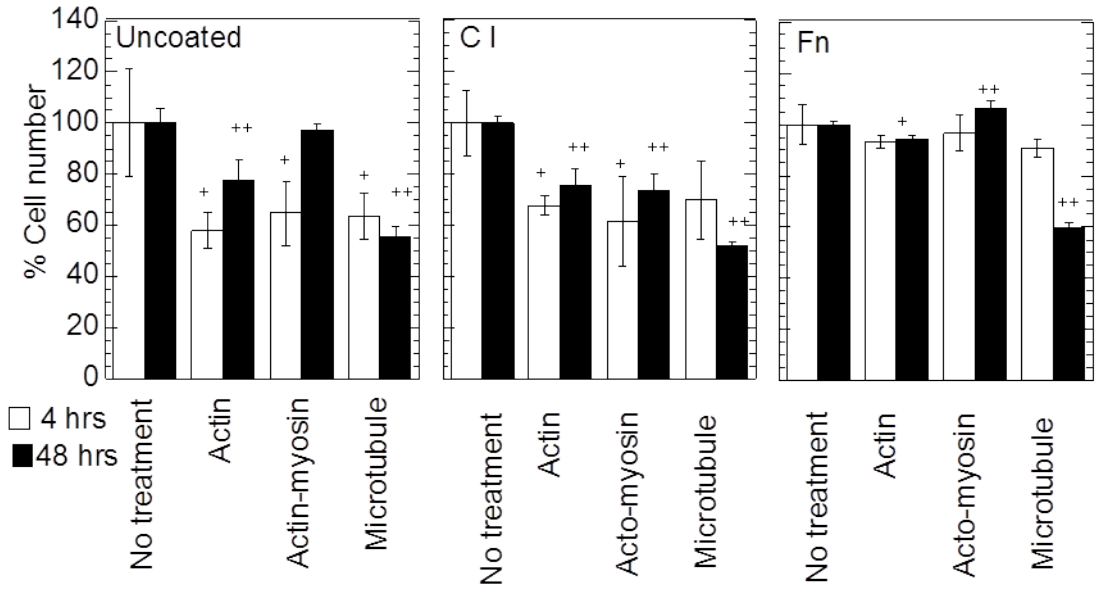

Figure 6-5: Cell viability after cytoskeleton inhibitor treatment. Cells were plated on uncoated (**A**), or C I (50 μg/ml) coated (**B**) or Fn (40 μg/ml) coated (**C**) surfaces. Cells were treated for 30 minutes, after which media was replaced and polyplexes added. Cell viability was analyzed 4 and 48 hours post addition of polyplexes using MTT assay. Statistical analysis was done using Dunnett multiple comparison test, which compares each treatment condition to the control. The symbols + and ++ represent a significant change to the level of $p < 0.05$ and $p < 0.01$, respectively

trafficking of the polyplexes toward the nucleus. Further, the results suggest that cellular contractility, a result of actin-myosin interactions, is low for cells seeded on C I coated surfaces since there is no effect when they are disrupted, while actin-myosin interactions are high for cell seeded on Fn coated surfaces since when they are disrupted enhanced gene transfer occurs.

Disruption of microtubule polymerization significantly increased transgene expression on uncoated, C I coated and Fn coated surfaces ($p < 0.001$, **Figure 6-6A**), while the polyplex internalization significantly decreased on Fn and uncoated surfaces ($p < 0.05$, **Figure 6-6B**). The microtubular network has been implicated with caveolae-mediated endocytosis [85] and lysosomal trafficking of endosomes [83]. Thus, the increase in gene transfer on all surfaces can be attributed to reduced trafficking to the lysosomes and reduced DNA intracellular degradation. Since the enhancement in gene transfer was observed for all the surface coatings, the effect appears independent of protein surface coating.

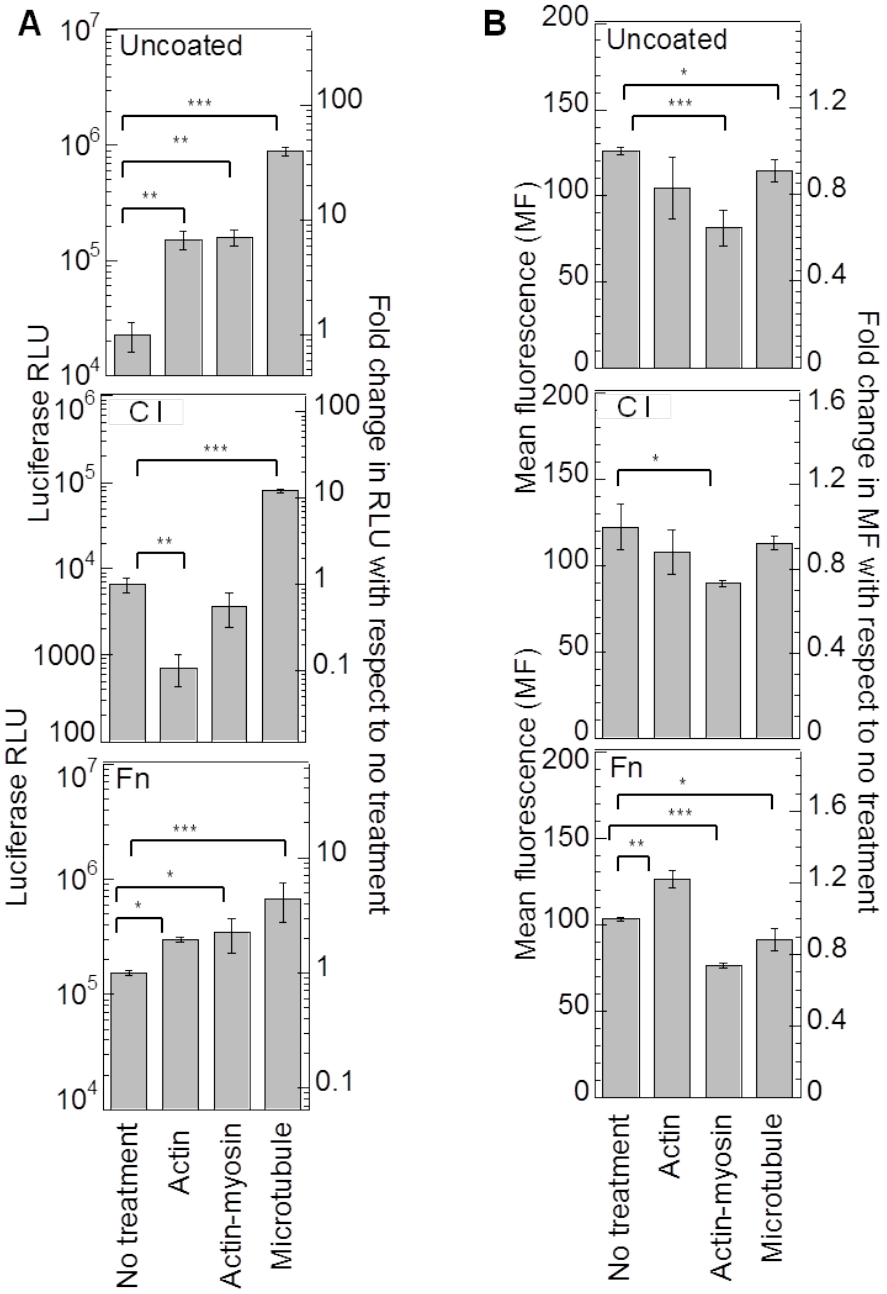

Figure 6-6: Role of cell cytoskeleton in transgene expression and polyplex internalization. Cells were plated on uncoated, C I (50 µg/mL) coated or Fn (40 µg/mL) coated surfaces for 14-16 hours prior to treating the cells with CD, BDM and Noc for 30 minutes to inhibit actin polymerization, myosin ATPase and microtubule polymerization, respectively. Immediately after treatment with inhibitor, the medium was replaced and bolus transfection was done with or without YOYO-1 labeled polyplexes. Transgene expression was analyzed 48 hours post transfection using luciferase assay (**A**) and internalization was assessed 2 hours post transfection using flow cytometry (**B**). A total of 7000 events were analyzed per sample. Gating was done such that the negative control had 5% positive events. The transgene expression and internalization obtained after specific inhibitor treatment were statistically compared with untreated sample using the unpaired t-test (two tail p value). The symbols *, **, and *** represent a significant change to the level of $p < 0.05$, $p < 0.01$, and $p < 0.001$, respectively

As with the inhibitors for the endocyotic pathways, the action of the cytoskeletal inhibitors is not solely specific to cell cytoskeleton and affect the related pathways. Nocodazole interferes with

microtubule polymerization affecting related processes such as mitotic spindle formation [138]. This explains the significant decrease in proliferation observed 48 hours post nocodazole treatment (**Figure 6-5**). Cytochalasin D (CD) which is a potent inhibitor of actin polymerization, has also been reported to arrest the cell cycle at G1-S transition by activating the p53-dependent pathways [139]. However, the concentration or time period for the inhibitor treatments used in our investigation have been widely used to study cell cytoskeleton specifically [140, 141], and are different than those used for related actions such as cell cycle arrest mentioned before [138, 139].

2,3-Butanedione monoxime (BD) which is widely used as a skeletal myosin II inhibitor has been shown be a cytoprotectant [142] as well as affects multiple mechamisms such as muscle contraction, ionic current flow and synaptic transmission [143]. As with the endocytotic inhibitors, all the different conditions were treated the same and we believe that differences between protein coatings are beyond changes in proliferation.

These studies indicate that the structural ECM constituents affect the efficiency of non-viral gene transfer by modulating cell cytoskeletal dynamics, uptake mechanisms and the resultant intracellular trafficking. An in depth understanding of the underlying mechanisms of gene transfer in cells would provide cues to design cell pretreatments, develop scaffolds and gene delivery protocols, which are able to enact efficient gene transfer.

6.4 Conclusion

In conclusion, non-viral gene transfer to mMSCs plated on surfaces coated with C I or Fn resulted in different levels of gene expression and polyplex internalization. The differences observed are due to differences in the endosomal pathways used for polyplex uptake and

differences in the cellular cytoskeleton of the cell. In particular, we found that efficient gene transfer to mMSCs plated on protein-coated surfaces is achieved when polyplexes are internalized through clathrin-mediated endocytosis and that Fn promotes clathrin-mediated endocytosis. Further, overall transgene expression for mMSCs plated on C I coated surfaces was inhibited and this inhibition was attributed to the promotion of internalization through caveolae-mediated endocytosis and reduced actin polymerization. Lastly, in this chapter we have shown that the amount of cellular tension affects non-viral gene transfer with decreased actin-myosin interactions resulting in decreased internalization on all surfaces. The understanding of how the cellular microenvironment affects the efficiency of non-viral gene transfer to MSCs can aid in the design of effective strategies to genetically modify these cells and achieve their therapeutic potential.

Chapter 7

RhoGTPases Modulate Non-Viral Gene Delivery

7.1 Introduction

Chapter 4 and 5 have elucidiated that cellular microenvironment modulates non-viral gene delivery to mouse mesenchymal stem cells (mMSCs). Specifically six different ECM proteins and their combinations were screened for their ability to enhance gene transfer to mouse mesenchymal stem cells (mMSCs) using poly(ethylenimine) polyplexes. Proteins that promoted well spread cells (e.g. fibronectin and collagen IV) resulted in polyplexes being trafficked to the nucleus and enhanced gene transfer, while those that resulted in less spread cells (e.g. collagen I) resulted in polyplexes that did not colocalize with the nucleus and inhibited gene transfer [144]. In chapter 6, on comparing the internalization pathway of polyplexes for cells seeded on fibronectin or collagen I, different endocytic pathways were found to be used with clathrin-mediated endocytosis being the primary pathway used for cells plated on fibronectin [145]. Further, polymerized actin, actin-myosin interactions, and the microtubular network were found

to influence non-viral gene transfer to different extents for cells seeded on fibronectin versus collagen I [145].

Structural components of the ECM such as Fn actively mediate crosstalk between the ECM and RhoGTPases by associating with cell surface receptors, namely integrins [89] and syndecans [129], which effectively engage RhoGTPases leading to adhesion signaling [109, 130].

The RhoGTPases along with their functions and downstream effectors have been described in detail in chapter 3. In active GTP-bound state, RhoGTPases interact with and stimulate the activity of effectors which participate in signaling cascades that coordinate various cellular processes such as migration, proliferation [92], gene expression [93] and cytoskeletal organization. Specifically, Cdc42 mediates cell polarity and filipodia, Rac mediates protrusion of lamellipodia, and Rho maintains cell adhesion during migration [99]. Furthermore, bacterial internalization [100, 101], adenovirus internalization [102] and recently receptor-mediated internalization of transferrin [103] has been shown to be a resultant of host cell actin cytoskeleton manipulation at level of RhoGTPases. However, the role of RhoGTPases in non-viral gene transfer has not been previously investigated.

We had hypothesised that the Rho family of small GTPases play a role in the mechanism by which ECM modulates gene transfer in two dimensions (Hypothesis 3). The research study covered in this chapters examines if the interplay between Fn and integrins communicated via the RhoGTPases [95] and the resultant signaling cascades affecting cytoskeletal dynamics, endocytosis, gene transcription and proliferation regulated non-viral gene transfer in cells plated on Fn. Herein, to begin to understand the cellular molecules involved in modulating gene delivery to mMSCs plated on Fn coated surfaces, the role of Rho, Rac and Cdc42 RhoGTPases in the uptake and transgene expression of DNA/PEI polyplexes was studied. The RhoGTPases

were specifically inhibited using chemical inhibitors and dominant negative gene products, as well as activated to determine their role in gene transfer and DNA/PEI internalization. *The research related to AIM 3 and Hypothesis 3 was covered in this chapter.*

7.2 Materials and methods

7.2.1 Cell Culture. Mouse bone marrow cloned mesenchymal stem (D1, CRL12424) were purchased from ATCC (Manassas, VA, USA). Cells were maintained in Dulbecco's modified eagle's medium (Sigma-Aldrich, St. Louis, MO) containing 10% bovine growth serum (BGS, Hyclone, Logan, Utah) and 1% penicillin/streptomycin antibiotics (Invitrogen, Grand Island, NY) and cultured at 37˚C and 5% CO_2.

7.2.2 Protein coating. Stock solution fibronectin (1 mg/ml, Millipore, Billerica, MA) was diluted to 40 μg/ml in phosphate buffered saline (PBS), and added in each well of a tissue culture plate. The plate was incubated over night at 4˚C in a humid environment, followed by incubation at 37˚C for 2 hours [146]. The solution was removed and wells were washed twice with PBS to remove unbound proteins. Wells were further incubated with BSA (1% in PBS) for 30 minutes at 37˚C followed by two washings with PBS.

7.2.3 Analysis of RhoGTPase activation by fibronectin or collagen I. Poly-dimethoxy silane (PDMS) sheets were made by mixing Sylgard 184 PDMS prepolymer thoroughly in a 10:1 mass ratio of silicone elastomer to curing agent, degassing and casting in a square dish at 60°C overnight. After the cured PDMS sheets were removed, they were cut into strips and oxygen plasma treated using Technics RIE (Reactive Ion Etching) for 3 minutes at 100 mTorr of O2, 100

W or 15 minutes at 200 mTorr of O2, 200 W. The PDMS strips were subsequently placed in a 1:1 v/v methanol and hydrochloric acid solution for 30 minutes, then dried and incubated overnight in a 5% v/v amino-propyl triethoxysilane (APTES, Sigma-Aldrich, St. Louis, MO) solution in ethanol, at room temperature and in inert atmosphere [147]. The sheets were sterilized in 70% ethanol prior to cell plating. The cells were cultured for a day till confluent and then serum starved overnight before exposing them to fibronectin or collagen I coated surfaces. Five minutes before exposing cells to fibronectin or collagen I, sodium orthovanadate (0.1 mM) was added to the cell culture media. Sodium orthovanadate is an inhibitor of protein tyrosine phosphatases and alkaline phosphatases and was used to preserve the phosphorylation of RhoGTPases through inhibiting endogenous phosphatases [109].

The PDMS cell sheets were exposed to fibronectin or collagen I for 20 minutes or 1 hour, which have been shown to be the duration of RhoGTPase activation in different cells after interaction with the extracellular matrix [89, 107-109]. After exposure to ECM protein at 37°C, the strips were placed in Petri dishes on ice and rinsed once with ice cold PBS supplemented with 0.2 mM sodium orthovanadate. The lysis buffer provided with the GLISA kit (Cytoskeleton, Inc., Denver, CO) was modified to include 5 mM sodium orthovanadate, 50 mM sodium fluoride and 0.5 mM phenylmethylsulfonyl fluoride (PMSF), along with 1x protease inhibitor cocktail provided with Kit [109, 148] After aspirating all liquid from the PDMS strips, 100 µl of lysis buffer was added and scraped. Cell lysate was immediately clarified by centrifugation at 9,000 rcf, 4°C for 2 minutes, aliquoted into microcentrifuge tubes and snap frozen in liquid nitrogen, as indicated by the manufacture's protocol. After 1 or 2 days, the frozen aliquots were analyzed and RhoGTPases activity assessed, as per manufacture's protocol.

7.2.4 Chemical inhibition of RhoGTPases. Difficile toxin B (TcdB, List Biologicals, Campbell, CA) was used to pharmacologically inhibit Rho, Rac and Cdc42 [100-102, 104, 149]. Rho was specifically inhibited using cell permeable C3 transferase (C3, Cytoskeleton, Denver, CO) [100, 104, 149]. mMSCs were seeded on fibronectin coated 48 well plates or 24 well plates at cell densities of 20,000 and 50,000 cells/well, respectively. The cells were allowed to attach for 14-15 hours before the media in the wells was replaced with serum free media containing 0-1 μg/ml C3 transferase (C3) or 0-300 ng/ml TcdB for 4 hours. Immediately post treatment, media was changed with serum containing media and DNA/PEI internalization and overall transgene expression studied. To assess RhoGTPase inhibition, cell morphology was analyzed and the respective GLISA assays were performed, immediately after inhibitor treatment.

7.2.5 Chemical activation of RhoGTPases. Cells were allowed to attach on fibronectin-coated plates for 8 hours followed by overnight incubation in serum free media. Rho was pharmacologically activated by incubating cells in presence 25 μg/ml Calpeptin (CP, Cytoskeleton, Inc., Denver, CO) for 10 minutes while Rac and CDC42 were activated by incubating cells in presence of 50 ng/ml Epidermal growth factor (EGF, Cytoskeleton) for 2 minutes. Immediately after treatment cell morphology, internalization and gene expression were analyzed. For analysis of non-viral gene transfer, cells were transfected with polyplexes in serum free media for 2-4 hours, following which media was replaced with serum containing media. Activated Rho, Rac and Cdc42 were confirmed by performing respective activation G-LISA assays (RhoA, Rac1,2,3 and Cdc42 G-LISA Activation Assays; Cytoskeleton) with lysates from activated and control samples as per manufacturer's protocol. Overnight serum starved cells were treated as the control sample. To assess activity, samples were subsequently treated with 25

μg/ml calpeptin for 10 minutes or with 50 ng/ml EGF for 2 minutes. Activity of RhoA, Rac and Cdc42, respectively, was assessed using a GLISA assay and normalized to values obtained for control lysates.

7.2.6 Transient inhibition and activation of RhoGTPases. Specific inhibition and activation of the RhoGTPases was done by a method described by Burnham et al. [101] with minor modification. Plasmids expressing dominant negative Rac1 (pcDNA3-EGFP-Rac1-T17N), RhoA (pcDNA-EGFP-RhoA-T19N) and Cdc42 (pcDNA-EGFP-Cdc42-T17N), as well as plasmids expressing constitutively active mutants of RhoA (pcDNA-EGFP-RhoA-Q63L), Rac1 (pcDNA-EGFP-RhoA-Q61L) and Cdc42 (pcDNA-EGFP-Cdc42-Q61L) were kindly provided by Dr Garry Bokoch (The Scripps Research Institute, La Jolla, CA) [150, 151]. $5x10^4$ and $25x10^4$ cells were plated per well in a 24 and 6 well plate respectively, and cultured for 24 hours prior to transfection. For every 1 μg of DNA, 2 μl of Lipofectamine^{TM} 2000 transfection reagent was added to the DNA solution, vortexed for 15 seconds and incubated at room temperature for 20 minutes. Complexes were added directly to the medium of the plated cells at a final DNA concentration of 1 μg per well for 24 well plates and 2.5 μg per well for 6 well plates. Analysis of GFP expression in transfected cells using FACS showed 30-40% cells to be successfully transfected with dominant negative or constitutively active genes and control plasmid (**Figure 7-9**). 24 hours post transfection, cells were harvested and used to study the effect of RhoGTPase inhibition or activation on transgene expression as well as internalization. Activation or inhibition was analyzed by assessing RhoGTPases activity using respective GLISA assays (RhoA, Rac and Cdc42 G-LISA Activation Assays; Cytoskeleton) as per manufacturer's protocol. Cells transfected with pEGFP using Lipofectamine^{TM} 2000, were used as control for

studies involving transfection with dominant negative and constitutively active genes. For assessing activation, 24 hours post transfection with constitutive active genes, cells were serum starved overnight and then harvested for performing respective activation G-LISA assays and studying morphology. For assessing inhibition, 24 hours post transfection with dominant negative genes, cells were replated on fibronectin coated surface overnight and harvested for performing GLISA assays and studying morphology.

7.2.7 Transfection. pEGFP-luc plasmid was purchased from clontech (Palo Alto, CA) and expanded using a Giga Prep Kit from Qiagen following the manufacturer's protocol. Linear poly-(ethylene imine) (25kDa, PEI) was purchased from Polysciences (Warrington, PA). The cells were allowed to attach and cultured under various conditions as per required for the experiments mentioned. For gene transfer studies, DNA/PEI polyplexes were formed by mixing equal volumes of plasmid DNA with PEI**.** For every 1 μg of DNA, 1.65 μg of PEI was added to the DNA solution to get N/P of 12, vortexed for 15 seconds and incubated at room temperature for 15 minutes. Polyplexes were added directly to the medium of the plated cells at a final DNA concentration of 0.5 μg for 48 well plates. Salt was added directly to the wells post addition of transfection solution to get the final concentration of 150 mM NaCl. Transfection was quantified at 48 hours post transfection using the Promega Luciferase Assay System following the manufacturer's instructions. Subsequently, the total amount of protein in samples was analyzed using Peirce BCA assay with or without compat-Able protein assay preparation kit as per manufacturer's protocol. Experiments were carried out in triplicates and results were expressed as relative light units (RLU) per mg of cell protein.

7.2.8 Internalization of polyplexes. Plasmid DNA (pEGFPluc) and the fluorescent DNA-intercalator YOYO-1 or YOYO-3 were mixed at a ratio of 1 dye molecule per 50 base pairs and allowed to complex for 60 minutes at room temperature. YOYO-1 or YOYO-3 labeled DNA was then used to prepare PEI/DNA complexes at a N/P of 12, bolus transfection was performed and cells were exposed to polyplexes for 2 hours. For YOYO-1 labeled complexes, cells were washed with PBS, trysinized with 50 µl of 0.25% trypsin-EDTA and suspended in 350 µl of 0.04% tryphan blue in 1% BGS in PBS to quench the flourescence of extracellular associated DNA. For YOYO-3 labeled complexes, cells were washed twice for 10 minutes with cellscrub to remove extracellular associated DNA, trysinized and suspended in 1% BGS in PBS. YOYO-1 fluorescent cells having were detected by flow cytometry with a FACScan X and data was analyzed with CELLQuest (Beckton Dickinson). YOYO-3 fluorescent cells were detected by flow cytometry using BD LSR II and data was analyzed with FACSDiVa (Beckton Dickinson). Experiments were performed in triplicates analyzing 7000 or 10000 total events per sample.

7.2.9 Microscopy and quantification of stress fibers. Cells were plated on fibronectin coated plastic coverslips prior to culture. Immediately after treatment with Rho protein activators or inhibitors, cells were fixed with 5% paraformaldehyde for 15 minutes and permeabilized with 0.1% tritonX100 in 1x PBS for 3 minutes. The cells were stained for actin using Alexa488-phalloidin and for DNA using Hoechst 33258 dye. The staining solution was added in each well and left in dark for 30-60 minutes at room temperature followed by washings with 0.05% tween-20. Images were taken with a Zeiss AxioObserver Z1 inverted microscope at 100x magnification. The number of stress fibers per cell was quantified by counting the individual fibers observed in 100x pictures taken of cells in the respective condition.

7.2.10 Statistical methods. All statistical analysis were performed using the computer program Instat (GraphPad, San Diego, CA). Experiments were statistically analyzed using a one-way ANOVA followed by a post-hoc test if the ANOVA result was $p < 0.05$. Experiments were statistically analyzed using the Tukey test, which compares all pairs of columns using a 95% confidence interval or using the Dunnet test which compares all columns versus a control column or using the unpaired t-test (two tail p value), which compares two different columns. Statistical significance was determined using a 95% confidence interval. Data was plotted as the mean of at least three independent measurements and standard deviation.

7.3 Results and discussion

7.3.1 Fibronectin exposure activates RhoGTPases in mMSCs.

The activation of RhoGTPases in mMSCs by fibronectin was assessed using fluorescence immunohistochemistry and molecular assays. Fluorescence immunohistochemistry of the actin cytoskeleton revealed that cells plated on fibronectin-coated surfaces resulted in an increase in stress fibers compared to cells plated on tissue culture plastic (**Figure 7-1A and B**, $p < 0.05$), indicative of active RhoGTPases. The level of RhoGTPase activation was determined using GLISA assays for RhoA, Rac1,2,3 and Cdc42. To ensure that the observed activation was due to the interaction of the cell with the fibronectin coated surface and not the dynamics of cell spreading, cells were allowed to attach and spread on amine functionalized PDMS sheets. Following cell spreading, the cell sheet was flipped on top of fibronectin coated or uncoated tissue culture plastic and incubated for 20 minutes or 1 hour. At 20 minutes of exposure to fibronectin-coated surfaces, RhoA was significantly activated ($p < 0.05$), while Cdc42 was not

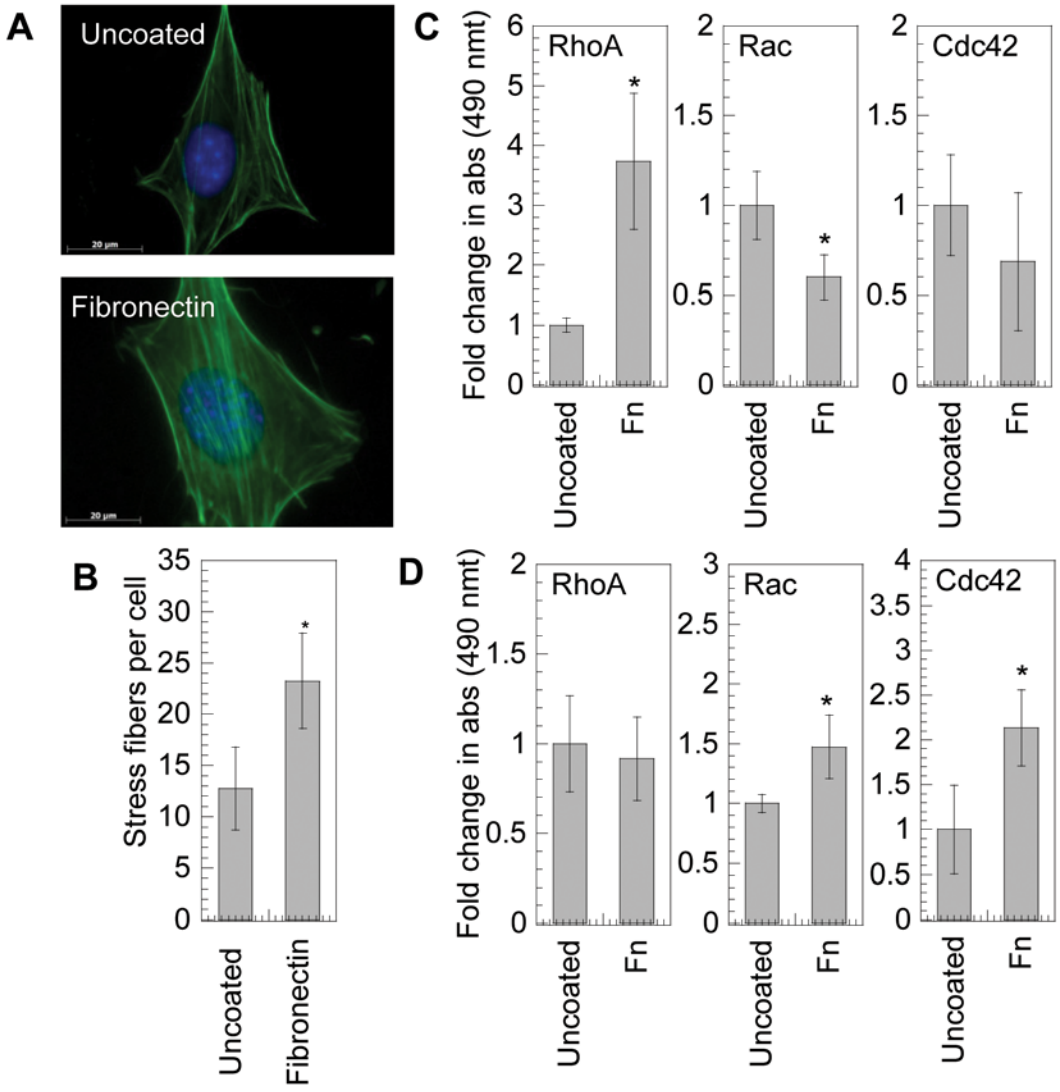

Figure 7-1: RhoGTPase activation on fibronectin. (**A**) mMSCs were plated on uncoated or fibronectin (40 µg/mL) coated surfaces for 16 hours and cell morphology was studied by staining cells for actin using Alexa488 conjugated phalloidin (green), and for DNA using Hoechst 33258 dye (blue). Images were taken with a Zeiss AxioObserver Z1 inverted microscope at 100x magnification. (**B**) Stress fiber quantification. (**C and D**) Active RhoGTPase quantification was performed using GLISA specific for RhoA, Rac1,2,3 and Cdc42. Cells were cultured in PDMS sheets and allowed to attach and spread before exposing them to protein modified plastic for 20 minutes or 1 hour. The average of three samples was plotted. The level of active RhoGTPase in samples exposed to fibronectin was compared with untreated sample using the unpaired t-test (two tail p value). The symbol * represents a significant change to the level of $p < 0.05$. The error bars represent the standard deviation in all plots.

activated and Rac1,2,3 was inhibited compared to exposure to bare tissue culture plastic (**Figure 7-1C**). After 1 hour exposure to fibronectin-coated surfaces, Rac1,2,3 and Cdc42 were significantly activated ($p < 0.05$), while RhoA was not activated (**Figure 7-1D**).

RhoGTPases have been primarily implicated as the controlling factors in guiding cell motility, morphology, contractility and proliferation [99]. RhoGTPases have also been implicated in regulating phagocytosis [104], endocytic trafficking [105], as well as mediating the various steps of vesicular trafficking [106]. Thus, RhoGTPases can play a role in polyplex uptake and polyplex intracellular trafficking. Fibronectin has been previously shown to enhance signaling through RhoGTPases [89, 107-109]. Initial activation of Rac and Cdc42 by fibronectin has been shown to mediate cell spreading in NIH/3T3 cells [108, 109]. Our results show that the exposure of mMSCs to fibronectin coated surfaces results in enhanced activation of the RhoGTPases namely RhoA, Rac1,2,3 and Cdc42, in mMSCs. To study the role of RhoGTPases on non-viral gene transfer for mMSCs plated on fibronectin coated surfaces, systematic inhibition and activation by molecular inhibitors as well as dominant negative or positive genes was subsequently used.

7.3.2 Inactivation of RhoGTPases for cells plated on fibronectin inhibits transgene expression.

Inactivation of RhoGTPases was used to screen their potential involvement in mediating non-viral gene transfer in mMSCs. TcdB irreversibly inactivates Rho, Rac and Cdc42 by glycosylation of the threonine residue [152, 153], while C3 selectively inhibits RhoA, B and C [154], but not Rac or Cdc42, by modifying the aspargine41 at the effector region of the GTPase. Inactivation of RhoGTPase using difficile toxin B was characterized using actin staining and

GLISAs for RhoGTPases. Cells with inactivated RhoGTPases resulted in less spread cells with a significant decrease in stress fibers ($p < 0.01$, **Figure 7-2 A and B**) and amount of active RhoA, Rac1,2,3 and Cdc42 (p at least < 0.05, **Figure 7-2C**). Cell viability was not significantly affected immediately after treatment with TcdB and 48 hrs post transfection (**Figure 7-8A**). RhoA,B,C were selectively inactivated using C3 transferase and resulted in a significant decrease in actin stress fibers ($p < 0.01$, **Figure 7A and B**) and a significant decrease in active RhoA ($p < 0.01$, **Figure 7-2D**). Cell viability was maintained at >60% immediately post C3 transferase treatment as well as 48 hours after treatment and transfection (**Figure 7-8B**).

Cells were transfected immediately following the inhibitory treatments and transgene expression was analyzed using a luciferase assay at 48 hours and the extent of polyplex internalization was assessed using flow cytometry analysis (FACS) after 2 hours. More than 90% decrease in transgene expression of cells plated on fibronectin-coated surfaces was noticed after treatment with TcdB and C3 transferase ($p < 0.001$, **Figure 7-2E**). However, internalization of the complexes was significantly increased following treatment (p at least < 0.05, **Figure 7-2F**).

To further understand the individual role of RhoGTPases, mMSCs were transiently transfected with GFP fused plasmid constructs of dominant negative mutants of either RhoA (RhoA-T19N), or Rac1 (Rac1-T17N) or Cdc42 (Cdc42-T17N) [101, 151]. At least 80% cell viability was maintained in cells expressing EGFP control plasmid and dominant negative genes 16 hours post plating cells on fibronectin (at time of bolus transfection) and 48 hours post gene delivery (**Figure 7-9**). Expression of RhoA-T19N by cells plated on fibronectin coated surface resulted in a significant decrease ($p < 0.01$) in stress fibers; however, no significant difference in stress fibers was observed in cells expressing dominant negative mutants of Rac1 and Cdc42 (**Figure 7-3 A and B**). GLISA analysis of active Rho, Rac1,2,3 and Cdc42 showed a significant decrease

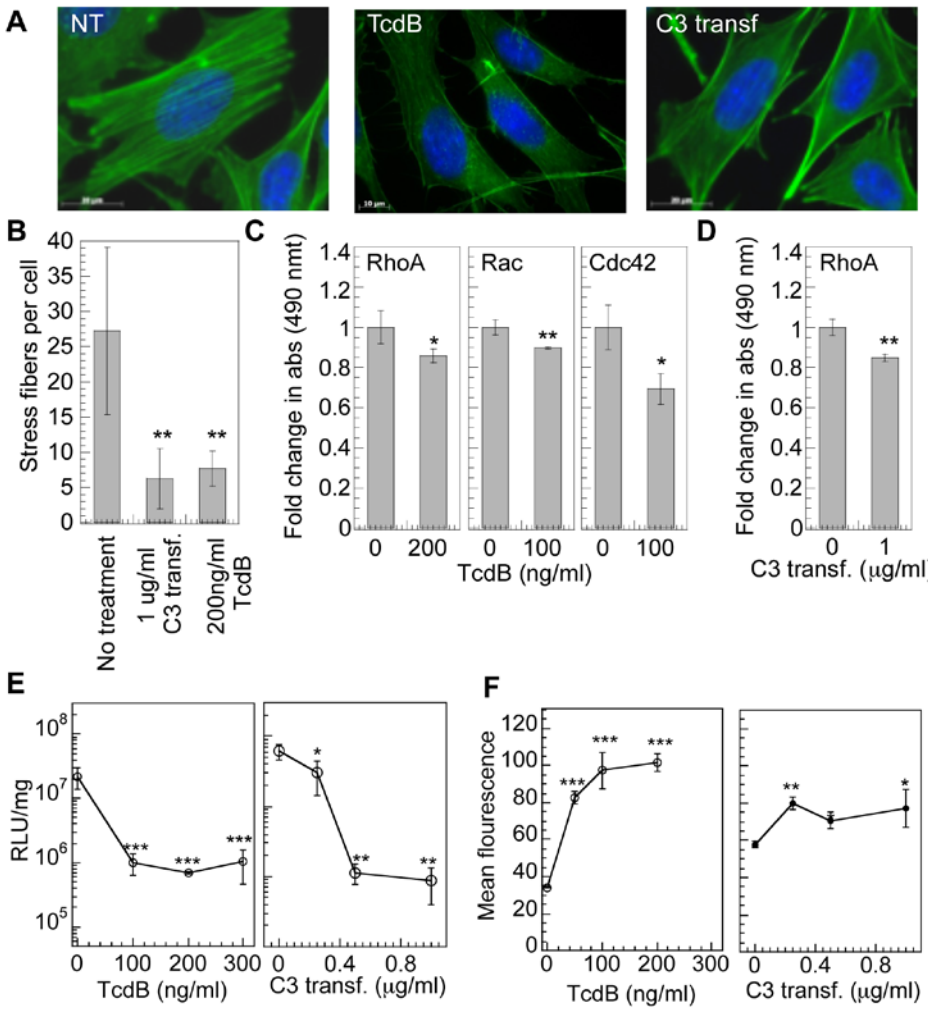

Figure 7-2: RhoGTPase inhibition using TcdB and C3 transferase decreases transgene expression. mMSCs were plated on fibronectin (40 μg/mL) coated tissue culture plastic for 16 hours prior to being treated with 0-300 ng/ml TcdB for 4 hours in serum free media, or 0-1 μg/ml C3 transferase for 4 hours. (**A**) Cell morphology was studied immediately after treatment with inhibitor, by staining cells for actin using Alexa488 (green) conjugated phalloidin, and for DNA using Hoechst 33258 dye (blue). Images were taken with a Zeiss AxioObserver Z1 inverted microscope at 100x magnification. **B**) Stress fiber quantification.Statistical analysis was done using a one-way Anova followed by the Dunnett Multiple Comparison test. The Anova p value was 0.0052. The symbol ** represents a significant change in stress fibers with respect to untreated cells to the level of $p < 0.01$. (**C**) Active RhoGTPase quantification was performed using GLISA specific for RhoA, Rac1,2,3 and Cdc42. (**D**) Active RhoA quantification was performed using GLISA specific for RhoA. Statistical analysis was done using the unpaired t-test (two tail p value) where active RhoGTPase level in treated cells was compared with untreated cells. The symbols * and ** represent a significant change to the level of $p < 0.05$ and $p < 0.01$, respectively. (**E**) Cells were transfected immediately post treatment and transgene expression was analyzed at 48 hours using luciferase assay and normalized with total protein quantified using Peirce BCA assay. (**F**) Cells were transfected immediately post treatment with YOYO-1 labeled polyplexes and after 2 hours cells were collected with trypsin and polyplex internalization analyzed by flow cytometry. A total of 7000 events were analyzed per sample. Experiments were performed in triplicate and the average plotted with the error bars representing the standard deviation. Fold increase in transgene expression and internalization was calculated with respect to the untreated control. Statistical analysis for gene transfer and internalization was done using a one-way Anova followed by the Tukey-Kramer Multiple Comparison test, which compares all columns. The Anova p values for transgene expression were 0.004 and 0.0052 for TcdB and C3 transferase, respectively and the Anova p values for internalization were < 0.0001 and 0.0067 for TcdB and C3 transferase, respectively. The symbols ***, ** and * represent a significant change in gene expression or internalization with respect to sample not treated with inhibitor to the level of $p < 0.001$, $p < 0.01$ and $p < 0.05$, respectively.

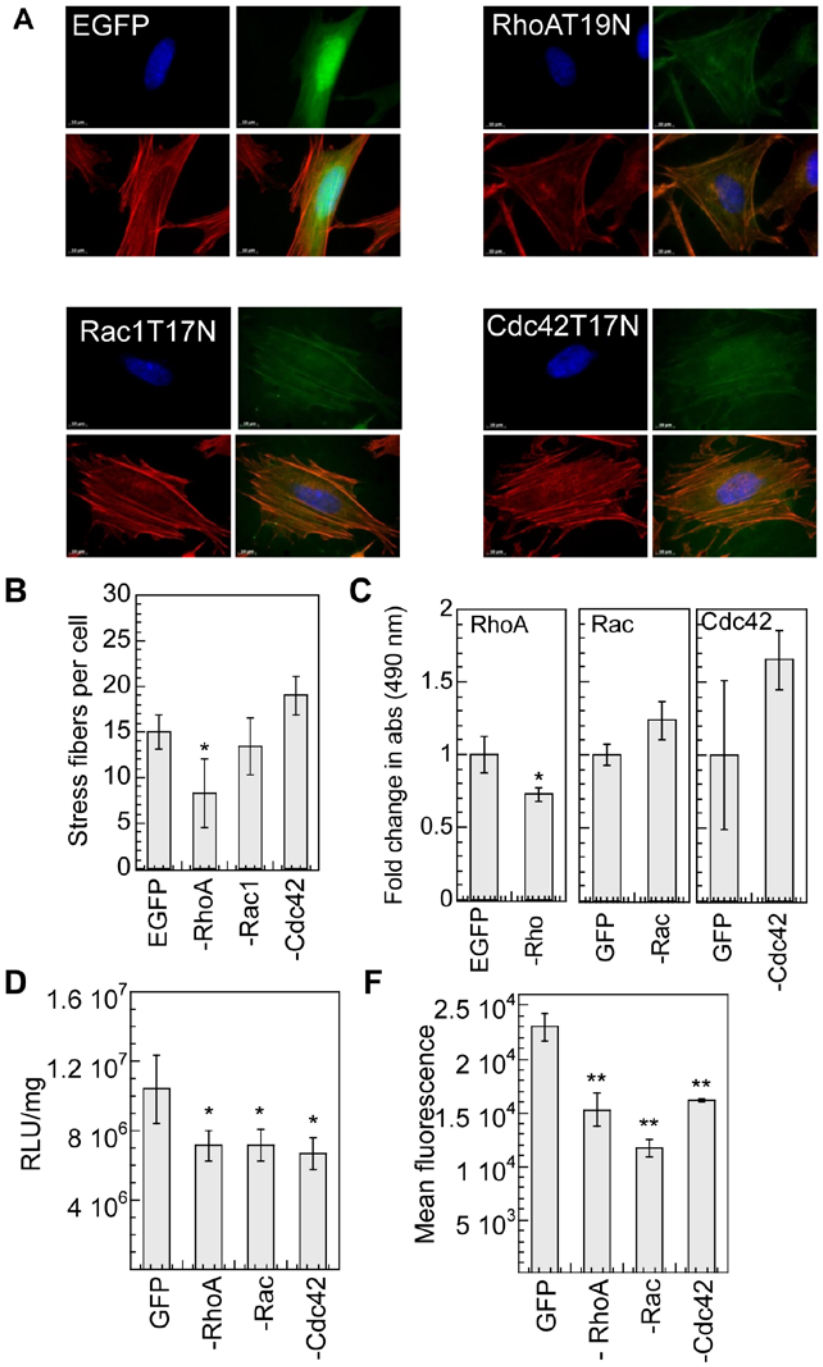

Figure 7-3: RhoGTPase inhibition using dominant negative gene products decreases transgene expression. mMSCs were transiently transfected with dominant negative forms of RhoA, Rac1 or Cdc42 with a plasmid also containing EGFP. 24 hours post transfection, cells were replated on fibronectin coated plates and cultured for 16 hours prior to bolus transfection. Cells transfected with pEGFP were used as control. (**A**) Alexa488 conjugated phalloidin (green), and Hoechst dye (blue) staining. Images were taken with a Zeiss AxioObserver Z1 inverted microscope at 100x magnification. (**B**) Stress fiber quantification. Statistical analysis was done using a one-way Anova followed by the Dunnett Multiple Comparison test. The Anova p value was 0.0015. The symbol * represents a significant change in stress fibers with respect to untreated cells to the level of $p < 0.05$. (**C**) Active Rho, Rac and Cdc42, was assessed for cells replated on fibronectin for 16 hours using GLISA assays specific for RhoA, Rac1,2,3 and Cdc42. Statistical analysis was done using the unpaired t-test (two tail p value). The symbol * represents a significant change to the level of $p < 0.05$. (**D**) The transgene expression was analyzed 48 hours post transfection using luciferase assay and normalized with total protein analyzed using Peirce BCA assay. (**E**) Internalization was analyzed using YOYO-3 labeled polyplexes 2 hours post transfection using flow cytometry. A total of 10,000 events were analyzed per sample and the mean fluorescence of events positive for both GFP and YOYO-3 was analyzed. Statistical analysis for gene transfer and internalization was done using a one-way Anova followed by the Dunnett Multiple Comparison test. The Anova p values were 0.0219 and < 0.0001 for transfection (D) and internalization (E), respectively. The symbols * and ** represent a significant change with respect to cells transfected with control plasmid (pEGFP) to the level of $p < 0.05$ and $p < 0.01$, respectively.

in active RhoA upon transfection with RhoA-T19N ($p < 0.05$), but no change in active Rac or Cdc42 upon transfection with Rac1-T17N or Cdc42-T17N compared to cells transfected with EGFP (**Figure 7-3C**).

Since for both inhibition protocols namely use of bacterial toxins and dominant negative genes, cells are seeded on fibronectin, these results indicate that the dominant negative gene could inhibit RhoA even though the cells are plated on fibronectin, but the dominant negative gene could only reduce the activation of Rac and Cdc42 to background levels when the cells are plated on fibronectin.

Transgene expression was significantly reduced in the cells expressing dominant negative form of RhoA, Rac1 and Cdc42 ($p < 0.05$, **Figure 7-3D**). The effect of dominant negative mutants on internalization was studied by analyzing the uptake of YOYO-3 labeled complexes in GFP positive cells only. A significant decrease in internalization was observed for cells expressing dominant negative form of RhoGTPases ($p < 0.01$, **Figure 7-3E**).

Consistent with our hypothesis of the involvement of RhoGTPases on non-viral gene transfer, inhibition of RhoGTPases led to a significant decrease in transgene expression. Although the exact mechanism of how RhoGTPases influence successful non-viral gene transfer cannot be determined from our data, we predict that the regulation of actin-microtubule dynamics, cell proliferation [92] and gene transcription via integrin-dependent intracellular signaling pathways [93] positively influence non-viral gene transfer. RhoGTPases have been implicated in endocytosis of bacteria and viruses by mammalian cells. For example, Rac1, RhoA, and Cdc42 are required for HeLa cell invasion by group B streptococcus [101], RhoA positively regulates the pathway by which Madin-Darby canine kidney (MDCK) cells internalize P. aeruginosa strain

PA103 [100], and Rho C enhances macropinocytosis and modulates entry of Ebola virus and vesicular stomatitis virus pseudotyped vectors.

Interestingly, the effect on polyplex internalization was not the same for the bacterial toxins and transfection with dominant negative genes. While inhibition of RhoGTPases using TcdB and C3 transferase led to an increase in polyplex internalization, inhibition with dominant negative genes led to a decrease in internalization. We cannot offer a definitive reason for these findings. The observed increase in internalization on treatment with TcdB could be due to TcdB-mediated activation of phospholipase C and D [153], leading to regulation of receptor-mediated endocytosis [155, 156]. The increase observed on C3 treatment correlates with our previous study where depolymerization of actin using cytochalasin D enhanced polyplex uptake in mMSCs cultured on fibronectin [145]. The observed decrease in internalization for inhibition with dominant negative genes could possibly be due to inhibition of macropinocytosis by dominant negative mutants of Cdc42 and Rac1, as was shown for bone marrow derived dendritic cells [157].

7.3.3 Activation of RhoGTPases for cells plated on fibronectin does not influence transgene expression.

Since RhoGTPase inactivation leads to a significant decrease in gene transfer efficiency for cells plated on fibronectin-coated surfaces, next we wanted to determine if further activation of RhoGTPases enhanced transgene expression. RhoGTPases were activated using calpeptin, EGF and transfection with constitutively active RhoGTPase mutants. Calpeptin (CP) is a cell permeable calpain inhibitor known to activate Rho leading to stress fiber formation [158, 159]. Treatment with CP did not significantly change the number of stress fibers in the cell (**Figure 7-**

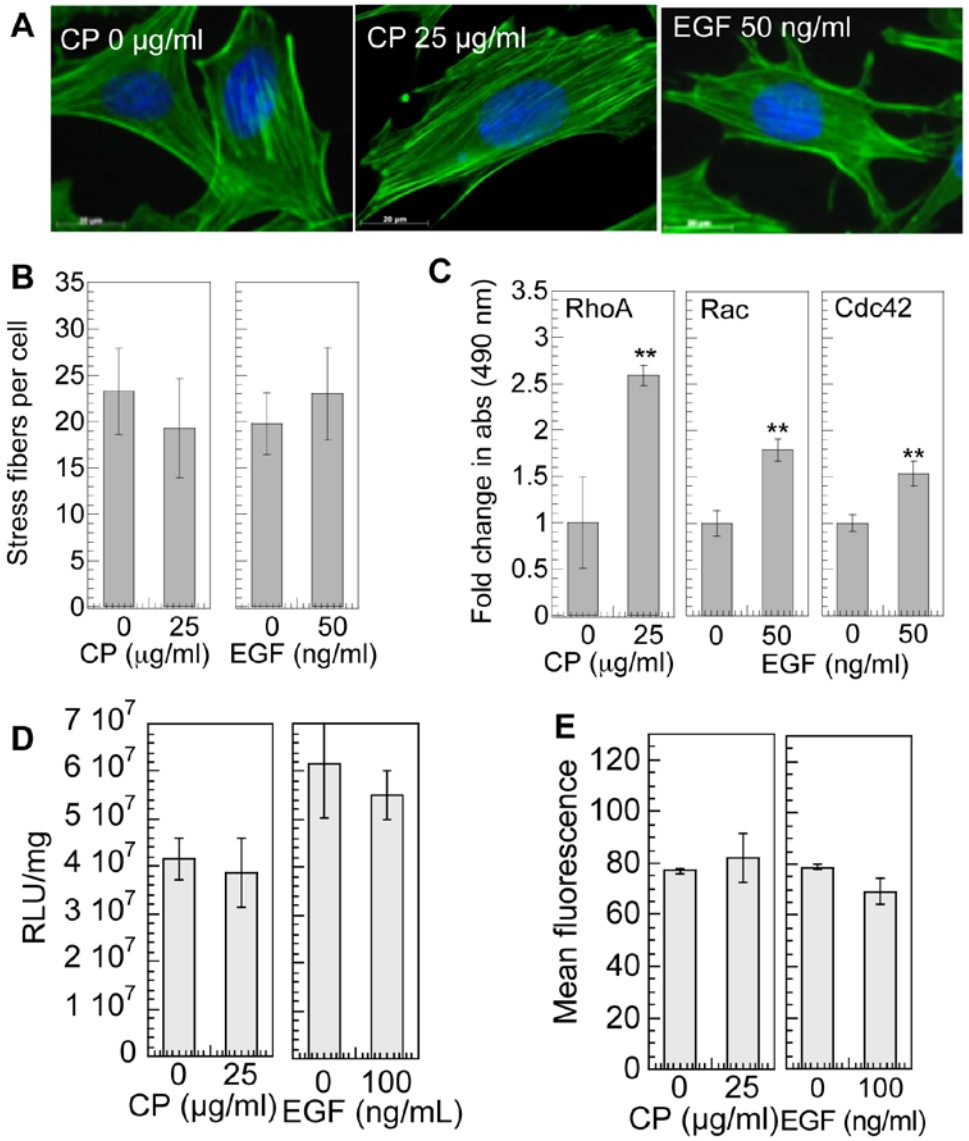

Figure 7 4: Effect of RhoGTPase activation using calpeptin (CP) and epidermal growth factor (EGF) on gene transfer. mMSCs cells were cultured for 8 hours on fibronectin wells, followed by overnight serum starvation and then treated with 0-100 µg/ml CP for 10 minutes or 0-100 ng/ml EGF for 2 minutes in serum free media. (**A**) After treatment, the changes in cell morphology were visualized through lexa488 conjugated phalloidin (green) and for DNA using Hoechst 33258 dye (blue) staining. Images were taken with a Zeiss AxioObserver Z1 inverted microscope at 100x magnification. (**B**) Stress fiber quantification. (**C**) Active RhoGTPase quantification after treatment was performed using GLISA specific for RhoA, Rac1,2,3 and Cdc42. (**D**) Transfection was performed immediately post treatment in serum free media. 4 hours post transfection media was replaced with complete media. The transgene expression was analyzed 48 hours post transfection using luciferase assay and normalized with total protein analyzed using Peirce BCA assay. (**E**) Internalization was analyzed 2 hours post transfection using flow cytometry of YOYO-1 labeled polyplexes. A total of 7000 events were analyzed per sample. Statistical analysis for the level of active RhoGTPase, transgene expression and internalization, was done using the unpaired t-test (two tail p value) where treated sample was compared with untreated sample. The symbols ** and *** represent a significant change to the level of $p < 0.01$ and $p < 0.001$, respectively.

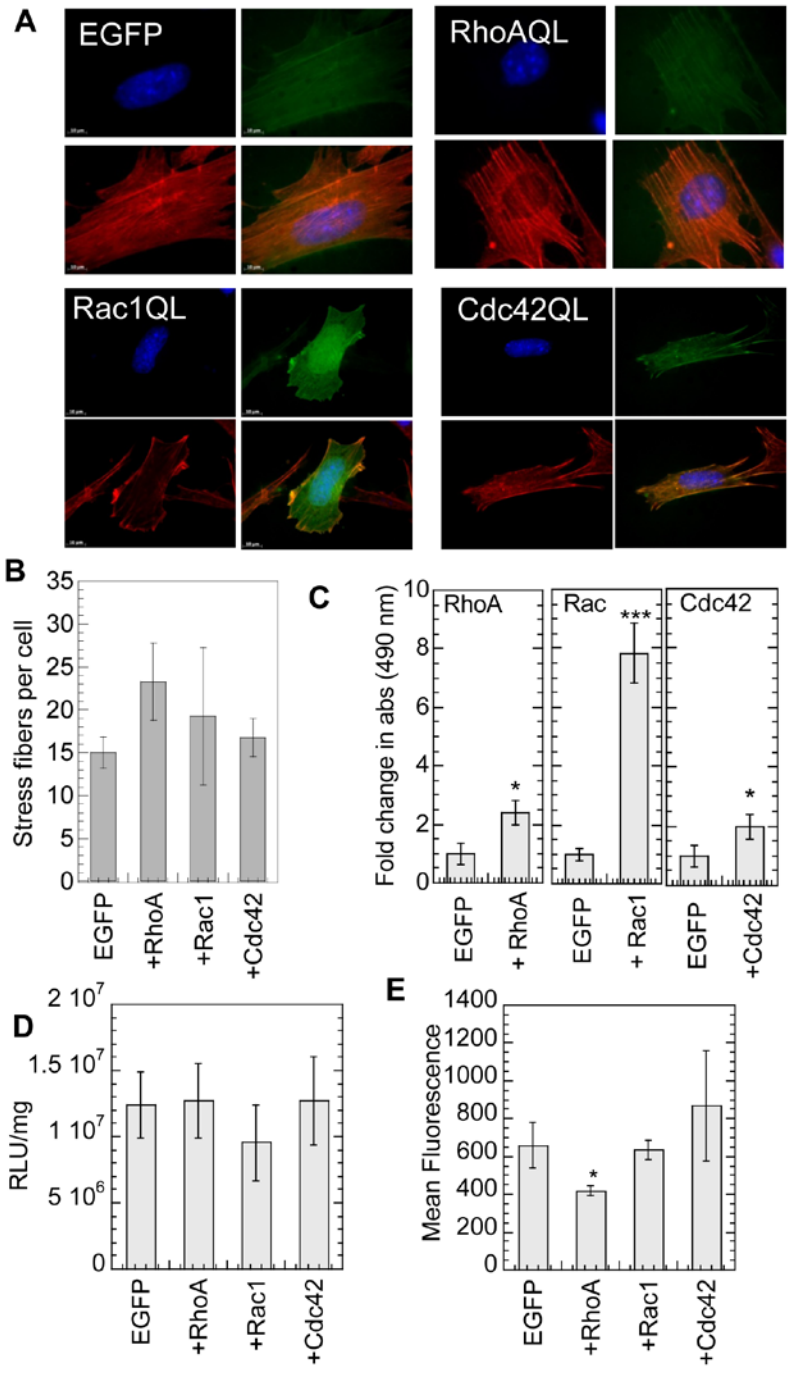

Figure 7-5: Effect of expression of constitutively active mutants of RhoGTPases on gene transfer. mMSCs plated on a 6-well plate were transiently transfected with constitutive active forms of RhoA, Rac1 or Cdc42 conjugated with GFP, using lipofectamine^{TM}2000. Cells transfected with pEGFP were used as control. After 24 hours, cells were harvested and replated on fibronectin-coated surfaces. (**A**) 24 hours post transfection with constitutive active forms of RhoGTPases in cells plated on tissue culture plastic, changes in cell morphology were analyzed through actin and DNA staining using Alexa488 conjugated phalloidin (green), and Hoechst 33258 dye (blue), respectively. (**B**) The number of stress fibers per cell were counted. (**C**) Active Rho, Rac and Cdc42-GTPases were assessed using GLISA assays 24 hours post transfection with constitutive active forms of RhoGTPases and overnight serum starvation. (**D**) The replated cells were cultured for 16 hours on fibronectin before bolus transfection. The transgene expression was analyzed 48 hours post transfection using luciferase assay and normalized with total protein analyzed using Peirce BCA assay. (**E**) Internalization was analyzed 2 hours post transfection using flow cytometry and YOYO-3 labeled polyplexes. A total of 10,000 events were analyzed per sample and the mean fluorescence of events positive for both GFP and YOYO-3 was analyzed. Statistical analysis for number of stress fibers, ruffles, transgene expression and internalization was done using the Dunnett multiple comparison test.

4 A and B), but significantly increased the amount of active Rho (by 2.5 fold) ($p < 0.01$, **Figure 7-4C**) compared to cells seeded on fibronectin coated surfaces that did not receive treatment**.** Viability was maintained at 90% or greater compared to cells not treated with CP immediately after treatment as well as 48 hours post treatment and addition of polyplexes (**Figure 7-8C**). Epidermal growth factor (EGF) is an efficient activator of Rac1,2, and Cdc42 [160]. Treatment with EGF resulted in a significant increase in active Rac1,2,3 and Cdc42 ($p < 0.01$ and < 0.01, **Figure 7-4C**) compared to cells seeded on fibronectin-coated surfaces that did not receive treatment. No significant change in cell viability was observed immediately post treatment and 48 hours post treatment and transfection (**Figure 7-8D**). No significant difference in transgene expression (**Figure 7-4E**) and internalization (**Figure 7-4F**) was observed using treatment with CP or EGF for cells placed on fibronectin.

Although we show that EGF activates Rac and Cdc42, EGF also stimulates macropinocytosis [161]. To confirm the CP and EGF findings, mMSCs were transiently transfected with GFP fused plasmid constructs of constitutive active mutants of either RhoA (RhoA-Q63L), or Rac1 (Rac1-Q61L) or Cdc42 (Cdc42-Q61L) [151]. At least 80% cell viability was maintained in cells expressing EGFP control plasmid and active genes 16 hours post plating cells on fibronectin (at time of bolus transfection) and 48 hours post gene delivery (**Figure 7-9D**). Transfection with constitutively active RhoA mutant resulted in an increase in stress fiber formation (**Figure 7-5 A and B**). Further, a significant increase in the amount of active RhoA, Rac1 and Cdc42 was observed for cells transfected with the constitutively active genes (p at least < 0.05, **Figure 7-5D**). Similar to the results obtained for CP and EGF further activation of RhoGTPases did not enhance transgene expression beyond that observed for cells seeded on fibronectin and transfected with EGFP (**Figure 7-5D**). Expression of constitutively active form of RhoA, Rac1

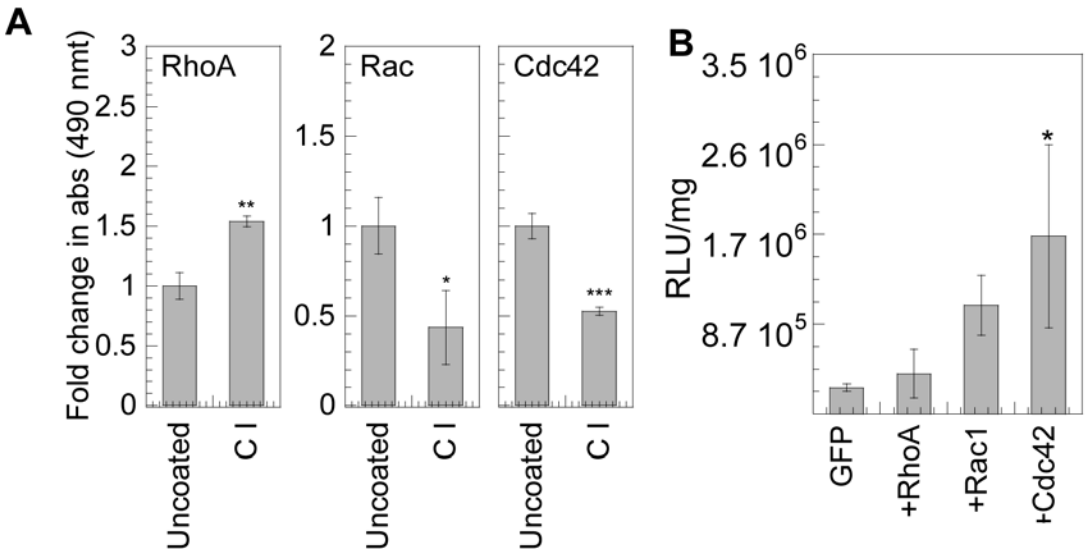

Figure 7-6: Effect of expression of constitutively active mutants of RhoGTPases on gene transfer for cells cultured on collagen I substrates. (**A**) mMSCs were cultured on amine functionalized PDMS strips and serum starved overnight before exposing to collagen I coated surfaces for 20 minutes to assess Rho-GTP and 1 hour to assess Rac and Cdc42-GTPases. The cells were subsequently lysed and respective GLISA assays were performed to quantify RhoA, Rac1,2,3 and Cdc42. Statistical analysis was done using the unpaired t-test (two tail p value). (**B**) mMSCs transiently transfected with constitutively active negative of RhoA, Rac1 or Cdc42 conjugated with GFP were cultured on collagen I coated plates for 16 hours prior to bolus transfection with polyplexes. The transgene expression was analyzed 48 hours post transfection using luciferase assay and normalized with total protein analyzed using Peirce BCA assay. Statistical analysis was done using a one-way Anova followed by the Dunnett multiple comparison test. The Anova p value was 0.0203. The symbols *, ** and *** represent a significant change to the level of $p < 0.05$, $p < 0.01$ and $p < 0.001$, respectively.

and Cdc42 did not affect internalization (**Figure 7-5E**). These results confirm that further activation of RhoA, Rac1 or Cdc42 over what fibronectin achieves on its own (**Figure 7-1 C and D**) does not alter transgene expression. A further activation of RhoGTPases does not increase transgene expression in mMSCs cultured on fibronectin-coated dishes.

7.3.4 Activation of RhoGTPases for cells plated on collagen I enhances transgene expression.

As mentioned we previously observed that gene transfer to mMSCs plated on collagen I was inhibited [145]. Activation of RhoGTPases for cells plated on collagen I was significantly lower

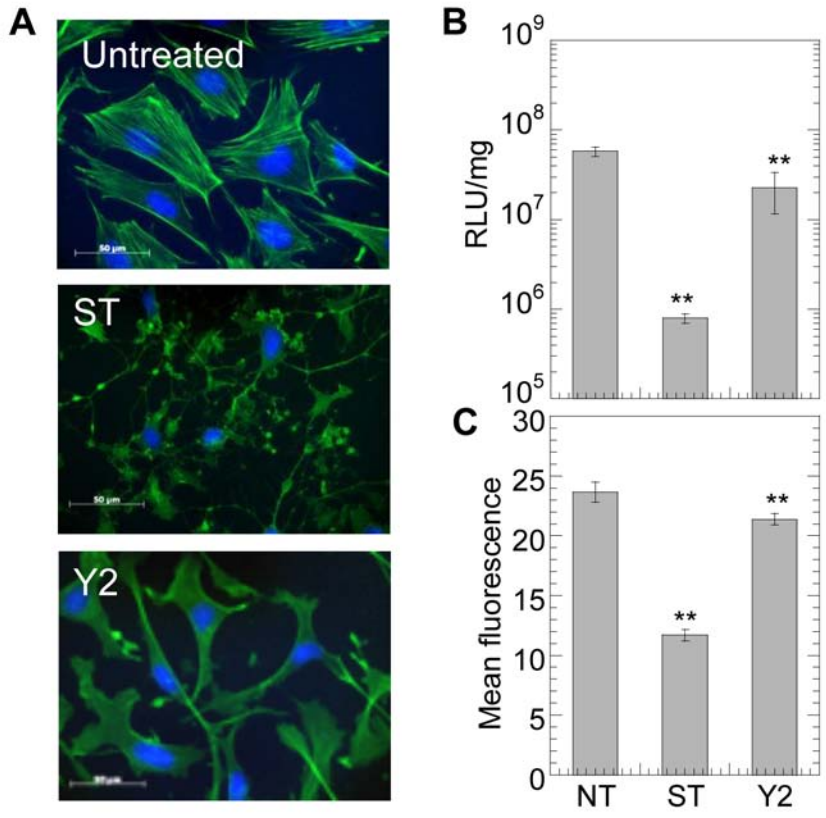

Figure 7-7: Inhibition of PKC and ROCK inhibits gene transfer in cells plated on fibronectin. mMSCs were cultured for 16 hours on fibronectin coated plates prior to treatment with 10 μM Y27632 (Y2) or 100 nM Staurosporine (ST) for 2 hours to inhibit ROCK and PKC, respectively. (**A**) Changes in mMSC cell morphology were visualized through staining for actin using Alexa488 conjugated phalloidin and for DNA using Hoechst 33258 dye. Images were taken with a Zeiss AxioObserver Z1 inverted microscope at 40x magnification. Immediately after treatment with inhibitor, the medium was replaced and bolus transfection was done. (**B**) Transgene expression was analyzed 48 hours post transfection using luciferase assay and normalized with total protein analyzed using Peirce BCA assay. Internalization was assessed 2 hours post transfection using flow cytometry and YOYO-1 labeled polyplexes (**C**). A total of 7000 events were analyzed per sample. Statistical analysis was done using a one-way Anova followed by the Dunnett multiple comparison test. The Anova p value was 0.0003 and < 0.0001 for transgene expression and internalization, respectively. The symbol ** represents a significant change to the level of $p < 0.01$.

compared to cells plated on fibronectin (**Figure 7-6** vs. **Figure 7-1**). Thus, we used transfection experiments on collagen I to further test our hypothesis of the importance of active RhoGTPases on non-viral gene transfer. Rho was enhanced 4-fold on fibronectin coated surfaces but only 1.5-fold for cells plated on collagen I. Rac was enhanced 1.5-fold for cells plated on fibronectin but inhibited by 50% for cells plated on collagen I. Cdc42 was enhanced by 2-fold for cells plated on fibronectin, but inhibited by 50% for cells seeded on collagen I (**Figure 7-6A**). Cells were transfected with constitutively active RhoA, Rac1 and Cdc42 and replated on collagen I coated surfaces for 16 hours before transfection. Rac1 and Cdc42 activation were able to enhance the

transgene expression by 4.1- and 6.7-fold compared to EGFP mock transfected cells respectively, while RhoA activation had no difference (**Figure 7-6B**). Since RhoA was activated by cell exposure to collagen I (**Figure 7-6A**), this result shows that further activation of RhoA is not beneficial to achieve higher transgene expression similar to what was observed for cells plated on fibronectin. On the other hand, Rac and Cdc42 were inhibited on Collagen I coated surfaces, and thus the fact that transfection with constitutively active Cdc42 and Rac1 increased transgene expression indicates that these RhoGTPases can promote transgene expression in cells with less active RhoGTPases.

7.3.5 Rho effector protein Rho-Kinase (ROCK) and PKC mediated phosphorylation modulate gene transfer

The small RhoGTPases employ downstream effectors to mediate their effects on cell morphology, focal adhesion and migration. RhoGTPase binds to serine/threonine kinases [96] namely Rho Kinase, ROK and the related p160ROCK; and elevate their activity. The role of Rho downstream effector ROCK in non-viral gene transfer was also investigated. ROCK was inhibited using Y27632 (Y2) which is a specific inhibitor of ROCK. Treatment with Y27632 reduced the number of actin stress fiber (**Figure 7-7A**). No significant change in cell viability was observed immediately after inhibitor treatment, and 48 hours post treatment and transfection (**Figure 7-8E**). Treatment with Y27632 resulted in a significant decrease in overall transgene expression and polyplex internalization ($p < 0.01$, **Figure 7-7 B and C**). This suggests that cell contractility mediated by ROCK contributes to the regulation of polyplex uptake by RhoGTPase. Besides ROCK, there are other Rho effector molecules like Phosphatidyl inositol 4-phosphate 5-

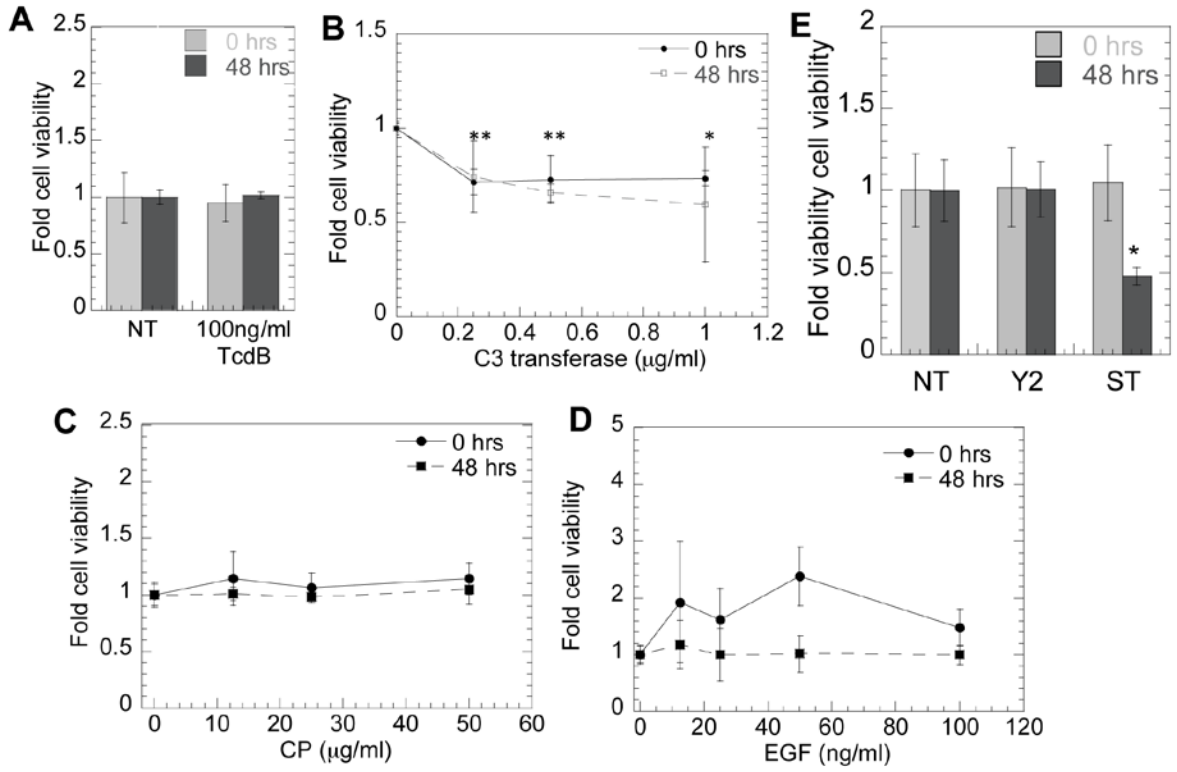

Figure 7-8: Effect of inhibitors and activators on cell viability. To study the effect of RhoGTPase inhibition on gene transfer, mMSCs were plated on fibronectin (40 μg/mL) coated tissue culture plastic surfaces for 16 hours prior to being treated with 0-300 ng/ml TcdB for 4 hours in serum free media, or 0-1μg/ml C3 transferase for 4 hours. Cells were transfected immediately post treatment with inhibitors. For studying the effect of RhoGTPase activation, mMSCs were cultured for 8 hours on fibronectin, followed by overnight serum starvation and then treated with 0-100 μg/ml CP for 10 minutes or 0-100 ng/ml EGF for 2 minutes in serum free media. Subsequently, immediately post treatment with activators, bolus transfection was done for 4 hours in serum free media. For assessing the role of ROCK and PKC in gene transfer, mMSCs were cultured for 16 hours on fibronectin prior to treatment with 10 μM Y27632 (Y2) for 2 hours or 100 nM Staurosporine (ST) for 2 hours to inhibit ROCK and PKC, respectively. Immediately after treatment with ST or Y2, the medium was replaced and bolus transfection was done. Cell proliferation was analyzed immediately after treatment with TcdB (**A**), C3 transferase (**B**), CP (**C**), EGF (**D**) and ST or Y2 (**E**), as well 48 hours post treatment and transfection by measuring calcien AM fluorescence after live/dead staining. The cell viability obtained after specific inhibitor treatment was statistically compared using Tukey-Kramer multiple comparison test, which compares all pairs with each other. The symbols *, **, and *** represents a significant change to the level of $p < 0.05$, $p < 0.01$, and $p < 0.001$, respectively.

kinase (PIP5-kinase) and p140mDia that also regulate actin polymerization [97, 98] and could play a role in mediating gene transfer and would be interesting to study in future.

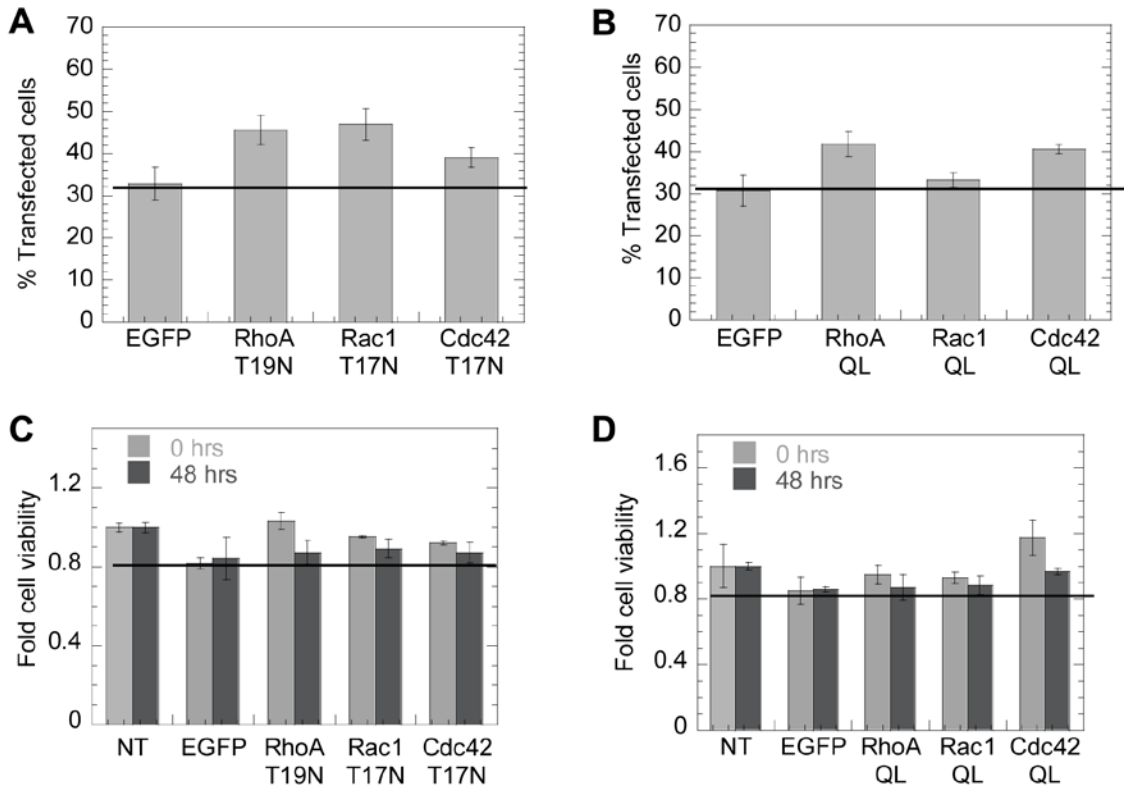

Figure 7-9: Percent cells transfected with dominant negative and constitutively active genes, and the effect on cell viability. To study the effect of direct inhibition and activation of RhoGTPase on gene transfer in cells plated on fibronectin tissue culture plastic, D1 cells were transiently transfected using lipofectamine^{TM}2000, with dominant negative or constitutively active forms of RhoA, Rac1 or Cdc42 conjugated with GFP. The distribution and percentage of cells transfected with dominant negative genes (**A**) or constitutively active genes (**B**), was assessed by analyzing GFP expression using flow cytometry. The cells were subsequently cultured on Fn for 16 hours prior to bolus transfection using linear polyethylenimine (LPEI). The cell viability was determined 16 hours after culturing cells on fibronectin as well as 48 hours post addition of polyplexes using live/dead assay, for cells transfected with dominant negative genes (**C**) or constitutively active genes (**D**).

Besides integrins, syndecans also mediate cell-fibronectin interactions [162] and activate PKC, which acts upstream to activate RhoGTPases [163] and mediate cell contractility. Syndecan-4 directly recruits PKC-α and facilitates focal adhesion formation on fibronectin [164]. To determine the function of PKC in non-viral gene transfer, it was inhibited using staurosporine (ST). Treatment with staurosporine led to a loss of cystoskeletal integrity (**Figure 7-7A**). No significant change in cell viability was observed immediately after ST treatment. However, 48 hours post treatment and transfection, ST significantly reduced cell viability ($p < 0.05$, **Figure 7-**

8E). PKC inhibition resulted in a severe decrease in transgene expression and polyplex uptake ($P < 0.01$). Therefore, a decrease in transgene expression was seen on PKC inhibition as an effect of decreased internalization and proliferation. PKC stimulation has been shown to induce clathrin mediated endocytosis of $\alpha_5\beta_1$ [165] and actin dependent uptake of cationic DNA complexes [132]. These results indicate RhoGTPase activity regulated by PKC [163] is required for effective transgene expression.

7.4 Conclusions

The mechanisms activated upon ECM binding that influenced effective gene transfer had not been elucidated. In chapter 4, mMSCs plated on fibronectin coated surfaces resulted in enhanced gene transfer, while cells plated on collagen I resulted in inhibited gene transfer compared to cells seeded on uncoated surfaces [145]. In this study we determined if RhoGTPase activation was one of the contributing factors for the observed enhancement in transgene expression for cells plated on fibronectin-coated surfaces. The results indicated that RhoGTPases modulated non-viral gene transfer for mMSCs plated on fibronectin coated surfaces. The results showed that the engagement of the ECM dictated the RhoGTPase activation level, which in turn dictated the efficiency of transgene expression. Activation of RhoGTPases for cells with inactive RhoGTPases led to enhanced transgene expression, but activation of RhoGTPases for cells with already active RhoGTPases did not result in further enhancement. Since only RhoA, Rac1 and Cdc42 were studied, the conclusions about the involvement of RhoGTPases (e.g. RhoB/C) in non-viral gene transfer cannot be offered. A molecular understanding of the process of non-viral gene transfer is necessary to engineer systems that achieve efficient gene delivery.

Chapter 8

Role of RhoGTPases in Non-Viral Gene Delivery is Cell Type Specific

8.1 Introduction

Chapter 7, showed that RhoGTPases play a role in non-viral gene transfer in mMSCs cultured on Fn coated surface. However, it did not prove that RhoGTPases had an underlying role in non-viral gene transfer in other cell types. Morever, this role could be same in all cell types or could be cell-type dependent. To investigate the underlying role of RhoGTPPases in non-viral gene transfer, the modulation of gene transfer by RhoGTPases was studied in another cell-type.

The effect of various inhibitors, such as difficile toxin B [166, 167] and C3 transferase [158] as well as activators Calpeptin [158, 159] and EGF [160] on fibroblast cells has been previously studied. Considering the fact that fibroblast cells have been widely employed in Rho related studies [99, 108, 130, 168], NIH/3T3 fibroblast cells represented a model cell line to next study the function of RhoGTPases in non-viral gene transfer which would determine whether this role is cell-type dependent or not.

In this study, the role of RhoGTPases, specifically Rho, Rac and Cdc42 in the uptake and effective intracellular transfer of DNA/PEI to mouse fibroblasts (NIH/3T3) plated on Fn coated surfaces was analyzed.

Hence, the study done for mMSCs in chapter 7 was repeated for NIH/3T3 fibroblast cells. The RhoGTPses were specifically inhibited using chemical inhibitors gene products, as well as activated to determine their role in gene transfer and DNA/PEI internalization.

Materials and methods used for studying the role of RhoGTPases in gene transfer in NIH/3T3 cells have been mentioned in chapter 7, and are same as the materials and methods used for studying the role of RhoGTPases in mMSCs.

8.2 Results and discussion

8.2.1 Effect of inactivation of RhoGTPases on gene transfer in NIH/3T3 cells plated on fibronectin.

To examine if RhoGTPases play an underlying role in modulation of non-viral gene transfer and whether this role is cell-type dependent or not, we studied the function of RhoGTPases in non-viral gene transfer in NIH/3T3 cells. As observed in mMSCs in chapter 7, collective inhibition of Rho, Rac and Cdc42 using TcdB significantly increased ($p < 0.001$) polyplex internalization in NIH/3T3 cells, while the overall transgene expression was significantly ($p < 0.001$) inhibited (**Figures 8-1 A and B**). Furthermore, inhibition of Rho using 0-1 μg/ml C3 tranferase led to greater than 90% decrease in transgene expression (**Figure 8-1C**). Though treatment with 0.125 μg/ml C3 tranferase resulted in a significant increase ($p < 0.05$) in internalization, but no effect was observed for 0.25-1 μg/ml C3 transferase treatment (**Figure 8-1D**).

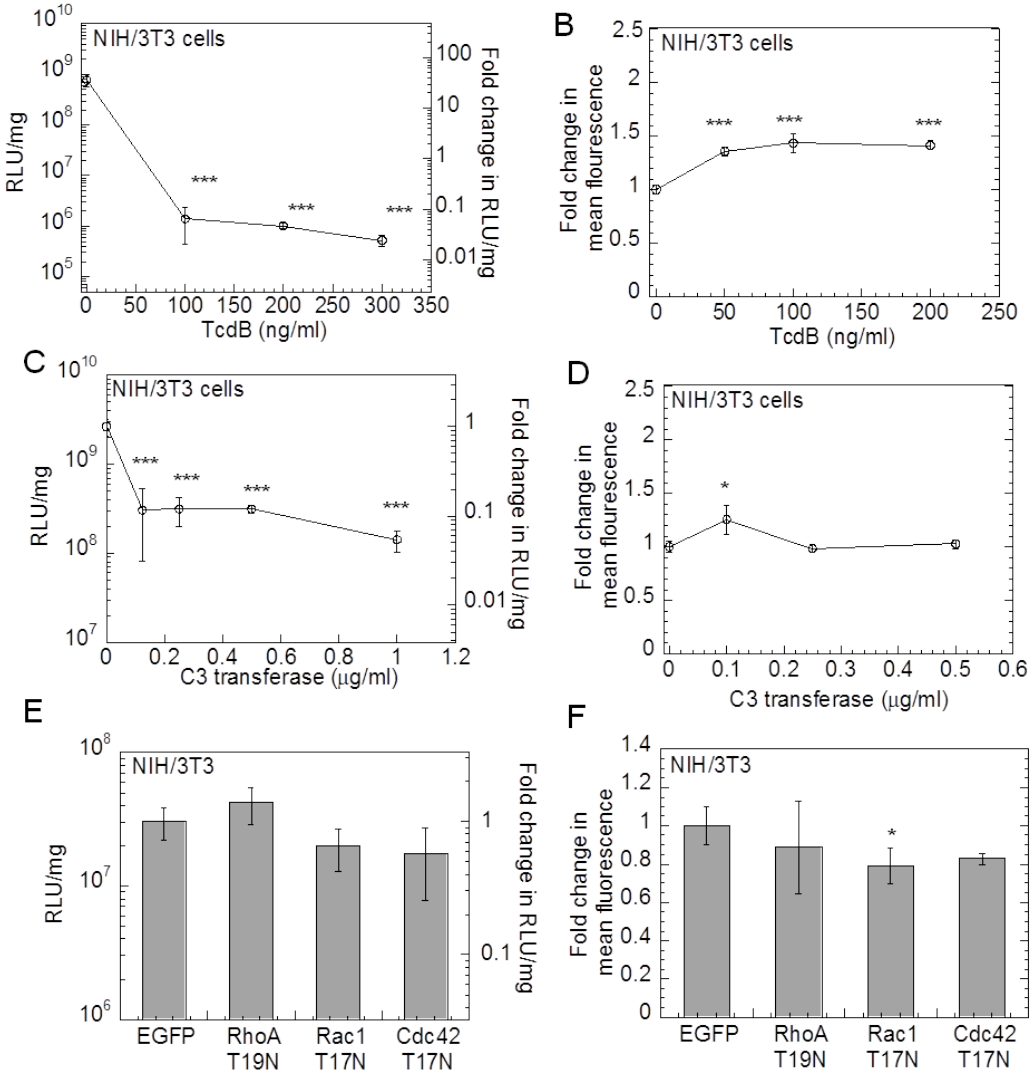

Figure 8-1. Effect of inhibition of RhoGTPases on gene transfer in NIH/3T3 cells. NIH/3T3 **cell**s were plated on Fn (40 μg/mL) coated surfaces for 16 hours prior to being treated with 0-300ng/ml TcdB or 0-1 μg/ml C3 transferase for 4 hrs in serum free media. Cells were transfected immediately post treatment.

For inhibition using dominant negative gene products, NIH/3T3 cells were transiently transfected with dominant negative forms of RhoA, Rac1 or Cdc42 with a plasmid also containing EGFP. 24 hours post transfection, cells were replated on fibronectin coated plates and cultured for 16 hours prior to bolus transfection. Cells transfected with pEGFP were used as control. The symbol * represents a significant change to the level of $p < 0.05$.

(**A, C, and E**) The transgene expression was analyzed 48 hours post transfection using luciferase assay and normalized with total protein analyzed using Peirce BCA assay. (**B, D and F**) Internalization was analyzed using YOYO-3 labeled polyplexes 2 hours post transfection using flow cytometry. A total of 7000 or 10,000 events were analyzed per sample. For analyzing the effect of gene products, the mean fluorescence of events positive for both GFP and YOYO-3 was analyzed. Statistical analysis was done using the Tukey-Kramer multiple comparison test. The symbols * and *** represent a significant change in gene expression or internalization with respect to control (untreated or transfected with pEGFP) to the level of $p < 0.05$ and $p < 0.001$, respectively.

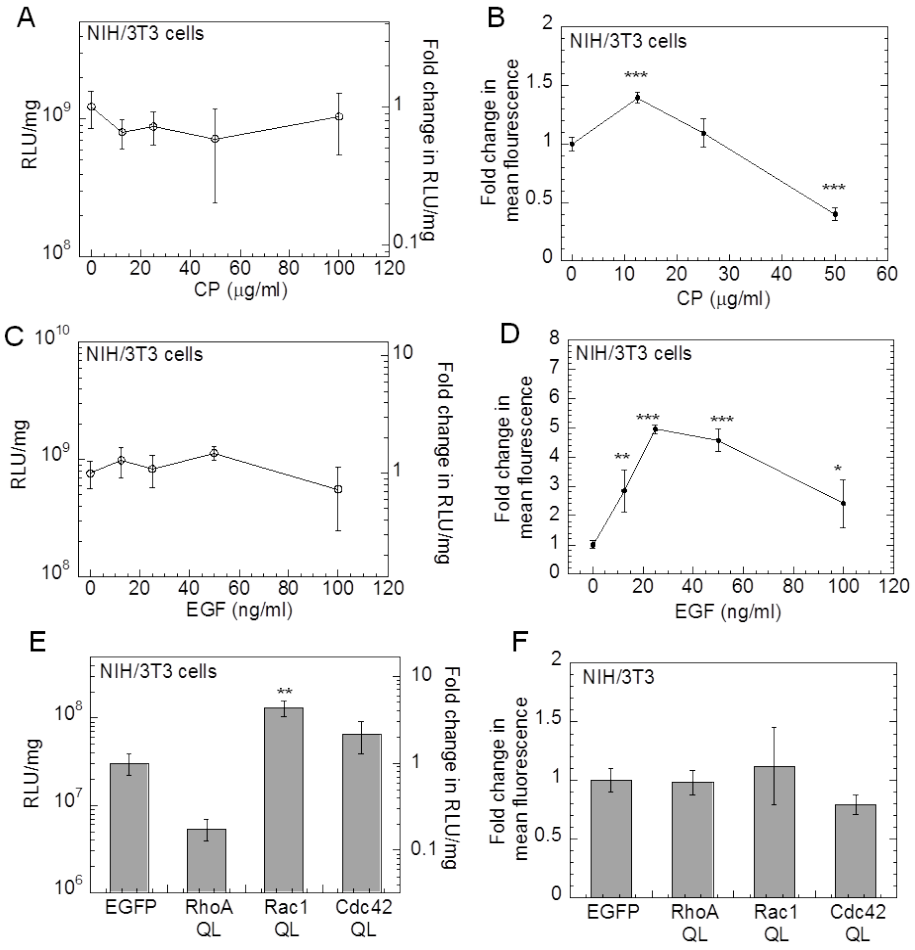

Figure 8-2. Effect of activation of RhoGTPases on gene transfer in NIH/3T3 cells. NIH/3T3 cells were cultured for 8 hours on fibronectin wells, followed by overnight serum starvation and then treated with 0-100 μg/ml CP for 10 minutes or 0-100 ng/ml EGF for 2 minutes in serum free media. Transfection was performed immediately post treatment in serum free media. 4 hours post transfection media was replaced with complete media.

For activation using constitutively active gene products, NIH/3T3 cells were transiently transfected with dominant negative forms of RhoA, Rac1 or Cdc42 with a plasmid also containing EGFP. 24 hours post transfection, cells were replated on fibronectin coated plates and cultured for 16 hours prior to bolus transfection. Cells transfected with pEGFP were used as control. The symbol * represents a significant change to the level of $p < 0.05$.

(**A, C and E**) The transgene expression was analyzed 48 hours post transfection using luciferase assay and normalized with total protein analyzed using Peirce BCA assay. (**B, D and F**) Internalization was analyzed using YOYO-3 labeled polyplexes 2 hours post transfection using flow cytometry. A total of 7000 or 10,000 events were analyzed per sample. For analyzing the effect of gene products, the mean fluorescence of events positive for both GFP and YOYO-3 was analyzed. Statistical analysis was done using the Tukey-Kramer multiple comparison test. The symbols * and *** represent a significant change in gene expression or internalization with respect to control (untreated or transfected with pEGFP) to the level of $p < 0.05$ and $p < 0.001$, respectively.

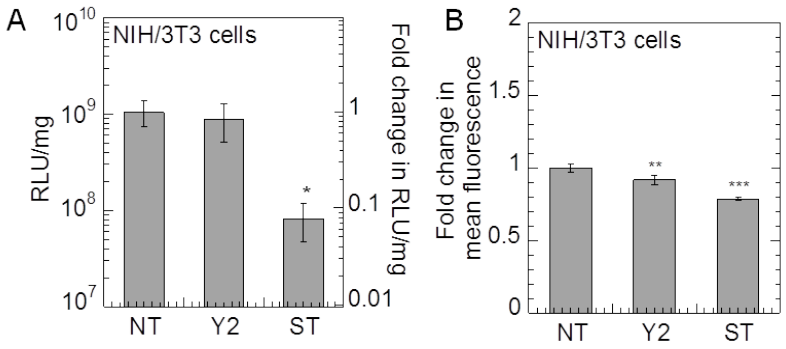

Figure 8-3:. Role of PKC and ROCK inhibition on gene transfer in NIH/3T3 cells plated on fibronectin. Cells were cultured for 16 hours on fibronectin coated plates prior to treatment with 10 μM Y27632 (Y2) or 100 nM Staurosporine (ST) for 2 hours to inhibit ROCK and PKC, respectively. Immediately after treatment with inhibitor, the medium was replaced and bolus transfection was done. (**A**) Transgene expression was analyzed 48 hours post transfection using luciferase assay and normalized with total protein analyzed using Peirce BCA assay. (**B**) Internalization was assessed 2 hours post transfection using flow cytometry and YOYO-1 labeled polyplexes. A total of 7000 events were analyzed per sample. Statistical analysis was done using a one-way Anova followed by the Dunnett multiple comparison test. The Anova p value was 0.0003 and < 0.0001 for transgene expression and internalization, respectively. The symbol ** represents a significant change to the level of $p < 0.01$.

On the other hand, a significant decrease was observed in internalization (**Figure 8-1F)** by specifically inhibiting Rac1. A decrease in internalization was also observed by specifically inhibiting Cdc42, but was not statistically significant, while no significant effect was seen on transgene expression (**Figure 8-1E)**

8.2.2 Effect of activation of RhoGTPases on gene transfer in NIH/3T3 cells plated on fibronectin.

On studying the effect of activation of RhoGTPases on gene transfer to NIH/3T3 cells, it was observed that activation of Rho using treatment with CP did not affect transgene expression, whereas internalization (**Figure 8-2 A and B**) significantly increased ($p < 0.001$) for lower concentration of CP (12.5 μg/ml) and decreased ($p < 0.001$) for higher concentration (50 μg/ml)

of CP. As observed in mMSCs, Rac and Cdc42 activation using treatment with 0-100 ng/ml EGF did not affect the transgene expresession but significantly ($p < 0.05$) increased internalization in NIH/3T3 cells (**Figures 8-2 C and D**). The increase in internalization was significantly more ($p < 0.05$) using 25 and 50 ng/ml EGF as compared to 12.5 and 100 ng/ml EGF.

Additionally, the effect of transiently expressing constitutively active RhoGTPase genes on gene transfer to NIH/3T3 cells plated on Fn was studied (**Figures 8-2 E and F**). Specific activation of Rac1 and Cdc42 increased the transgene expression by 4.3-fold and 2.1-fold, respectively, while RhoA activation resulted in a >80% decrease in transgene expression (**Figure 8-2E**). The specific activation of RhoGTPases did not significantly modulate internalization (**Figure 8-2F**). This indicates that as observed in mMSCs, the RhoGTPases also play an integrap role in mediating gene transfer in NIH/3T3 cells plated on a precoated Fn surface.

8.2.3 Effect of ROCK and PKC on gene transfer in NIH/3T3 cells plated on fibronectin.

To divulge the role of ROCK and protein kinase C (PKC) in gene transfer, ROCK was inhibited using Y27632 and PKC was inhibited using staurosporine. The effect of these inhibitors on cell morphology and viability was studied using mMSCs in chapter 7.

Y27632 is a specific inhibitor of ROCK. Treatment with Y27632 resulted in a significant decrease in polyplex internalization in NIH/3T3 cells, as was observed for mMSCs. However, unlike in the mMSCs, the overall trangene expression was not influenced significantly in NIH/3T3 cells (**Figure 8-3A**).

On analyzing the effect of PKC inhibition on gene transfer, it was observed that the transgene expression as well as polyplex uptake was significantly reduced ($P < 0.001$, **Figures 8-3 A and B**).

Our studies showed that the Rho subfamily of small GTPases modulate non-viral gene transfer, with Cdc42 and Rac activation, resulting in a significant increase in non-viral gene transfer to mMSCs and NIH/3T3 cells.

8.3 Discussion: Comparing the role of RhoGTPases in gene transfer in NIH/3T3 cells with mMSCs.

Collective inhibition of Rho, Rac and Cdc42 and specific inhibition Rho, Rac and Cdc42 using dominant negative genes increased polyplex internalization, but severely limited transgene expression in both mMSCs and NIH/3T3 cells pointing out their positive role in mediating transfection in both cell types. Specific inhibition of RhoA, Rac1 and Cdc42 using dominant negative genes had decreased polyplex internalization and transgene expression in mMSCs, as shown in chapter 7. However, specific inhibition of the RhoGTPases did not signifcantly influence the gene transfer in NIH/3T3 cells, except that inhibition of Rac led to a significant decrease in internalization ($p < 0.05$).

RhoGTPases can regulate intracellular processing of polyplexes by influencing actin-microtubule dynamics, cell proliferation [92] and gene transcription via integrin-dependent intracellular signaling pathways [93]. Rho activation using CP and Rac/Cdc42 activation using EGF did not influence the transgene expression in both cell types. However, Rac and Cdc42 activation using EGF significantly increased polyplex uptake in NIH/3T3, although we show that EGF activates Rac and Cdc42, EGF also stimulates macropinocytosis [161]. Therefore, the role of activated RhoA, Rac1 and Cdc42 was specifically studied by transiently expressing constitutively active RhoGTPase mutants. In chapter 7, transfection with constitutively active RhoGTPases resulted in increased amounts of active RhoA, Rac and Cdc42.

As was observed with CP and EGF treatment, the expression of constitutively active RhoA, Rac1 and Cdc42 had not influenced transgene expression or uptake for mMSCs plated on fibronectin as shown in chapter 7. On the other hand, specific activation of RhoA inhibited the transgene expression by 0.8-fold in NIH/3T3 cells, however activation of Rac1 and Cdc42 increased transgene expression by 4.3- and 2.1- fold, respectively.

Activation of Rac/Cdc42 using EGF significntly increased internalization, specific inhibition of Rac significantly decreased internalization, and specific activation of Rac increased transgene expression in NIH/3T3 cells but not in mMSCs. This indicated that Rac and Cdc42 play a more consequential role in efficient transgene expression in NIH/3T3 cells as compared to mMSCs.

It seems that the role of RhoGTPases in non-viral gene transfer is cell dependent as has been observed for bacterial internalization which employs RhoGTPases differently in HeLa versus MDCK cells [100] .

8.4 Conclusion

In conclusion, RhoGTPases play a significant role in the modulation of efficient delivery of non-viral vectors to mMSCs and NIH/3T3 cells. The inhibition and activation studies conducted for studying the role of RhoGTPases on non-viral gene transfer showed varying results for mMSCs and NIH/3T3 cells. Fn has been shown to activate RhoGTPases in cells [108, 109]. Experiments performed to test whether activation of RhoGTPases would further increase gene transfer on Fn, indicated that a further activation of RhoGTPases did not increase transgene expression in mMSCs on Fn, but a further activation of RacGTP and Cdc42GTP increased the transgene expression in NIH/3T3 cells plated on Fn. These results taken together further indicated that the role of RhoGTPases in non-viral gene transfer is cell-type dependent.

Chapter 9

Stem Cell Culture in Three Dimensions Using Fibrin Hydrogels

9.1 Introduction

3-D matrices provide a better model system for studying cellular physiological processes as cells in tissues exist in a 3-D system, constituting characteristic ECM molecules. Cellular processes of differentiation and morphogenesis for tissue engineering have been shown to occur preferentially in 3-D instead of 2-D [75, 76]. Certain MSCs significantly upregulate the expression of smooth muscle specific proteins, such as αSMA and myosin, when cultured in 3-D PEG hydrogels as compared to on a tissue culture plastic surface [77]. Therefore, the culture of cells in 3-D is able to mimic the natural in-vivo environment more closely.

Tissue like hydrogels as 3-D scaffolds embody tissue like flexibility while possessing viscoelastic properties, interstitial flow, and diffusive transport characteristics similar to tissues. In this chapter, 3-D culture of cells in fibrin hydrogels has been explored. Fibrin alone or in combination with other biomaterials has been applied as a biological scaffold to regenerate adipose tissue, cartilage, bone, ligaments and cardiac tissue [169, 170]. Fibrin gels also allow facile incorporation of ECM proteins.

While fibrin has domains for cell interaction and adhesion, it lacks useful domains of ECM proteins that mediate cell behavior. In this chapter, the objective was to develop fibrin gels incorporating ECM proteins that would support mesenchymal stem cell (MSC) culture and mediate efficient gene transfer. These gels were to be developed to study the influence of ECM proteins and different culture conditions on gene transfer to stem cells.

9.1.1 Advantages of using fibrin hydrogel for tissue engineering.

Fibrin is a fibrous protein involved in the clotting of blood. Fibrin is made from fibrinogen, a soluble plasma glycoprotein that is synthesized by the liver. Processes in the coagulation cascade activate prothrombin to the serine protease thrombin, which is responsible for converting fibrinogen into fibrin. Fibrin is then cross linked by factor XIII to form a clot. This covalent crosslinking of the fibrin strands using Factor XIIIa also associates fibrin with extra-cellular matrix proteins like fibronectin, vitronectin, collagen and von Willebrand factor (vWF), while immobilizing the clot at the site of injury. Fibrin gels provide a unique platform for studies of cells cultured in 3-D [171], as 1) fibrin is non-toxic as a macromer, 2) can be polymerized to form gels as well as 3) is degraded in-vivo by cell secreted proteases allowing its remodeling.

9.1.2 Incorporation of ECM proteins in fibrin hydrogels

Fibrin has certain domains like the RGD sequence which allows cell adhesion, however, it lacks the other useful domains contained in the ECM proteins like fibronectin, vitronectin, laminin and collagen that are able to guide cell behavior and function.

Factor XIIIa (FXIIIa) plays an important role in the final stages of the coagulation cascade by covalently crosslinking the fibrin strands [172]. Studies have shown that in wound healing,

thrombin activated FactorXIII stabilizes the fibrin clots while simultaneously sequestering various ECM proteins. Since most ECM proteins have sites for Factor XIIIa or for other tissue transglutaminases, such transglutaminases offer a facile approach to incorporate the ECM proteins in a 3-D matrix using Factor XIIIa for gelation [173, 174]. The incorporation of the various ECM proteins like collagen [175, 176], fibronectin [177, 178] and vitronectin [179] into fibrin gels by employing factorXIIIa mediated crosslinking has been illustrated in previous studies analyzing the interactions between the ECM protein and fibrin.

The binding site of fibronectin with fibrin for factorXIIIa mediated covalent crosslinking has been extensively studied [178, 180]. The quantity of fibronectin incorporated in the gel increases linearly with increase in fibronectin concentration in the presence of factorXIII and thrombin [173]. Studies have shown that the covalent crosslinking of fibronectin to fibrin by factorXIIIa is required for maximal cell adhesion to a fibronectin-fibrin matrix [177]. Recently, a study on the osteogenic differentiation of MSCs in response to fibronectin fragments interacting with specific integrins as well as full length fibronectin, demonstrated the incorporation of full length fibronectin in 3-D fibrin scaffolds, and showed that it assisted cell adhesion, spreading and proliferation [181].

The incorporation of four laminin-derived oligopeptides (RGD, IKVAV, YIGSR, RNIAEIIKDI) conjugated to FactorXIIIa substrate (N terminus of α_2-plasmin inhibitor) in fibrin gels using FactorXIIIa enhances the number of regenerated axons by 85% relative to animals treated with tubes filled with unmodified fibrin [182]. This exemplifies a way of incorporating the various proteins that have a factorXIIIa reactive site naturally, in fibrin gels using factorXIIIa mediated chemistry. The hMSC morphology, proliferation and osteogenic differentiation in fibrin gels has been shown to be dependent on the fibrinogen and thrombin ratio [131].

9.1.3 Use of fibrin gels for delivery of bioactive factors and gene delivery

Fibrin gels have been used for delivery of various bioactive factors for therapeutic purposes. Cell demanded release of VEGF tethered within fibrin implants using FactorXIIIa mediated crosslinking had been shown to significantly induce non-leaky blood vessel growth in embryonic chicken chorioallantoic membrane (CAM) and in adult mice [183]. Fibrin gels were applicable for delivering growth factors [183] to augment tissue regeneration, as well as for gene delivery [27], in addition to allowing the facile incorporation of ECM proteins along with the ability to mediate cell infiltration, adhesion and proliferation. The applicability of fibrin gels for in-vivo gene based therapies had been demonstrated using peptide-DNA nanoparticles entrapped in fibrin gels for local induction of angiogenesis in dermal wounds in mice [184]. Fibrin gels mediated the delivery of the incorporated lipoplexes to the encapsulated cells as well as infiltrating NIH/3T3 cells in in-vitro 3-D model for at least 10 days [185]. Another study demonstrated that fibrin gels mediated significantly enhanced transfection as compared to bolus transfection on 2-D tissue cultured treated wells for 293T/17 and NIH/3T3 cells. The transfection efficiency was significantly higher in encapsulated cells as compared to cells on top of fibrin gel, which was attributed to their uptake of lipoplexes by gel degradation in cell vicinity [186]. These studies validated the concept of utilizing fibrin gels for in-vitro and in-vivo gene transfer. However, the inclusion of optimum ECM signals in fibrin gels would further help stimulate the bioactivity and the gene transfer to the cells.

On a whole, the use of factorXIIIa would enable a natural incorporation of the ECM structural proteins having constituent factorXIIIa reactive sequences in the fibrin gels, without having to chemically modify each protein in order to covalently sequester them in the gels. This would

further enhance the bioactivity of the gels and provide a scaffold that could be used to deliver bioactive factors to cells.

In this chapter, it was aimed to develop and examine fibrin gels for MSC culture and gene transfer, wherein various ECM proteins would be incorporated using factor XIII mediated chemistry along with polyplexes to facilitate gene delivery. The purpose was to utilize fibrin gels as a model system to study gene transfer in 3-D with respect to the cellular microenvironment. Fibrin gels were chosen for this study as they allowed facile incorporation of the various ECM proteins via factor XIII mediated chemistry, as well as represented the natural in-vivo environment generated at the site of wound healing allowing cell infiltration and adhesion.

9.2 Materials and methods.

9.2.1 Materials. Human fibrinogen, bovine plasma thrombin and linear poly(ethylene imine) (25 kDa, PEI) were bought from Enzyme Research Laboratories, Sigma and Polysciences, respectively. Sodium hyaluronan (HA) was a kind gift from Genzyme Corporation (60 kDa MW, Cambridge, MA). All other chemicals were purchased from Fisher Scientific unless otherwise noted. Vectors expressing mammalian secreted alkaline phosphatase (pSEAP) and gaussia luciferase (pGLuc) were obtained from Genlantis and New England Biolabs, respectively. A Giga Prep kit from Qiagen was used to expand all the plasmids.

9.2.2 Cell culture. Mouse bone marrow cloned mesenchymal stem cells (D1, CRL12424) were purchased from ATCC (Manassas, VA, USA). Cells were maintained in Dulbecco's modified eagle's medium (Sigma-Aldrich) containing 10% bovine growth serum (BGS, Hyclone, Logan,

Utah) and 1% penicillin/streptomycin antibiotics (Invitrogen, Grand Island, NY) and cultured at 37˚C and 5% CO_2.

Human mesenchymal stem cells containing mito red (hMSCs, U.S. Patent 5,716,616) were purchased from the Texas A&M Health Science Center, University of Texas-A & M. hMSCs were maintained in α-MEM media with glutamine , 16.5% FBS, 2-4 mM L-glutamine and P/S (penicillin and streptomycin at a final concentration of 100 U/ml and 100 ug/ml), and cultured at 37˚C and 5% CO_2.

9.2.3 Cell proliferation. To analyze cell proliferation and spreading, phase pictures were taken at 10x and 20x magnification, or Alamar blue assay was performed. To perform alamar blue assay, media was replaced with 100 µl of phenol red free C-DMEM. 20 µl of alamar blue (5%v/v) was added to each well and incubated at 37˚C for 4 hours. 100 µl of media (sample) was transferred to another plate. Absorption was measured at 570 nm and 600 nm. Pheno red free complete media was used as blank and 100 µl of CDMEM with alamar blue (incubated for 4 hours, no cells) was used as negative control.

9.2.4 Polyplex lyophilization. The CnE approach developed by *Lei et.al.,J Control Release, 2011* was used. To make lyophilized polyplexes at NP 9, plasmid DNA (10 µg) and PEI (11.74 µg) were mixed in 3.5 ml water in the presence of 35 mg (0.10 mmol) of sucrose (Ultra pure,MP Biomedicals) and incubated at room temperature for 15 min. 1.5 ml of 0.67 mg/ml Agarose in water was added before lyophilization (UltraPure™ Agarose, Tm=34.5 to 37.5 °C, Invitrogen).

9.2.5 Phospha-light kit/SEAP reporter gene assay. The CSPD substrate was diluted 1:20 with reaction buffer. The reaction buffer and assay buffer were warmed to room temperature.1x dilution buffer was prepared. 25 µl of sample was diluted in 75 µl dilution buffer, heated to 65˚C for 30 minutes and then cooled on ice to room temperature. 100 µl of assay buffer was then added to 100 ul of sample, incubated for 5 minutes. 100 ul of assay buffer was added and incubated for 20 minutes. Finally, readings were taken in luminometer**.**

9.2.5 Formation of fibrin gels. Fibrin matrices were made using 2.5-8 mg/ml fibrinogen, 2 U/ml factor XIIIa, fibronectin at concentrations ranging from 0 to 10% (wt/wt) of fibrin concentration and cells using 2 U/ml thrombin in 1x buffer with 1g/lt $CaCl_2$. 50 µl of precursor gel solution was transfered to each well of a 96-well low binding plate. For gelation, the precursor solution was incubated at 37°C for 20 minutes and subsequently swelled with 150 µl DMEM. The change medium was changed after 10 minutes, 30 minutes, 2 hours and then daily.

9.2.6 Encapsulation of polyplexes in fibrin gels. To encapsulate polyplexes in fibrin hydrogels through CnE, 100 µl fibrin gel precursor solution was mixed with lyophilized polyplexes and initiated to form gels at 37°C for 20 minutes with thrombin (2 U/ml).
For analyzing transgene expression, media was collected daily and stored at -20°C till SEAP assay was performed using manufacturer's protocol.

9.2.7 Incorporation of ECM proteins in fibrin gels. To incorporate ECM proteins, the specific ECM protein at the required amount to constitute 2.5-7.5 wt/wt% of fibrin gel as required by the experiment, was added to the precures or gel solution containing fibrin and 2 U/ml factorXIIIa.

Lypholized polyplexes and 1 U/ml thrombin were then added to the precursor solution before initiating gelation at 37°C for 20 minutes.

9.2.8 Modification of HA. Acrylated hyaluronic acid (HA-AC) was prepared using a two-step synthesis [187, 188]. Briefly, HA (60,000 Da, Genzyme Corporation, Cambridge, MA) (2.0 g, 5.28 mmol, 60 kDa) was reacted with 18.0 g (105.5 mmol) of adipic dihydrazide (ADH) at pH 4.75 in the presence of 4.0 g (20 mmol) of 1-ethyl-3-(3-dimethylaminopropyl) carbodiimide (EDC) hydrochloride overnight and purified through dialysis (8000 MWCO) in deionized (D1) water for 2 days. The purified intermediate (HA-ADH) was lyophilized and stored at 20°C until used. A portion of 29% of the carboxyl groups was modified with ADH based on the trinitrobenzene sulfonic acid (TNBSA, Pierce, Rockford, Illinois) assay. HA-ADH was then reacted 5 molar excess of N-acryloxysuccinimide (NHS-Ac) in HEPES buffer (pH 7.2) overnight, and purified

through dialysis in DI water for 2-3 days. All the primary amines were acrylated based on the 2,4,6-trinitrobenzene sulfonic acid (TNBSA, Thermo Scientific) assay performed following the product manual.

9.2.9 HA Hydrogel Synthesis. Hydrogels were prepared with 3% HA and with the ratio of thiols to acrylates (r ratio) as 0.4-0.44. HA hydrogels were subsequently formed by Michael-type addition of biscysteine containing MMPxl peptides onto HA-AC functionalized with cell adhesion peptides (RGD). A lyophilized aliquot of RGD peptides (0.1 mg) was dissolved in 15 µl of 0.3 M TEOA buffer (pH = 8.4), mixed with HA-AC, and allowed to react for 15-20 min at 37°C. A lyophilized aliquot of the cross-linker (0.91 mg MMPxl) was then diluted in 18.2 µl of

0.3M TEOA buffer (pH = 8.4) immediately before mixing with HA-RGD (final concentration of 100 μM RGD), and the cell solution (500,000 cells per 100 μl of final gel volume). The final gel solution had a pH= 8-8.1. Gelation was achieved by placing drops of 10 μl of the precursor solution between sigmacoted glass slides for 30 min at 37°C. The final gel was placed inside 96-well plates for culture. Thorough mixing was used to ensure the homogeneity in cell and crosslinker distribution in the precursor solution.

9.2.10 Incorporation of ECM proteins in HA gels.

ECM proteins namely Fn, laminin (Lm), collagen IV (C IV) and collagen I (C I) were modified by reacting with Nacryloxysuccinimide (NHS-Ac) at 10,000 molar access of NHS-Ac with respect to the ECM protein. NHS-Ac was dissolved in PBS at a concentration of 10 mg/ml and immediately added to the ECM protein, mixed and left overnight on a rotational shaker at 4°C. The acrylated ECM protein was filtered and concentrated using centricon with 10 KDa NMWL membrane (Millipore, Billerica, MA). The concentration of the protein was determined and subsequently used in experiments. The amount of ECM protein required to obtain a specific concetration in the hydrolgel, was added directly to the HA gel precursor solution, before addition of crooslinker

9.2.11 Bolus transfection in HA hydrogels. DNA/PEI polyplexes were formed by mixing equal volumes of plasmid DNA with 25 kDa-Linear PEI**.** For every 1 μg of DNA, 0.913 μg of PEI was added to the DNA solution to get N/P of 7, vortexed for 15 seconds and incubated at room temperature for 15 minutes. Subsequently salt was added to the polyplex solution to get a final

concentration of 150 mM NaCl. Polyplexes were then added directly to the medium of the plated cells at a final DNA concentration of 5 μg per gel (10 μl) per well of 96 well low binding plate. Transfection was quantified at 48 hours post transfection using the Gaussia Luciferase Assay System following the manufacturer's instructions.

9.3 Results and discussion

9.3.1 Fibrin gels for 3-D culture of mMSCs.

To assess the use of fibrin gels for culturing MSCs, fibrin gels were made using 1U/ml thrombin, with or without factorXIIIa, Fn and polyplexes. Cell proliferation was analyzed on day 2 and 4 of cell culture using alamar blue assay. As shown in **figure 9-1A,** the rate of cell proliferation on day 2 and 4 was statistically similar for fibrin-thrombin gels with or without factor XIIIa. For gels incorporating polyplexes the rate of proliferation on day 2 was significantly lower as compared to fibrin-thrombin gel ($p < 0.01$). The rate of proliferation of cells on day 4 in fibrin-thrombin gels having Fn incorporated using factorXIIIa, was statistically higher than the fibrin-thrombin gels without Fn ($p < 0.05$).

The extent of cell spreading observed on day 3 corresponded to the results obtained for proliferation using alamar blue. Well spread cells were observed in fibrin gels using thrombin, with or without factorXIIIa (**Figure 9-1B)**. For fibrin-thrombin with factorXIIIa and Fn, more

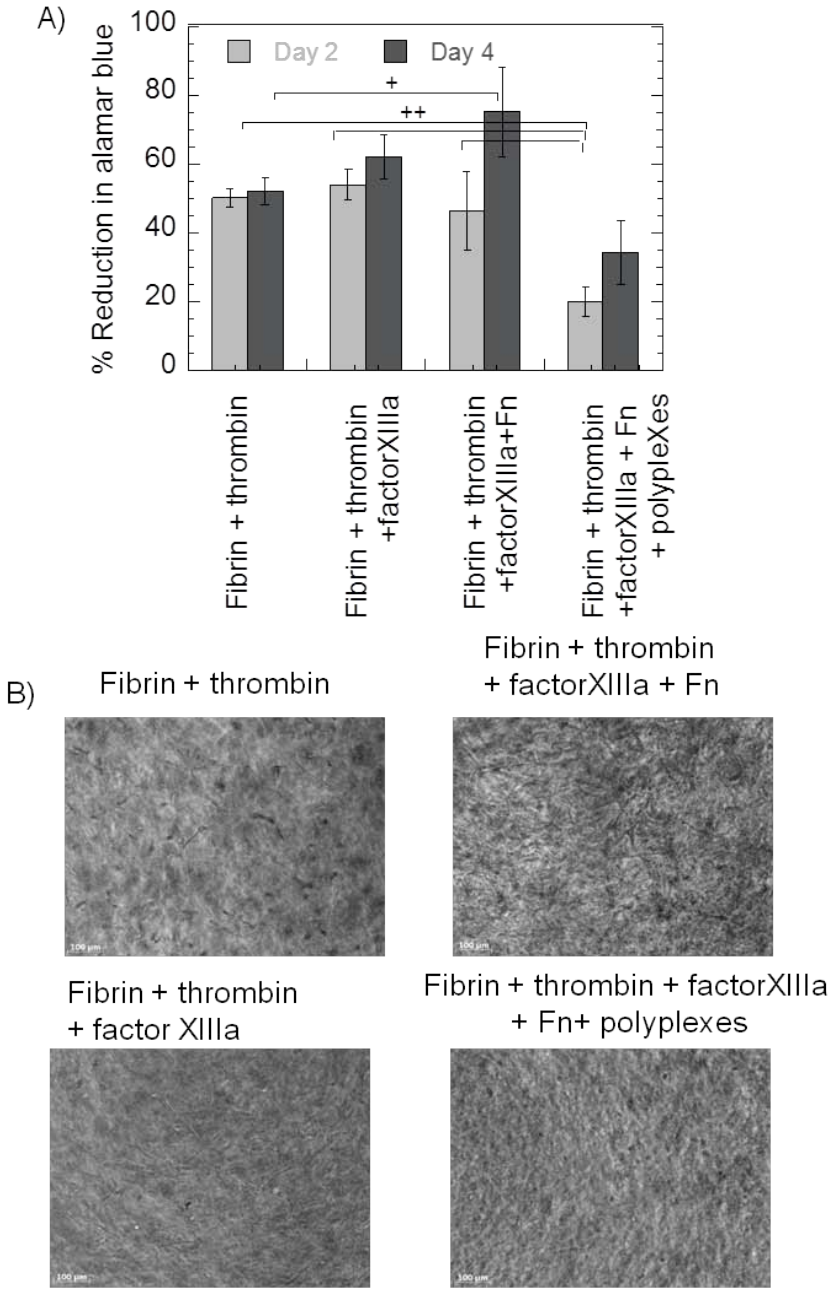

Figure 9-1: mMSC culture in fibrin gels. 3 mg/ml fibrin gels were made using 1 U/ml thrombin with or without 2 U/ml factorXIIIa, 2.5 wt/wt% Fn and polyplexes. **A**) Cell proliferation in different gels was analyzed on day 2 and 4 of cell culture, using alamar blue assay. **B**) Cell spreading was analyzed on day 3 taking phase images using a Zeiss AxioObserver Z1 inverted microscope, at 10. Statistical analysis for internalization was done using Tukey-Kramer multiple comparison test which compares all pairs within the same protein coat. The symbols + and ++ represent the significant change to the level of $p < 0.05$, and $p < 0.01$, respectively.

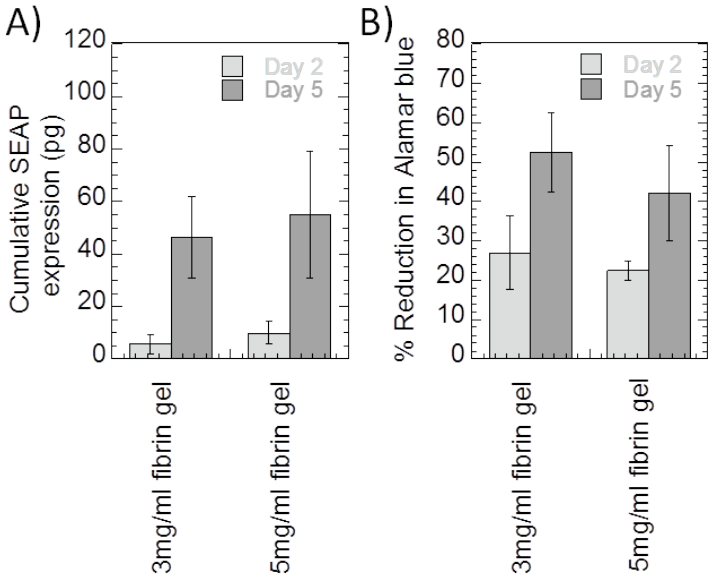

Figure 9-2: Transfection ability of fibrin gels. 3 mg/ml and 5 mg/ml fibrin gels were made using 2 U/ml thrombin. 5 µg of DNA was included per 100 µl of gel. Media was collected daily. **A**) The cumulative SEAP expression was calculated on day 2 and 5 using SEAP reporter gene assay kit. **B**) Cell proliferation was analyzed on day 2 and 5 using alamar blue assay. All experiments were performed in triplicates.

cells were observed to spread, while for gel with polyplexes, less cell spreading was observed (**Figure 9-1B)**. 5 µg of pSEAP in polyplexes was incorporated per 100 µl of the gel.

These results indicate that the addition of ECM protein Fn increased proliferation while addition of only factorXIIIa to the fibrin gel did not increase proliferation. These gels promote cell spreading and proliferation of the mMSCs.

9.3.2 Fibrin gels for 3-D culture of mMSCs.

After fibrin-thrombin gels were found to support cell spreading and proliferation, the next step was to determine if these gels mediated effective non-viral gene transfer. Media was collected daily and the amount of SEAP protein was quantified using Phospha-light^{TM} SEAP

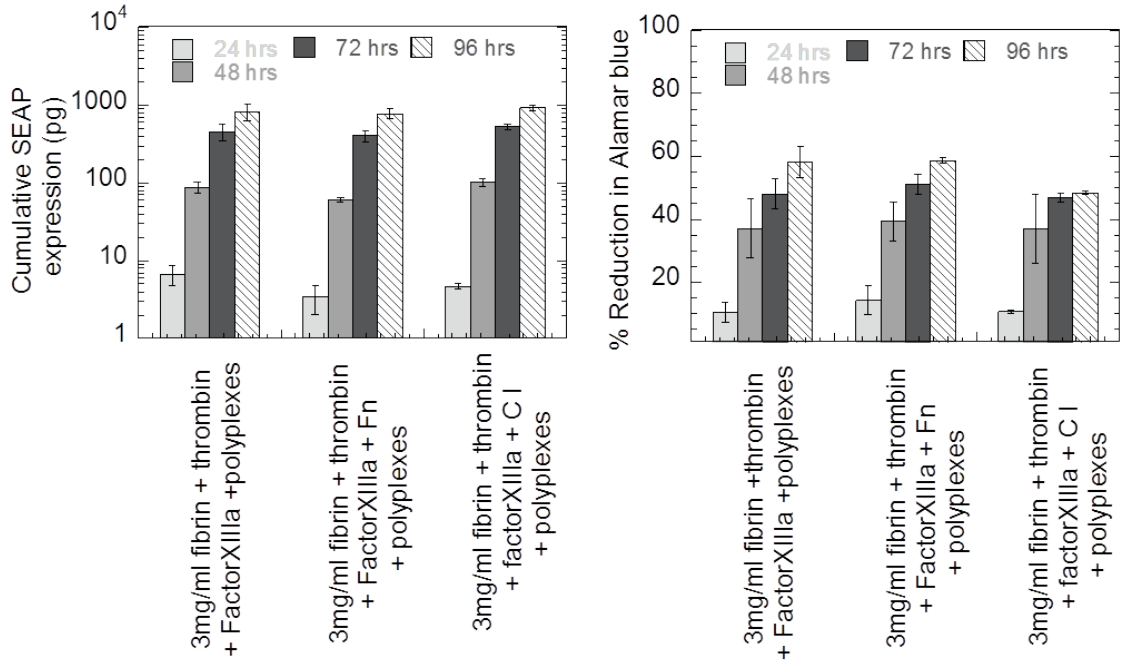

Figure 9-3: Effect of incorporation of Fn or C I on transfection mediated by fibrin gels. 3 mg/ml fibrin gels were made with inclusion of polyplexes and factorXIIIa, with or without 2.5% (wt/wt) Fn or 2% (wt/wt) C I. 100,000 cells and 2.5 µg pDNA were incorporated per 100 µl gel. The media was collected daily and SEAP expression was analyzed. **A**) Cumulative SEAP expression for day 1 till 4 was plotted. **B**) Proliferation was analyzed on day 1 till day 4 using alamar blue assay. All experiments were performed in triplicates.

Reporter Gene Assay. Triplicate samples were examined and cumulative SEAP expression calcalulated and plotted. It was observed that fibrin gels led to transfection and transgene expression of SEAP (**Figure 9-2A**). Transfection and proliferation in 3 mg/ml and 5 mg/ml fibrin gels was statistically the same (**Figures 9-2 A and B**). This indicated that the transfection ability of these gels does not depend on fibrin concentration in the range of 3-5 mg/ml.

9.3.3 Incorporation of ECM proteins Fn or C I in fibrin gels did not enhance transgene expression.

3 mg/ml fibrin gels were made and 5 µg pDNA was included per 200 µl of gel. The level of

transgene expression obtained in gels without ECM proteins, gels with Fn or gels with C I was similar (**Figure 9-3A**). The rate of proliferation as determined by alamar blue assay was also similar for the gels from day 1 to day 3 (**Figure 9-3B**).

This indicated that fibrin gels interact with mMSCs to promote cell proliferation and effective transfection, even without the inclusion of ECM proteins Fn or C I.

9.3.4 Influence of ECM proteins on gene transfer in fibrin gels and hyaluronic acid gels.

It has been demonstrated that fibrin gels mediate cell spreading, proliferation and transgene expression. The objective to develop such a hydrogel was to be able to employ it for studying the role of ECM and mechanism of gene transfer in mMSCs cultured in 3-D.

3 mg/ml fibrin gels were made which included 5% (wt/wt) ECM protein or did not include any ECM protein. 5 µg of pGLuc in the form of lypholized polyplexes, was included per 200 µl of gel. ECM proteins tested were laminin (Lm), fibronectin (Fn), vitronectin (Vt), collagen IV (C IV) and collagen I (C I). On analyzing the transgene expression using gaussia luciferase assay, similar level of transgene expression was observed for different ECM protein containing gels (**Figure 9-4A**). Fibrin gels made using thrombin, but without factor XIIIa and ECM protein, mediated similar or higher transgene expression as compared to gels with ECM proteins.

We then studied the influence of ECM proteins in HA hydrogels. Since HA does not interact with integrins and support cell adhesion, HA conjugated with adhesion peptide (RGD) was used as control. Here, bolus transfection was done. Different ECM proteins were found to mediate varied levels of gene transfer. The transgene expression mediated by laminin was significantly more than collagen IV and fibronectin ($p < 0.05$, **Figure 9-4B**). A decrease was observed with

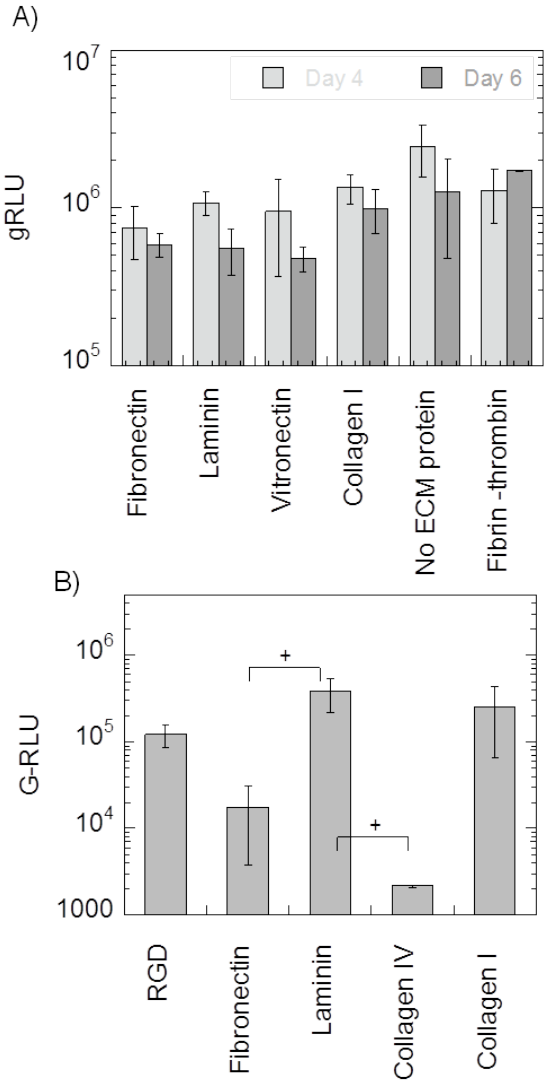

Figure 9-4: Influence of ECM proteins on transfection in 3 mg/ml fibrin gels and 3% HA gels.
A) 3 mg/ml fibrin gels were made incorporating 5% (wt/wt) of different ECM proteins, 2.5 µg pGLuc and 100,000 cells per 100 µl gel. 50 µl gel was added per well of a 96-well low binding plate. Media was collected daily and transfection was analyzed using gaussia luciferase assay as per manufacturer's protocol. The gLuc expression on respective days haD been plotted.
B) 3% HA gels were made incorporating either 100 µM RGD, or 4.25 µM Fn, or 1.9 µM laminin, or 1.8 µM collagen IV or 22.5 µM collagen I. 500,000 cells were included per 100 µl gel. 10 µl HA gel was added to each well of a 96-well low binding plate. Bolus transfection was done and 5 µg pGLuc was added per well, for HA hydrogels. Transgene expression was analyzed 48 hours post transfection using gaussia luciferase assay. Statistical analysis for internalization was done using Tukey-Kramer multiple comparison test, which compares all pairs within the same protein coat. The symbo + represents the significant change to the level of $p < 0.05$. All experiments were done in triplicates.

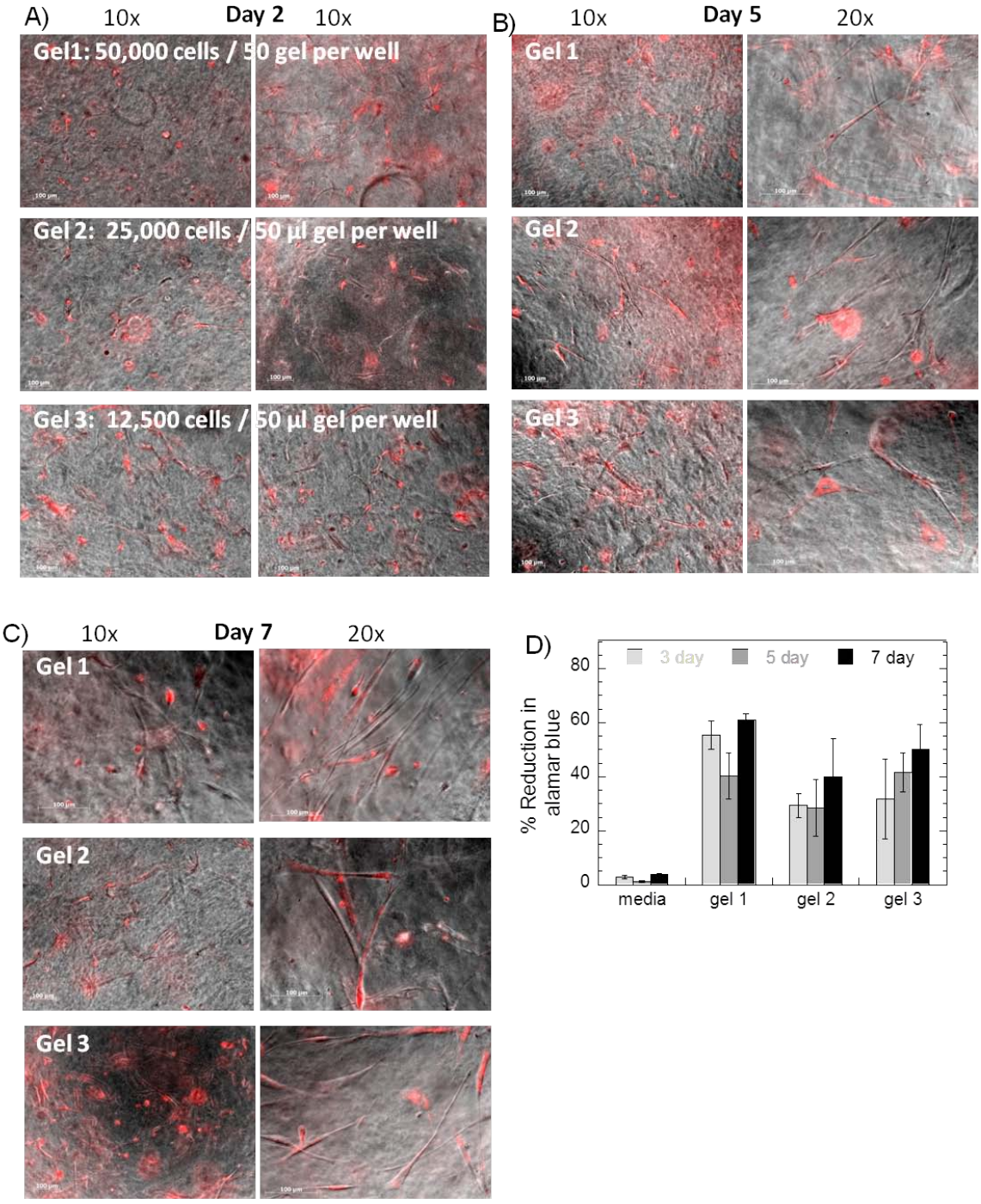

Figure 9-5: hMSC culture in fibrin gels. 3 mg/ml fibrin gels were made using thrombin. hMSCs were cultured at different cell densities. **(A)**, (**B**) and (**C**) Phase and fluorescent images using AxioObserver Z1 inverted microscop at 40x. **D**) Proliferation rate was analyzed using alamar blue assay.

Fn and C IV while an increase was observed with laminin, as compared to HA gels wirh RGD (**Figure 9-4B**).

9.3.5 Fibrin gels for hMSC culture.

To assess the application of fibrin gels for culture of human mesenchymal stem cells (hMSCs), hMSCs with mito red were incorporated at different intial seeding densities, to determine the optimum seeding density for 3-D culture. Fibrin gels sustained hMSC spreading and proliferation at an initial seeding density of 12,500 cells till 50,000 cells per 50 µl gel per well of a 96 well low binding plate (**Figure 9-5A**). Cell spreading was evident in the phase and flourescent images of hMSCs with mito red in fibrin gels. The proliferation was analyzed using alamar blue assay. Fibrin gels supported proliferation until day seven in all gels, having different initial seeding density of hMSCs (**Figure 9-5B**). The observed proliferation was consistent with the observed cell spreading of hMSCs in fibrin gels.

9.4 Conclusion

Fibrin gels supported the culture of mouse as well as human mesenchymal stem cells, thereby promoting cell spreading and growth. Fibrin gels were found to be a good tool to mediate gene delivery in-vitro to mMSCs. However, since the fibrin gels themselves supported good cell viability and transfection, no significant differences were observed on incorporating ECM proteins. Subsequently, hydrogels using hyaluronic acid (HA) were tested. HA does not interact with integrins to support cell adhesion and subsequent proliferation. Conjugation of adhesion peptides such as RGD is required to initiate cell attachment and spreading. Incorporation of different ECM proteins in HA hydroels mediated varied levels of transgene expression with

laminin enhancing the transgene expression, and fibronectin and collagen IV inhibiting transgene expression. Interestingly, this result was opposite as compared to 2-D in tissue culture plastes, wherein fibronectin and collagen IV enhanced transgene expression, as shown in chapter 4 and 5. This indicated that ECM proteins differentially influenced non-viral gene transfer to cells plated in 2-D in coventional tissue culture plastic and in cells cultured in 3-D using HA hydrogels.

HA gels with RGD were taken as control, and any change observed in gene transfer and cell behavior on varying the culture conditions as with respect to the control, was due to the condition or response to other constituents of the gel. This was not the case with fibrin gels where the influence of ECM proteins on gene transfer could not be detected as fibrin gels themselves promoted transfection.

Hence, for studying gene transfer mechanism in mMSCs cultured in 3-D in the next chapter, 3% hyaluronic acid gels with incoporated RGD adhesion peptide were employed.

Chapter 10

Non-Viral Gene Delivery to Mouse Mesenchymal Stem Cells in 2-D on Tissue Culture Plastic Surface and in 3-D in Hyaluronic Acid Hydrogels

10.1 Introduction

The cell microenvironment has been shown to modulate non-viral gene delivery in 2-D surfaces [1, 6, 42, 144], as established in the previous chapters. Recent studies have shown that cell microenvironment is able to influence gene transfer in 3-D [185, 187]. While the underlying mechanisms mediating gene transfer to cells plated in 2-D had been widely studied [34, 122, 144, 189], the mechanisms involved in gene transfer to cells in 3-D had not been studied in detail. Chapter 3 and 8 provided insight about the benefits of culturing cells in 3-D as compared to 2-D. Cells in tissues are in a three-dimensional environment having characteristic biophysical and biomechanical signals. The biophysical signals embedded in three dimensional (3-D) matrix influence cell functions like migration, adhesion, proliferation, gene expression and secretion of biological molecules [70-74]. Cellular processes like proliferation and migration as well as cellular morphology have been shown to be significantly different in 2-D versus 3-D system. The cell behavior in 2-D cannot be compared with cell behavior in 3-D. Furthermore, 2-D and 3-D could differentially modulate transfection [186]. Hence, the gene transfer mechanism and

efficiency were likely to be influenced by dimensionality [182, 186]. If so, then the cell behavior and underlying mechanisms for gene transfer involving endocytosis pathways, cytoskeletal dynamics and RhoGTPases, that regulate gene transfer in 2-D (as shown in chapter 4,5,6 and 7) cannot be applied to the development of gene transfer systems in 3-D.

Local gene delivery using hydrogel scaffolds has been studied for over a decade primarily through the encapsulation of naked DNA during hydrogel formation. In this study we used hyaluronic acid (HA) hydrogels which are rapidly gaining popularity as a tissue engineering scaffold [190, 191]. Hyaluronic acid is a polysaccharide that is also known as hyaluronan or HA. It is an unmodified glycosaminoglycan (GAG) in the extracellular matrix (ECM) and is found in all connective tissues. HA is a linear copolymer of D-glucorinc acid and N-acetyl-D-glucosamine, and is visco-elastic with the ability to highly absorb water [192]. HA plays a dynamic role in many biological processes. HA influences tissue organization via interactions with cell surface receptors such as CD44 and RHAMM (receptor for HA-mediated motility). HA promotes the migration of cells, facilitates ECM remodeeling , promotes inflammatory response and can inhibit cell adhesion [190].

A MMP degradable HA hydrogel scaffold for stem cell culture and non-viral gene delivery had been composed [187, 188]. HA was cross-linked to form a hydrogel material using a MMP degradable peptide and Michael addition chemistry. Internalization pathways, cytoskeletal dynamics and RhoGTPases modulate non-viral gene delivery to mMSCs cultured in 2-D [146, 193]. In this chapter we use this hydrogel scaffold to investigate the role of different endocytosis pathways, cytoskeleton constituents and RhoGTPases in non-viral gene transfer to mMSCs plated in 3-D in HA hydrogels, in comparison to 2-D on conventional tissue culture plastic

surface (TCPS) , as 3-D culture of cells mimics its natural environment more closely. *Aims and hypothesis covered in this chapter are: Aim 4 and Hypothesis 4.*

10.2 Materials and Methods

10.2.1 Materials. Peptides Ac-GCRDGPQGIWGQDRCG-NH2 (MMPxl) and Ac-GCGWGRGDSPG-NH2 (RGD) were obtained from Genescript (Piscataway, NJ). Sodium hyaluronan was a gift from Genzyme Corp. (Boston,MA). Gaussia luciferase expression vector (pGluc, New England BioLabs, Ipswich, MA) was expanded using an endotoxin-free Giga Prep kit from Qiagen following the manufacturer's instructions. Linear PEI (25 kg/mol) was purchased from Polysciences (Warrington, PA).

Amiloride hydrochloride hydrate, Methyl-β-cyclodextrin, Cytochalasin D, Nocodazole, Butanedione monoxime (BD), IPA-3 and Y27632 were purchased from Sigma Aldrich (St Louis, MO). Genistein, Chlorpromazine hydrochloride and were purchased from Fisher scientific. Jasplikinolide was purchased from Invitrogen (Grand Island, NY) and Endothelin I was purchased from Calbiochem (EMD biosciences, San Diego, CA). Difficile toxin B (TcdB) was purchased from List Biologicals (Campbell, CA). C3 transferase (C3), Paclitaxel, , Rho/Rac/Cdc42 activator I and Rho activator II were purchased from Cytoskeleton Inc (Denver, CO). All other products were purchased from Fisher Scientific unless noted otherwise.

10.2.2 Cell culture. Mouse bone marrow cloned mesenchymal stem cells (D1, CRL12424) were purchased from ATCC (Manassas, VA, USA). Cells were maintained in Dulbecco’s modified eagle’s medium (Sigma-Aldrich) containing 10% bovine growth serum (BGS, Hyclone, Logan,

Utah) and 1% penicillin/streptomycin antibiotics (Invitrogen, Grand Island, NY) and cultured at 37˚C and 5% CO_2.

10.2.3 Modification of HA. Acrylated hyaluronic acid (HA-AC) was prepared using a two-step synthesis as previously described [187, 188]. Briefly, HA (60,000 Da, Genzyme Corporation, Cambridge, MA) (2.0 g, 5.28 mmol, 60 kDa) was reacted with 18.0 g (105.5 mmol) of adipic dihydrazide (ADH) at pH 4.75 in the presence of 4.0 g (20 mmol) of 1-ethyl-3-(3-dimethylaminopropyl) carbodiimide hydrochloride (EDC) overnight and purified through dialysis (8000 MWCO) in deionized (D1) water for 2 days. The purified intermediate (HA-ADH) was lyophilized and stored at 20 °C until used. A portion of 29% of the carboxyl groups was modified with ADH based on the trinitrobenzene sulfonic acid (TNBSA, Pierce, Rockford, Illinois) assay. HA-ADH was then reacted 5 molar excess of Nacryloxysuccinimide (NHS-Ac) in HEPES buffer (pH 7.2) overnight, and purified through dialysis in DI water for 2-3 days. All the primary amines were acrylated based on the 2,4,6-trinitrobenzene sulfonic acid (TNBSA, Thermo Scientific) assay performed following the product manual.

10.2.4 HA Hydrogel Synthesis. Hydrogels were prepared with 3% HA and with the ratio of thiols to acrylates (r ratio) as 0.4-0.44. HA hydrogels were subsequently formed by Michael-type addition of biscysteine containing MMPxl peptides onto HA-AC functionalized with cell adhesion peptides (RGD). A lyophilized aliquot of RGD peptides (0.1 mg) was dissolved in 15 µl of 0.3 M TEOA buffer (pH = 8.4), mixed with HA-AC, and allowed to react for 15-20 min at 37°C. A lyophilized aliquot of the cross-linker (0.91 mg MMPxl) was then diluted in 18.2 µl of 0.3M TEOA buffer (pH = 8.4) immediately before mixing with HA-RGD (final concentration of

100 μM RGD), and the cell solution (500,000 cells per 100 μl of final gel volume). The final gel solution had a pH=8-8.1. Gelation was achieved by placing drops of 10 μl of the precursor solution between sigmacoted glass slides for 30 min at 37°C. The final gel was placed inside 96-well plates for culture. Thorough mixing was used to ensure the homogeneity in cell and crosslinker distribution in the precursor solution.

10.2.5 Characterization of HA Hydrogel Mechanical Properties. The storage and loss modulus were measured with a plate-to-plate rheometer (Physica MCR, Anton Paar, Ashland, VA) using a 8 mm plate under a constant strain of 0.01 and frequency ranging from 0.1 to 10 rad/s. Hydrogels were made as detailed above and cut to a size of 8.0 mm in diameter to fit the plate. A humid hood was used to prevent the hydrogel from drying, and the temperature was kept at 37°C.

10.2.6 Cell morphology. Cells were fixed and stained for actin and nuclear DNA using Alexa488-phalloidin and Hoechst dye following the manufacturer's instructions and standard staining protocols. Briefly, after two PBS washes the cells were fixed with 4% paraformaldehyde (PFA) for 30 minutes at room temperature and the cell membrane was weakened with 0.1% tritonX100 in PBS for 6 minutes. Hoechst dye and Alexa488-phalloidin were then added and left in the dark for 60 minutes at room temperature followed by three washes with 0.05% tween-20. The samples were imaged using confocal microscopy at 20x magnification.

10.2.7 Cell proliferation. The Cell Titer 96®Aqueous One Solution Cell Proliferation Assay (Promega) was performed to determine the cytotoxicity and proliferation of the cells in different

ECM proteins. The Aqueous One Solution (20 µl) was added in each well to be assayed and incubated for 2 hours. SDS (25 µl of a 10% solution) was added to each well after the incubation. The fluorescence was measured using a plate reader at 490 nm. Three gels for each condition were analyzed at each time point.

10.2.8 Transfection in 2-D. The cells were allowed to attach and cultured under various conditions as per required for the experiments mentioned. For gene transfer studies, DNA/PEI polyplexes were formed by mixing equal volumes of plasmid DNA with PEI**.** For every 1 µg of DNA, 1.65 µg of PEI was added to the DNA solution to get N/P of 12, vortexed for 15 seconds and incubated at room temperature for 15 minutes. Polyplexes were added directly to the medium of the plated cells at a final DNA concentration of 0.5 µg for 48 well plates. Salt was added directly to the wells post addition of transfection solution to get a final concentration of 150 mM NaCl. Transfection was quantified at 48 hours post transfection using the Gaussia Luciferase Assay System following the manufacturer's instructions.

10.2.9 Internalization of polyplexes in 2-D. Plasmid DNA (pGluc) and the fluorescent DNA-intercalator YOYO-1 were mixed at a ratio of 1 YOYO-1 molecule per 50 base pairs and were allowed to complex for 60 minutes at room temperature. YOYO-1 labeled DNA was then used to prepare PEI/DNA complexes at a N/P of 12 (as mentioned above) and bolus transfection was performed. Two hours after exposure to the polyplexes, cells were washed with PBS, trysinized with 50 µl of 0.25% trypsin-EDTA and finally suspended in 350 µl of 0.04% tryphan blue in 1% BGS in PBS. Fluorescent cells were detected by flow cytometry with a FACScan X and data was analyzed with CELLQuest (Beckton Dickinson). Experiments were performed in triplicates

analyzing 5000 total events per sample and and mean fluorescence intensity of total events was plotted.

10.2.10 Transfection in hydrogels. DNA/PEI polyplexes were formed by mixing equal volumes of plasmid DNA with 25 kDa-Linear PEI**.** For every 1 μg of DNA, 0.913 μg of PEI was added to the DNA solution to get N/P of 7, vortexed for 15 seconds and incubated at room temperature for 15 minutes. Subsequently salt was added to the polyplex solution to get a final concentration of 150 mM NaCl. Polyplexes were then added directly to the medium of the incoporated cells at a final DNA concentration of 5 μg per gel (10 μl) per well of 96 well low binding plate. Transfection was quantified at 48 hours post transfection using the Gaussia Luciferase Assay System following the manufacturer's instructions.

10.2.11 Internalization in hydrogels. Plasmid DNA (pSEAP) and the fluorescent DNA-intercalator YOYO-1 were mixed at a ratio of 1 YOYO-1 molecule per 50 base pairs and were allowed to complex for 60 minutes at room temperature. YOYO-1 labeled DNA was then used to prepare PEI/DNA complexes at a N/P of 7 (as mentioned above for transfection in hydrogels) and bolus transfection was performed. Two hours after exposure to the polyplexes, gels were washed with PBS, degraded by trysinization with 50 μl of 0.25% trypsin-EDTA for 5 minutes, and finally suspended in 250 μl of 0.04% tryphan blue in 1% BGS in PBS. Fluorescent cells were detected by flow cytometry with a FACScanX and data was analyzed with CELLQuest (Beckton Dickinson). Experiments were performed in triplicates analyzing 5000 total events per sample and mean fluorescence intensity of total events was plotted.

10.2.12 Analyzing endocytic pathways. For 2-D cell culture 20,000 cells per well were cultured in a 48 well plate for 13-14 hours before pretreatment with inhibitors for endocytosis to determine the endocytic pathways active in cells. For 3-D cell culture 50,000 cells per 10 µl hydrogel per well were cultured in a 96 well plate for 2 days before pretreatment. Clathrin mediated endocytosis was inhibited by using 10 µg/ml chloropromazine (-clathrin I) and indirectly inhibited using 50 µM dynasore (-clathrin II), caveolae mediated endocytosis was inhibited using 200 µM genestein (-caveolae I) and 0.5-1 mM cyclodextrin (-caveolae II), and macropinocytosis was inhibited using 100 µM ameloride (-macropinocytosis). A 1.5 hours pretreatment for genistein, chlorpromazine and amiloride, and 1 hour pretreatment for cyclodextrin and dynasore was given in 2-D and 3-D. Subsequently, cells were incubated with polyplexes for 4 hours and overnight (12-13 hours) in 2-D and 3-D, respectively. The media was then replaced with fresh media. 48 hours post addition of media, transgene expression and cell proliferation were analyzed using above-mentioned method.

10.2.13 Studying the role of cytoskeleton in gene transfer. For 2-D cell culture 20,000 cells per well were cultured in a 48 well plate for 13-14 hours before pretreatment. For 3-D cell culture 50,000 cells per 10 µl hydrogel per well were cultured in a 96 well plate for 2 days before pretreatment. The media in the wells was replaced with media containing the inhibitor for 0.5 and 1.5 hours for 2-D and 3-D respectively, or activator for 2 hours for both 2-D and 3-D. For endothelin I, a 2.5 minute pretreatment was given in 2-D and 3-D. 20 µM Cytochalasin D (-actin) treatment was given to inhibit actin polymerization and the resultant tension, 10 µM nocodazole (-microtubulin) treatment was given to depolymerize microtubules and 10 mM butanedione monoxime (-actin-myosin) treatment was given to inhibit myosin ATPase. For activation, 500

nM jasplakinolide (+actin), 10 μM paclitaxel (+microtubule) and 20 nM endothelin I (+actin-myosin) was given for actin. microtubule, and actin-myosin interactions, respectively. Media was replaced after pretreatment for cells cultured in 2-D, following which cells were transfected and transgene expression and proliferation were analyzed after 48 hours post transfection. For 3-D, after pretreatment overnight transfections were done in presence of inhibitor or activator. The media was then replaced with fresh media and gene expression and proliferation were analyzed after 48 hours.

10.2.14 Inhibition of RhoGTPases in hydrogels. 200 ng/ml difficile toxin B (-Rho,Rac,Cdc42, List Biologicals, Campbell, CA) was used to pharmacologically inhibit Rho, Rac and Cdc42, Rho was specifically inhibited using cell permeable 1 μg/ml C3 transferase (-RhoA,B,C, Cytoskeleton, Denver, CO) and Rac and Cdc42 were both inhibited using 10 μM IPA3 (-PAK1). 20,000 cells per well in a 48 well plate were cultured for 14-15 hours in 2-D and 50,000 cells per 10 μl hydrogel per well were cultured in a 96 well plate in 3-D for 2 days before pretreatment. The media in the wells was then replaced with serum free media containing -Rho,Rac,Cdc42 or -ROCK for four hours or -PAK1 for 0.5 hours. Immediately after pretreatment, media was replaced and transfection was done for cells cultured in 2-D. Transgene expression and proliferation were analyzed 48 hours post transfection in 2-D. For cells cultured in 3-D, after pretreatment overnight transfections were done in presence of the inhibitor. The media was then replaced with fresh media and gene expression and proliferation were analyzed after 48 hours.

10.2.15 Activation of RhoGTPases. 1 μg/ml Rho/Rac/Cdc42 activator I (+Rho, Rac,Cdc42) and 1 μg/ml Rho direct activator II (+RhoA,B,C) were used to activate all three Rho, Rac and Cdc42,

and to activate only Rho respectively. 20,000 cells per well in a 48 well plate were cultured and 50,000 cells per 10 µl hydrogel per well in a 96 well plate were cultured in 2-D and 3-D, respectively, for 2 days before pretreatment. Media was changed to serum free media and cells were cultured in hydrogels in serum free media for 1 day. Subsequently, pre-treatment was given for 4 hours with activators in serum free media. Media was replaced after pretreatment for cells cultured in 2-D with serum free media without activator and subsequently bolus transfection was done with or without YOYO-1 labeled polyplexes for 4 hours. For 3-D after pretreatment, bolus transfection was done overnight in presence of activators in serum free media with or without YOYO-1 labeled polyplexes. The media was then replaced with fresh media and gene expression and proliferation were analyzed after 48 hours, as described above.

10.2.16 Statistics. All statistical analysis were performed using the computer program Instat (GraphPad, San Diego, CA). Experiments were statistically analyzed using the Tukey test, which compares all pairs of columns, using a 95% confidence interval or using unpaired t-test (two tail p value) which compared any two columns.

10.3 Results

10.3.1 RGD functionalized hyaluronic acid (HA) hydrogels for 3-D culture of mouse mesenchymal stem cells (mMSCs).

HA was cross-linked to form a hydrogel material using Michael-type addition of biscysteine containing MMPxl peptides onto HA-AC functionalized with cell adhesion peptides (RGD) (**Figure 10-1A**). The storage (G') and loss moduli (G'') of hydrogels with DNA polyplexes were measured at 37°C using plate-to-plate rheology with 8 mm geometry. An evaporation blocker

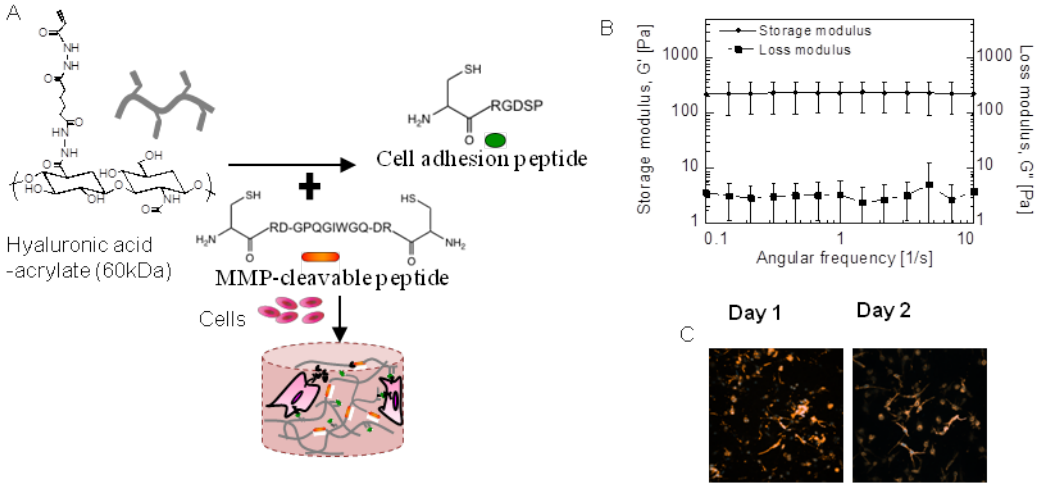

Figure 10-1: Adhesion peptide functionalized hyaluronic acid hydrogel for 3 dimensional cell culture. (**A**) HA hydrogels were formed by Michael-type addition of biscysteine containing MMPxl peptides onto HA-AC functionalized with cell adhesion peptides (RGD) and cells were encapsulated within the hydrogel. (**B**) The mechanical properties of the hydrogels were determined using plate-to-plate rheometry. The storage and loss modulus over a frequency range of 0.1-10 rad/s at a constant strain of 0.01 was plotted. (**C**) 10 µl gel was placed per well in 96-well plates with 50,000 cells per well, for culture. Cell spreading after 1 and 2 days of culture was analyzed through actin and DNA staining using Alexa488 conjugated phalloidin, and Hoechst dye, respectively.

was utilized to avoid drying of the hydrogel sample. It was observed that G' and G" did not cross at any measured frequency (0.1 to 10 Hz) and were frequency-independent (**Figure 10-1B**), both of which are consistent with hydrogel characteristics indicating that they are crosslinked. Cells proliferated well within HA gels as observed in fluorescent pictures on day 1 and 2. Cells were observed to start spreading on day 1, and were well spread by day 2 (**Figure 10-1C**).

10.3.2 Polyplex internalization pathways differ for cells cultured inside hydrogel scaffolds.

Amiloride (-macropinocytosis) was used to inhibit macropinocytosis, genistein (-caveolae I) and methyl-cyclodextrin (-caveolae II) were used to inhibit caveolae mediated endocytosis, and chlorpromazine (-clathrin I) and dynasore (-dynamin) were used to inhibit clathrin mediated endocytosis.

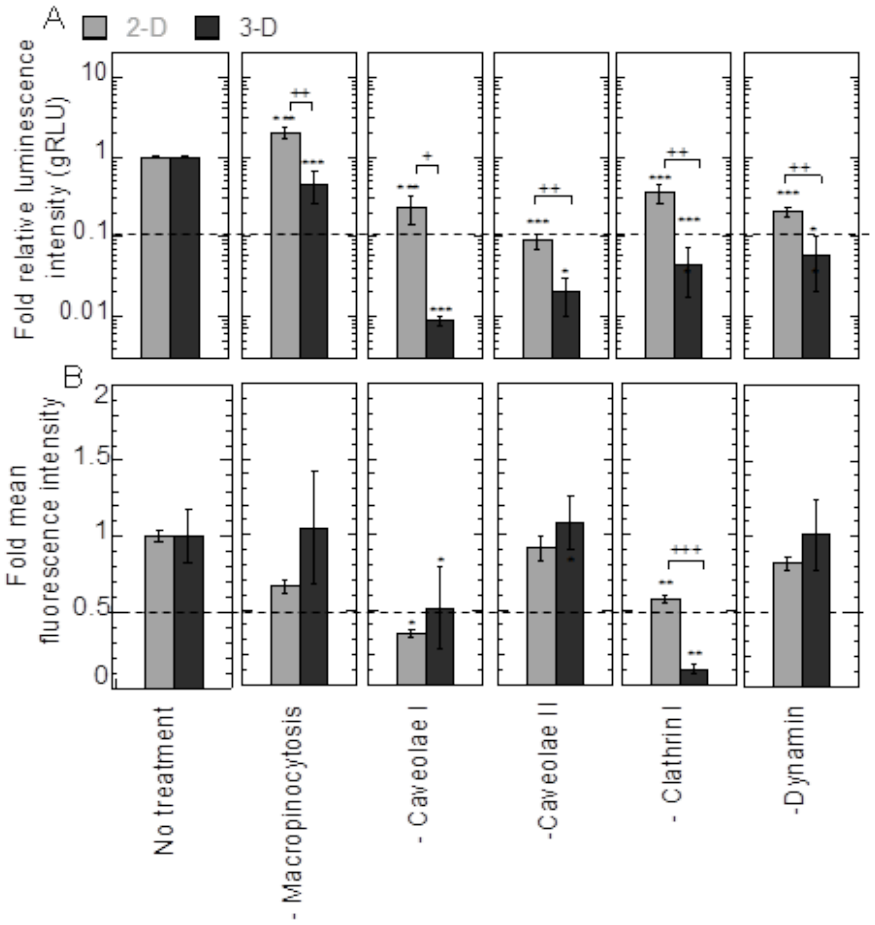

Figure 10-2: Effect of endocytic inhibitors on LPEI/DNA complex mediated gene transfer. Macropinocytosis and clathrin mediated endocytosis was inhibited using 100 µM amiloride (-macropinocytosis) and 200 µM genestein (-clathrin I). Caveolae mediated pathway was inhibited using 10 ug/ml chlorpromazine (-caveolae I) and 5 mM cyclodextrin (-caveolae II). Dynamin plays a role in the clathrin pathway and was inhibited using 50 µM dynasore (-clathrin II). Cells were cultured in 2-D on tissue culture surface for 13-14 hours before pretreatment and for 2-days in 3-D before pretreatment. A 1.5 hrs pretreatment for -clathrin I, -caveolae I and -macropinocytosis, and 1 hour pretreatment for -caveolae II and -dynamin was given in 2-D and 3-D. Subsequently, cells were incubated with or without YOYO-1 labeled polyplexes for 4 hours and 12-13 hrs in 2-D and 3-D, respectively. (**A**) The transgene expression was analyzed 48 hours post transfection in 2-D and post overnight transfection in 3-D by using gaussia luciferase assay. (**B**) Internalization was analyzed 2 hours post transfection in 2-D, and after overnight transfection in 3-D using flowcytometry. A total of 7000 events for 2-D and 5000 events for 3-D were analyzed per sample and the mean fluorescence of events was plotted. Statistical analysis was done using tukey Multiple Comparison test, which compares all columns with each other for 2-D and 3-D, respectively. The symbols *, ** and *** represents a significant change to the level of $p < 0.05$, $p < 0.01$ and $p < 0.001$, respectively, as compared to untreated sample for 2-D and 3-D respectively. For each treatment, transgene expression and internalization in 2-D was statistically compared with 3-D using the unpaired t-test (two tail p value). The symbols +,++ and +++ represents a significant change to the level of $p < 0.05$, $p < 0.01$ and $p < 0.001$, respectively, between 2-D and 3-D reading.

Inhibition of caveolae and clathrin significantly decreased transgene expression while inhibition of macropinocytosis significantly increased transgene expression in 2-D (atleast $p < 0.01$, **Figure 10-2A**). In 3-D, inhibition of macropinocytosis resulted in a 54% decrease, and inhibition of both caveolae and clathrin endocytosis led to a >90% decrease in transgene expression.

The level of internalization did not correspond with transgene expression in all conditions. In 2-D, inhibition using -caveolae I, -clathrin I and -macropinocytosis significantly decreased internalization by 66, 42 and 34%, respectively, ($p < 0.001$, **Figure 10-2B**). However, -caveolae II did not significantly influence internalization and -dynamin led to a low significant decrease ($p < 0.05$, 17.5%↓) in internalization in 2-D. In 3-D, inhibition using -caveolae I and -clathrin I led to a significant decrease in internalization (atleast $p < 0.05$) and inhibition with -caveolae II, -dynamin and -macropinocytosis had no significant influence on internalization (**Figure 10-2B**). The cell viability in 3-D was not influenced by treatment with endocytic inhibitors at the time of transgene expression analysis, which is 48 hours post removal of polyplexes after overnight transfection (**Figure 10-5**).

10.3.3 Role of cytoskeletal dynamics in gene transfer in hydrogels. Cytochalasin-D (-actin), nocodazole (-microtubule) and butanedione-monoxime (-actin-myosin) were used for studying the effect of inhibition of cell cytoskeleton, while jasplakinolide (+actin), paclitaxel (+microtubule) and endothelin I (+actin-myosin) were used for studying the affect of activation on gene transfer.

For cells cultured in 2-D on TCPS, inhibition of actin, microtubule and actin-myosin interactions increased transgene expression by 6.8-, 7- and 39-fold, respectively (**Figure 10-3A**). On the

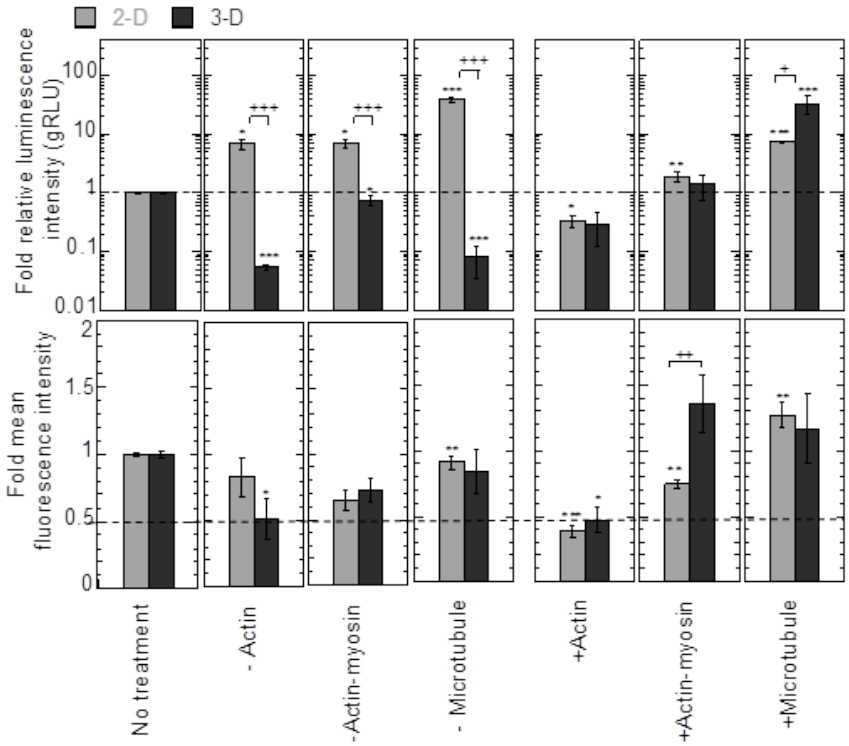

Figure 10-3: Effect of cytoskeletal inhibitors and activators on LPEI/DNA complex mediated gene transfer. Actin polymerization, actin-myosin interactions and microtubule polymerization were inhibited using 20 uM cytochalasin D (-actin), 10 mM BDM (-actin-myosin) and 10 μM nocodazole (-microtubule). Treatment using 500 nM jasplakinolide (+actin), 10 μM paclitaxel (+microtubule) and 20 treatment, the cells were cultured for 14-15 hours and 2 days on tissue culture plastic (2-D) and in nM endothelin I (+actin-myosin) was given for enhancing actin polymerization, microtubule polymerization, and actin-myosin interactions respectively. For hydrogels (3-D). The media in the wells was replaced with media containing the inhibitor for 0.5 and1.5 hours for 2-D and 3-D respectively, or activator for 2 hours for both 2-D and 3-D. Media was replaced after pretreatment for cells cultured in 2-D and subsequently bolus transfection was done with or without YOYO-1 labeled polyplexes. For 3-D after pretreatment, bolus transfection was done overnight with or without YOYO-1 labeled polyplexes. (**A**) The transgene expression was analyzed 48 hours post transfection in 2-D and post overnight transfection in 3-D by using gaussia luciferase assay. (**B**) Internalization was analyzed 2 hours post transfection in 2-D, and after overnight transfection in 3-D using flow cytometry. A total of 7000 events for 2-D and 5000 events for 3-D were analyzed per sample and the mean fluorescence of events was plotted. Statistical analysis was done using Tukey-Kramer multiple comparison test, which compares all columns with each other for 2-D and 3-D, respectively. The symbols *, ** and *** represent a significant change to the level of $p < 0.05$, $p < 0.01$ and $p < 0.001$, respectively, as compared to untreated sample for 2-D and 3-D, respectively. For each treatment, transgene expression and internalization in 2-D was statistically compared with 3-D using the unpaired t-test (two tail p value). The symbols +,++ and +++ represent a significant change to the level of $p < 0.05$, $p < 0.01$ and $p < 0.001$, respectively, between 2-D and 3-D reading.

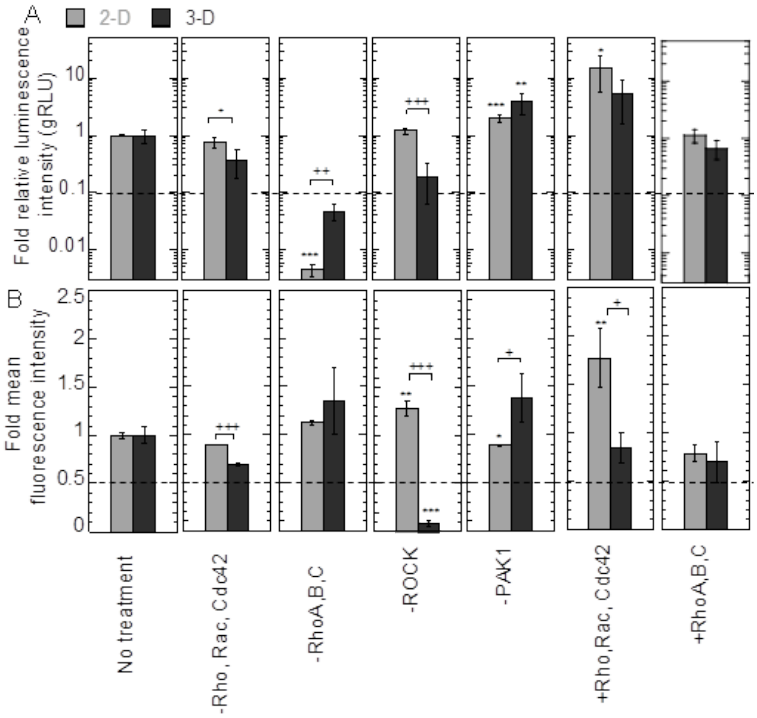

Figure 10-4: Effect of RhoGTPase mediated signaling on gene transfer. Rac, Cdc42 and Rho were inhibited using 200 ng/ml difficile toxin B (-Rho,Rac,Cdc42), Rho was inhibited using 1 µg/ml C3 transferase (-RhoA,B,C), and Rac and Cdc42 were both inhibited using 20 µM IPA3 (-Rac,cdc42). ROCK was inhibited using 10 µM Y27632 (-ROCK). The effect of activation of RhoGTPases was studied by activation of Rho, Rac and Cdc42 with 1 µg/ml Rho,Rac,Cdc42 activator I (+Rho,Rac,Cdc42) and by specific activation of Rho using 1 µg/ml Rho direct activator II (+RhoA,B,C). For inhibitor treatment, the cells were cultured for 14-15 hours and for 2 days in 2-D and 3-D, respectively before the media in the wells was replaced with serum free media containing -Rho,Rac,Cdc42 or -ROCK for four 4 or -PAK1 for 0.5 hours.

For activator treatment cells were cultured for 2 days in 2-D and in 3-D, respectively. Media was then changed to serum free media and cells were cultured in serum free media for 1 day in 2-D and 3-D. Subsequently pretreatment was given for 4 hours with activators in serum free media. Media was replaced after pretreatment for cells cultured in 2-D with serum free media without activator and subsequently bolus transfection was done with or without YOYO-1 labeled polyplexes for 4 hours. For 3-D after pretreatment, bolus transfection was done overnight in presence of activators in serum free media with or without YOYO-1 labeled polyplexes. (**A**) The transgene expression was analyzed 48 hours post transfection in 2-D and post overnight transfection in 3-D by using gaussia luciferase assay. (**B**) Internalization was analyzed 2 hours post transfection in 2-D, and after overnight transfection in 3-D using flow cytometry. A total of 7000 events for 2-D and 5000 events for 3-D were analyzed per sample and the mean fluorescence of events was plotted. Statistical analysis was done using Tukey -Kramer multiple comparison test, which compares all columns with each other for 2-D and 3-D, respectively. The symbols *, ** and *** represent a significant change to the level of $p < 0.05$, $p < 0.01$ and $p < 0.001$, respectively, as compared to untreated sample for 2-D and 3-D, respectively. For each treatment, transgene expression and internalization in 2-D was statistically compared with 3-D using the unpaired t-test (two tail p value). The symbols +,++ and +++ represent a significant change to the level of $p < 0.05$, $p < 0.01$ and $p < 0.001$, respectively, between 2-D and 3-D reading.

other hand, activation of actin significantly decreased transgene expresssion, while enhancement of microtubule polymerization increased transgene expression by 7.5-fold and enhancement of actin-myosin interactions had no influence in 2-D. For 3-D, inhibition of actin and microtubule polymerization led to >90% decrease in transgene expression and inhibition of actin-myosin significantly decreased transgene expression by 24.5% ($p < 0.05$). Treatment with +actin led to a 70% decrease in transgene expression, and +microtubule and +actin-myosin significantly increased transgene expression by 35- and 1.4-fold, respectively, in 3-D (at least $p < 0.05$, **Figure 10-3A**).

For 2-D, inhibition of actin polymerization had no effect on internalization while inhibition of microtubule polymerization and actin-myosin interactions significantly decreased internalization (**Figure 10-3B**). Conversely, enhancement of actin polymerization significantly decreased internalization while enhancement of microtubule polymerization increased internalization in 2-D. For cells cultured in 3-D inhibition, as well as enhancement of actin polymerization significantly decreased internalization (atleast $p < 0.05$, **Figure 10-3B**). No significant effect was observed in polyplex internalization after both inhibition or enhancement of microtubule polymerization or actin-myosin interactions. At the time of transgene expression analysis same level of proliferation was observed for all conditions as compared to untreated cells (**Figure 10-5**).

10.3.4 Role of RhoGTPases in gene transfer in hydrogels.

Inhibition of Rho, Rac and Cdc42 using TcdB (-Rho,Rac,Cdc42), RhoA,B,C using C3 transferase (-RhoA,B,C) and ROCK using Y27632 (-ROCK) did not influence transgene expression in 2-D but significantly decreased transgene expression in 3-D ($p < 0.05$, **Figure 10-**

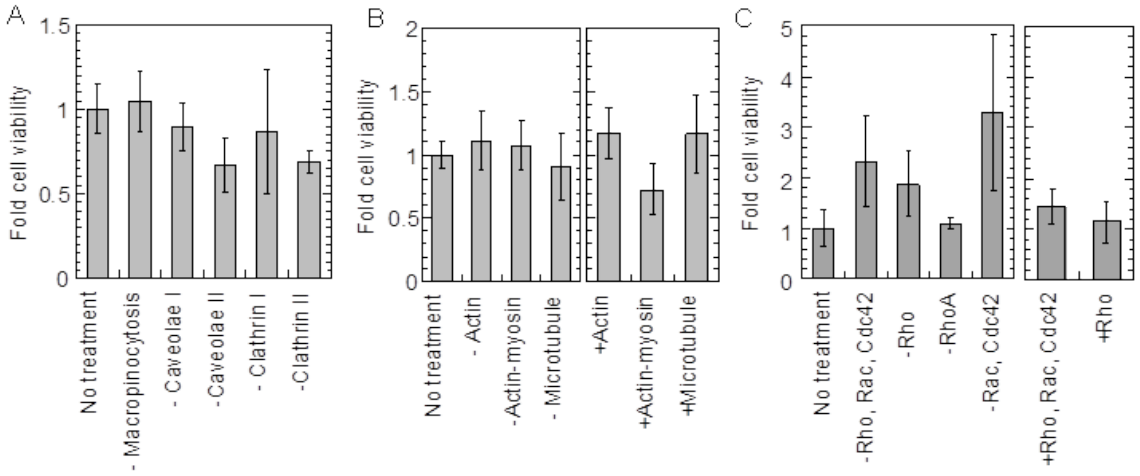

Figure 10-5: Viability of cells cultured in 3-D after treatments namely: (**A**) Endocytic inhibitors, (**B**) Cytoskeletal inhibitors and activators and (**C**) RhoGTPases inhibitors and activators.

4A). Inhibition of PAK1, downstream effector of Rac and Cdc42, using IPA3 (-PAK1) significantly increased transgene expression in 2-D and 3-D by two- and four- fold, respectively. Activation of Rho, Rac and Cdc42 significantly increased transgene expression in 2-D and 3-D by 15- and 5.4-fold, respectively, (**Figure 10-4A**). Activation of RhoA,B,C influence the transgene expression significantly in 2-D and 3-D.

Treatment with -Rho,Rac,Cdc42 and -RhoA,B,C did not statistically influence internalization in cells cultured in 2-D and 3-D (**Figure 10-4B**). Treatment with -ROCK did not significantly affect the internalization in 2-D and resulted in a significant decrease in internalization in 3-D. Inhibition of ROCK decreased internalization by >90% in 3-D. Interestingly, treatment with -PAK1 significantly decreased internalization in 2-D ($p < 0.001$) and did not significantly influence (increase) internalization in 3-D (**Figure 10-4B**). Activation of Rho, Rac and Cdc42-GTPases significantly increased internalization in 2-D but not in 3-D. Activation of only Rho (+RhoA,B,C) did not influence internalization in 2-D as well as in 3-D.

The cell viability was significantly not influenced by treatment with RhoGTPase inhibitors and activators at the time of transgene expression analysis (**Figure 10-5**).

10.4 Discussion

3-D matrices provide a better model system for studying cellular physiological processes as cells in tissues exist in a 3-D system. Cellular processes like proliferation and migration, cellular morphology, biosynthesis of differentiated products as well as apoptosis [194] have been shown to be significantly different in 2-D versus 3-D system. For primary fibroblasts, cell-viability and metabolism assessed by mitochondrial activities was upregulated in 3-D culture versus 2-D patterning, keeping surface area of adhesion and rigidity constant [195]. Integrin function was regulated by the dimensions and dynamics of the cell microenvironment [196]. In standard 2-D cell culture, cells including mesenchymal stem cells formed focal adhesions or fibrillar adhesions and in 3-D matrices cells formed 3-D matrix adhesions which employed fibronectin receptor $\alpha_5\beta_1$ [196]. Furthermore, gene transfer is modulated by the mechanical properties of the substrate [1] and these adhesion sites act as mechanosensors [197, 198]. Hence the cell behavior specifically pertaining to non-viral gene transfer in 2-D cannot be compared with cell behavior in 3-D as they utilize different types of adhesion structures [199].

Gene transfer to cells cultured in two dimensions (2-D) on coventional tissue culture plastic surfacs (TCPS) versus cells cultured in three dimension (3-D) scaffolds had previously not been studied in detail. As shown in chapter 6 and 7, internalization pathways, cytoskeletal dynamics and RhoGTPases modulated non-viral gene delivery to mMSCs cultured in cells cultured in 2-D [146, 193]. In this chapter, the gene transfer mechanism in cells cultured in 3-D HA hydrogels was studied and compared with gene transfer mechanism in cells cultured in 2-D on tissue culture plastic surface. This study indicated that the internalization pathways are differentially

Table 10-1: Effect of endocytic inhibitors on gene transfer in 2-D versus 3-D.

	% Transgene expression			% Internalization	
	2D	3D		2D	3D
-Caveolae I	49%↓, ***	99.1%↓, ***		72.9%↓, ***	48.6%↓,**
-Caveolae II	91%,↓, ***	98%↓, ***		9.5%↓	107%↑
-Clathrin I	69%↓, ***	95.4%↓, *		28.3%↓, ***	89.4%↓, **
-Clathrin II	79%↓, ***	94%↓, ***		17.53%↓, **	102%↑
-Macropinocytosis	124%↑, *	54.6%↓, *		2.2%↓	104%↑

Table 10-2: Effect of cytoskeletal inhibitors and activators on gene transfer in 2-D versus 3-D

	% Transgene expression			% Internalization	
	2D	3D		2D	3D
-Actin	32.4%↓	94.4%↓, ***		172.2%↑, ***	47.9%↓,*
-Microtubule	1012%↑, ***	92%↓, ***		101.3%↑	16%↓
-Actin-myosin	21.5%↓	24.5%↓, *		111.4%↑	27.8%↓
+Actin	67%↓, *	70%↓		61.4%↓, ***	52%↓,**
+Microtubule	750%↑, ***	3552%↑, ***		126%↑, **	136%,↑
+Actin-myosin	195%↑, **	139%↑		25.8%↓, **	116.7%,↑

Table 10-3: Effect of RhoGTPase mediated signaling on gene transfer in 2-D versus 3-D

	% Transgene expression			% Internalization	
	2D	3D		2D	3D
-Rho, Rac, Cdc42	12.8%↓,	64%↓, *		23.7%↓	30.8%↓
-Rho	99.3%↓,	95.3%↓, **		112.4%↑	134.6%↑
-RhoA	119.7%↑,	81%↓, **		31.8%↓	91%↓,**
-Rac,Cdc42	198%↑, ***	387.7%↑, *		32.86%, ↓ ***	138%↑,
+Rho, Rac, Cdc42	1516%↑,*	536%↑*		177.3%↑,**	15.5%↓
+Rho	112.3%↑	25%↓		21.5%↓	30.5%↓

modulated in 2-D on TCPS and in 3-D in hydrogels. All three pathways contributed in mediating efficient gene transfer in 3-D HA hydrogels, while only caveolae and clathrin mediated

endocytosis were involved in efficient gene transfer in 2-D (≥77% and 64%, respectively, **Table 10-1**).

Unlike -caveolae I inhibition using -caveolae II did not influence internalization in 2-D and 3-D. Caveolae mediated endocytosis is dependent on tyrosine phosphorylation [200]. Genestein (-caveolae I) inhibited caveolae pathway by inhibiting tyrosine kinase. Cyclodextrin (-caveolae II) inhibited by depleting cholesterol. After extraction of cholesterol, calveolin remained clustered in the plasma membrane, as if caveolae (invaginations) were not flattened or disappeared. The influence of -caveolae II on internalization may not have been fully detected as polyplexes possibly remain associated with caveolae giving a false positive reading.

Inhibition with dynasore (-dynamin) did not influence the internalization in 3-D while a low significant decrease of 17.5% was observed in internalization in 2-D on TCPS ($p < 0.05$, **Table 10-1**). Dynasore inhibited clathrin-mediated endocytosis which depends on dynamin by rapidly blocking coated vesicle formation [201]. Two types of coated pit intermediates accumulated during dynasore treatment, U-shaped, half formed pits and O-shaped, fully formed pits, captured while pinching off [201]. Inhibition using -dynamin on internalization was not fully detected as a positive reading was observed from polyplexes that possibly remain attached to the pits as the clathrin lattice was not disrupted while endocytosis is inhibited.

Primary fibroblast assembled actin cytoskeleton when cultured on flat 2-D substrates but did not assemble a detectable cytoskeleton when cultured in soft 3-D microwells [195]. Our results showed that inhibition and enhancement of actin polymerization significantly increased and decreased transgene expression, respectively, in mMSCs cultured on 2-D (atleast $p < 0.01$). This indicated that inhibiting actin polymerization resulted in decreased cellular tension which aids

trafficking in 2-D on TCPS. Contrarily, the decrease in transgene expression on enhancing actin polymerization in 2-D correlated with significant decrease in internalization ($p < 0.001$).

In the other aspect, inhibition and enhancement of actin polymerization in 3-D in hydrogels decreased transgene expression by 94% and 70%, respectively (**Table 10-2**). Our results showed that this decrease in transgene expression was a consequence of significantly decreased internalization (at least $p < 0.05$).

Inhibition of actin-myosin interactions increased transgene expression by 7-fold and enhancement of actin-myosin interactions had no effect in 2-D. In contrast, inhibition and enhancement of actin-myosin interactions significantly decreased and increased transgene expression in 3-D, respectively. This indicated that actin-myosin interactions mediated efficient gene transfer leading to transgene expression in cells cultured in 3-D in HA hydrogels.

It has been shown that cytoskeletal elements regulate each other [202]. It is important to note that even though specific functions had been assigned to different cytoskeletal elements, they were overlapping and not separate. Actin played a role in membrane trafficking and microtubules were involved in the control of protrusive and contractile forces [202].

A 39-fold increase in transgene-expression was observed after inhibition of microtubule polymerization in 2-D (**Table 10-2**). Inhibition of microtubule polymerization increased contractile force and promoted focal adhesions in 2-D [203]. Therefore the enhancement of transgene expression could have been a resultant of increased actin-dynamics which aided in efficient trafficking of the polyplexes. However, a >90% decrease in transgene expression was observed in 3-D indicating that microtubules played a pivotal role in trafficking. Microtubules played a role in vesicular transport and depolymerization of microtubules possibly disrupted the vesicular transport.

Furthermore, a 7.5- and 35-fold increase in transgene expression was observed after enhancement of microtubule polymerization in 2-D and 3-D, respectively (**Table 10-2**). This could be attributed to increased vesicular transport. A higher increase in transgene expression on +microtubule treatment was observed in 3-D as compared to 2-D, which was consistent with the drastic decrease observed on inhibition of microtubule polymerization in 3-D. This indicated that microtubule polymerization positively regulated and highly contributed to efficient gene transfer in cells cultured in hydrogels.

On the other hand, inhibition and enhancement of microtubule polymerization significantly increased and decreased polyplex internalization, respectively, in 2-D while no effect was observed on internalization in 3-D. This indicated that microtubules had a role in internalization in cells cultured in 2-D on TCPSs.

RhoGTPases specifically Rho, Rac and Cdc42 modulate non-viral gene transfer in cells cultured in 2-D and 3-D. Results indicate that RhoA,B,C and contractility mediated by RhoA through downstream effector ROCK highly contributes to obtaining transgene expression in hydrogels (**Table 10-3**). The decrease observed in transgene expression after treatment with -ROCK can be explained with significantly decreased internalization on ROCK inhibition in 3-D in hydrogels. Moreover, it corresponds with the role of actin-myosin interactions in mediating efficient transgene expression in 3-D, as mentioned above. On the contrary inhibition of RhoA,B,C or ROCK does not significantly influence gene transfer in TCPSs (**Table 10-3**). Futhermore, a significant increase (2-fold) and decrease (33%), in transgene expression and internalization, respectively, was observed after inhibition of Rac and Cdc42 in 2-D. This indicates that on treatment with -Rac,Cdc42, the polyplexes are possibly internalized by a different pathway that leads to overall increased transgene expression for cells cultured on a 2-D

tissue culture surface. Decreased internalization leading to overall increased transgene expression occurs in mMSCs when they are plated on Fn coated surfaces in 2-D [145]. -Rac, Cdc42 does not influence internalization in 3-D but increases transgene expression by 3.9-fold in 3-D.

10.5 Conclusion

To conclude, in this chapter it has been shown that endocytic pathways, cytoskeletal dynamics and RhoGTPase mediated signaling differentially influenced non-viral gene transfer in cells cultured in 2-D on tissue culture plastic surfaces and in 3-D in HA hydrogels. Caveolae and clathrin mediated endocytosis contributed to efficient gene transfer in 2-D, while all three pathways namely macropinocytosis, caveolae and clathrin mediated endocytosis contributed to efficient gene transfer in 3-D. Unlike 2-D, actin polymerization highly contributed to efficient transgene expression in 3-D and on inhibition led to a >90% decrease in transgene expression. Enhancement of actin polymerization decreased transgene expression as a resultant of decreased internalization in both 2-D and 3-D. Microtubule polymerization had contrasting roles in gene transfer in cells cultured on TCPS and in cells cultured in hydrogels. The inhibition of microtubule polymerization increased transgene expression by 39-fold in 2-D. The enhancement of microtubule polymerization resulted in 35-fold increase in transgene expression in 3-D. RhoA,B,C and ROCK highly contributed to efficient transgene expression in 3-D and had no significant influence on gene transfer in 2-D. Also, RhoA mediated contractility contributed more than 90% to internalization in 3-D but not in 2-D. These results provided an understanding of non-viral gene transfer in three dimensional cell microenvironment, to obtain efficient gene transfer for the purpose of tissue regeneration and gene therapy.

Chapter 11

CONCLUSIONS

11.1 Introduction

The development of gene therapy and tissue regeneration as potential treatments necessitates efficient and safe gene delivery to cells. The purpose of gene delivery directly at the site of interest is to be able to produce endogenous protein over a longer period of time as compared to the direct administration of the protein itself. The clearance rate for proteins is usually too fast to achieve a significant biological effect as is needed to guide localized tissue repair and regeneration [204]. DNA delivery is likely to sustain a level of the functional protein applicable for guiding the biological processes.

Though non-viral gene delivery is safe, it is limited by its lower efficiency as compared to viral gene delivery. Most of the studies aiming to improve non-viral vectors have focused on vector design while the cellular microenvironment has not been studied in detail. Cells bound to the ECM activate specific signaling pathways which guide cell behavior, proliferation, differentiation and apoptosis. This thesis systematically investigates and examines the role of extracellular matrix structural proteins in mouse mesenchymal stem cells (mMSCs), to divulge the characteristic microenvironment required to enhance non-viral gene delivery.

11.2 Specific AIMs

11.2.1 Specific AIM 1

We had first aimed to study the role of the cellular microenvironment and the related mechanistic pathways in gene transfer, in an attempt to improve on non-viral gene-delivery efficiency. In chapter 4 and 5, density, identity and combination of ECM structural proteins were observed to modulate non-viral gene transfer to mouse mesenchymal stem cells in 2-D. Protein coatings that resulted in well spread cells, such as Fn, ECMg and C IV, resulted in 10-, 6.5- and 5- fold increase in transgene expression, respectively, when compared to uncoated surfaces. On the other hand, upto 90% inhibition was observed on C I coated surface which led to less spread cells. Notably, protein coats that resulted in less spread cells, such as C I and Vt significantly increased polyplex internalization compared to uncoated and Fn coated surfaces. Protein density also affected the amount of transgene expression for C I, Fn and ECMg. C I had a dominant influence and inhibited the transgene expression when combined with Fn or Lm. Furthermore surfaces coated with a combination Vt, C IV and Lm mediated statistically similar level of transgene expression, internalization and cell spreading as was seen on Fn. While the transgene expression of C I and Fn corresponded with rate of proliferation, the cell proliferation was the same on surfaces with increasing concentration of ECM proteins. Thus, a different mechanism must be involved in the dose dependent response on Fn, Cl I and ECMg. Moreover the transgene expression for all other ECM combinations was also independent of proliferation. *For all ECM combinations analyzed, the extent of cell spreading mediated by the ECM protein had a 70% correlation with the extent of overall gene transfer observed. These results agree with Hypothesis 1.*

Through this study we have gained a better understanding of the characteristics of the microenvironment that will assist in guiding the formation 2-D culture systems with the incorporation of characteristics that specifically aid in enhancing in-vitro non-viral delivery for application in tissue regeneration and therapy.

11.2.2 Specific AIM 2

In chapter 4 and 5, AIM 1 and Hypothesis 1 was addressed and it was illustrated that the cell cytoskeleton and endocytosis pathway affect the process of non-viral gene transfer for adherent cells. Subsequently, we investigated if the possible differences in non-viral gene transfer for mMSCs plated on either collagen I or Fn were due to differences in their cytoskeleton and internalization pathways. In chapter 6, AIM2 was addressed. *We further showed that the mechanism by which these ECM proteins affected non-viral gene transfer involved the endocytosis pathway used for uptake of DNA complexes and intracellular tension.* Efficient gene transfer to mMSCs plated on protein-coated surfaces was achieved when polyplexes were internalized through clathrin-mediated endocytosis and that Fn promoted clathrin-mediated endocytosis. Further, the amount of cellular tension affected non-viral gene transfer and decreased actin-myosin interactions resulted in decreased internalization on all surfaces.

These results agree with our 2nd Hypothesis that "the varied ECM proteins influence the efficiency of gene transfer by mediating differential endocytic pathways and cytoskeletal dynamics, that subsequently modulate the process of gene transfer".

Chapter 4, 5, and 6 together indicates that the cellular microenvironment can be manipulated and engineered to achieve optimal non-viral gene transfer. The investigation of the effects of the cellular microenvironment on non-viral gene transfer will result in a comprehensive

understanding of the limitations of gene transfer, which could further improve the current methods and vectors used for non-viral gene delivery.

11.2.3 Specific AIM 3

So far, it had been established that extracellular proteins have varied cell areas and gene transfer efficiencies. RhoGTPases are the controlling factors in guiding cell motility [99], morphology and behavior [87]. There exists a crosstalk between the ECM and the RhoGTPases where the RhoGTPases in return regulate cell-cell and cell-matrix adhesion [89]. However, the role of RhoGTPases in non-viral gene delivery as a consequence of cell-ECM interactions had not been studied. To further study the underlying mechanism by which ECM modulates gene transfer, AIM3 of this research project had been to investigate the role of RhoGTPases in gene transfer and internalization in mMSCs plated on a Fn coated surface by inhibiting them as well as by activating them, and analyzing the resultant affects on gene transfer. As reported in chapter 7, inactivation of RhoGTPases significantly reduced the transgene expression in both mMSCs and NIH/3T3 cells. On the other hand, the activation of RhoGTPases was able to rescue the transfection ability of mMSCs plated on C I. The role of RhoGTPases in gene transfer was found to be cell-type specific. Overall this study indicated that RhoGTPases play an important role in the modulation of efficient delivery of non-viral vectors. *These results prove and agree with our 3rd hypothesis that " the Rho family of small GTPases plays a role in the mechanism by which ECM modulates gene transfer in two dimensions".*

This investigation of the effects of the cellular microenvironment on non-viral gene transfer via RhoGTPases, along with the results established in chapters 4, 5 and 6, provides a comprehensive

understanding of the limitations of gene transfer, which could further improve the current methods and vectors used for non-viral gene delivery.

11.2.4 Specific AIM 4

The last AIM of the thesis had been to elucidate the gene transfer mechanism in mouse bone marrow mesenchymal stem cells (D1 cells) cultured in a 3-D microenvironment. Hyaluronic acid hydrogels were used to study the gene transfer in 3-D in-vitro.

The influence of dimensionality on mechanism of gene transfer in cells was elucidiated in chapter 10 by studying the role endocytic pathways, cytoskeletal dynamics and RhoGTPases, in cells cultured in a 3-D microenvironment in comparison to cells cultured in a 2-D microenvironment. Caveolae and clathrin mediated endocytosis regulated gene transfer in 2-D, while all three pathways of endocytosis namely clathrin and caveolae mediated endocytosis, and macropinocytosis regulated gene transfer in 3-D. This study indicated that microtubule polymerization, actin polymerization and RhoA mediated contractility had varied roles in gene transfer in TCPS and in hydrogels. Moreover, Rac- and Cdc42-GTPases influenced internalization in 2-D surfaces but not in 3-D hydrgels.

On the whole, endocytic pathways, cytoskeletal dynamics and RhoGTPase mediated signaling differentially modulate non-viral gene transfer in cells cultured in 2-D on tissue culture plastic surfaces and in 3-D HA hydrogels. *These results agree with our 4th Hypothesis.* Henceforth, the cell behavior specifically pertaining to non-viral gene transfer in conventional 2-D surface cannot be compared with cell behavior in 3-D.

MSC can be isolated from the bone marrow, expanded in culture and genetically modified to serve as cell carriers for local and systemic therapy. This research provides an in-depth

understanding of the characteristics of the cellular microenvironment, that will guide the formation of scaffolds. These scaffolds will incorporate characteristics that would specifically enhance non-viral delivery to cells in-vitro, and in-vivo, for application in tissue regeneration and therapy.

Chapter 12

BIBLIOGRAPHY

1. Kong, HJ, Liu, J, Riddle, K, Matsumoto, T, Leach, K, and Mooney, DJ (2005). Non-viral gene delivery regulated by stiffness of cell adhesion substrates. *Nature materials* **4**: 460-464.
2. Teo, BK, Goh, SH, Kustandi, TS, Loh, WW, Low, HY, and Yim, EK. The effect of micro and nanotopography on endocytosis in drug and gene delivery systems. *Biomaterials* **32**: 9866-9875.
3. Kong, HJ, Hsiong, S, and Mooney, DJ (2007). Nanoscale cell adhesion ligand presentation regulates nonviral gene delivery and expression. *Nano Lett* **7**: 161-166.
4. Yoshikawa, T, Uchimura, E, Kishi, M, Funeriu, DP, Miyake, M, and Miyake, J (2004). Transfection microarray of human mesenchymal stem cells and on-chip siRNA gene knockdown. *J Control Release* **96**: 227-232.
5. Okazaki, A, Jo, JI, and Tabata, Y (2006). A Reverse Transfection Technology to Genetically Engineer Adult Stem Cells. *Tissue Eng*.
6. Bengali, Z, Rea, JC, and Shea, LD (2007). Gene expression and internalization following vector adsorption to immobilized proteins: dependence on protein identity and density. *The journal of gene medicine* **9**: 668-678.
7. Uchimura, E, *et al.* (2005). On-chip transfection of PC12 cells based on the rational understanding of the role of ECM molecules: efficient, non-viral transfection of PC12 cells using collagen IV. *Neurosci Lett* **378**: 40-43.
8. Lee, KD (2008). Applications of mesenchymal stem cells: an updated review. *Chang Gung medical journal* **31**: 228-236.
9. Caplan, AI (2007). Adult mesenchymal stem cells for tissue engineering versus regenerative medicine. *Journal of cellular physiology* **213**: 341-347.
10. Chen, XD, Dusevich, V, Feng, JQ, Manolagas, SC, and Jilka, RL (2007). Extracellular matrix made by bone marrow cells facilitates expansion of marrow-derived mesenchymal progenitor cells and prevents their differentiation into osteoblasts. *J Bone Miner Res* **22**: 1943-1956.
11. Bosnakovski, D, Mizuno, M, Kim, G, Takagi, S, Okumura, M, and Fujinaga, T (2006). Chondrogenic differentiation of bovine bone marrow mesenchymal stem cells (MSCs) in

different hydrogels: influence of collagen type II extracellular matrix on MSC chondrogenesis. *Biotechnology and bioengineering* **93**: 1152-1163.
12. Mauney, JR, Volloch, V, and Kaplan, DL (2005). Matrix-mediated retention of adipogenic differentiation potential by human adult bone marrow-derived mesenchymal stem cells during ex vivo expansion. *Biomaterials* **26**: 6167-6175.
13. Uccelli, A, Moretta, L, and Pistoia, V (2006). Immunoregulatory function of mesenchymal stem cells. *European journal of immunology* **36**: 2566-2573.
14. Kumar, S, Chanda, D, and Ponnazhagan, S (2008). Therapeutic potential of genetically modified mesenchymal stem cells. *Gene therapy* **15**: 711-715.
15. Kanehira, M, *et al.* (2007). Targeted delivery of NK4 to multiple lung tumors by bone marrow-derived mesenchymal stem cells. *Cancer gene therapy* **14**: 894-903.
16. Studeny, M, Marini, FC, Champlin, RE, Zompetta, C, Fidler, IJ, and Andreeff, M (2002). Bone marrow-derived mesenchymal stem cells as vehicles for interferon-beta delivery into tumors. *Cancer research* **62**: 3603-3608.
17. Tang, J, Xie, Q, Pan, G, Wang, J, and Wang, M (2006). Mesenchymal stem cells participate in angiogenesis and improve heart function in rat model of myocardial ischemia with reperfusion. *Eur J Cardiothorac Surg* **30**: 353-361.
18. Okubo, Y, Bessho, K, Fujimura, K, Iizuka, T, and Miyatake, SI (2001). In vitro and in vivo studies of a bone morphogenetic protein-2 expressing adenoviral vector. *The Journal of bone and joint surgery* **83-A Suppl 1**: S99-104.
19. Partridge, K, *et al.* (2002). Adenoviral BMP-2 gene transfer in mesenchymal stem cells: in vitro and in vivo bone formation on biodegradable polymer scaffolds. *Biochemical and biophysical research communications* **292**: 144-152.
20. Li, S, and Huang, L (2000). Nonviral gene therapy: promises and challenges. *Gene therapy* **7**: 31-34.
21. Vernejoul, F, *et al.* (2002). Antitumor effect of in vivo somatostatin receptor subtype 2 gene transfer in primary and metastatic pancreatic cancer models. *Cancer research* **62**: 6124-6131.
22. Yamamoto, M, and Tabata, Y (2006). Tissue engineering by modulated gene delivery. *Advanced drug delivery reviews* **58**: 535-554.
23. Bleiziffer, O, Eriksson, E, Yao, F, Horch, RE, and Kneser, U (2007). Gene transfer strategies in tissue engineering. *Journal of cellular and molecular medicine* **11**: 206-223.
24. Kofron, MD, and Laurencin, CT (2006). Bone tissue engineering by gene delivery. *Advanced drug delivery reviews* **58**: 555-576.
25. Giordano, C, *et al.* (2008). Gene delivery systems for gene therapy in tissue engineering and central nervous system applications. *The International journal of artificial organs* **31**: 1017-1026.
26. Hoeller, D, Petrie, N, Yao, F, and Eriksson, E (2002). Gene therapy in soft tissue reconstruction. *Cells, tissues, organs* **172**: 118-125.
27. Saul, JM, Linnes, MP, Ratner, BD, Giachelli, CM, and Pun, SH (2007). Delivery of non-viral gene carriers from sphere-templated fibrin scaffolds for sustained transgene expression. *Biomaterials* **28**: 4705-4716.
28. Kessler, MW, Ackerman, G, Dines, JS, and Grande, D (2008). Emerging technologies and fourth generation issues in cartilage repair. *Sports medicine and arthroscopy review* **16**: 246-254.

29. Steinert, AF, Noth, U, and Tuan, RS (2008). Concepts in gene therapy for cartilage repair. *Injury* **39 Suppl 1**: S97-113.
30. Martinek, V, Ueblacker, P, and Imhoff, AB (2003). Current concepts of gene therapy and cartilage repair. *J Bone Joint Surg Br* **85**: 782-788.
31. Gao, X, Kim, KS, and Liu, D (2007). Nonviral gene delivery: what we know and what is next. *The AAPS journal* **9**: E92-104.
32. Felgner, PL, *et al.* (1987). Lipofection: a highly efficient, lipid-mediated DNA-transfection procedure. *Proceedings of the National Academy of Sciences of the United States of America* **84**: 7413-7417.
33. Boussif, O, *et al.* (1995). A versatile vector for gene and oligonucleotide transfer into cells in culture and in vivo: polyethylenimine. *Proceedings of the National Academy of Sciences of the United States of America* **92**: 7297-7301.
34. Friend, DS, Papahadjopoulos, D, and Debs, RJ (1996). Endocytosis and intracellular processing accompanying transfection mediated by cationic liposomes. *Biochimica et biophysica acta* **1278**: 41-50.
35. Labat-Moleur, F, *et al.* (1996). An electron microscopy study into the mechanism of gene transfer with lipopolyamines. *Gene therapy* **3**: 1010-1017.
36. Khalil, IA, Kogure, K, Akita, H, and Harashima, H (2006). Uptake pathways and subsequent intracellular trafficking in nonviral gene delivery. *Pharmacological reviews* **58**: 32-45.
37. Pack, DW, Hoffman, AS, Pun, S, and Stayton, PS (2005). Design and development of polymers for gene delivery. *Nature reviews* **4**: 581-593.
38. Akinc, A, Thomas, M, Klibanov, AM, and Langer, R (2005). Exploring polyethylenimine-mediated DNA transfection and the proton sponge hypothesis. *The journal of gene medicine* **7**: 657-663.
39. Wightman, L, *et al.* (2001). Different behavior of branched and linear polyethylenimine for gene delivery in vitro and in vivo. *The journal of gene medicine* **3**: 362-372.
40. Lungwitz, U, Breunig, M, Blunk, T, and Gopferich, A (2005). Polyethylenimine-based non-viral gene delivery systems. *Eur J Pharm Biopharm* **60**: 247-266.
41. Mairhofer, J, and Grabherr, R (2008). Rational vector design for efficient non-viral gene delivery: challenges facing the use of plasmid DNA. *Molecular biotechnology* **39**: 97-104.
42. Uchimura, E, *et al.* (2005). On-chip transfection of PC12 cells based on the rational understanding of the role of ECM molecules: efficient, non-viral transfection of PC12 cells using collagen IV. *Neuroscience Letters* **378**: 40-43.
43. Lungwitz, U, Breunig, M, Blunk, T, and Gopferich, A (2005). Polyethylenimine-based non-viral gene delivery systems. *European Journal of Pharmaceutics and Biopharmaceutics* **60**: 247-266.
44. Boussif, O, *et al.* (1995). A Versatile Vector for Gene and Oligonucleotide Transfer into Cells in Culture and in-Vivo - Polyethylenimine. *Proceedings of the National Academy of Sciences of the United States of America* **92**: 7297-7301.
45. Akinc, A, Thomas, M, Klibanov, AM, and Langer, R (2005). Exploring polyethylenimine-mediated DNA transfection and the proton sponge hypothesis. *J Gene Med* **7**: 657-663.
46. Chen, J, *et al.* (2008). Galactose-poly(ethylene glycol)-polyethylenimine for improved lung gene transfer. *Biochemical and biophysical research communications* **375**: 378-383.

47. Kircheis, R, Wightman, L, and Wagner, E (2001). Design and gene delivery activity of modified polyethylenimines. *Advanced drug delivery reviews* **53**: 341-358.
48. Mi Bae, Y, *et al.* (2007). Dexamethasone-conjugated low molecular weight polyethylenimine as a nucleus-targeting lipopolymer gene carrier. *Bioconjugate chemistry* **18**: 2029-2036.
49. Luo, X, Pan, S, Feng, M, Wen, Y, and Zhang, W (2009). Stability of poly(ethylene glycol)-graft-polyethylenimine copolymer/DNA complexes: influences of PEG molecular weight and PEGylation degree. *Journal of materials science*.
50. Saito, Y, Higuchi, Y, Kawakami, S, Yamashita, F, and Hashida, M (2008). Immunostimulatory Characteristics Induced by Linear Polyethyleneimine/plasmid DNA Complexes in Cultured Macrophages. *Human gene therapy*.
51. Erbacher P, BT, Brion E, Coll JL, Plank C, Behr JP, Remy JS. (2004). Genuine DNA/polyethylenimine (PEI) complexes improve transfection properties and cell survival. *J Drug Target* **12**: 223-236.
52. Godbey, WT, Wu, KK, and Mikos, AG (1999). Poly(ethylenimine) and its role in gene delivery. *J Control Release* **60**: 149-160.
53. Helander, IM, Alakomi, HL, Latva-Kala, K, and Koski, P (1997). Polyethyleneimine is an effective permeabilizer of gram-negative bacteria. *Microbiology (Reading, England)* **143 (Pt 10)**: 3193-3199.
54. Helander, IM, Latva-Kala, K, and Lounatmaa, K (1998). Permeabilizing action of polyethyleneimine on Salmonella typhimurium involves disruption of the outer membrane and interactions with lipopolysaccharide. *Microbiology (Reading, England)* **144 (Pt 2)**: 385-390.
55. Klemm, AR, Young, D, and Lloyd, JB (1998). Effects of polyethyleneimine on endocytosis and lysosome stability. *Biochemical pharmacology* **56**: 41-46.
56. Oku, N, Yamaguchi, N, Yamaguchi, N, Shibamoto, S, Ito, F, and Nango, M (1986). The fusogenic effect of synthetic polycations on negatively charged lipid bilayers. *Journal of biochemistry* **100**: 935-944.
57. Lambert, RC, *et al.* (1996). Polyethylenimine-mediated DNA transfection of peripheral and central neurons in primary culture: probing Ca2+ channel structure and function with antisense oligonucleotides. *Molecular and cellular neurosciences* **7**: 239-246.
58. Bonnet, ME, Erbacher, P, and Bolcato-Bellemin, AL (2008). Systemic delivery of DNA or siRNA mediated by linear polyethylenimine (L-PEI) does not induce an inflammatory response. *Pharmaceutical research* **25**: 2972-2982.
59. Davies, LA, *et al.* (2008). Enhanced lung gene expression after aerosol delivery of concentrated pDNA/PEI complexes. *Mol Ther* **16**: 1283-1290.
60. Hassani, Z, *et al.* (2007). A hybrid CMV-H1 construct improves efficiency of PEI-delivered shRNA in the mouse brain. *Nucleic acids research* **35**: e65.
61. Liao, HW, and Yau, KW (2007). In vivo gene delivery in the retina using polyethylenimine. *BioTechniques* **42**: 285-286, 288.
62. Ohana, P, *et al.* (2005). Regulatory sequences of H19 and IGF2 genes in DNA-based therapy of colorectal rat liver metastases. *The journal of gene medicine* **7**: 366-374.
63. Lisziewicz, J, *et al.* (2005). DermaVir: a novel topical vaccine for HIV/AIDS. *The Journal of investigative dermatology* **124**: 160-169.

64. Lutolf, MP, and Hubbell, JA (2005). Synthetic biomaterials as instructive extracellular microenvironments for morphogenesis in tissue engineering. *Nature biotechnology* **23**: 47-55.
65. Shi, YB, Li, Q, Damjanovski, S, Amano, T, and Ishizuya-Oka, A (1998). Regulation of apoptosis during development: input from the extracellular matrix (review). *International journal of molecular medicine* **2**: 273-282.
66. Hadjipanayi, E, Mudera, V, and Brown, RA (2009). Guiding cell migration in 3D: a collagen matrix with graded directional stiffness. *Cell motility and the cytoskeleton* **66**: 121-128.
67. Lo, C-M, Wang, H-B, Dembo, M, and Wang, Y-l (2000). Cell Movement Is Guided by the Rigidity of the Substrate. *Biophysical Journal* **79**: 144-152.
68. Hadjipanayi, E, Mudera, V, and Brown, RA (2009). Close dependence of fibroblast proliferation on collagen scaffold matrix stiffness. *Journal of tissue engineering and regenerative medicine* **3**: 77-84.
69. Perlstein, I, *et al.* (2003). DNA delivery from an intravascular stent with a denatured collagen-polylactic-polyglycolic acid-controlled release coating: mechanisms of enhanced transfection. *Gene Ther* **10**: 1420-1428.
70. Qutub AA, PA (2009). Elongation, proliferation & migration differentiate endothelial cell phenotypes and determine capillary sprouting.
. *BMC Syst Biol* **3**.
71. Ayala P, LJ, Desai TA (2010). Microtopographical cues in 3D attenuate fibrotic phenotype and extracellular matrix deposition: implications for tissue regeneration. *Tissue Eng Part A* **16**: 2519-2527.
72. Bott K, UZ, Schrobback K, Ehrbar M, Hubbell JA, Lutolf MP, Rizzi SC. (2010). The effect of matrix characteristics on fibroblast proliferation in 3D gels. *biomaterials* **31**: 8454-8464.
73. Li CL, TT, Nan KJ, Zhao N, Guo YH, Cui J, Wang J, Zhang WG. (2008). Survival advantages of multicellular spheroids vs. monolayers of HepG2 cells in vitro. *Oncol Rep* **29**: 1465-1471.
74. Hong, H, and Stegemann, JP (2008). 2D and 3D collagen and fibrin biopolymers promote specific ECM and integrin gene expression by vascular smooth muscle cells. *Journal of biomaterials science* **19**: 1279-1293.
75. Bonaventure J, KN, Cohen-Solal L, Ng KH, Bourguignon J, Lasselin C, Freisinger P. (1994). Reexpression of cartilage-specific genes by dedifferentiated human articular chondrocytes cultured in alginate beads. *Exp Cell Res* **212**: 97-104.
76. Chang TT, H-FM (2009). Monolayer and spheroid culture of human liver hepatocellular carcinoma cell line cells demonstrate distinct global gene expression patterns and functional phenotypes. *Tissue Eng Part A* **15**: 559-567.
77. Adelow, C, Segura, T, Hubbell, JA, and Frey, P (2008). The effect of enzymatically degradable poly(ethylene glycol) hydrogels on smooth muscle cell phenotype. *Biomaterials* **29**: 314-326.
78. Place, ES, George, JH, Williams, CK, and Stevens, MM (2009). Synthetic polymer scaffolds for tissue engineering. *Chemical Society reviews* **38**: 1139-1151.
79. Ondrej, V, Lukasova, E, Falk, M, and Kozubek, S (2007). The role of actin and microtubule networks in plasmid DNA intracellular trafficking. *Acta biochimica Polonica* **54**: 657-663.

80. Suh, J, Wirtz, D, and Hanes, J (2003). Efficient active transport of gene nanocarriers to the cell nucleus. *Proceedings of the National Academy of Sciences of the United States of America* **100**: 3878-3882.
81. Lindberg, J, Fernandez, MA, Ropp, JD, and Hamm-Alvarez, SF (2001). Nocodazole treatment of CV-1 cells enhances nuclear/perinuclear accumulation of lipid-DNA complexes and increases gene expression. *Pharmaceutical research* **18**: 246-249.
82. Brisson, M, Tseng, WC, Almonte, C, Watkins, S, and Huang, L (1999). Subcellular trafficking of the cytoplasmic expression system. *Human gene therapy* **10**: 2601-2613.
83. Li, D, Li, P, Li, G, Wang, J, and Wang, E (2009). The effect of nocodazole on the transfection efficiency of lipid-bilayer coated gold nanoparticles. *Biomaterials* **30**: 1382-1388.
84. Grosse, S, Aron, Y, Thevenot, G, Monsigny, M, and Fajac, I (2007). Cytoskeletal involvement in the cellular trafficking of plasmid/PEI derivative complexes. *J Control Release* **122**: 111-117.
85. Wong, AW, Scales, SJ, and Reilly, DE (2007). DNA internalized via caveolae requires microtubule-dependent, Rab7-independent transport to the late endocytic pathway for delivery to the nucleus. *The Journal of biological chemistry* **282**: 22953-22963.
86. Douglas, KL, Piccirillo, CA, and Tabrizian, M (2008). Cell line-dependent internalization pathways and intracellular trafficking determine transfection efficiency of nanoparticle vectors. *European Journal of Pharmaceutics and Biopharmaceutics* **68**: 676-687.
87. Hall, A (2005). Rho GTPases and the control of cell behaviour. *Biochemical Society transactions* **33**: 891-895.
88. Evers, EE, *et al.* (2000). Rho family proteins in cell adhesion and cell migration. *Eur J Cancer* **36**: 1269-1274.
89. Arthur, WT, Noren, NK, and Burridge, K (2002). Regulation of Rho family GTPases by cell-cell and cell-matrix adhesion. *Biological research* **35**: 239-246.
90. Clark, EA, King, WG, Brugge, JS, Symons, M, and Hynes, RO (1998). Integrin-mediated signals regulated by members of the rho family of GTPases. *The Journal of cell biology* **142**: 573-586.
91. Hotchin, NA, and Hall, A (1995). The assembly of integrin adhesion complexes requires both extracellular matrix and intracellular rho/rac GTPases. *The Journal of cell biology* **131**: 1857-1865.
92. Olson, MF, Ashworth, A, and Hall, A (1995). An essential role for Rho, Rac, and Cdc42 GTPases in cell cycle progression through G1. *Science (New York, NY* **269**: 1270-1272.
93. Schmidt, A, and Hall, MN (1998). Signaling to the actin cytoskeleton. *Annual review of cell and developmental biology* **14**: 305-338.
94. Ridley, AJ, Paterson, HF, Johnston, CL, Diekmann, D, and Hall, A (1992). The small GTP-binding protein rac regulates growth factor-induced membrane ruffling. *Cell* **70**: 401-410.
95. Boudreau, NJ, and Jones, PL (1999). Extracellular matrix and integrin signalling: the shape of things to come. *The Biochemical journal* **339 (Pt 3)**: 481-488.
96. Van Aelst, L, and D'Souza-Schorey, C (1997). Rho GTPases and signaling networks. *Genes Dev* **11**: 2295-2322.
97. Tolias, KF, Cantley, LC, and Carpenter, CL (1995). Rho family GTPases bind to phosphoinositide kinases. *The Journal of biological chemistry* **270**: 17656-17659.

98. Ren, XD, Bokoch, GM, Traynor-Kaplan, A, Jenkins, GH, Anderson, RA, and Schwartz, MA (1996). Physical association of the small GTPase Rho with a 68-kDa phosphatidylinositol 4-phosphate 5-kinase in Swiss 3T3 cells. *Molecular biology of the cell* **7**: 435-442.
99. Nobes, CD, and Hall, A (1999). Rho GTPases control polarity, protrusion, and adhesion during cell movement. *J Cell Biol* **144**: 1235-1244.
100. Kazmierczak, BI, Jou, TS, Mostov, K, and Engel, JN (2001). Rho GTPase activity modulates Pseudomonas aeruginosa internalization by epithelial cells. *Cell Microbiol* **3**: 85-98.
101. Burnham, CA, Shokoples, SE, and Tyrrell, GJ (2007). Rac1, RhoA, and Cdc42 participate in HeLa cell invasion by group B streptococcus. *FEMS microbiology letters* **272**: 8-14.
102. Li, E, Stupack, D, Bokoch, GM, and Nemerow, GR (1998). Adenovirus endocytosis requires actin cytoskeleton reorganization mediated by Rho family GTPases. *J Virol* **72**: 8806-8812.
103. Lamaze, C, Chuang, TH, Terlecky, LJ, Bokoch, GM, and Schmid, SL (1996). Regulation of receptor-mediated endocytosis by Rho and Rac. *Nature* **382**: 177-179.
104. Tosello-Trampont, AC, Nakada-Tsukui, K, and Ravichandran, KS (2003). Engulfment of apoptotic cells is negatively regulated by Rho-mediated signaling. *The Journal of biological chemistry* **278**: 49911-49919.
105. Ellis, S, and Mellor, H (2000). Regulation of endocytic traffic by rho family GTPases. *Trends in cell biology* **10**: 85-88.
106. Ridley, AJ (2001). Rho proteins: linking signaling with membrane trafficking. *Traffic (Copenhagen, Denmark)* **2**: 303-310.
107. Bourdoulous, S, Orend, G, MacKenna, DA, Pasqualini, R, and Ruoslahti, E (1998). Fibronectin matrix regulates activation of RHO and CDC42 GTPases and cell cycle progression. *J Cell Biol* **143**: 267-276.
108. Ren, XD, Kiosses, WB, and Schwartz, MA (1999). Regulation of the small GTP-binding protein Rho by cell adhesion and the cytoskeleton. *Embo J* **18**: 578-585.
109. Price, LS, Leng, J, Schwartz, MA, and Bokoch, GM (1998). Activation of Rac and Cdc42 by integrins mediates cell spreading. *Mol Biol Cell* **9**: 1863-1871.
110. Chang, C, Wang, X, Niu, D, Zhang, Z, Zhao, H, and Gong, F (2009). Mesenchymal stem cells adopt beta-cell fate upon diabetic pancreatic microenvironment. *Pancreas* **38**: 275-281.
111. Chen, LB, Jiang, XB, and Yang, L (2004). Differentiation of rat marrow mesenchymal stem cells into pancreatic islet beta-cells. *World J Gastroenterol* **10**: 3016-3020.
112. Thomas, CE, Ehrhardt, A, and Kay, MA (2003). Progress and problems with the use of viral vectors for gene therapy. *Nature Reviews Genetics* **4**: 346-358.
113. Schaffert, D, and Wagner, E (2008). Gene therapy progress and prospects: synthetic polymer-based systems. *Gene therapy* **15**: 1131-1138.
114. Hubbell, JA (2006). Non-viral gene delivery: multifunctional polyplexes as locally triggerable nonviral vectors. *Gene therapy* **13**: 1371-1372.
115. Panetti, TS, and McKeown-Longo, PJ (1993). The alpha v beta 5 integrin receptor regulates receptor-mediated endocytosis of vitronectin. *The Journal of biological chemistry* **268**: 11492-11495.

116. Felding-Habermann, B, and Cheresh, DA (1993). Vitronectin and its receptors. *Current opinion in cell biology* **5**: 864-868.
117. White, DJ, Puranen, S, Johnson, MS, and Heino, J (2004). The collagen receptor subfamily of the integrins. *The international journal of biochemistry & cell biology* **36**: 1405-1410.
118. Mecham, RP (1991). Receptors for laminin on mammalian cells. *Faseb J* **5**: 2538-2546.
119. Zhang, Z, Morla, AO, Vuori, K, Bauer, JS, Juliano, RL, and Ruoslahti, E (1993). The alpha v beta 1 integrin functions as a fibronectin receptor but does not support fibronectin matrix assembly and cell migration on fibronectin. *The Journal of cell biology* **122**: 235-242.
120. De Laporte, L, Yan, AL, and Shea, LD (2009). Local gene delivery from ECM-coated poly(lactide-co-glycolide) multiple channel bridges after spinal cord injury. *Biomaterials* **30**: 2361-2368.
121. Wilke, M, Fortunati, E, van den Broek, M, Hoogeveen, AT, and Scholte, BJ (1996). Efficacy of a peptide-based gene delivery system depends on mitotic activity. *Gene therapy* **3**: 1133-1142.
122. Mortimer, I, Tam, P, MacLachlan, I, Graham, RW, Saravolac, EG, and Joshi, PB (1999). Cationic lipid-mediated transfection of cells in culture requires mitotic activity. *Gene therapy* **6**: 403-411.
123. Brunner, S, Sauer, T, Carotta, S, Cotten, M, Saltik, M, and Wagner, E (2000). Cell cycle dependence of gene transfer by lipoplex, polyplex and recombinant adenovirus. *Gene therapy* **7**: 401-407.
124. Chowdhury, EH, *et al.* (2005). Integrin-supported fast rate intracellular delivery of plasmid DNA by extracellular matrix protein embedded calcium phosphate complexes. *Biochemistry* **44**: 12273-12278.
125. Prowse, AB, Chong, F, Gray, PP, and Munro, TP. Stem cell integrins: implications for ex-vivo culture and cellular therapies. *Stem Cell Res* **6**: 1-12.
126. Zuhorn, IS, Kalicharan, D, Robillard, GT, and Hoekstra, D (2007). Adhesion receptors mediate efficient non-viral gene delivery. *Mol Ther* **15**: 946-953.
127. Terrisse, AD, *et al.* Internalization of microparticles by endothelial cells promotes platelet/endothelial cell interaction under flow. *J Thromb Haemost* **8**: 2810-2819.
128. O'Neill, AM, *et al.* Resistance of canine lymphoma cells to adenoviral infection due to reduced cell surface RGD binding integrins. *Cancer Biol Ther* **11**: 651-658.
129. Morgan, MR, Humphries, MJ, and Bass, MD (2007). Synergistic control of cell adhesion by integrins and syndecans. *Nat Rev Mol Cell Biol* **8**: 957-969.
130. Defilippi, P, Olivo, C, Venturino, M, Dolce, L, Silengo, L, and Tarone, G (1999). Actin cytoskeleton organization in response to integrin-mediated adhesion. *Microsc Res Tech* **47**: 67-78.
131. Catelas, I, Sese, N, Wu, BM, Dunn, JC, Helgerson, S, and Tawil, B (2006). Human mesenchymal stem cell proliferation and osteogenic differentiation in fibrin gels in vitro. *Tissue engineering* **12**: 2385-2396.
132. Kopatz, I, Remy, JS, and Behr, JP (2004). A model for non-viral gene delivery: through syndecan adhesion molecules and powered by actin. *J Gene Med* **6**: 769-776.
133. Kruger-Krasagakes, S, Grutzkau, A, Krasagakis, K, Hoffmann, S, and Henz, BM (1999). Adhesion of human mast cells to extracellular matrix provides a co-stimulatory signal for cytokine production. *Immunology* **98**: 253-257.

134. Markovits, J, *et al.* (1989). Inhibitory effects of the tyrosine kinase inhibitor genistein on mammalian DNA topoisomerase II. *Cancer Res* **49**: 5111-5117.
135. Peroutka, SJ, and Synder, SH (1980). Relationship of neuroleptic drug effects at brain dopamine, serotonin, alpha-adrenergic, and histamine receptors to clinical potency. *Am J Psychiatry* **137**: 1518-1522.
136. Goncalves, C, Mennesson, E, Fuchs, R, Gorvel, JP, Midoux, P, and Pichon, C (2004). Macropinocytosis of polyplexes and recycling of plasmid via the clathrin-dependent pathway impair the transfection efficiency of human hepatocarcinoma cells. *Mol Ther* **10**: 373-385.
137. von Gersdorff, K, Sanders, NN, Vandenbroucke, R, De Smedt, SC, Wagner, E, and Ogris, M (2006). The internalization route resulting in successful gene expression depends on both cell line and polyethylenimine polyplex type. *Mol Ther* **14**: 745-753.
138. Hsu, SL, *et al.* (2006). Caspase 3, periodically expressed and activated at G2/M transition, is required for nocodazole-induced mitotic checkpoint. *Apoptosis* **11**: 765-771.
139. Rubtsova, SN, Kondratov, RV, Kopnin, PB, Chumakov, PM, Kopnin, BP, and Vasiliev, JM (1998). Disruption of actin microfilaments by cytochalasin D leads to activation of p53. *FEBS Lett* **430**: 353-357.
140. Bhadriraju, K, Yang, M, Alom Ruiz, S, Pirone, D, Tan, J, and Chen, CS (2007). Activation of ROCK by RhoA is regulated by cell adhesion, shape, and cytoskeletal tension. *Experimental Cell Research* **313**: 3616-3623.
141. Polte, TR, Eichler, GS, Wang, N, and Ingber, DE (2004). Extracellular matrix controls myosin light chain phosphorylation and cell contractility through modulation of cell shape and cytoskeletal prestress. *American journal of physiology* **286**: C518-528.
142. Thum, T, and Borlak, J (2001). Butanedione monoxime increases the viability and yield of adult cardiomyocytes in primary cultures. *Cardiovasc Toxicol* **1**: 61-72.
143. Sellin, LC, and McArdle, JJ (1994). Multiple effects of 2,3-butanedione monoxime. *Pharmacol Toxicol* **74**: 305-313.
144. Dhaliwal, A, Lam, J, Maldonado, M, Lin, C, and Segura, T (2011). Extracellular matrix modulates non-viral gene transfer to mouse mesenchymal stem cells. *Soft Matter*.
145. Dhaliwal, A, Maldonado, M, Han, Z, and Segura, T. Differential uptake of DNA-poly(ethylenimine) polyplexes in cells cultured on collagen and fibronectin surfaces. *Acta Biomater*.
146. Dhaliwal, A, Maldonado, M, Han, Z, and Segura, T. Differential uptake of DNA-poly(ethylenimine) polyplexes in cells cultured on collagen and fibronectin surfaces. *Acta Biomater* **6**: 3436-3447.
147. Wang, B, Oleschuk, RD, and Horton, JH (2005). Chemical force titrations of amine- and sulfonic acid-modified poly(dimethylsiloxane). *Langmuir* **21**: 1290-1298.
148. Khatiwala, CB, Kim, PD, Peyton, SR, and Putnam, AJ (2009). ECM Compliance Regulates Osteogenesis by Influencing MAPK Signaling Downstream of RhoA and ROCK. *JOURNAL OF BONE AND MINERAL RESEARCH* **24**: 886-898.
149. Tkachenko, E, Lutgens, E, Stan, RV, and Simons, M (2004). Fibroblast growth factor 2 endocytosis in endothelial cells proceed via syndecan-4-dependent activation of Rac1 and a Cdc42-dependent macropinocytic pathway. *J Cell Sci* **117**: 3189-3199.
150. Zhang, S, *et al.* (1995). Rho family GTPases regulate p38 mitogen-activated protein kinase through the downstream mediator Pak1. *The Journal of biological chemistry* **270**: 23934-23936.

151. Subauste, MC, *et al.* (2000). Rho family proteins modulate rapid apoptosis induced by cytotoxic T lymphocytes and Fas. *The Journal of biological chemistry* **275**: 9725-9733.
152. Aktories, K, and Just, I (2005). Clostridial Rho-inhibiting protein toxins. *Curr Top Microbiol Immunol* **291**: 113-145.
153. Genth, H, Dreger, SC, Huelsenbeck, J, and Just, I (2008). Clostridium difficile toxins: more than mere inhibitors of Rho proteins. *Int J Biochem Cell Biol* **40**: 592-597.
154. Aktories, K (1997). Bacterial toxins that target Rho proteins. *J Clin Invest* **99**: 827-829.
155. Benya, RV, Akeson, M, Mrozinski, J, Jensen, RT, and Battey, JF (1994). Internalization of the gastrin-releasing peptide receptor is mediated by both phospholipase C-dependent and -independent processes. *Mol Pharmacol* **46**: 495-501.
156. Kanematsu, T, *et al.* (2007). Phospholipase C-related inactive protein is implicated in the constitutive internalization of GABAA receptors mediated by clathrin and AP2 adaptor complex. *J Neurochem* **101**: 898-905.
157. Garrett, WS, *et al.* (2000). Developmental control of endocytosis in dendritic cells by Cdc42. *Cell* **102**: 325-334.
158. Kim, SJ, Lee, ZW, Kweon, SM, Kim, S, and Ha, KS (2002). Regulation of reactive oxygen species and stress fiber formation by calpeptin in Swiss 3T3 fibroblasts. *Cellular signalling* **14**: 205-210.
159. Schoenwaelder, SM, and Burridge, K (1999). Evidence for a calpeptin-sensitive protein-tyrosine phosphatase upstream of the small GTPase Rho. A novel role for the calpain inhibitor calpeptin in the inhibition of protein-tyrosine phosphatases. *The Journal of biological chemistry* **274**: 14359-14367.
160. Ridley, AJ, and Hall, A (1992). The small GTP-binding protein rho regulates the assembly of focal adhesions and actin stress fibers in response to growth factors. *Cell* **70**: 389-399.
161. Koivusalo, M, *et al.* Amiloride inhibits macropinocytosis by lowering submembranous pH and preventing Rac1 and Cdc42 signaling. *J Cell Biol* **188**: 547-563.
162. Mostafavi-Pour, Z, Askari, JA, Parkinson, SJ, Parker, PJ, Ng, TT, and Humphries, MJ (2003). Integrin-specific signaling pathways controlling focal adhesion formation and cell migration. *J Cell Biol* **161**: 155-167.
163. Pan, J, *et al.* (2005). PKC mediates cyclic stretch-induced cardiac hypertrophy through Rho family GTPases and mitogen-activated protein kinases in cardiomyocytes. *J Cell Physiol* **202**: 536-553.
164. Koo, BK, *et al.* (2006). Structural basis of syndecan-4 phosphorylation as a molecular switch to regulate signaling. *J Mol Biol* **355**: 651-663.
165. Ng, T, *et al.* (1999). PKCalpha regulates beta1 integrin-dependent cell motility through association and control of integrin traffic. *Embo J* **18**: 3909-3923.
166. Weernink, PA, Guo, Y, Zhang, C, Schmidt, M, Von Eichel-Streiber, C, and Jakobs, KH (2000). Control of cellular phosphatidylinositol 4,5-bisphosphate levels by adhesion signals and rho GTPases in NIH 3T3 fibroblasts involvement of both phosphatidylinositol-4-phosphate 5-kinase and phospholipase C. *Eur J Biochem* **267**: 5237-5246.
167. Halabi-Cabezon, I, *et al.* (2008). Prevention of the cytopathic effect induced by Clostridium difficile Toxin B by active Rac1. *FEBS Lett* **582**: 3751-3756.

168. Hall, A, and Nobes, CD (2000). Rho GTPases: molecular switches that control the organization and dynamics of the actin cytoskeleton. *Philos Trans R Soc Lond B Biol Sci* **355**: 965-970.
169. Ahmed, TA, Dare, EV, and Hincke, M (2008). Fibrin: a versatile scaffold for tissue engineering applications. *Tissue Eng Part B Rev* **14**: 199-215.
170. Karp, JM, Sarraf, F, Shoichet, MS, and Davies, JE (2004). Fibrin-filled scaffolds for bone-tissue engineering: An in vivo study. *Journal of biomedical materials research* **71**: 162-171.
171. Janmey, PA, Winer, JP, and Weisel, JW (2009). Fibrin gels and their clinical and bioengineering applications. *Journal of the Royal Society, Interface / the Royal Society* **6**: 1-10.
172. Wilmer, M, Schroder, V, and Kohler, HP (2002). [Methods for the determination of factor XIII/XIIIa]. *Hamostaseologie* **22**: 32-42.
173. Okada, M, Blomback, B, Chang, MD, and Horowitz, B (1985). Fibronectin and fibrin gel structure. *The Journal of biological chemistry* **260**: 1811-1820.
174. Sun, Y, Giraudier, O, and Garde, VL (2005). Rheological characterization and dissolution kinetics of fibrin gels crosslinked by a microbial transglutaminase. *Biopolymers* **77**: 257-263.
175. Duckert, F, and Nyman, D (1978). Factor XIII, fibrin and collagen. *Supplementum* **63**: 391-396.
176. Saito, Y, Imada, T, Takagi, J, Kikuchi, T, and Inada, Y (1986). Platelet factor XIII. The collagen receptor? *The Journal of biological chemistry* **261**: 1355-1358.
177. Corbett, SA, Lee, L, Wilson, CL, and Schwarzbauer, JE (1997). Covalent cross-linking of fibronectin to fibrin is required for maximal cell adhesion to a fibronectin-fibrin matrix. *The Journal of biological chemistry* **272**: 24999-25005.
178. Makogonenko, E, Tsurupa, G, Ingham, K, and Medved, L (2002). Interaction of fibrin(ogen) with fibronectin: further characterization and localization of the fibronectin-binding site. *Biochemistry* **41**: 7907-7913.
179. Podor, TJ, *et al.* (2002). Incorporation of vitronectin into fibrin clots. Evidence for a binding interaction between vitronectin and gamma A/gamma' fibrinogen. *The Journal of biological chemistry* **277**: 7520-7528.
180. Matsuka, YV, Medved, LV, Brew, SA, and Ingham, KC (1994). The NH2-terminal fibrin-binding site of fibronectin is formed by interacting fourth and fifth finger domains. Studies with recombinant finger fragments expressed in Escherichia coli. *The Journal of biological chemistry* **269**: 9539-9546.
181. Martino, MM, Mochizuki, M, Rothenfluh, DA, Rempel, SA, Hubbell, JA, and Barker, TH (2009). Controlling integrin specificity and stem cell differentiation in 2D and 3D environments through regulation of fibronectin domain stability. *Biomaterials* **30**: 1089-1097.
182. Schense, JC, Bloch, J, Aebischer, P, and Hubbell, JA (2000). Enzymatic incorporation of bioactive peptides into fibrin matrices enhances neurite extension. *Nature biotechnology* **18**: 415-419.
183. Ehrbar, M, *et al.* (2004). Cell-demanded liberation of VEGF121 from fibrin implants induces local and controlled blood vessel growth. *Circulation research* **94**: 1124-1132.
184. Trentin, D, Hall, H, Wechsler, S, and Hubbell, JA (2006). Peptide-matrix-mediated gene transfer of an oxygen-insensitive hypoxia-inducible factor-1alpha variant for local

induction of angiogenesis. *Proceedings of the National Academy of Sciences of the United States of America* **103**: 2506-2511.
185. des Rieux, A, Shikanov, A, and Shea, LD (2009). Fibrin hydrogels for non-viral vector delivery in vitro. *J Control Release* **136**: 148-154.
186. Lei, P, Padmashali, RM, and Andreadis, ST (2009). Cell-controlled and spatially arrayed gene delivery from fibrin hydrogels. *Biomaterials* **30**: 3790-3799.
187. Gojgini, S, Tokatlian, T, and Segura, T. Utilizing cell-matrix interactions to modulate gene transfer to stem cells inside hyaluronic Acid hydrogels. *Mol Pharm* **8**: 1582-1591.
188. Lei, Y, Rahim, M, Ng, Q, and Segura, T. Hyaluronic Acid and Fibrin Hydrogels with Concentrated DNA/PEI Polyplexes for Local Gene Delivery. *J Control Release*.
189. Xiang, S, *et al.* Uptake mechanisms of non-viral gene delivery. *J Control Release*.
190. Allison, DD, and Grande-Allen, KJ (2006). Review. Hyaluronan: a powerful tissue engineering tool. *Tissue engineering* **12**: 2131-2140.
191. Gurski, LA, Jha, AK, Zhang, C, Jia, X, and Farach-Carson, MC (2009). Hyaluronic acid-based hydrogels as 3D matrices for in vitro evaluation of chemotherapeutic drugs using poorly adherent prostate cancer cells. *Biomaterials* **30**: 6076-6085.
192. Kim J, PY, Tae G, Lee KB, Hwang SJ, Kim IS, Noh I, Sun K. (2008). Synthesis and characterization of matrix metalloprotease sensitive-low molecular weight hyaluronic acid based hydrogels. *J Mater Sci Mater Med* **19**
193. Dhaliwal A, MM, Lin C, Segura T. (2012). Cellular Cytoskeleton Dynamics Modulates Non-Viral Gene Delivery through RhoGTPases. *PLoS One* **7**: e35046.
194. Weaver VM, LS, Lakins JN, Chrenek MA, Jones JC, Giancotti F, Werb Z, Bissell MJ. (2002). beta4 integrin-dependent formation of polarized three-dimensional architecture confers resistance to apoptosis in normal and malignant mammary epithelium. *Cancer Cell* **2**: 205-216.
195. Mirjam Ochsner1¤b, MT, Viola Vogel2, Michael L. Smith2¤a* (2010). Dimensionality Controls Cytoskeleton Assembly and Metabolism of Fibroblast Cells in Response to Rigidity and Shape. *PLoS One* **5**: e9445.
196. Yamada KM, PR, Cukierman E. (2003). Dimensions and dynamics in integrin function. *Braz J Med Biol Res* **36**: 959-966.
197. Balaban NQ, SU, Riveline D, Goichberg P, Tzur G, Sabanay I, Mahalu D, Safran S, Bershadsky A, Addadi L, Geiger B. (2001). Force and focal adhesion assembly: a close relationship studied using elastic micropatterned substrates. *Nat Cell Biol* **3**: 466-472.
198. Bershadsky AD, BC, Carramusa L, Zilberman Y, Gilquin B, Khochbin S, Alexandrova AY, Verkhovsky AB, Shemesh T, Kozlov MM. (2006). Assembly and mechanosensory function of focal adhesions: experiments and models. *Eur J Cell Biol* **85**: 165-173.
199. Cukierman E, PR, Stevens DR, Yamada KM. (2001). Taking cell-matrix adhesions to the third dimension. *Science* **294**: 1708-1712.
200. Sverdlov M, SA, Minshall RD. (2007). Tyrosine phosphorylation-dependence of caveolae-mediated endocytosis. *J Cell Mol Med* **11**: :1239-1250.
201. Macia, E, Ehrlich, M, Massol, R, Boucrot, E, Brunner, C, and Kirchhausen, T (2006). Dynasore, a cell-permeable inhibitor of dynamin. *Dev Cell* **10**: 839-850.
202. S, E-M (2004). Actin and microtubules in cell motility: which one is in control? *Traffic* **5**: 470-477.

203. Elbaum M, CA, Levy ET, Shtutman M, Bershadsky AD. (1999). Microtubule involvement in regulating cell contractility and adhesion-dependent signalling: a possible mechanism for polarization of cell motility. *Biochem Soc Symp* **65**: 147-172.
204. Trentin, D, Hubbell, J, and Hall, H (2005). Non-viral gene delivery for local and controlled DNA release. *J Control Release* **102**: 263-275.